

1981

Natural Convection, Two-Phase Flow, and Crystallization in a Vacuum Pan Sugar Crystallizer.

Jack Jerome Bunton

Louisiana State University and Agricultural & Mechanical College

Follow this and additional works at: https://digitalcommons.lsu.edu/gradschool_disstheses

Recommended Citation

Bunton, Jack Jerome, "Natural Convection, Two-Phase Flow, and Crystallization in a Vacuum Pan Sugar Crystallizer." (1981). *LSU Historical Dissertations and Theses*. 3587.

https://digitalcommons.lsu.edu/gradschool_disstheses/3587

This Dissertation is brought to you for free and open access by the Graduate School at LSU Digital Commons. It has been accepted for inclusion in LSU Historical Dissertations and Theses by an authorized administrator of LSU Digital Commons. For more information, please contact gradetd@lsu.edu.

INFORMATION TO USERS

This was produced from a copy of a document sent to us for microfilming. While the most advanced technological means to photograph and reproduce this document have been used, the quality is heavily dependent upon the quality of the material submitted.

The following explanation of techniques is provided to help you understand markings or notations which may appear on this reproduction.

- 1. The sign or "target" for pages apparently lacking from the document photographed is "Missing Page(s)". If it was possible to obtain the missing page(s) or section, they are spliced into the film along with adjacent pages. This may have necessitated cutting through an image and duplicating adjacent pages to assure you of complete continuity.**
- 2. When an image on the film is obliterated with a round black mark it is an indication that the film inspector noticed either blurred copy because of movement during exposure, or duplicate copy. Unless we meant to delete copyrighted materials that should not have been filmed, you will find a good image of the page in the adjacent frame.**
- 3. When a map, drawing or chart, etc., is part of the material being photographed the photographer has followed a definite method in "sectioning" the material. It is customary to begin filming at the upper left hand corner of a large sheet and to continue from left to right in equal sections with small overlaps. If necessary, sectioning is continued again—beginning below the first row and continuing on until complete.**
- 4. For any illustrations that cannot be reproduced satisfactorily by xerography, photographic prints can be purchased at additional cost and tipped into your xerographic copy. Requests can be made to our Dissertations Customer Services Department.**
- 5. Some pages in any document may have indistinct print. In all cases we have filmed the best available copy.**

**University
Microfilms
International**

300 N. ZEEB ROAD, ANN ARBOR, MI 48106
18 BEDFORD ROW, LONDON WC1R 4EJ, ENGLAND

8117617

BUNTON, JACK JEROME

NATURAL CONVECTION, TWO-PHASE FLOW, AND CRYSTALLIZATION
IN A VACUUM PAN SUGAR CRYSTALLIZER

The Louisiana State University and Agricultural and Mechanical Col. PH.D. 1981

University
Microfilms
International 300 N. Zeeb Road, Ann Arbor, MI 48106

PLEASE NOTE:

In all cases this material has been filmed in the best possible way from the available copy. Problems encountered with this document have been identified here with a check mark ✓.

1. Glossy photographs or pages _____
2. Colored illustrations, paper or print _____
3. Photographs with dark background _____
4. Illustrations are poor copy _____
5. Pages with black marks, not original copy _____
6. Print shows through as there is text on both sides of page _____
7. Indistinct, broken or small print on several pages _____
8. Print exceeds margin requirements _____
9. Tightly bound copy with print lost in spine _____
10. Computer printout pages with indistinct print ✓
11. Page(s) _____ lacking when material received, and not available from school or author.
12. Page(s) _____ seem to be missing in numbering only as text follows.
13. Two pages numbered _____. Text follows.
14. Curling and wrinkled pages _____
15. Other _____

**University
Microfilms
International**

NATURAL CONVECTION, TWO-PHASE FLOW,
AND CRYSTALLIZATION
IN A
VACUUM PAN
SUGAR CRYSTALLIZER

A Dissertation

Submitted to the Graduate Faculty of the
Louisiana State University and
Agricultural and Mechanical College
in partial fulfillment of the
requirements for the degree of
Doctor of Philosophy

in

The Department of Chemical Engineering

by

Jack Jerome Bunton
B.S., University of South Alabama, 1976
M.S., Louisiana State University, 1978

May 1981

To My Daughter Brianna,
With Love

ACKNOWLEDGEMENT

Foremost, I would like to express my special gratitude to my wife Toni, whose patience, love, and understanding allowed me to complete this research.

I would like to express my appreciation to my Committee members, Drs. Lawrence Mann, Bert Wilkins, Ralph W. Pike, and Joseph Polack for their comments and suggestions based upon their review of this work. Special thanks to Armando B. Corripio and Richard C. Farmer for advice and guidance in the development of this research.

Special appreciation to Hazel LaCoste and other members of the staff of the department of Chemical Engineering, as well as, the members of the staff of the Audubon Sugar Institute for their continuing support of graduate students pursuing an advanced degree.

I am grateful for the financial assistance provided by the Audubon Sugar Institute. Also, I would like to thank the Dr. Charles E. Coates Memorial Fund, donated by Charles E. Coates, for financial aid in the preparation of this manuscript.

TABLE OF CONTENTS

	page
ACKNOWLEDGEMENT.....	iii
LIST OF TABLES.....	vi
LIST OF FIGURES.....	vii
ABSTRACT.....	viii
 CHAPTER	
1. INTRODUCTION.....	1
2. PARTICLE EQUATIONS.....	10
3. MATHEMATICAL MODEL.....	23
1. Overall Balances.....	29
2. General Homogeneous Model.....	31
3. Sectionalization.....	33
4. Pertinent Equations.....	43
5. Non-Dimensionalization and Boundary Conditions.....	62
6. Discussion of the Assumptions.....	70
4. COMPUTATIONAL METHODS.....	73
1. Development of the Philosophy of the Finite Difference Equations.....	81
2. Numerical Model for Vacuum Pan.....	101
5. RESULTS.....	124
1. Sensitivity of Calculation to the Kinematic Viscosity and Thermal Diffusivity.....	127
2. Effect of Pan Design and Operating Conditions.....	130

CHAPTER	page
3. Comparison of Predicted Tube Velocities Against Literature.....	168
4. Numerical Problems and Hydrostatic Head Assumption.....	172
6. DYNAMIC GRID.....	175
7. SUMMARY AND CONCLUSIONS.....	183
8. RECOMMENDATIONS.....	190
REFERENCES.....	191
NOMENCLATURE.....	199
APPENDIX	
I LISTING OF COMPUTER PROGRAM.....	205
II VELOCITY PROFILES DEMONSTRATING EFFECT OF THERMAL DIFFUSIVITY AND KINEMATIC VISCOSITY.....	306
III EXAMPLE OF DYNAMIC GRID.....	316
VITA.....	321

LIST OF TABLES

TABLE		page
3.4.1	Coefficient of Concentration.....	47
3.4.2	Coefficient of Thermal Expansion.....	47
3.4.3	Viscosity Correlation Statistics.....	55
3.4.4	Viscosity Data.....	55
3.4.5	Evaporation Coefficient.....	61
3.5.1	Non-Dimensional Variables.....	64
3.5.2	Boundary Conditions.....	68
4.1.1	Upwind Differencing Algorithm.....	96
5.1.1	Log of Model Runs Varying the Thermal and Momentum Diffusivity.....	129
5.2.1	Typical Pan Designs.....	141
5.2.2	Log of Model Runs Varying Pan Design and Operating Conditions.....	142
5.2.3	Summary of Model Results.....	143
5.3.1	Webre's Data.....	171
5.3.2	Clausen's Data.....	171

LIST OF FIGURES

FIGURE		page
1.0.0	Idealized Vacuum Pan.....	5
2.0.0	Well Stirred Tank Crystallizer.....	11
2.0.1	Typical Crystal Size Distribution.....	13
2.0.2	Typical Crystal Number Density Function.....	18
3.3.1	Sectionalized Vacuum Pan.....	42
4.1.1	Well Stirred Tank.....	86
4.1.2	Grid Representation of Well Stirred Tank.....	87
4.1.3	Typical Two-Dimensional Finite Difference Grid.....	88
4.1.4	Computational Grid Cell.....	95
4.2.1	Typical Grid Arrangement.....	112
4.2.2	Differencing Vertical Pressure Gradient.....	123
5.2.1	Velocity Profiles-Generated From Experimental Runs Varying Pan Design and Operating Conditions.....	144
5.2.2	Growth Profiles-Generated From Experimental Runs Varying Pan Design and Operating Conditions.....	156

ABSTRACT

A mathematical model of a Vacuum Pan Sugar Crystallizer is developed. This mathematical model is based on the fundamentals of the physics of two-phase flow. Because of the complexity of the model, the time dependent solution is accomplished using numerical methods designed to be executed by a digital computer. The model generates velocity, pressure, temperature, and supersaturation profiles for the Pan, in response to the operating conditions and the design of the Pan. The motivation for the development of this model is to give an analytical tool to study the effects of Pan design, control systems, and operating conditions on the product crystal size distribution.

The emphasis of this research is on the development of the numerical methods that are consistent with conservative and transportive principles reflected in the equations of motion. Important features of the numerical code are that it employs a dynamic grid system designed for free surface flows, and is compatible with viscous two-phase flows exhibited in the Pan. The modeling equations are two-dimensional for the volume above the Calandria, but in other areas where two-dimensional equations are an extravagance, one-dimensional and lumped equations are used.

The velocity and growth rate profiles provides the information needed for a distributed population balance equation needed to analyze the effect of these profiles on the crystal size distribution. The development of such a population balance is discussed but is not part of the present numerical code. Nonetheless, the model provides valuable information concerning the effects of Pan design, control systems, and operating conditions in a qualitative sense, as demonstrated in the results. Sensitivity studies varying Pan design and operating conditions demonstrate that of the cases studied, the volumn fraction crystals, pan level, heat load, pan pressure, and whether or not the pan major diameter is flared, had the most significant effects on the pan performance. These variations of Pan design and operating conditions were judged significant based on their effect on the velocity and growth profiles, maximum and minimum supersaturation, and average supersaturation. A summary of the results is presented in Chapter 7 and discussions concerning particular cases along with raw data are presented in Chapter 5.

CHAPTER 1

INTRODUCTION

The purpose of this research is to develop a mathematical model of the transport phenomena in a Vacuum Pan Sugar Crystallizer and to use it to study its effect on the crystal size distribution (CSD), and its control. The proper conservative equations will be found or derived, that under proper assumptions and simplifications, and when given the proper boundary conditions, will adequately describe the conditions of fluid flow in the pan. Once the proper equations have been found, further assumptions will be made to model sections of the pan where the characteristics of the flow are different.

The development of the mathematical model is based on the fundamental conservation equations of mass, momentum, and energy as applied to a multi-phase system. The phases present during the operation of the Vacuum Pan are the liquid sugar solution, solid sugar crystals, and water vapor because the mixture is boiling. The mathematical model is spatially distributed rather than lumped. The motive for development of this model is to study the effect of spatially varying growth rates on the resulting CSD. The growth variations are the result of the distributed nature of the temperature profiles in the

Vacuum Pan. Although, the purpose of this research is to develop the model describing the fluid mechanics, emphasis is placed on the use of this model to analyze the CSD. In fact, Chapter 2 is a summary of the equations used in the literature to model particulate systems such as the Vacuum Pan.

Before going any further, let's describe the Vacuum Pan with enough detail so that the reader may understand subsequent discussion in reference to the Pan.

Figure 1.0.0 is the symmetrical half-section of an idealized pan divided into sections that will have meaning later.

Basically, the Vacuum Pan is a Calandria type evaporator with a central downtake. The objective of the Vacuum Pan is to provide a supersaturated environment to promote crystal growth. Sugar content in the water solution is depleted by crystal growth and replenished by unsaturated liquid feed. Thus, water is evaporated continuously to maintain supersaturated conditions. Careful consideration is given to pan temperature, therefore, the pan is operated under vacuum to maintain low boiling temperature because the sugar crystals are heat sensitive. The massecuite (a sugar solution with crystalline sugar in suspension), is heated in the Calandria and the hot mixture rises as the result of density differences between the column of the mixture

above the Calandria Downtake and the column above the Calandria Heating Section. Boiling may occur as the mixture rises towards the surface. The heat generated in the Calandria is released at the surface in the form of vapor, if the boiling point of the mixture has been reached. That which has not left the pan in the form of vapor is recirculated back through the Calandria via the Downtake. Because of the highly viscous nature of the sugar solution, sugar crystals generally flow with approximately the same velocity as the surrounding fluid even though the density difference is significant. The amount of sugar in the solution remains relatively constant throughout the pan volume at any given time, but, the local solution temperature may change drastically relative to local sugar concentration changes. Thus, growth profiles result due to temperature profiles in the Pan.

Important features of the Vacuum Pan Sugar Crystallizer needed for consideration in the derivation of the mathematical model describing the fluid flow are that, the flow is by natural convection, free surface, possibly boiling, and highly viscous. However, different sections may be characterized independently and if these characteristics are capitalized upon, a more efficient numerical computer code may be formulated without neglecting the major features mentioned above. The following sections are separated as shown in

Figure 1.0.0 because of their different characteristics.

1. Pan Proper
2. Bottom and Downtake
3. Calandria
4. Free Surface

To this point, the significance of the CSD is not apparent. A narrow CSD is desirable and it is the objective of the Vacuum Pan to grow an initially uniform seed CSD to an acceptable size, dictated by the maximum volume of crystal that the mother liquor can suspend and still be reasonably fluid. The volume fraction of crystal is usually less than forty percent at the end of the batch. A wide CSD or large variance of the CSD reduces the fluidity of the mixture for a given volume fraction of crystals. This makes the separation of the crystals at the end of the batch by centrifuging difficult and also hinders circulation in the Vacuum Pan. Circulation in the Pan must be maintained to prevent further widening of the CSD.

A narrow CSD is also desirable because a wider CSD is not generally marketable as a consumer product. Of course, a narrow CSD indicates that nucleation has been avoided. Since nucleation causes crystal aggregates to be formed, which occludes mother liquor containing impurities, and noting that purity is also important, a

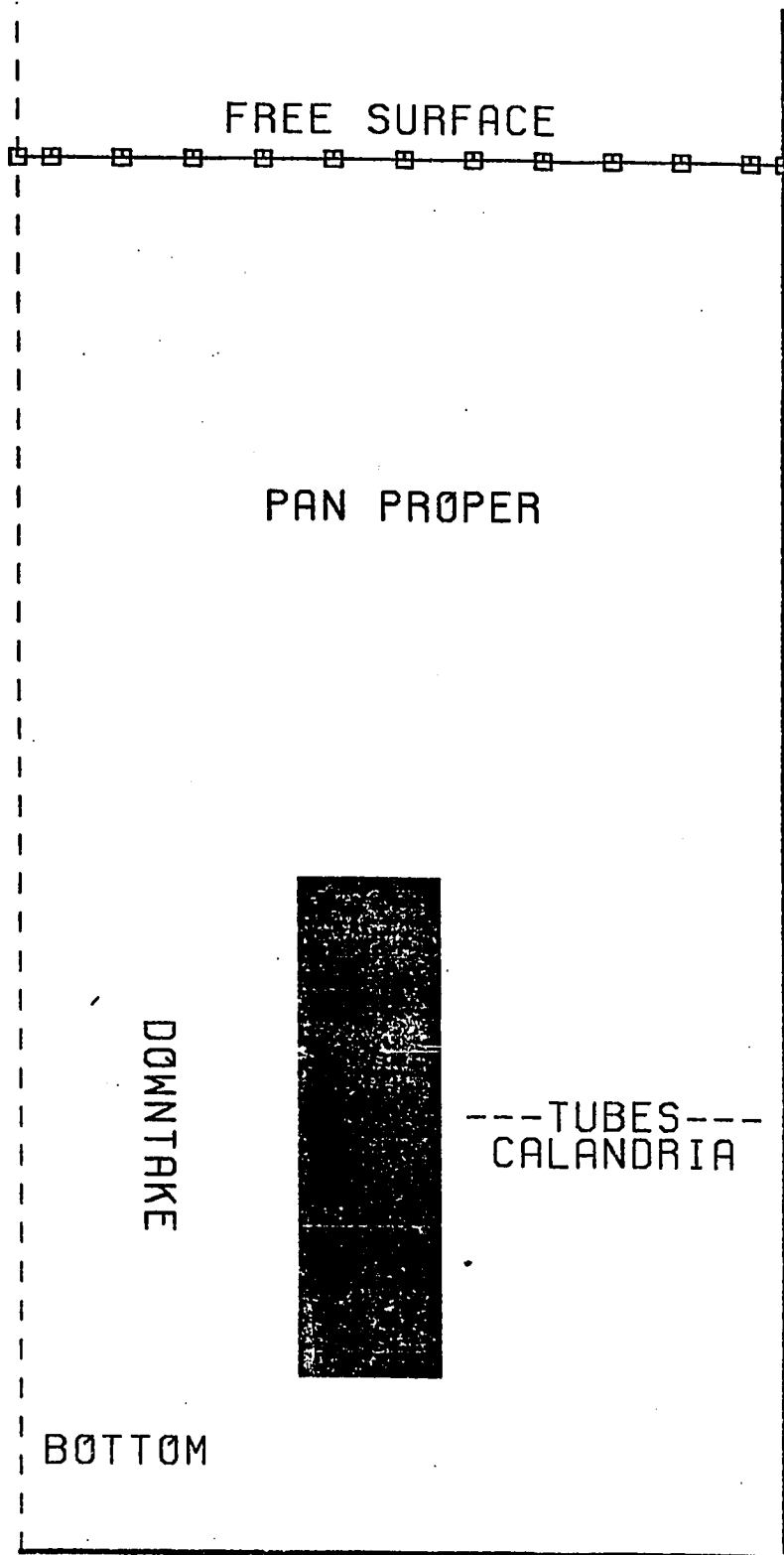


FIGURE 1.0.0 IDEALIZED VACUUM PAN

narrow CSD is desirable. Thus, a narrow CSD is important from the standpoint of the operation of the Pan, separation of the product, and from customer specifications. Therefore, a model capable of predicting the conditions that cause a widening of the CSD and studying control methods to minimize these conditions as much as possible, is desirable.

Previous work in modeling the Vacuum Pan for the purpose of simulation and control studies have been based on the Well Stirred Tank (WSTRT) principle. These models employ the basic material and energy balances as applied to the WSTRT, as well as, the basic physical properties and kinetic information as pertaining to the sucrose crystallizer. Recent advances in modeling particulate systems through the use of the particle population balance aid in the understanding of the operation of the Vacuum Pan. Wright (1974), Frew (1973), and Mukhopadhyay (1980) use these recent advances in studying particulate systems along with the overall material and energy balance to develop a mathematical model of the Vacuum Pan. Both Wright (1974) and Mukhopadhyay (1980) develop the model as a simulation tool to study the effects of certain variables. However, Mukhopadhyay (1980) considers the competing kinetics of nucleation and growth to change the CSD, while Wright (1974) ignores nucleation but includes an empirical dispersion coefficient that describes the

widening of the CSD due to mixing effects. Frew (1973), on the other hand, develops the model in order to apply optimal control theory to optimize the operation of the batch. However, Frew's conclusions are the same as might be concluded based on experience or with a little engineering insight. Earlier modeling efforts by Doucet (1966), Mori (1968), Evans (1970), and Batterham (1974) do not employ the population balances and are aimed at understanding and designing the basic material and energy balance control systems. Doucet, Evans, and Batterham develop and apply their models in the time domain, but Mori linearizes the modeling equations and places them in the Laplace domain in a more traditional control theory approach.

Although the emphasis here is on semi-continuous or the batch Vacuum Pan, Randolph (1978) and Sawal (1979) have published articles concerning continuous sucrose crystallizers and the application of the particle balances.

In the following chapters, the mathematical model of the Vacuum Pan will be developed. Although the main purpose of this research is to develop a model describing the fluid mechanics, for the sake of completeness, the population balances for spatially distributed and lumped systems will be discussed in Chapter 2. However, these balances will not be integrated into the numerical model,

instead, the crystal growth will be treated very simply for material balance purposes. The spatial dependence of the growth rate will be demonstrated with local calculation of the growth rate based on the local temperature and the pan sucrose and impurities concentrations. Extensions of this model to include the lumped or distributed particle balances will allow a direct analysis of the effects of pan design, operating conditions, and control systems on the CSD. Concluding this research, sensitivity studies will be performed to demonstrate the effects of pan design and operating conditions on the velocity profiles and growth rate profiles. These, of course, directly affect the CSD and demonstrate the usefulness of the model as a research tool. In addition to the velocity and growth rate profiles, the model also generates temperature and pressure profiles in the Pan.

Because of the system of equations describing the physics of fluid motion in the Vacuum Pan are complex, the numerical solution of these equations is particularly difficult. It is for this reason that the derivation of the applied equations, under the proper assumptions, is so important in order to facilitate the numerical solution and reduce the complexity of the numerical solution. The solution method described for the modeling equations and concepts brought out in this research are

very much at the forefront of the state of the art in computational fluid mechanics for free surface flows. Much of the emphasis of this research is therefore, placed on the development of the modeling equations and their numerical solution.

Application of the model to other problems involving a free surface is obvious, since it is based on the fundamentals of fluid mechanics. As this research is an extension of earlier research done at Louisiana State University, by Waldrop (1972) and Pitts (1976), on modeling bays and estuaries, the improvements and extensions accomplished in this research are directly applicable to these earlier codes. The code described here can be easily extended to study circulation patterns caused by hot submerged jets in bodies of water. The Oak Ridge Simplified Marker and Cell Code, developed by Park (1980), was developed to simulate such a situation, but the code developed in this research is simpler and more efficient with computer time, which are obvious advantages. In addition, the development of the dynamic grid system, which is essential when modeling free surface flows, is presented with more mathematical rigor than presented in the literature and should aid in the development of other free surface fluid dynamic codes.

CHAPTER 2

PARTICLE EQUATIONS

The analysis of particulate systems such as dryers, fluidized beds, and crystallizers, among others, has been greatly enhanced by the development of the population balances. An excellent source of discussion and application of these population balances is contained in a book by Randolph and Larson (1971).

Because the biological sciences are also interested in information concerning the ages or sizes of biological organisms, these equations apply directly to the analysis of those systems. The concise mathematical framework of this set of equations, through analytical or numerical solutions of the applied equations, allows analysts to simulate particulate systems or interpret experimental data.

As applied to crystallizers, the growth and nucleation rate of crystals may be identified from experiments or the CSD predicted. To demonstrate how kinetic data might be interpreted, the continuous Well Stirred Tank (WSTRT) crystallizer will be described mathematically with reference to Figure 2.0.0. This population balance will serve to identify the kinetics of the crystallizer or model the crystallizer. The important point, however, is that once the kinetics have

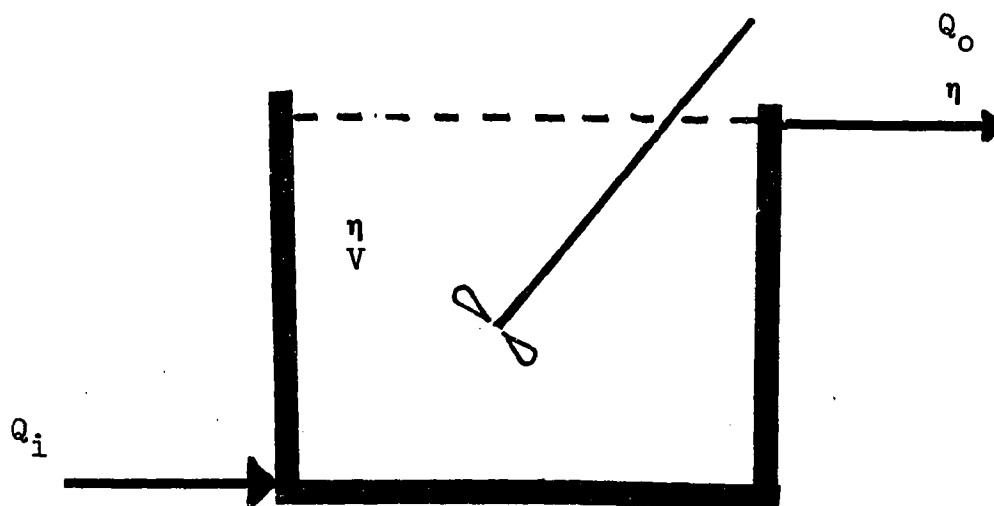


FIGURE 2.0.0 WELL STIRRED TANK CRYSTALLIZER

been identified, the population balances can be derived for more complex physical systems and hopefully, the kinetics still apply.

The population balances for the WSTRT are derived like the material and energy balances, except, the conserved quantity is the number of particles in a particular size range. The function that mathematically describes the population in question is its crystal size distribution (CSD). The function is generally approximated by a continuous function rather than a discrete function. Figure 2.0.1 is a typical CSD, that might be obtained by a sieve analysis or various other methods. Since the crystals are suspended in a volume of mother liquor, in a crystallizer, to facilitate the analysis, a new variable will be defined as the crystallizer number density, as defined by Equation 2.0.0.

$$\eta = \frac{\text{CSD}}{V} N_c \quad 2.0.0$$

Where V is the volume of the mother liquor rather than the total volume. The number of crystals per unit volume in the crystallizer between the sizes of L to $L+dL$ is then defined by Equation 2.0.1.

$$V \int_L^{L+dL} \eta dL = V \eta(L) dL \quad 2.0.1$$

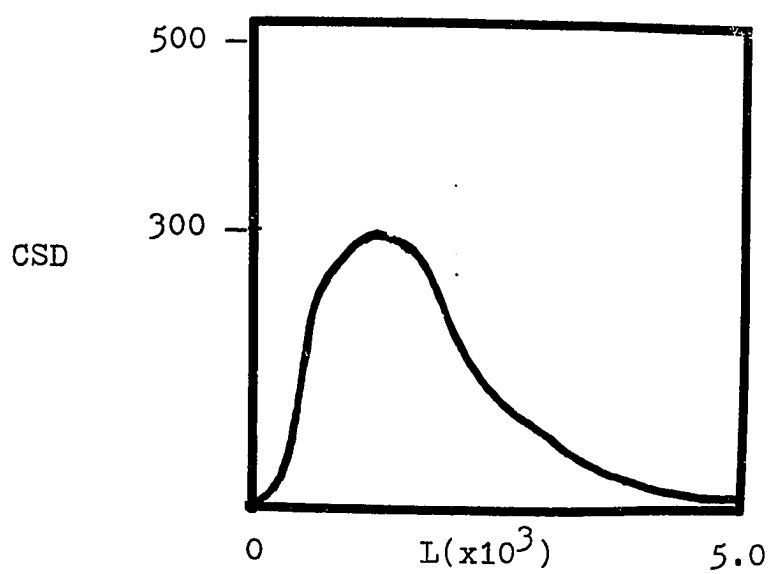


FIGURE 2.0.1 TYPICAL CRYSTAL SIZE DISTRIBUTION

The change in time of the number of crystals in the size range is the result of the birth or the nucleation rate of new crystals, the input of seed crystals with the feed, and output of crystals in the output stream, and the growth of crystals. The function which describes the rate at which nuclei are produced in all size ranges per unit volume of mother liquor, is the nucleation rate density function (NRDF), and is approximated with a continuous function (B). The mechanisms that cause nucleation and the theory behind them are discussed in Mullin (1975). For most modeling efforts the nucleation of new crystals is described mathematically as a power law function of the growth rate or supersaturation. The growth rate (G) of the crystals in the solution is generally expressed as a power law function of supersaturation. The theory of growth of crystals is also discussed in Mullin. Although, birth of crystals can be thought of as occurring in all sizes, for the purposes here, the NRDF describes the nucleation of crystals at the zero size. For this analysis, no crystals will be supplied with the feed. The population balance is expressed mathematically in Equation 2.0.2.

$$\frac{\partial (V\eta(L)dL)}{\partial t} \Delta t = - \Delta t Q_o \eta(L)dL + \Delta t V B(L)dL \quad 2.0.2$$

$$+ V(\eta(L-G\Delta t)G\Delta t - \eta(L)G\Delta t)$$

Dividing both sides of Equation 2.0.2 by dL , Δt , and V and taking the limit as dL and Δt , go to zero, Equation 2.0.3 is the resulting equation. The domain of Equation 2.0.3 is crystal sizes greater than or equal to zero.

$$\frac{\partial \eta V}{V \partial t} = \frac{\partial \eta}{\partial t} + \frac{d \ln V}{dt} = - \frac{\eta}{V} Q_0 - \frac{\partial \eta G}{\partial L} + B \quad 2.0.3$$

Equation 2.0.3 is the population balance for the WSTRT model. However, to obtain information about the kinetics from experimental data collected from the WSTRT, Equation 2.0.3 can be simplified to allow an analytic solution. Equation 2.0.4 results from neglecting the dynamic terms. The boundary conditions for Equation 2.0.4 are given below the equation, the functionality of B is also given.

$$\begin{aligned} \frac{d \eta G}{\partial L} &= - \frac{\eta}{V} Q_0 \\ \eta(0) &= \eta_0 = B_0 / G \\ \eta(\infty) &= 0 \\ B(0) &= B_0 \\ B(L) &= 0 \quad L > 0 \end{aligned} \quad 2.0.4$$

Equation 2.0.4 applies for crystal sizes greater than zero but is made to include zero size by applying the boundary condition at the zero crystal size. This

boundary condition is derived by doing a particle balance for the zero size as given by Equation 2.0.5.

$$\frac{d\eta_o}{dt} = -\eta_o G + B_o \quad 2.0.5$$

Therefore at steady state, the nuclei density (η_o) is simply the ratio of the nucleation rate to the growth rate. The solution to Equation 2.0.4, given the functional definition of B, the boundary conditions and growth rate not a function of the length, is given in Equation 2.0.6 below.

$$\eta = \eta_o \text{EXP}\left(-\frac{LQ_o}{VG}\right) \quad 2.0.6$$

Therefore, by taking experimental data from a WSTRT crystallizer at a steady state, one may obtain the growth rate and nucleation rate at the conditions in the crystallizer. Then, by studying various conditions, a functional relationship may be obtained between the conditions (supersaturation, impurities, etc.) in the WSTRT and the growth and nucleation rates. The traditional method of analysis is to plot the logarithm of the crystal number density function (η) as a function of the crystal size and extract the slope and intercept,

but other mathematical techniques may be used.

Figure 2.0.2 is a typical plot.

Once the kinetics of the system have been established, by experiment, one may use Equation 2.0.3 to model the dynamics of the continuous WSTRT in response to changes in operating conditions or the effect of various control systems. However, Equation 2.0.3 is too complex for analytical solution and, therefore, a numerical solution must be attempted. Since Equation 2.0.3 is a partial differential equation, the equation could be partitioned into a set of particle size ranges and integrated as partial differential equations are traditionally treated. This is the approach Grimmett (1980) takes in studying Fluidized-Bed Dryers. However, generally speaking, the complete distribution need not be reproduced during a numerical simulation, instead, a few descriptive parameters are all that are needed, specifically, the average particle size, the total number of particles, and the variance of the CSD. Of course, all of these can be obtained from the crystallizer number density function, since it is related to the CSD via Equation 2.0.0. Thus, following the moments of the crystallizer number density function, one can follow the performance of the crystallizer. Following the moments also eliminates the problems of a partial differential equation, since the particle size dimension is integrated out when Equation 2.0.3 is

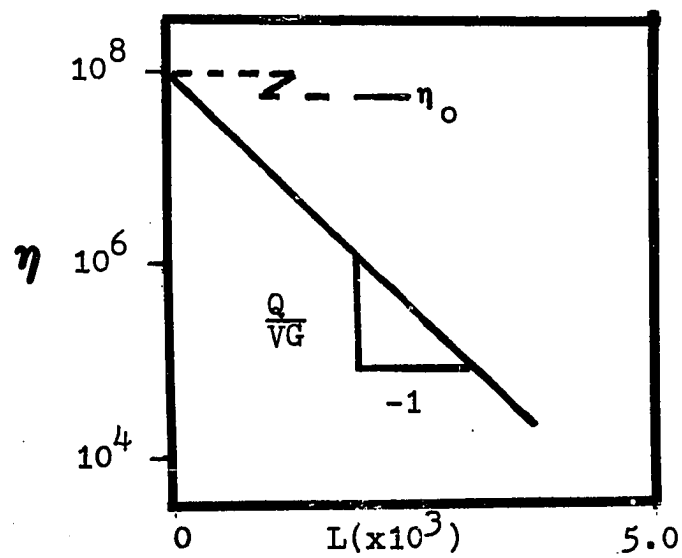


FIGURE 2.0.2 TYPICAL CRYSTAL NUMBER DENSITY FUNCTION

converted to a moment equation. This is done by the integration described in the equation below.

$$\begin{aligned} \int_0^{\infty} L^k \frac{\partial \eta}{\partial t} dL + \frac{d \ln V}{dt} \int_0^{\infty} L^k \eta dL = - Q_0/V \int_0^{\infty} L^k \eta dL \\ - G \int_0^{\infty} L^k \frac{\partial \eta}{\partial L} dL + \int_0^{\infty} L^k B(L) dL \end{aligned} \quad 2.0.7$$

$k = 0, 1, 2, \dots$

Equation 2.0.7 can be integrated for each value of k , given the definition of the k th moment of η ,

Equation 2.0.8, and by using integration by parts for moments higher than zeroth moment.

$$M_k = \int_0^{\infty} L^k \eta dL \quad k = 0, 1, 2, \dots \quad 2.0.8$$

The results of the integration are summarized below.

$$B_k = \int_0^{\infty} L^k B dL \quad k = 0, 1, 2, \dots \quad 2.0.9$$

$$\frac{dM_k}{dt} + M_k \frac{d \ln V}{dt} = - M_k Q_0/V + k G M_{k-1} + B_k \quad 2.0.10$$

$$M_{-1} = \eta_0 \quad 2.0.11$$

$$B_k(k=0) = B_0 \quad 2.0.12$$

$$B_k = 0 \quad k = 1, 2, 3, \dots$$

The total number of crystals in the WSTRT, the average length, and the variance of the CSD, is then related to the moments, as shown in Equation 2.0.12 thru 2.0.15.

$$N_c = M_0 V \quad 2.0.13$$

$$\bar{L} = M_1 / M_0 \quad 2.0.14$$

$$\sigma^2 = M_2 / M_0 - (M_1 / M_0)^2 \quad 2.0.15$$

These equations can be integrated along with the overall material and energy balances and be used to study the dynamics of the WSTRT.

Although, in many cases, the WSTRT principle is adequate for most industrial applications where particulate processing is involved, there are cases where this is not true. Such a case is the semi-continuous operation of the Vacuum Pan Sugar Crystallizer. Because the sugar solution is viscous and mixing is generally caused by natural convection and boiling, growth and

supersaturation profiles exist. Crystals flowing with the fluid are, therefore, subjected to a varying growth environment which contributes to the widening of the CSD. Because supersaturation at points may be excessive, even though the average supersaturation is satisfactory, nucleation may occur which further disturbs the CSD. Analysis of this system can only be done satisfactorily when these problems are taken into account in the modeling effort. One way to model such a system is to use a distributed population balance. Hulburt and Katz (1964) develop such a distributed population balance, based on continuum principles. The development of the distributed equation considers distributed conditions to promote growth and nucleation and convection of the crystals with the fluid. Unfortunately, Hulburt and Katz developed the equations for incompressible flow only, therefore, the equations do not directly apply to the Vacuum Pan because of the boiling phenomenon. Because the use of the distributed equations requires the velocity, growth, and nucleation profiles, these equations must be combined with the distributed equations of mass, momentum, and energy. To be compatible with the fluid dynamic equations and their numerical solution, as developed in the pages to follow, additional research will be needed to construct the proper crystal size number density and the form of the

population balance. Possible alternative formulations of the distributed population balance accommodating compressible flow, might be to express the number density (η) on a per unit mass of mixture basis, to be compatible with the homogeneous flow assumption used in the development of the equations of motion in the following chapters. On a per mass basis, the population balance will have the form of the mixture momentum equation without the diffusion terms. A more physical alternative would be to consider the crystals as remaining in the liquid phase all the time, in which case, the incompressible flow assumption will be valid and the population balance will only have to be modified to include the volume fraction of liquid. Although the distributed analysis is a formidable test, analyses of this type have been attempted successfully, but not for the crystallizer. For example, Bracco (1974) analyzes the combustion of flammable liquid drops falling in hot air using the distributed population balance with fluid flow. Thus, such a modeling effort is possible and if carried out, should aid in the understanding of the operation of the Vacuum Pan and help eliminate some of the problems that cause a widening of the CSD.

CHAPTER 3

MATHEMATICAL MODEL

Over the past twenty years with the advent of fast computers, the utility of studying physical systems by numerically solving the fundamental mathematical equations describing the physical system has increased. This is the result of the high cost of failure of the designed system to meet specifications or safety requirements. For most mathematical formulations of the physical systems, analytical solutions of the set of equations are not possible, therefore, a solution must be found through the use of numerical methods. The ease of solving these equations depends on the complexity of the problem and the particular characteristics of the numerical formulation of the problem. Once a realistic and solvable mathematical model has been developed, the model can then be used to simulate the system of interest. The advantage here is that computational experiments can be performed that can optimize the systems complete design, including control systems as well as safety systems. All of this can be done before large expenditures are wasted on building plant scale equipment which later must be modified. The model does not replace the lab and pilot lab experiments necessarily, but may be used as a tool in order to reduce risk to capital expenditures. The

field of fluid dynamics, as applied to physical systems, in which more than one phase exist, is of particular interest to this research. Application of computational fluid dynamics of multi-phase to physical system has helped designers build safer and more economical equipment. In particular, computational fluid dynamics has contributed greatly to the development of a nuclear industry. In fact, much of the research in the two-phase flow was done explicitly to develop numerical codes to simulate loss of coolant situations and to simulate reactor cores for the nuclear industry. These numerical methods saved literally millions of dollars in experimental costs of designing safety systems by using the model to predict results that otherwise would have to be measured experimentally.

In this chapter a similar approach will be used as applied to a Vacuum Pan Sugar Crystallizer. The applied equations describing viscous two-phase flow with a free surface will be presented. These equations will be considered as adequately describing conditions promoting natural circulation in a Vacuum Pan Sugar Crystallizer. The numerical methods needed to solve the mathematical formulation of the problem will be developed and presented in another chapter. The development of the fluid dynamic equations describing two-phase flow under various assumptions has been done in the literature. Therefore, such development will not be done here, instead,

literature will be cited in order to indicate the available sources of information.

The one-dimensional homogeneous flow is the most basic of the fluid dynamic models of the two-phase flow phenomena. The basic assumption of this model is that the two-phase fluid can be presented as one fluid with proper averages applied to the physical properties. Wallis (1969) has a good applied presentation of this model. He continues his discussions of one-dimensional models with the two-phase stratified flow models. The stratified model considers each phase separately, but the equations are coupled by exchange functions that describe the exchange of mass, momentum, and energy across the interface. The development of multi-dimensional stratified and homogeneous models are done in detail in Ishii (1975). Ishii's approach is to develop the complete mathematical model of two-phase flow in as much detail as possible and then identify the areas where development of phenomenological models are needed to give closure to the set of equations. These phenomenological models describe the interchange of mass, energy, and momentum across the interfaces between phases. Each phase is considered a continuum. The results are a set of equations that based on the magnitude of certain dimensionless numbers can be simplified. Soo (1967) has written a book that is very comprehensive in the analysis

of applied multi-phase flow. Soo (1978) has also written an article in an attempt to bring out the distinguishing differences between continuum mechanics and multi-phase flow, Soo makes the point that only when the multi-phase mixture is considered as completely homogeneous can continuum mechanics be used to derive the models.

Solbrig (1978) reviews the literature concerning the development of the applied two-phase flow equations and multi-phase flow equations. In addition, he also derives a set of equations. Because of the complexity of the multi-phase flow equations and their solution, the hope in developing a workable model in a limited amount of time and computer resources is bleak unless a great many assumptions can be made to simplify the complexities. Hopefully these assumptions can be justified.

The development of the mathematical model for the Vacuum Pan will be done in several parts as pertaining to several sections of the Pan. These sections are the Pan Proper, Downtake and Bottom, and Calandria (or tube section). The various sections of the Pan were discussed earlier in reference to Figure 1.0.0. The development of the model is done in this fashion to insure that the main characteristics of each section are modeled. Thus, when all the sections are combined, a model is formulated that describes the main characteristics of Pan operation without overkilling the simpler sections with complexity.

The formulation of the mathematical model for the free surface will be deferred to the chapter on the numerical model, since the differences in this section and the Pan Proper are only the results of the numerical solution technique.

Before stating any of the conservative equations of mass, energy, and momentum, some assumptions will be made and the conservative equations will reflect these assumptions from the outset. Further modifications and assumptions will be made if needed in subsequent discussions concerning sectionalization as mentioned above. These assumptions are listed below.

- (1) Homogeneous flow of the mixture.
i.e., The solid and vapor phases are completely dispersed in the predominant liquid phase.
- (2) All phases are moving with the same velocity.
- (3) There is instantaneous thermal and mechanical equilibrium between all phases.
- (4) Laminar flow exists.
- (5) Newton's law of viscosity and Fourier's law of heat conduction apply.
- (6) The viscosity terms reflect the incompressible nature of the liquid.
i.e., The substantial derivative of the density changes little spatially.
- (7) The substantial derivative of the pressure is

negligible compared to the other terms in the energy equation.

- (8) Viscous heating of the fluid is negligible.
- (9) The heat of crystallization is negligible.
- (10) No spatial variation of the concentration of sucrose, impurities, and crystals.
- (11) The flow is axisymmetric with no circulatory motion about the vertical axis, therefore, two-dimensional with the coordinates being the radial and vertical directions.
- (12) No nucleation of new crystals.
- (13) The hydrostatic head assumption is applicable to reduce the vertical momentum equation to the density and pressure term.

3.1 OVERALL BALANCES

As indicated in assumption (10), no species continuity will be stated for the spatial variation of the concentration of sucrose, impurities, or crystals. The dynamics of these components will be described with Equations 3.1.1 thru 3.1.5, which are the lumped overall material balances for the whole Pan. The hold-up of vapor was assumed to be negligible and a overall material balance for the vapor was not written. The mass fractions of each component are calculated as according to Equations 3.1.6 thru 3.1.9. Since these overall mass balances were used instead of distributed balances, several assumptions will have to be made with regards to the calculation of mixture enthalpy and density, these assumptions will be discussed later.

$$\text{sugar: } \frac{dS}{dt} = F X_{SF} - \frac{dC}{dt} \quad 3.1.1$$

$$\text{impurity: } \frac{dIMP}{dt} = F X_{IMF} \quad 3.1.2$$

$$\text{water: } \frac{dW}{dt} = F X_{WF} - ER \quad 3.1.3$$

$$\text{crystal: } C = N_c \rho_c \frac{\pi}{6} L^3 \quad 3.1.4$$

$$\text{crystal size: } \frac{d\bar{L}}{dt} = G \quad 3.1.5$$

mass fractions:

$XSP=S/TMASS$	3.1.6
$XIP=IMP/TMASS$	3.1.7
$XWP=W/TMASS$	3.1.8
$XCP=C/TMASS$	3.1.9

The overall balances for the sugar, impurities, and crystal content were taken from a model developed by Wright (1974). However, Wright included dispersion of the CSD by an empirical equation. One of the objects of this research, is to show that the model for the fluid dynamics developed in this dissertation in combination with a distributed particle balance can calculate the dispersion of the CSD directly. Although, the particle balances discussed earlier were not programmed, the growth rate variations in the pan will be demonstrated in the results. As mentioned above, it is assumed that local variations in concentration of the sucrose and impurities are negligible, therefore, the cause of growth variations is assumed to result from the temperature differences in the Pan. These temperature differences have to be significant if natural convection is to be the mechanism to circulate the batch.

3.2 GENERAL HOMOGENEOUS MODEL

The homogeneous equations, as taken from Ishii (1975) page 229, after neglecting the effects of the interfaces on the momentum and energy equations, are presented below in vector form in Equations 3.2.1 thru 3.2.7.

$$\text{continuity: } \frac{\partial \rho}{\partial t} + \nabla \cdot \rho \mathbf{U} = 0 \quad 3.2.1$$

$$\begin{aligned} \text{momentum: } \frac{\partial \mathbf{U}}{\partial t} + \nabla \cdot \rho \mathbf{U} \mathbf{U} &= -\nabla P \\ &+ \nabla \cdot \boldsymbol{\tau} + \mathbf{F}_B \end{aligned} \quad 3.2.2$$

$$\begin{aligned} \text{energy: } \frac{\partial \rho H}{\partial t} + \nabla \cdot \rho \mathbf{U} H &= K \nabla^2 T \\ &+ \frac{DP}{Dt} + \phi_c \end{aligned} \quad 3.2.3$$

$$\text{density: } \rho = \sum \gamma_i \rho_i \quad 3.2.4$$

$$\text{velocity: } \mathbf{U} = \frac{\sum \gamma_i \rho_i \mathbf{U}_i}{\rho} \quad 3.2.5$$

$$\text{enthalpy: } H = \frac{\sum \gamma_i \rho_i H_i}{\rho} \quad 3.2.6$$

$$\text{stress tensor: } \boldsymbol{\tau} = \mu (\nabla \mathbf{U} + (\nabla \mathbf{U})^+) \quad 3.2.7$$

Applying the following assumptions: (2), (4), (6), (7), (8), and (9), and transforming to the cylindrical coordinate system, Ishii's equations are reduced to Equations 3.2.8 thru 3.2.14. Equations 3.2.8 thru 3.2.14 are exactly the same equations that could be developed

under the assumptions above, if the single-phase equations from Bird, Stewart, and Lightfoot (1960) were simplified and the same mixing rules for the physical properties applied. These equations are offered as the general model for the Vacuum Pan Sugar Crystallizer under the assumptions applied. The boundary conditions for the system will be discussed later.

$$\text{continuity:} \quad \frac{\partial \rho}{\partial t} + \frac{1}{r} \frac{\partial r}{\partial r} \frac{\rho u}{\partial r} + \frac{\partial \rho w}{\partial z} = 0 \quad 3.2.8$$

$$\begin{aligned} \text{radial momentum:} \quad & \frac{\partial \rho u}{\partial t} + \frac{1}{r} \frac{\partial r}{\partial r} \frac{\rho u^2}{\partial r} \\ & + \frac{\partial \rho w u}{\partial z} = -\frac{\partial P}{\partial r} + \rho v \left(\frac{1}{r} \frac{\partial}{\partial r} \left(r \frac{\partial u}{\partial r} \right) - \frac{u^2}{r^2} + \frac{\partial^2 u}{\partial z^2} \right) \end{aligned} \quad 3.2.9$$

$$\begin{aligned} \text{vertical momentum:} \quad & \frac{\partial \rho w}{\partial t} + \frac{1}{r} \frac{\partial r}{\partial r} \frac{\rho u w}{\partial r} + \\ & \frac{\partial \rho w^2}{\partial z} = -\frac{\partial P}{\partial z} + \rho v \left(\frac{1}{r} \frac{\partial}{\partial r} \left(r \frac{\partial w}{\partial r} \right) + \frac{\partial^2 w}{\partial z^2} \right) - g \rho \end{aligned} \quad 3.2.10$$

$$\begin{aligned} \text{energy:} \quad & \frac{\partial \rho H}{\partial t} + \frac{1}{r} \frac{\partial r}{\partial r} \frac{\rho u H}{\partial r} \\ & + \frac{\partial \rho w H}{\partial z} = \rho \alpha \left(\frac{1}{r} \frac{\partial}{\partial r} \left(r \frac{\partial T}{\partial r} \right) + \frac{\partial^2 T}{\partial z^2} \right) \end{aligned} \quad 3.2.11$$

$$\text{density:} \quad \rho = \sum \gamma_i \rho_i \quad 3.2.12$$

$$\text{velocity:} \quad U = U_i \quad 3.2.13$$

$$\text{enthalpy:} \quad H = \frac{\sum \gamma_i \rho_i H_i}{\rho} \quad 3.2.14$$

3.3 SECTIONALIZATION

The general homogeneous equations presented above, along with other pertinent equations, fully describe the operation of the Vacuum Pan Sugar Crystallizer. But, application of these fully two-dimensional equations would lead to a very complex model. This complexity for all portions of the Pan is unwanted because the characteristics of each section differ. In the following sectionalization of the model, all equations can be simplified from the general homogeneous flow Equations 3.2.8 thru 3.2.11. However, the Pan Proper is the only section where the general equations can be most easily seen to apply. This is intentional because the Pan Proper is the most complex of the sections modeled.

a. Pan Proper

The Pan Proper makes up the largest volume of the Pan and exhibits the most spatial differences in the velocity and temperature profiles. Complex convection currents occur in this section resulting from the hot liquid rising from the Calandria and backmixing of the cooler liquid that has released its vapor at the surface. The modeling of the Pan would be completely inadequate if this section of the Vacuum Pan was treated as one lump.

Because of its distributed nature, this section will be modeled by applying the general model equations presented earlier. In addition to the assumptions inherent in Equations 3.2.8 thru 3.2.13, it is also assumed that the hydrostatic head assumption is adequate as a description of pressure profiles in the Pan Proper. Actually, this assumption neglects all the terms in the vertical momentum equation except the pressure and the body force terms, that is, the effects of inertia, convection of momentum, and the viscous forces are assumed negligible. The resulting equations are presented below in Equations 3.3.1 thru 3.3.4.

$$\text{continuity:} \quad \frac{\partial \rho}{\partial t} + \frac{1}{r} \frac{\partial r \rho u}{\partial r} \quad 3.3.1$$

$$+ \frac{\partial \rho w}{\partial z} = 0$$

$$\text{radial momentum:} \quad \frac{\partial \rho u}{\partial t} + \frac{1}{r} \frac{\partial r \rho u^2}{\partial r} + \quad 3.3.2$$

$$\frac{\partial \rho w u}{\partial r} = - \frac{\partial P}{\partial r} + \rho v \left(\frac{1}{r} \frac{\partial}{\partial r} (r \frac{\partial u}{\partial r}) - \frac{u^2}{r^2} + \frac{\partial^2 u}{\partial z^2} \right)$$

$$\text{vertical momentum:} \quad - \frac{\partial P}{\partial z} - \rho g = 0 \quad 3.3.3$$

$$\text{energy:} \quad \frac{\partial \rho H}{\partial t} + \frac{1}{r} \frac{\partial r \rho u H}{\partial r} + \quad 3.3.4$$

$$\frac{\partial \rho w H}{\partial z} = \rho \alpha \left(\frac{1}{r} \frac{\partial}{\partial r} (r \frac{\partial T}{\partial r}) + \frac{\partial^2 T}{\partial z^2} \right)$$

b. Calandria

The Calandria is basically a heating section and is generally made of a number of tubes into which massecuite flows vertically upward on the inside and is heated by condensing steam on the outside of the tubes. Since the radial distances of the Pan Proper are much larger than the radial distances of the tubes, each tube can be considered as one-dimensional.

Because each tube has a different radial position it may be subject to different conditions and thus, different conditions could exist in each tube. Considering each tube independently could cost a great deal of computer time and programming time, therefore, it was decided to use an average tube to represent all the tubes. The one-dimensional model for the tubes are presented below in Equations 3.3.5 thru 3.3.8. These equations are exactly the same as the model for a boiler tube given in Wallis (1969), but, the hydrostatic head assumption has been applied. However, the pressure drop due to friction has been retained because friction restricts flow in the tubes considerably. The laminar flow equation is used to calculate the pressure drop, if vapor is present the velocity of the liquid for the same mass flux will be used. The equation for the local friction pressure drop is given in Equation 3.3.8. The

equations below can also be derived directly from the general homogeneous flow equations presented earlier. This can be done by integrating the equations over the cross-sectional area of the tubes. Once the proper boundary conditions are applied, the resulting equations are identical to those below.

$$\text{continuity:} \quad \frac{\partial \rho}{\partial t} + \frac{\partial \rho w}{\partial z} = 0 \quad 3.3.5$$

$$\text{vertical momentum:} \quad - \frac{\partial P}{\partial z} - \rho g - FR = 0 \quad 3.3.6$$

$$\text{energy:} \quad \frac{\partial \rho H}{\partial t} + \frac{\partial \rho w H}{\partial z} = \quad 3.3.7$$

$$\rho \alpha \frac{\partial^2 T}{\partial z^2} + UPOA(T - T_{\text{STEAM}})$$

$$\text{frictional pressure drop: } FR = 32 \mu w / D_t^2 \quad 3.3.8$$

c. Bottom

The Bottom and Downtake serve basically as a conduit to recirculate the massecuite back through the heating section. When modeling, several observations can be made. The conditions in this section are obviously non-boiling because the pressure is higher than the pressure in the Pan Proper that feeds this section. The dynamics of temperature changes are slow, since the profiles in the Pan Proper change only in response to the level of the Pan and the total solids fraction in the Pan which are slow dynamically. That is, assuming the two-phase boiling transients in the Pan Proper that occur on a small time scale have a negligible effect on the Pan Bottom and Downtake. In addition, most of the liquid that recirculates through the Downtake comes from the surface after it has boiled. Thus, the flux of liquid in the Bottom is of fairly constant temperature.

Since the conditions in the Bottom and Downtake are non-boiling and temperature changes are slow, it makes no sense to treat this area in a distributed fashion. Therefore, the Bottom and Downtake are treated as one lump for the energy and continuity equation. Because the effect of temperature on the density is small, the time derivative of the density in the continuity equation or mass balance for the Bottom and Downtake is neglected.

However, a problem occurs when writing the unsteady lumped momentum balance as presented in Bird, Stewart, and Lightfoot (1960), and presented in Equation 3.3.9. The formulation of the equation is made in reference to Figure 3.3.1.

$$\begin{aligned} \frac{\partial P}{\partial t} = (P + \rho w^2)_1 A_1 - (P + \rho w^2)_5 A_5 \\ - FR_{1-5} + F_B \quad 1-2 \end{aligned} \quad 3.3.9$$

The problem results from the fact that there is no specific cross-sectional area to base the momentum in the radial Pan Bottom. Splitting the Equation 3.3.9 into two lumps, Equations 3.3.10 for the Downtake and Equation 3.3.11 for the Bottom, isolates the problem in determining the lumped inertial term to Equation 3.3.11.

$$\begin{aligned} \frac{\partial P}{\partial t} \quad 1-2 = (P_1 - P_2) A_1 - FR_{1-2} \\ + \rho A_1 \text{ TUBEH } g \end{aligned} \quad 3.3.10$$

$$\begin{aligned} \frac{\partial P}{\partial t} \quad 2-5 = (P + \rho w^2)_2 A_2 \\ - (P + \rho w^2)_5 A_5 - FR_{2-5} \end{aligned} \quad 3.3.11$$

The inertial term in Equation 3.3.11 cannot be determined without knowing the velocity profiles in the Pan Bottom. This means a lumped analysis will not allow the inertial term to be evaluated. If the lumped momentum analysis is to be used for the Bottom, the inertial term in Equation 3.3.11 will have to be neglected, thus, a steady

state assumed. In order to maintain the dynamics of the problem and avoid the problem with Equation 3.3.11 in determining the inertial term, the cross-sectional area between the Downtake and the Calandria is taken as a basis for a one-dimensional momentum balance. Referring to Figure 3.3.1 will pin point the area under discussion. Equation 3.3.12 is the one-dimensional momentum balance for this section of the Pan, it can be obtained from Equation 3.2.9 by neglecting all the derivatives in the vertical direction. Equation 3.3.12 can be integrated over this area by applying the continuity equation for the cross-section to obtain the momentum at each point. Equation 3.3.18 is the resulting equation, the steps for its derivation are outlined in Equations 3.3.13 thru 3.3.17.

In the derivation of Equation 3.3.18, each of the terms in Equation 3.3.12 are integrated over the volume between point (3) and (4) i.e., V_{34} . The dynamic term, Equation 3.3.14, is integrated by applying Leibnitz's Rule (Bird, Stewart, and Lightfoot (1960)). The bar over the radial velocity indicates that it is the volume averaged radial velocity, for convenience this will be taken as being evaluated at the average radial position between points (3) and (4). Likewise, the pressure term is evaluated similarly. The gradient of pressure is then approximated assuming pressure to be a linear function of radial position. The viscous terms drop out directly by

applying Equation 3.3.13.

$$\frac{\partial u}{\partial t} = -u \frac{\partial u}{\partial r} - \frac{1}{\rho} \frac{\partial P}{\partial r} + v \left(\frac{1}{r} \frac{\partial}{\partial r} (r \frac{\partial u}{\partial r}) - \frac{u}{r^2} \right) \quad 3.3.12$$

$$r u = c_1 \quad 3.3.13$$

$$\int_{V_{3-4}} \frac{\partial u}{\partial t} dV = \frac{\partial \bar{u}}{\partial t} V_{3-4} \quad 3.3.14$$

$$-\int_{V_{3-4}} u \frac{\partial u}{\partial r} dV = -c_1^2 \left(\frac{1}{r} \right) \Big|_{r_3}^{r_4} 2\pi \text{ BOTTH} \quad 3.3.15$$

$$-\frac{1}{\rho} \int_{V_{3-4}} \frac{\partial P}{\partial r} dV = -\frac{\Delta P}{\Delta r} V_{3-4} \quad 3.3.16$$

$$\frac{1}{r} \frac{\partial}{\partial r} (r \frac{u}{r}) - \frac{u}{r^2} = 0 \quad 3.3.17$$

$$\frac{\Delta \bar{u}}{\Delta t} = -\frac{1}{\rho} \frac{\Delta P}{\Delta r} - 2 c_1^2 (\Delta \frac{1}{r}) / (\Delta r^2) \quad 3.3.18$$

The use of Equation 3.3.18 requires an assumption concerning the pressure profile, referring to Figure 3.3.1, from point (2) to point (3) and from point (4) to point (5). Since the flow is slow and the pressure drop across the area between the Downtake and the Calandria is, by pan design, small, it is assumed that the pressure at point (2) is equal to the pressure at point (3) and the pressure at point (4) is equal to the pressure at

point (5).

In summary, the equations modeling the Downtake and Bottom are presented in Equations 3.3.19 thru 3.3.22. Equation 3.3.19 is the lumped energy equation. Equation 3.3.20 is the continuity relation or the mass balance for the Downtake and Bottom. The momentum and equations are split into Equation 3.3.21 for the Downtake and Equation 3.3.22 for the Bottom. The continuity relation for the one-dimensional section in which Equation 3.3.22 is based on is Equation 3.3.13. Notice that Equations 3.3.19 and 3.3.20 reflect the input of mass and energy by the feed. The momentum of the feed is neglected.

$$\begin{aligned} \text{energy:} \quad \rho V \frac{dH}{dt} &= (-\rho w)_1 H_1 & 3.3.19 \\ &- (\rho w)_5 H_5 + F HF \end{aligned}$$

$$\begin{aligned} \text{continuity:} \quad (\rho w)_5 A_5 &= (\rho w)_1 A_1 & 3.3.20 \\ &+ F \end{aligned}$$

$$\begin{aligned} \text{vertical downtake: } P_2 &= P_1 + FR_{1-2} & 3.3.21 \\ + \rho \text{ TUBEH } g \quad FR_{1-2} &= \frac{8\mu w \text{ TUBEH}}{R_{\text{dwn}}^2} \end{aligned}$$

$$\begin{aligned} \text{radial momentum bottom: } \frac{d\bar{u}}{dt} &= - \frac{1(P_5 - P_2)}{\rho(r_4 - r_3)} & 3.3.22 \\ - 2(\bar{r} \bar{u})^2 (\Delta \frac{1}{r}) / (\Delta r^2) \end{aligned}$$

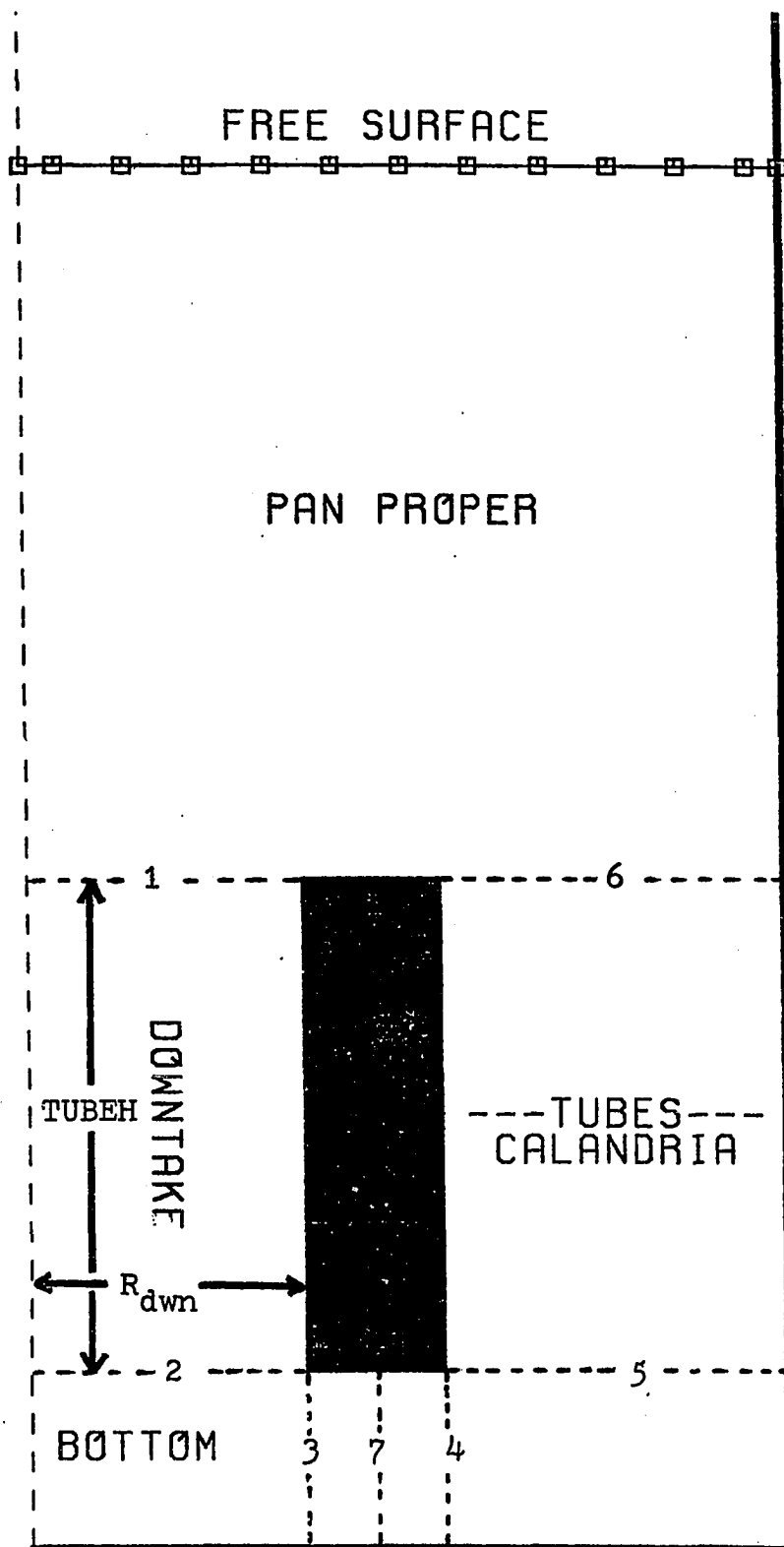


FIGURE 3.3.1 SECTIONALIZED VACUUM PAN

3.4 PERTINENT EQUATIONS

In order to give closure to the set of equations presented earlier and distinguish the model for application to an Industrial Vacuum Pan Sugar Crystallizer, certain pertinent equations are needed. These equations include a mathematical definition of the equations of state, thermodynamic state, kinetics, equilibrium conditions, and heat transfer relationships. These relationships will be supplied in the following discussions.

a. Equations Of State Three-Phase System

The proper average density for the homogeneous model has been given in Equation 3.2.4. The average density is the volume average of the component densities. Equation 3.2.4, however, which is implicit in the average density, for computational reasons is not in a good form. Assuming there is no volume change due to mixing, the mixture volume is the sum of the component volumes. Equation 3.4.1 states the alternate form of Equation 3.2.4, which is in a better computational form. Multiplying Equation 3.4.1 through by the mixture density defines the volume fraction of each component as shown in Equation 3.4.2.

$$\frac{1}{\rho} = \sum \frac{x_i}{\rho_i} \quad 3.4.1$$

$$\gamma_i = \frac{x_i \rho}{\rho_i} \quad 3.4.2$$

During the operation of the Pan there is the possibility of the three phases. Those phases are an aqueous solution of sugar, sugar crystals, and water vapor. It is assumed that the water vapor density can be adequately explained for pressure and temperature changes relative to a reference density as suggested by the Ideal Gas Law. But since pressure in the Pan may more than double from top to bottom of the Pan, while temperature effects are not so drastic, the equation of state for the vapor will be presented by Equation 3.4.3. This equation corrects only for pressure changes on the reference density. For computation convenience the reference density is evaluated at temperature and pressure of the vapor space.

$$\rho V = \rho_{VR} \left(\frac{P}{P_R} \right) \quad 3.4.3$$

The sugar crystal density given in Honig (1963) as 1.588 g/ml.

An extensive equation of state for sugar solutions was not found in the literature. Because of the limited range of temperature and sucrose concentration of

interest, a Taylor series expansion of the effects of these variables will be adequate. The liquid is assumed to be incompressible. Equation 3.4.4 is the Taylor series expansion truncated after the first term. Equation 3.4.5, the dimensionless form of Equation 3.4.4, is found by dividing the equation through by the reference density. The two parameters in the equations are then identified as the coefficient of thermal expansion and the coefficient of concentration.

$$\rho_L = \rho_{LR} + \frac{\partial \rho_L}{\partial T} \Delta T + \frac{\partial \rho_L}{\partial S} \Delta S \quad 3.4.4$$

$$\rho_L = 1 + \beta \Delta T + \beta_c \Delta S \quad 3.4.5$$

Both of these coefficients are functions of the temperature and concentration, but, only change a percent or so for typical changes about the base point that occur in the Pan during its operation. The reference temperature and concentration are variables that can be changed to reflect the conditions in the Pan for a particular simulation. Table 3.4.1 and 3.4.2 show functionality of the parameters with temperature and concentration. However, the effect of temperature on the coefficient of concentration was omitted, because its effect was insignificant compared to the effect of concentration. As can be seen in the Tables, the

insensitivity of the parameters to changes in temperature and concentration of sucrose is apparent. Therefore, the truncated Taylor series should serve well to describe the density of the sucrose solution over the limited conditions of the evaporator.

For computational convenience also, the water and sucrose density plus the crystal density will be combined into one density and considered as one phase. The reasons for this will be made clear when the enthalpy of the three-phase system is discussed. Equation 3.4.6 reflects this computational convenience.

$$\frac{1}{\rho_{LS}} = \frac{1-XCP}{\rho_L} + \frac{XCP}{\rho_C} \quad 3.4.6$$

TABLE 3.4.1: Coefficient of Concentration

BRIX	βC (1/BRIX)
.7	0.4611
.75	0.4635
.80	0.4655

TABLE 3.4.2: Coefficient of Thermal Expansion

$\beta \times 10^4 (1/(F))$			
TEMPERATURE (F)			
BRIX	131	149	185
.60	2.50	2.40	2.90
.75	2.46	2.62	2.86

b. Enthalpy Of Three-Phase System

The proper enthalpy per unit mass for the homogeneous model was presented earlier in Equation 3.2.6. However, like the density it is not in a good computational form. By direct substitution of the definition of the volume fraction, Equation 3.4.2, Equation 3.4.7 is derived that has computational advantages.

$$H = \sum x_i H_i \quad 3.4.7$$

Although the system is three-phase, the enthalpy will be treated as the density was earlier. That is, the liquid and the crystals will be treated as one-phase but distinguished from the vapor phase as shown in Equation 3.4.8.

$$H = (1-XV) HL + XV HV \quad 3.4.8$$

The enthalpy of the liquid and crystal mixture will be calculated via the heat capacity and temperature of the mixture. The heat capacity as represented by Equation 3.4.9 is taken from Hugot (1972). Equation 3.4.10 is the mathematical expression for the enthalpy of the liquid crystal mixture. The enthalpy of the vapor is by Equation 3.4.11.

$$CP = 1.0 - XSP(0.6 + XCP/0.6) \quad 3.4.9$$

$$HL = CP(T - TR) \quad 3.4.10$$

$$HV = 1075.8 + 0.43465(T - 32) + \quad 3.4.11$$

$$1.4877 \times 10^{-5}(T-32)^2 - 7.048 \times 10^{-7}(T-32)^3 + SH$$

$$* SH = 3.756599 P \text{ BPE} + 0.44973521 \text{ BPE}$$

$$- 6.9478 \times 10^{-5} \text{ BPE} P^2 - 6.959 \times 10^{-6} P \text{ BPE}^2$$

Notice the correlation for the vapor enthalpy has a correction for the amount of superheat. This is needed, assuming that the vapor will be in thermal equilibrium with the sugar solution which is boiling at an elevated temperature due to the presence of the sucrose and impurities.

The equilibrium relationship to distinguish when the vapor phase may be present is the boiling point of the sucrose, impurity, and water solution. Since the enthalpy of the vapor is greater than the liquid and crystal mixture, the vapor enthalpy will always contribute to an excess enthalpy. Therefore, once the boiling point is reached, the temperature of the mixture is given by Equation 3.4.12 and the excess enthalpy is given to the vapor. The calculation of the mass fraction is, thus, explicit via Equation 3.4.13.

* NOTE: Pressure expressed in psia.

$$T = f(P) + BPE \quad 3.4.12$$

$$XV = \frac{(H - HL)}{(HV - HL)} \quad 3.4.13$$

The equilibrium boiling point of the sucrose, impurity, and water solution is given by the saturation temperature of the water at the same pressure, plus, a boiling point elevation due to the presence of the sucrose and impurities in the water. These relationships are given below in Equations 3.4.14 thru 3.4.16. The boiling point elevation of the solution is the superheat needed to calculate the vapor enthalpy in Equation 3.4.11.

$$\text{boiling point elevation:} \quad 3.4.14$$

$$BPE = 2.2 \frac{(XIP+XSP)}{XWP} + 1.1 \frac{XIP}{(XSP+XIP)}$$

$$\text{temperature of water:} \quad 3.4.15$$

$$* TW = \frac{3061.596}{(6.306699 - \log P)} - 383.7148$$

$$\text{boiling point of solution:} \quad 3.4.16$$

$$T = TW + BPE$$

* note: Pressure expressed in psia.

As mentioned earlier, no specie calculation will be done for the sucrose, crystal, or impurities. Strictly speaking, the concentration of these components will change locally as the local vaporization occurs. Therefore, this formulation is restricted to small mass

fractions of vapor, vaporizing at any one time. However, this should not be viewed as a restriction, given the homogeneous flow assumption is valid, because small mass fractions of vapor cause large changes in the mixture density. In fact, a mass fraction of only 10^{-4} can cut the mixture density in half and at the same time only have a minute effect on the calculation of the heat capacity of the crystal and liquid mixture or the boiling point. Because of the large effect of the presence of vapor on the mixture density, it is hard to imagine mass fraction much larger than 10^{-4} in a natural convecting environment.

c. Viscosity Liquid and Solid Mixture

The viscosity of the mixture of sugar solution and the sugar crystals is the main reason for the poor recirculation through the tubes and low heat transfer coefficients observed in the Vacuum Pan. In addition, the viscosity is an integral part of some of the approaches taken in literature for the analysis of the kinetics of crystal growth. Therefore, the importance of a good equation for the dependence of the viscosity on temperature, concentration of the sugar solution, and the presence of crystals is obvious. A correlation for the liquid viscosity was taken from work by Evans (1970), but was found not to reproduce the viscosity data in Honig (1963) very well. Since the range of concentration and temperature encountered in the Pan are small, it was decided to take the form of the equation presented in the article by Evans and use it to correlate the data in Honig. An optimization program was used to select the parameters that minimize the sum of the squares differences between the experimental data and the value predicted by the equation. The statistics concerning that optimization are presented in Table 3.4.3. The correlation coefficient, as defined in Miller (1965), of the experimental data against the proposed equation is 0.97. Statistical weights were used to aid in

finding a better correlation. These weights were assumed to be proportional to the magnitude of the viscosity to reflect the percentage error in the viscometer measurement. The data points used to develop the correlation are given in Table 3.4.4. This is only a fraction of the data presented in Honig, the data that were more representative of the conditions in the Pan were used to find the parameters. The reason for using the restricted sample is because it was felt that the functionality of the viscosity is really more complicated, and using all the data available for the optimization would not allow the equation to predict the viscosity accurately in the range of interest. It also should be mentioned that data in Honig does not include supersaturated conditions, therefore, the equation will be used to extrapolate the data. Equation 3.4.17 is the equation for liquid viscosity.

$$\mu L = \text{EXP}(10195.02/(T+460.)) + 18.86(XSP+XIP)/(1-XCP) - 26.523)6.72 \times 10^{-4} \quad 3.4.17$$

The presence of solid crystals has an effect on the apparent viscosity of the mixture. This effect will be corrected by a multiplying factor. This multiplying factor is given by Equation 3.4.18, taken from work by Awang (1976).

$$\frac{\mu}{\mu_L} = \text{EXP}(8.959873 \text{ VCL } L^{0.15}) \quad 3.4.18$$

Equation 3.4.17 will be used to calculate the liquid viscosity when needed in the program. Equation 3.4.18 will correct the liquid viscosity for the presences of crystals for pressure drop calculations or when kinematic viscosity is needed.

TABLE 3.4.3: Viscosity Correlation Statistics

TOTAL SUM SQ.	RESIDUAL SUM SQ.	CORREL. COEFF.
9379	26	0.97
NO. PARAMETERS=3		NO. POINTS=18

TABLE 3.4.4: Viscosity Data

VISCOSITY(CP)			
TEMPERATURE(F)			
BRIX	140	158	176
.70	39.1	25.1	16.9
.71	46.7	29.5	19.6
.72	56.3	35.0	22.9
.73	68.6	41.8	27.0
.74	84.4	50.5	32.1
.75	105	61.6	38.4

d. Solubility And Kinetics Of Sucrose In Water

There are several different sources of the kinetics of sucrose crystals. Smythe (1971) has obtained data for sucrose crystallization in pure solutions as well as solutions with various impurities and additives, as well as, reviewing the literature concerning research in sucrose growth kinetics. His data were taken under conditions that eliminate the effects of mass transfer of the sucrose to the crystal surface. He did this in order to study the kinetics of the surface integration step. However, in an operating Pan the rate of growth of a crystal is limited by mass transfer as well as the surface kinetics. This was shown to be true by Buchler (1980), who took experimental growth rate with crystals in an environment similar to that found in an operating Pan. Hartel (1979) has obtained experimental data for pure sucrose solutions from a continuous well stirred tank. His analysis of the data from his experiments were based on the concepts presented in Chapter 2. The correlation for the growth rate of sucrose crystals that will be used in the model was obtained from an article by Wright (1974). The model is correlated from industrial data and includes the effects of impurities and temperature. The equation includes the mass transfer step and the surface integration step because the total

difference in concentration or oversaturation is used. The mass average linear growth rate of an equivalent spherical crystal was used for the correlation to avoid the problem of the crystal shape. The reason for using Wright's model was its applicability to industrial Pans and its simplicity. The model is presented below in Equations 3.4.19 thru 3.4.22.

$$G = \frac{dL}{dt} = \begin{cases} k_G \text{ OS} & \text{OS} > 0 \\ 5k_G \text{ OS} & \text{OS} < 0 \end{cases} \quad 3.4.19$$

$$k_G = k_G^0 \text{EXP}\left(-\frac{\text{EACT}}{2.303 R_g} \left(\frac{1}{(T+460)} - \frac{1}{599.7}\right)\right) \quad 3.4.20$$

$$\begin{aligned} \text{EACT} = & 11.0 - 0.011111(T - 140) \\ & + 8.0 \text{ XIP/XWP} \end{aligned} \quad 3.4.21$$

$$k_G^0 = 2.43 \times 10^{-2} \text{EXP}(1.75 \text{ XIP/XWP}) \quad 3.4.22$$

$$R_g = 1.104 \times 10^{-3}$$

As suggested by the model above, crystals only grow when exposed to a supersaturated environment of sucrose. Supersaturation is a measure of the excess amount of the sucrose above that when the solution is saturated. Therefore, the saturation point of the sucrose in water is of vital importance in order to determine when, and by what rate a crystal will grow. The saturation condition for pure

sucrose and water system is given by Equation 3.4.23, as taken from Wright's model.

$$\text{SAT} = 63.8188 - 5.1082 \times 10^{-3} T + 7.836 \times 10^{-4} T^2 - 1.5492 \times 10^{-6} T^3 \quad 3.4.23$$

The calculation of supersaturation must be consistent with the model for the growth rate of the crystal. Since Wright's model for the growth rate is used as presented above, the supersaturation relationships from Wright's article will also be used. These relationships are presented below in Equation 3.4.24 and 3.4.25.

$$\text{SS} = \frac{(100 - \text{SAT})}{\text{SAT}} \left(\frac{\text{XSP}}{\text{XWP}} \right) \left(\frac{1}{1 - 0.88 \text{XIP}/\text{XWP}} \right) \quad 3.4.24$$

$$\text{OS} = \text{SS} - 1 \quad 3.4.25$$

e. Heat Transfer Coefficients

Studies of heat transfer in Vacuum Pans are much lacking in the literature. No research has been done to quantify the mechanism of heat transfer in the tubes of the Vacuum Pan. The reason for this is partly because there has been no real need for accurate correlations for basic design. Also, it is partly because of the complexity of the problem. The heat transfer coefficients presented in Honig (1963), Hugot (1972), and Meade (1963), are based on steam consumption and the temperature difference between the steam and the temperature of the saturated liquid at the pressure of the pan vapor space. The absence of correlations for heat transfer coefficients, based on the local conditions in the tubes, will not prevent the development of the model or its subsequent use. But, without such local heat transfer coefficients, the effect of the pan level, steam temperature, and other operating conditions on heat transfer in tubes cannot be simulated properly. Since the heat load is the forcing function causing the flow, it seems important that the mechanism of heat flow be understood. Therefore, the need for research in this area is apparent.

While heat transfer in Vacuum Pans has not been studied extensively, evaporators have. Correlations have been given in a number of sources, Honig (1963),

Zagrodzki (1977), Saranin (1954), and Badger (1939).

Unfortunately, these correlations do not extend into the range of operation of the Vacuum Pan. However, studying these correlations may help in understanding the effects of the physical properties of the mixture and the effect of operating conditions on heat transfer in the Pan.

For the purposes of the development and demonstration of the numerical model, typical values of the evaporation coefficients will be used to calculate the heat input to the Pan. The evaporation coefficient is defined as the rate of steam consumed per unit heat transfer area. Typical values of the evaporation coefficient for various purity massecuites, as taken from Hugot (1963), are summarized in Table 3.4.5.

TABLE 3.4.5: Evaporation Coefficient

ECOEFF (LBS/FT ² /HR)		
	MAX	MIN
A MASSECUITE	14.6	6.6
B MASSECUITE	9.4	2.2
C MASSECUITE	7.5	0.34

3.5 NON-DIMENSIONALIZATION AND BOUNDARY CONDITIONS

In general, when solving a set of differential equations with numerical methods, the numerical solution is aided by putting the equations in dimensionless form. Picking the proper dimensional groups aids in reducing truncation errors because the dimensionless variable is scaled by the dimensional group. In some cases numerical solution speed is increased by picking dimensional groups involved in functional evaluations in the numerical code. In all cases, working with dimensionless equations adds a degree of flexibility in using the numerical coding of the equations, because the code no longer depends on units and at the same time, errors associated with dimensional inconsistency are reduced.

For the most part, the dimensional groups used here are adopted from Waldrop (1972) and Pitts (1976). However, dimensional groups were needed resulting from the variables associated with the energy equations for the Pan Proper and the Calandria. The non-dimensional forms of the variables are presented below in Table 3.5.1, as indicated by the prime mark. Applying these dimensional groups to the previously defined model equations, a non-dimensional set of equations are formulated. The non-dimensional equations appear the same as the dimensional equations and therefore, will not be repeated again.

Equation 3.1.1 thru 3.1.5 are not non-dimensionalized. These equations interact with the other equations only through the mass fractions which are already non-dimensional.

To complete the development of the model, the boundary conditions are presented in Table 3.5.2, Equations 3.5.15 thru 3.5.58. The table includes spatial as well as temporal boundary conditions. These initial conditions in combination with the spatial boundary conditions are necessary conditions that must be specified if a solution is to be attempted. The spatial boundary conditions, in some cases, are based on physical reasoning and in other cases, to insure the conservation of mass, energy, and momentum between sections. A discussion of the spatial conditions are given below.

For the Pan Proper, at the surface, the conditions of no normal or tangential viscous stresses are imposed. The exchange of mass, momentum, and energy between all modeled sections including the vapor space, which was not modeled, is done only through the convective terms. The only exception to this rule is at the top of the Calandria, at this point, thermal conduction is allowed because substantial temperature gradients can exist. At the center for the Pan Proper, the radial velocity is zero and symmetry is insured by making the enthalpy, vertical velocity, and pressure derivatives in the radial

TABLE 3.5.1: Non-Dimensional Variables

$$T' = T \beta / \text{CPW} \quad 3.5.1$$

$$H' = H \beta / \text{CPW} \quad 3.5.2$$

$$\mu' = \mu / R / h_{\max} / \sqrt{h_{\max} g} \quad 3.5.3$$

$$\kappa' = \kappa / \text{CPW} / R / h_{\max} / \sqrt{h_{\max} g} \quad 3.5.4$$

$$v' = v / h_{\max} / \sqrt{h_{\max} g} \quad 3.5.5$$

$$\alpha' = \alpha / h_{\max} / \sqrt{h_{\max} g} \quad 3.5.6$$

$$r' = r / h_{\max} \quad 3.5.7$$

$$z' = z / h_{\max} \quad 3.5.8$$

$$U' = U / \sqrt{h_{\max} g} \quad 3.5.9$$

$$t' = t / \sqrt{h_{\max} / g} \quad 3.5.10$$

$$\rho' = \rho / \rho_R \quad 3.5.11$$

$$P' = P / h_{\max} / \rho_R / h \quad 3.5.12$$

$$CP' = CP/CPW \quad 3.5.13$$

$$h' = h/h_{max} \quad 3.5.14$$

$$UU' = UU/CPW/\rho R/ \quad h_{max}/g \quad 3.5.15$$

direction equal to zero. At the walls, slip conditions are applied because for the most part, the numerical solutions will be done with large grid spacing, thus, the wall should have little influence on the point on the order of a foot away. The same reasoning was applied for the area across the bottom of the Pan Proper. In addition, the temperature gradient normal to the wall is taken as zero to indicate no conduction of heat through the wall. The velocities at the wall are zero. The pressure gradient in the radial direction normal to the wall is taken as zero. Refer to Figure 3.3.1 to clarify the notation concerning the boundary conditions for the Downtake and Calandria.

The most interesting of the boundary conditions are Equations 3.5.18 thru 3.5.20 involving the release of mass, momentum, and energy at the surface. These equations employ a functional relationship between the relative velocity of the vapor to the liquid and the volume fraction vapor at the surface. The function is taken from the literature and is typically used in the drift flux models as described in Wallis (1969) and Ishii (1975). The form of the function used in this research, describing the velocity of vapor relative to the surface, is shown in Equation 3.5.51

$$w_v - w_s = W_v^* (1-\gamma)^n \quad 3.5.51$$

The parameters in Equation 3.5.51, W_v^* and n , are a function of the evaporation rate, the physical properties of the fluid and the vapor bubble size. Experimental work is needed to establish the magnitude of these parameters for the conditions in the Pan. Therefore, for computational convenience, n is assumed to be zero and W_v^* is given sufficient magnitude such that the maximum evaporation rate can exceed the heat input.

TABLE 3.5.2: BOUNDARY CONDITIONS

SURFACE

$$\frac{\partial T}{\partial z} = 0 \quad \frac{\partial w}{\partial z} = 0 \quad \frac{\partial u}{\partial z} = 0 \quad 3.5.15-3.5.17$$

$$\rho V (w_v - w_s) = \rho V f(\gamma) \quad 3.5.18$$

$$\rho V (w_v - w_s) HV = \rho V HV f(\gamma) \quad 3.5.19$$

$$\rho V w_v = (f(\gamma) + w_s) \rho V \quad 3.5.20$$

$$P = P_s \quad 3.5.21$$

WALLS

$$\frac{\partial H}{\partial r} = 0 \quad \frac{\partial P}{\partial r} = 0 \quad \frac{\partial T}{\partial r} = 0 \quad 3.5.22-3.5.24$$

$$\frac{\partial u}{\partial r} = 0 \quad \frac{\partial w}{\partial r} = 0 \quad u = 0 \quad 3.5.25-3.5.27$$

CENTER LINE

$$u = 0 \quad \frac{\partial P}{\partial r} = 0 \quad \frac{\partial H}{\partial r} = 0 \quad 3.5.28-3.5.30$$

$$\frac{\partial T}{\partial r} = 0 \quad \frac{\partial u}{\partial r} = 0 \quad \frac{\partial w}{\partial r} = 0 \quad 3.5.31-3.5.33$$

DOWNTAKE - PAN PROPER

$$\frac{\partial T}{\partial z} = 0 \quad \frac{\partial w}{\partial z} = 0 \quad \frac{\partial u}{\partial z} = 0 \quad 3.5.34-3.5.36$$

$$u = 0 \quad w = w_1 \quad \rho = \rho_1 \quad 3.5.37-3.5.39$$

$$H_1 = \int H dA_1 \quad 3.5.40$$

CALANDRIA - BOTTOM

$$\frac{\partial T}{\partial z} = 0 \quad \frac{\partial w}{\partial z} = 0 \quad \rho = \rho_5 \quad 3.5.41-3.5.43$$

$$\rho w A = \rho_5 w_5 A_5 \quad H = H_5 \quad 3.5.44-3.5.45$$

CALANDRIA - PAN PROPER

$$\frac{\partial w}{\partial z} = 0 \quad \frac{\partial u}{\partial z} = 0 \quad u = 0 \quad 3.5.46-3.5.48$$

$$\rho w A = \rho_6 w_6 A_6 \quad H = H_6 \quad T = T_6 \quad 3.5.49-3.5.51$$

INITIAL CONDITIONS

$$I = I_0 \quad S = S_0 \quad C = C_0 \quad W = W_0 \quad 3.5.52-3.5.55$$

$$H = H_0 \quad U = U_0 \quad P = P_0 \quad 3.5.56-3.5.58$$

3.6 DISCUSSION OF THE ASSUMPTIONS

As presented earlier, many assumptions were made in the derivation of the mathematical model. These assumptions must be kept in mind when applying the model. The fluid dynamics of an operating Vacuum Pan are very complicated, the liquid is very viscous and contains solid particles and may be boiling vigorously. The hope of developing a numerical model that captures the minute details of the fluid dynamics of the Crystallizer, and be practical in terms of use of limited computer facilities is unrealistic. This problem prompted the assumptions used in the derivation of the model.

One of the fundamental assumptions made is the assumption of homogeneous flow. The homogeneous flow assumption represents the mixture of solids, liquid, and vapor as a quasi-fluid with physical properties that are mass averages of the species physical properties. This basically limits the calculation validity to a low volume fraction of vapor because when a large fraction of vapor exists, the vapor phase tends to separate. The effect of high volume fractions of crystals is not so critical because the high liquid viscosity restricts the tendency of the crystals to separate. Because the vapor phase tends to separate when the volume fraction of the vapor is large, the homogeneous model over estimates the mass average velocities

caused by buoyancy effects and the fluid drag caused by velocity gradients. This results because the vapor moves considerably faster than the liquid and solid phases but contributes greatly towards reducing mixture density. Further assumptions concerning the numerical flash calculation are valid only for low mass fractions of vapor (10^{-3}), because the solids and liquid phases are assumed to be one-phase in this calculation and neither the solid phase mass fraction nor the concentration of soluble sugar in solution are changed to find the real equilibrium position. However, the flash calculation is not a real limitation because the homogeneous assumption is much more limiting, besides, it is difficult for large vapor fractions to exist in the Pan Proper because vigorous mixing occurs when the vapor phase is present, and in most circumstances the heat input is too low to cause much flashing in the tubes.

The model also assumes that there is equilibrium between the phases and it occurs instantaneously. These assumptions are valid for all but very fast and highly accelerating flow and when the phases become separated. Although, Batterham (1975) indicates that there is evidence of measurable superheat in the Pan, its effect on the flow is small because the superheat is not large. Significant non-equilibrium between phases is also assumed to be small because the flow is slow and the heating rate

is low.

The model also neglects the heat loss to the environment by conduction through the walls of the Vacuum Pan, and the heat of crystallization. These effects are estimated to be about 5% of the total heat loads. However, these effects can be added easily enough if desired.

Another most important assumption of the model is the hydrostatic head assumption for the pressure profile. This assumption reduces the vertical momentum equation to only the density term and the pressure term. This assumption is common in the literature for modeling bays and estuaries as discussed by Pitts (1976). While it is true that these two terms are the dominant terms in the equation, the derivative of the vertical momentum equation with respect to the radial direction is the proper way to analyze the effect of these terms on the pressure profile. It becomes evident in this light that the other terms may be important depending on the flow, especially the convective terms. The application of the hydrostatic head assumption to fluid dynamics of the Vacuum Pan will have to be evaluated once the numerical model of the Pan has been developed.

CHAPTER 4

COMPUTATIONAL METHODS

In Chapter 3, a mathematical model of a Vacuum Pan Sugar Crystallizer was developed. The model is based on the fundamentals of the physics of fluid motion and the phenomena of two-phase flow. In this chapter, the discrete analogs of the governing equations will be derived. These discrete equations will form the base for the numerical solution of the governing equations. The development of the numerical methods as taken from the literature pertaining to this research will be overviewed to contrast the development here. These references will supply a wealth of information concerning numerical methods in computational fluid mechanics. Although the computer code will be attached in the appendix, the calculation sequence will be presented in enough detail to insure understanding.

The development of the numerical codes for multi-phase flow has been somewhat predicated upon the development of the codes for single-phase compressible and incompressible flow. This of course, results from the fact that, historically, the codes for single-phase flows were developed and tested first and their success dictates further application. Since typically, free surface flow multi-phase flow, and compressible flow calculations have

been done by directly solving the primitive equations, i.e., the equations of motion without transforming the variables, the discussion and references will be directed towards the solution of the primitive equations. The development of discrete analog equations and solution methods for the single-phase flow primitive equations are extensive in the literature. Several good references for these finite differencing and solution methods are Roache (1976), MacCormack (1978), Warming (1978), and Patankar (1980).

A particularly complex problem addressed in the context of incompressible fluid flow is the moving boundary or free surface problem. Such problems are exemplified by the presence of an interface. For the purposes here, the free surface problem will be typified by a cavity of a fluid, such as liquid in a partially filled tank or a large body of water, where in both cases the surface changes position in reaction to the forces which act upon it. The Los Alamos group developed the Marker Cell Method (MAC) to solve this class of problems. It is by far the most popular method to solve incompressible flow free surface problems. The method and its development are discussed in Roache (1976). The MAC method is quite general and capable of solving a wide variety of problems such as, waves crashing on the beach, dams breaking, and solid objects rising and falling in

liquids. Although a fixed grid system is used, the interface is simulated by adding or subtracting surface cells as the fluid flow suggests.

The MAC method uses the Poisson Equation to solve for the pressures and employs marker particles, which flow with fluid but do not affect the fluid dynamics, to locate the surface cells. The difficulty with the MAC method and its derivatives is that the solution is very complex and time consuming. This results because the solution of the Poisson Equation is an iterative one, a lot of bookkeeping must be done to keep track of the marker particles, and the boundary condition for all the different possible configurations of the surface cells are very complex and time consuming. In addition, a very small grid spacing is needed to insure proper conservation of mass.

Numerical calculations for compressible flow are based on the same finite differencing methods as used for incompressible flow. However, the pressure calculation is somewhat simplified because the pressure of the gas is a strong function of the density and internal energy. Many times an ideal gas approximation will suffice to supply the functional relationships between the pressure, density, and internal energy. This strong functional relationship ties the continuity equation strongly to the momentum and energy balances. This strong

functionality aids iterative techniques that manipulate the pressure profile until the continuity equation is satisfied. This is exactly what the MAC method does for incompressible flow calculations via the Poisson Equation but appears less apparent.

General numerical methods that handle both compressible and incompressible flow calculations have been developed by combining the methods of the pressure calculations used in both types of flows. These methods manipulate the pressure profile until the continuity is satisfied. Two such methods are discussed by Pracht (1975) and Pakantar (1980).

The development of the numerical methods for multi-phase flow have capitalized on the development of these hybrid codes for incompressible and compressible flow. In fact, for the case of homogeneous flow such as considered here, very little modification would be needed to accommodate homogeneous flow calculations. Lyczkowski (1978) reviews the state of the art in numerical calculation in a multi-phase medium. In his review, he discusses the numerical algorithms of some of the promising numerical codes. Among those codes reviewed, mixed implicit-explicit algorithms were typical. In all cases, the pressure was treated implicitly by the same iterative methods discussed earlier to enforce the continuity equation. Typical explicit phases of the

algorithm were the viscous terms and the energy equation. The convective momentum terms were at times treated implicitly, depending on the algorithm. For the most part, convergence of the pressure profile requires the presence of the compressible phase. Lyczkowski's discussion is directed towards codes for the two-fluid model, as developed in Ishii (1975), which is the most complicated of the multi-phase models. Nonetheless, the characteristics of the codes discussed should apply for all the modeling regimes.

The numerical solution method used here to solve the equations of motion, describing the Vacuum Pan, is an extension of the work of Waldrop (1972) and Pitts (1976). This method was developed to model incompressible free surface flows in bays and estuaries. The solution method is explicit and avoids the difficulty of the implicit pressure solution via the Poisson Equation and the use of marker particles to locate the free surface. The vertical momentum equation is used directly to calculate the pressure profile explicitly, and the continuity relationship is used to locate the free surface. The basic calculation method originated from the work of Waldrop (1972). However, Waldrop's method of locating the free surface was not consistent with the overall mass balance, but Pitts (1976) extending Waldrop's work corrected the problem by applying the continuity

equation to locate the surface position.

The method uses a fixed inner grid system with a floating top cell. Because of its method of locating the free surface, the method can be made to conserve momentum, mass, and energy very easily. And as long as the range of surface levels are small, which is the case for some tidal variations for bays and estuaries, the technique performs very well. But when large volume changes occur, either the accuracy or the problem is extremely strained, because much of the volume is in the surface cells, or the solution cannot continue because the volume in one or more of the surface cells is negative. Although this sounds like a serious disadvantage over the MAC method, the advantages come because a very coarse grid spacing may be used and still locate the interface accurately while the MAC method requires a very small grid spacing. Other redeeming qualities of Waldrop's method are that it is much simpler and many times more efficient with computer time. Although it is true that incompressible free surface flow does not have complexities that two-phase free surface flow does, but, hopefully the solution method still applies.

But because Waldrop's method is explicit, one might expect to encounter problems with the multi-phase homogeneous flow calculations for fast transients. If such problems occur, consideration will have to be given

to doing some calculations implicitly or at least multi-step. Because of the structure of Waldrop's method, implicit or multi-step calculations may not eliminate the problems associated with the flashing transients of multi-phase flow problem.

However, for the prupose of this research it will be assumed that the explicit calculation will serve as an adequate solution method. The applicability of the Waldrop method will be discussed later as part of the purpose of this research.

While the method of the solution of the free surface problem developed by Waldrop (1972) and extended by Pitts (1976), will be used in this research, many modifications will have to be made to incorporate the two-phase nature of the problem. In addition, many of the finite difference methods as used by both Waldrop and Pitts were found to be completely inadequate. The most noticeable problem with Waldrop's and Pitt's codes is the improper differencing of the surface cells. Because the volume and boundary areas of the surface cells differ from the inner cells, these cells must be given special consideration. However, Pitts and Waldrop did not distinguish the surface cells from the inner cells, which leads to inaccuracies and instabilities in the numerical calculation. This problem will be eliminated with the discrete analogs derived in this

section. The derivation of the discrete analog will include the cell volume and boundary areas, thus, when the areas and volume change during the course of the simulation, the grid system can automatically compensate. Also, a subtle problem with the differencing methods of Pitt's and Waldrop's codes occurs when the convective terms are differenced. The subtle point is that traditional differencing methods cannot be blindly applied without considering the whole system of difference equations. Even though Pitt's and Waldrop's differencing methods for the convective terms are conservative, they are not consistent with the differencing of the other equations. In particular, the convection of momentum is not consistent with continuity equation. This point will be demonstrated later with the Well Stirred Tank (WSTRT) analogy and with an example that uses the discrete analog equations. As the result of this research, a philosophy was developed that gives clues that aid in the development of numerical techniques in general and especially when fluid convection is involved. Further development of the numerical code includes an implicit free surface calculation and a dynamic grid.

4.1 DEVELOPMENT OF THE PHILOSOPHY OF THE FINITE DIFFERENCE EQUATIONS

The mathematical development of the modeling equations presented in Chapter 3 were based on the continuum principles, but, because Finite Difference Equations are discrete, there will always be a degree of approximation in a numerical solution describing the spatial and time dependence of the solution set. This degree of approximation can be formally analyzed by a truncated Taylor series, as discussed in Roache (1976), to be approximately first order but approaching second order. However, a shadow of doubt can be thrown on this analysis, based on the experience with the development of this work and as discussed by Patankar (1980), as the sole basis to judge the difference equations. Therefore, the formal truncation error may be used as an indication of the accuracy but not the absolute rule to judge differencing techniques. Instead, there are many rules by which to judge a set of difference equations modeling a physical system. Since the continuum equations also reflect the conservation and transportation of mass, momentum, and energy, the numerical equations should, as much as possible, reflect the same properties. The significance of these properties as applied to the discrete equations are discussed below.

The conservative property as applied to Finite Difference Equations of conservation of mass, momentum, and energy, simply means the Finite Difference Equation, when summed, satisfies the integral of that conservative equation over some volume. Therefore, if a Finite Difference form is conservative over a cell volume, fluxes of the conserved quantity enter at the cell boundary. And, if the Finite Difference form is conservative over all the Finite Difference cells, the terms left after all the cells are summed are the overall material, energy, and momentum balances.

The importance of this property is obvious if accurate results are to be obtained. If the Finite Difference form is conservative, then there are no source terms (or generation) that are non-physical and only associated with the numerical form of the equations. This is not to say that numerically stable non-conservative forms are not acceptable but stable conservative forms would appear to be more desirable. Numerical stability and conservative property are related in that the conservative form places bounds on the total change of conserved species over the total volume in time.

The transportive property means that the convection terms transport disturbances in the direction of flow. The transportive property has physical significance like

the conservative property and the Finite Difference form should have this property to simulate the physical problem more realistically. But, for the Finite Difference form to convey disturbances in the direction of flow, there must be a logical check in the code to determine the direction of flow.

Based on the above discussion, physical reasoning must go into the design of a good code. The conservative and transportive properties may not be the most important for a particular problem and may be sacrificed for other properties based on physical reasoning. For example, conservative and transportive properties of Finite Difference may not be consistent with the accuracy of a spatial derivative of a conserved quantities at a certain point, and the conservative and transportive properties may not be as important for that calculation.

However, for this problem, the conservative and transportive properties are considered to be most important, and great care was taken to insure that these properties are exemplified in the code. The reasoning for this is that accurate evaporation rates of water and liquid level in the Pan are needed, therefore, the conservation of energy and mass is paramount. Furthermore, if the conservative property is not a characteristic of mass balance, the pan level cannot be predicted accurately, and since the boiling phenomena is highly sensitive to

pressure changes, the problem is literally unstable for non-conservative Finite Difference Continuity Equation forms. The significance of the transportive property may not be apparent, but, for most industrially important problems, convection is the most important mechanism to transport mass, momentum, and energy. Therefore, a non-transportive form may diffuse the natural convecting flow regime and destroy, for example, the vertical rise of hot liquid to the surface to be boiled off, thus, the physical nature of the problem would be destroyed.

Because of the importance of the conservative and transportive properties in the discrete equations, and in order to capitalize on a familiar concept, the development of the discrete analogs for the distributed conservative equations will be aided by the WSTRT analogy. This analogy gives a visualization of the proper forms of discrete equations, so they may be constructed so as to be conservative and transportive. Also, some of the mystique of the distributed equations is eliminated through this analogy.

Figure 4.1.1 is an idealized situation involving a WSTRT. The conservative equations can be written without much thought. To aid in the extension of this concept to multi-dimensions, Figure 4.1.2 is an illustration of a grid representation of the WSTRT system. In Figure 4.1.3, a two-dimensional Finite Difference grid, the blacken

dots indicate the center of the cell which is indexed in order to identify the cell, and the crossmarks represent the areas where inputs or outputs in mass, energy, and momentum occur. Note the similarities between systems. The means to solve the WSTRT system are well known, therefore, solving the Finite Difference system should be analogous. The main problem in coding this WSTRT system is to determine if the mass flux of conservative quantity is an input or an output with regard to the cell and surrounding cells. This is simply taken care of with an algorithm for differencing the convective derivatives of conserved quantity. To complete the Finite Differencing of the conservative equations, the pressure and diffusion terms should also be differenced in a conservative fashion. If the viscous and compression forces are thought of as acting on the surface of the cell, a proper conservative scheme can be derived.

To place the analogy in a more mathematical plane, that will aid in the development of the Finite Difference Equations, especially when the dynamic grid is involved, a general property equation will be developed. This can then be used to describe the Finite Difference Equations for the dynamic grid. This general property equation is similar to the equation presented in Brodkey (1967), except the control volume will not be taken as moving

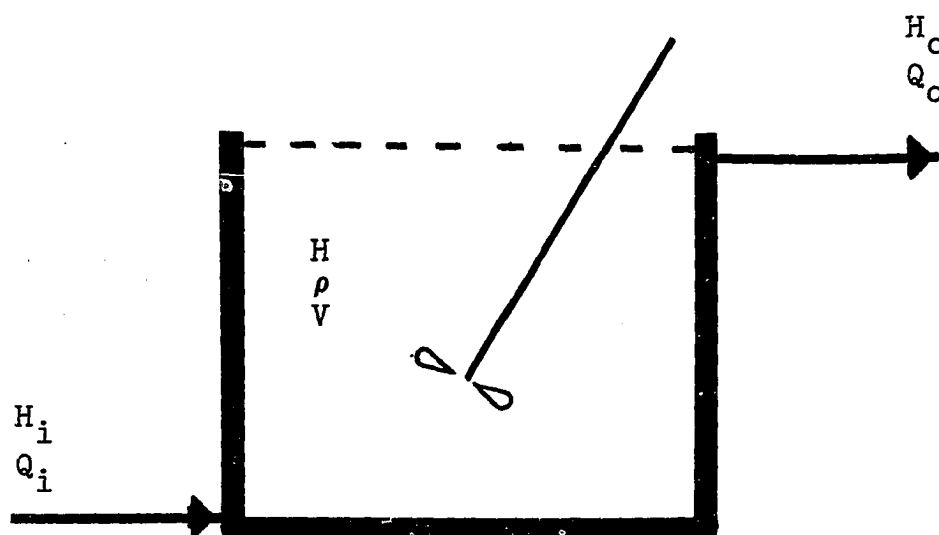


FIGURE 4.1.1 WELL STIRRED TANK

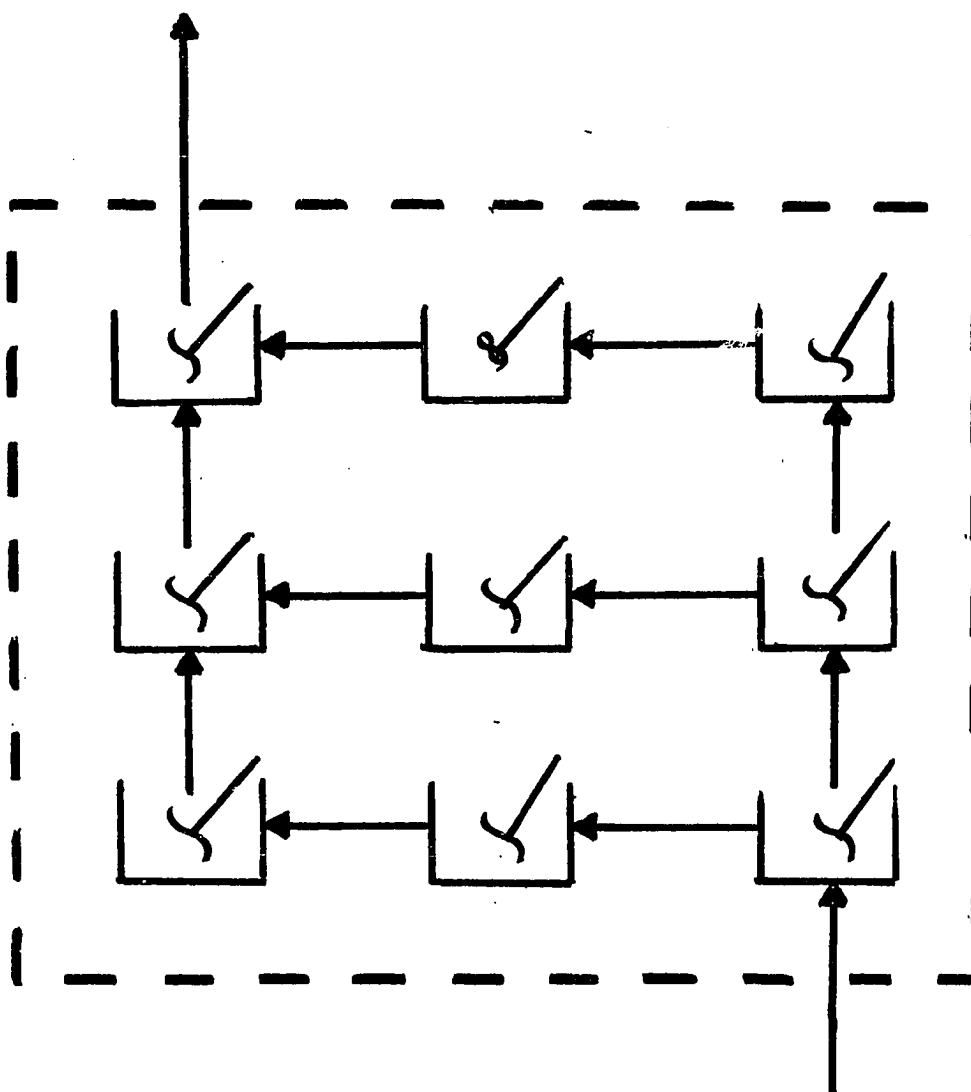


FIGURE 4.1.2 GRID REPRESENTATION OF WELL
STIRRED TANK

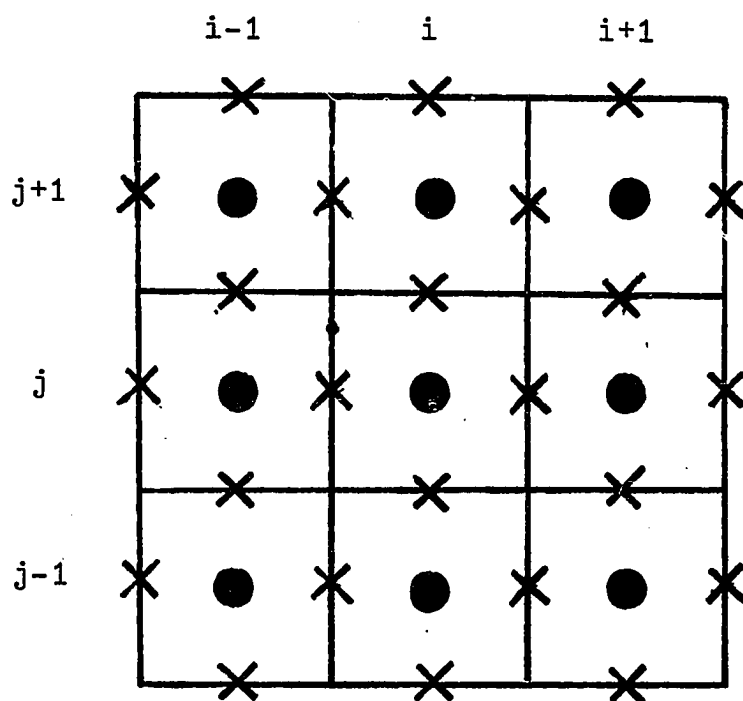


FIGURE 4.1.3 TYPICAL TWO-DIMENSIONAL
FINITE DIFFERENCE GRID

with the fluid, which implies that the time derivative will not be a total derivative. However, the distinction between the total derivative and the partial derivative of the conservative species with respect to time for this equation is dubious. This is because the flux terms will contain the convection of the conserved species relative to the surface of the volume in consideration. Therefore, the meaning of the derivative will change with the magnitude of the velocity of the surface boundaries, two special cases, being the total or substantial derivative and the partial derivative. Equation 4.1.1 is the general property equation for the whole volume.

$$\frac{d}{dt} \int \rho \phi \, dV = - \oint \phi_F \cdot d\bar{A} + \int \phi_g \, dV$$

$$\phi_F = \rho U_{RB} \phi + \bar{P}$$
4.1.1

The symbol ϕ is the general property per unit mass. The symbol ϕ_F is the sum of convection of the conserved species which crosses the cell boundary, plus, the terms which can be thought of as acting on the boundary or diffusing through the boundary. This function contains the viscous and compressive terms if ϕ is the specific momentum, and thermal conduction terms if ϕ is the specific enthalpy. The symbol ϕ_g is the generation of the general

property per unit volume.

Again, the analogy of the WSTRT is evident because the volume integrals can be thought of as the sum of the differential sized WSTRT cells. Remembering that if the sum of these small cells add to the total conservative general property equation for the total volume, the fluxes across each cell must cancel. Therefore, the discrete analogy of the fluxes should be constructed so that this is possible in the Finite Difference Equations. The volume terms, which are the accumulation of general property and its generation, which simply add as the integral suggests.

In order to derive the discrete Finite Difference Equations for each finite cell from the general property equation, the mean value theorem of calculus is used to arrive at the proper volume averages for the volume terms. The flux terms will be evaluated at the boundaries. Equation 4.1.2 is the discrete form of the general property equation as it applies to a cell in a Finite Difference grid. To avoid the problems associated with making a mathematically general statement, the discrete equation refers to the Finite Difference grid for the problem at hand, as shown in Figure 4.1.3. Furthermore, this discussion will be restricted to the two-dimensional case. Therefore, the discrete equation will refer directly to the Pan Proper and Free Surface. The

;

discrete models for the other sections can be arrived at through simple reasonings, based on the discussions here.

$$\begin{aligned}
 \frac{d}{dt}(\rho \phi V) = & - ((\rho u_{RB} \phi A)_{i+\frac{1}{2}} - (\rho u_{RB} \phi A)_{i-\frac{1}{2}})_r \\
 & - ((\rho w_{RB} \phi A)_{j+\frac{1}{2}} - (\rho w_{RB} \phi A)_{j-\frac{1}{2}})_z + \phi_g V \\
 & - ((\bar{P} A)_{i+\frac{1}{2}} - (\bar{P} A)_{i-\frac{1}{2}})_r - ((\bar{P} A)_{j+\frac{1}{2}} - (\bar{P} A)_{j-\frac{1}{2}})_z
 \end{aligned} \tag{4.1.2}$$

At this point, all the terms except the time derivative and the convections will be dropped, since the discussions to follow will not concern these terms. The discussions of these terms will be picked up later. Equation 4.1.3 is the resulting equation.

$$\frac{d(\rho \phi V)}{dt} = -\Delta_r(\rho u_{RB} \phi A) - \Delta_z(\rho w_{RB} \phi A) \tag{4.1.3}$$

As mentioned earlier, through general property equations, it is hoped that a way to incorporate the dynamic grid and construct the algorithm for the convective terms would be derived. Equation 4.1.3 contains a volume term, as well as boundary areas, which will be dynamic if the dynamic grid system is used. The convection terms are exactly as visualized by the WSTRT analogy, therefore, with the physical interpretation given by the

WSTRT analogy the proper algorithm can be constructed. Because of the way the numerical calculation proceeds, the time derivative will have to be split into its components. Equation 4.1.4 shows the result of the differentiation.

$$\rho V \frac{d\phi}{dt} + \phi \frac{d\rho V}{dt} = -\Delta_r(\rho u_{RB}\phi A) - \Delta_z(\rho w_{RB}\phi A) \quad 4.1.4$$

The rate of change of mass in the cell is given also by the overall mass balance for the cell. Equation 4.1.5 is the discrete form of the mass balance derived by taking ϕ as one in Equation 4.1.3.

$$\frac{d\rho V}{dt} = -\Delta_r(\rho u_{RB}A) - \Delta_z(\rho w_{RB}A) \quad 4.1.5$$

Equation 4.1.5 can then be used to eliminate the rate of change of mass in the cell from Equation 4.1.4. The resulting equation after rearranging the terms is Equation 4.1.6, because the subtraction is done before the multiplication computer truncation error is reduced.

$$\rho V \frac{d\phi}{dt} = -\Delta_r(\rho u_{RB}(\phi - \phi_i)A) - \Delta_z(\rho w_{RE}(\phi - \phi_i)A) \quad 4.1.6$$

Equation 4.1.6 is the discrete analogy of the differential conservative equations in the form presented

by Bird, Stewart, and Lightfoot (1960), in which the continuity or mass balance has been eliminated.

Equation 4.1.6 is a conservative discrete analogy in which the continuity relation has been eliminated but at the same time is mathematically satisfied.

The philosophical point is that the statement of conservation of momentum and energy involves the convection of mass, as does the mass balance or continuity equation. Therefore, the proper differencing method of the conservative equations must satisfy all the equations simultaneously. To make this point a little more clear, remember, for a WSTRT, when writing an energy balance, the mass balance is also involved, as shown by Equations 4.1.7 and 4.1.8. Therefore, the difference equations should use the proper difference forms so that the equations are not only conservative, in the sense that when all the equations are added the proper overall balances result, but also must locally be conservative or consistent with the mass balance for that cell.

$$\frac{dH\rho V}{dt} = \rho_i Q_i H_i - \rho_o Q_o H_o \quad 4.1.7$$

$$\frac{d\rho V}{dt} = \rho_i Q_i - \rho_o Q_o \quad 4.1.8$$

Equation 4.1.6 is conservative, if the property that is convected across the cell boundary is constructed consistently throughout the grid system. However, the transportive property is physically important, therefore, the WSTRT analogy must be invoked to arrive at the proper algorithm for the convection terms. Simply speaking, if the conserved property is an input, it is characteristic of the adjacent cell. Likewise, if the property is an output from the cell in question, it is characteristic of that cell. The upwind differencing algorithm presented in Roache (1976) accomplishes the WSTRT analogy. The algorithm is presented below in Table 4.1.1, with reference to Figure 4.1.4.

Only the radial term will be presented, since the vertical term is analogous. However, the mass rate leaving the top and bottom boundaries of the cell are calculated directly from the continuity equation. But the radial mass rate is assumed to be the linear average of the adjacent points. The algorithm is not exactly as presented by Roache, because of the way Equation 4.1.6 was derived. The algorithm presented in Roache was derived so that differencing would obey the transportive principle, which is exactly what has been accomplished through the WSTRT analogy.

Now that a consistent way to difference the

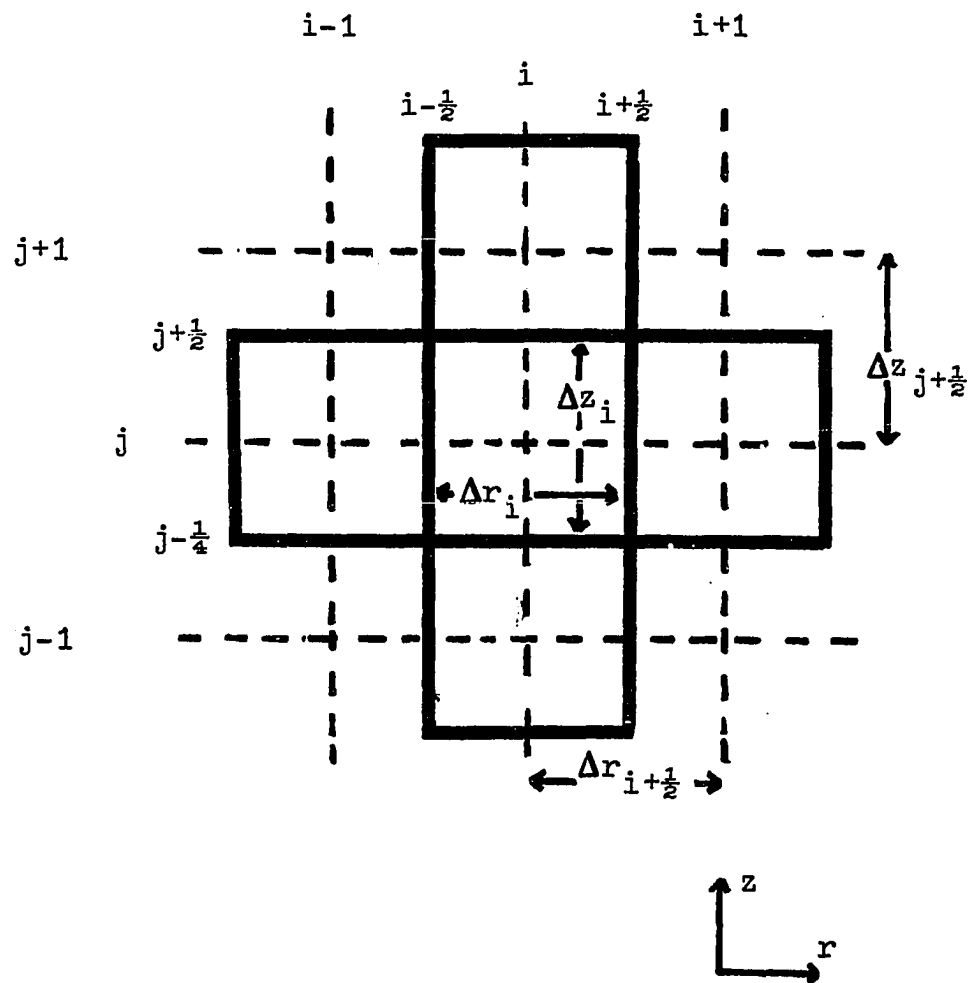


FIGURE 4.1.4 COMPUTATIONAL GRID CELL

TABLE 4.1.1: Upwind Differencing Algorithm

$$\text{IF } u_B = (\rho u_{RB}^A)_{i-\frac{1}{2}} > 0 \quad \phi - \phi_i = \phi_{i-1} - \phi_i$$

$$\text{IF } u_B = (\rho u_{RB}^A)_{i-\frac{1}{2}} < 0 \quad \phi - \phi_i = 0$$

$$\text{IF } u_F = (\rho u_{RB}^A)_{i+\frac{1}{2}} > 0 \quad \phi - \phi_i = 0$$

$$\text{IF } u_F = (\rho u_{RB}^A)_{i+\frac{1}{2}} < 0 \quad \phi - \phi_i = \phi_{i+1} - \phi_i$$

$$(\rho u_{RB}^A)_{i-\frac{1}{2}} = [(\rho u_{RB}^A)_{i-1} + (\rho u_{RB}^A)_i]/2$$

$$(\rho u_{RB}^A)_{i+\frac{1}{2}} = [(\rho u_{RB}^A)_i + (\rho u_{RB}^A)_{i+1}]/2$$

convective terms has been derived, the discrete form of the viscous, compressive, and body forces for the momentum equations shall be derived, as well as, the thermal diffusion terms for the energy equation. Because of the complexity of the viscous forces in their general form, the derivation of these terms will be omitted. Instead, the viscous forces will be taken directly from the modeling equation given in Chapter 3. The WSTRT analogy and Equation 4.1.2 will simply indicate that the diffusion terms should be differenced in a conservative fashion. The mathematical form of the viscous forces are given below in terms of the general property. These terms, of course, are differential diffusion forms of Equation 4.1.2 after dividing Equation 4.1.2 through by the volume, and then taking the limit, as the volume goes to zero. Equation 4.1.9 and 4.1.10 will serve as the definition of thermal diffusion also. Any discrete analogs for Equation 4.1.9 and 4.1.10 will, therefore, apply to the momentum equations as well as the energy equations.

$$D_{rr}(\phi) = \frac{1}{r} \frac{\partial}{\partial r} \left(r \frac{\partial \phi}{\partial r} \right) \quad 4.1.9$$

$$D_{zz}(\phi) = \frac{\partial^2 \phi}{\partial z^2} \quad 4.1.10$$

$$D_{\theta r}(\phi) = \frac{\phi_2}{r^2} \quad 4.1.11$$

Both Equations 4.1.9 and 4.1.10 are differenced in a conservative form as shown in Equations 4.1.12 and 4.1.13 below.

$$D_{rr}(\phi) = (\rho_{i+\frac{1}{2}} A_{i+\frac{1}{2}} (\phi_{i+1} - \phi_i) / \Delta r_{i+\frac{1}{2}} - \rho_{i-\frac{1}{2}} A_{i-\frac{1}{2}} (\phi_i - \phi_{i-1}) / \Delta r_{i-\frac{1}{2}}) / V_i \quad 4.1.12$$

$$D_{zz}(\phi) = (\rho_{j+\frac{1}{2}} (\phi_{j+1} - \phi_j) / \Delta z_{j+\frac{1}{2}} - \rho_{j-\frac{1}{2}} (\phi_j - \phi_{j-1}) / \Delta z_{j-\frac{1}{2}}) / \Delta z_j \quad 4.1.13$$

However, Equation 4.1.11 cannot be differenced in a conservative form because it looks like a source term, this is a problem that results from expressing the radial component of the stress tensor in the cylindrical coordinate system. Actually, mathematically, Equation 4.1.11 should cancel with the other terms for the inner cells if the overall momentum balance is to be observed. Since Equation 4.1.12 and 4.1.13 sum for the entire volume to give the stresses at the boundary, there might be some question as to why this should be included in the discrete analogy of the modeling equations.

Nonetheless, Equation 4.1.14 will be used as the discrete form of Equation 4.1.11 and used in programming.

$$D_{\theta r}(\phi) = \rho_i \frac{\phi_{i2}}{r_i} \quad 4.1.14$$

The generation term in Equation 4.1.2 is simply the body force for the vertical momentum equation. The discrete analog is Equation 4.1.15.

$$\phi_g V_i = \rho_i V_i \quad 4.1.15$$

To complete the definition of the force acting on a cell, a discrete analog of the compressive forces must be stated. The radial gradient is approximated by Equation 4.1.16

$$\frac{\partial P}{\partial r} = ((P_{i+1} + P_i) \Delta z_{i+\frac{1}{2}} - \quad 4.1.16$$

$$(P_i + P_{i-1}) \Delta z_{i-\frac{1}{2}}) / 2 \Delta z_i \Delta r_i$$

The pressure gradient of the vertical direction is simply approximated by Equation 4.1.17.

$$\frac{\partial P}{\partial z} = \frac{P_{j+\frac{1}{2}} - P_{j-\frac{1}{2}}}{\Delta z_j} \quad 4.1.17$$

The pressure along the vertical surfaces are not related to the grid points, because, the pressures will be calculated along the surface via the vertical momentum equation. This will be made clearer once the calculation sequence is outlined.

In the preceding discussions where the density is needed at the boundaries of the cell, this density is calculated simply by averaging the densities of the cells adjacent to the boundary. This applies in particular to Equation 4.1.12 and Equation 4.1.13.

4.2 NUMERICAL MODEL FOR VACUUM PAN

Now that the discrete analogs for the various terms presented in the modeling equations have been derived, the full set of numerical modeling equations will be presented and how the various modeling sections interact. The numerical modeling equations will be presented in the order that each equation for each modeling section supplies information to the calculation sequence. In summary, the calculation sequence is outlined below in steps (1) through (7).

- (1) Calculate the radial velocity from the radial momentum equation.
- (2) Calculate the enthalpy from the energy equation, then calculate the temperature and density.
- (3) Rezone the grid system.
- (4) Do any spatial averaging and integrate the overall balances, then calculate the mass fractions of components and spatial averaged physical properties.
- (5) Calculate vertical mass fluxes and velocities from the continuity equation and also the vapor flux leaving the surface.
- (6) Calculate the new surface position from the continuity equation.

- (7) Calculate the pressure profile from the vertical momentum equation.

In the derivation of the discrete modeling equations, it was pointed out that a dynamic grid system could be used in conjunction with these equations. This dynamic grid system is important to the numerical solution because moving boundary problems are plagued with the problem of keeping track of the location of the boundaries. In particular, free surface problems such as the present modeling effort, where curvature of the surface and volume changes occur, a fixed grid system is inadequate.

Although Waldrop's method as extended by Pitts, has a floating top cell, the volume changes during the course of operation of the Vacuum Pan are large enough to strain the accuracy of the solution or produce negative cell volume. Therefore, the grid system will have to be dynamic to be compatible with the solution techniques for the whole operation of the Vacuum Pan. The easiest way to prevent the surface cells from running dry or expanding too large is to absorb some of the volume changes in the inner cells. This is the method that will be used to develop the dynamic grid used here. The forms of the discrete analogs of the modeling equations will not change because they were derived with the dynamic grid systems in mind.

Because the natural convecting flow in the Pan does not permit large deviations of the radial surface height from the average surface height, there is no need to distinguish differences in the inner cell vertical heights in the radial direction. Adjustments for curvature can be done with surface cells. Also, radial variation of the radial increments is an unneeded complexity. Therefore, varying the inner cell vertical heights with volume change so as to maintain a positive surface volume is all that is needed in the way of a dynamic grid. A better description of this dynamic grid system along with the calculations involved, are present as part of the outline of the calculation sequence for solving the numerical model. A more general discussion of the dynamic grid systems developed in the literature as well as the dynamic grid system used here is included in Chapter 6, Appendix III includes an example.

Each computational grid cell in the grid system is aligned such that the boundaries of the cell correspond to the physical boundaries of the Pan and the boundaries of each sectional portion of the Pan. This arrangement allows the boundary conditions to be easily applied and ensures that the conservative and transportive nature of each cell is characteristic of the computational space. The dynamic portion of the grid system is limited to the Pan Proper. Therefore, free surface must always be contained in the

Pan Proper.

|

4.2.1 RADIAL MOMENTUM

Taking the general property as the specific radial momentum, the equations for the modeled section can be derived. An explicit method is used to integrate these equations. The equations for the Pan Proper, Free Surface, and the Bottom are presented below. The equation for updating the radial velocity in the Bottom is a little different because the convective term can be evaluated implicitly.

a. Free Surface and Pan Proper

$$\begin{aligned} \text{DUDT}_{ij}^n = & -\Delta_r \frac{(\rho u_{RB}^n A(u-u_i))}{\rho_i V_i} - \Delta_z \frac{(\rho w_{RB}^n A(u-u_j))}{\rho_i V_i} \\ & - \frac{\Delta P}{\Delta r} + v D_{rr}^n(u) + v D_{\theta r}^n(u) + v D_{zz}^n(u) \end{aligned} \quad 4.2.1$$

$$u_{ij}^{n+1} = u_{ij}^n + (\text{DUDT}_{ij}^n + \text{DUDT}_{ij}^{n-1}) \Delta t / 2 \quad 4.2.2$$

b. Bottom

$$\begin{aligned} u_7^{n+1} = & u_7^n - \frac{\text{PBIP1} - \text{PBIM1} \Delta t - (u_7^{n+1})^2}{\rho_7 \Delta r} c_2 \\ (u^{n+1})^2 \approx & u^{n+1} u^n \\ c_2 = & \Delta \left(\frac{1}{r} \right) / \Delta r^2 \Delta t \quad r_7^2 \\ u_7^{n+1} = & u_7^n - \frac{1}{\rho} \frac{\Delta P}{\Delta r} / (1 + c_2 u^n) \Delta t \end{aligned} \quad 4.2.3$$

4.2.2 ENTHALPY, TEMPERATURE, AND DENSITY

The energy equation, like the radial momentum, is solved explicitly via the equation below. The equations for the Pan Proper and the Free Surface will be lumped together again, but remember, the flux of energy leaving the surface is the result of vaporization. The flux of vapor leaving the surface cell will be calculated later, as will be outlined momentarily. Heat is transferred into the Pan in the Calandria. This flux of energy is given the symbol ECOEFF, this flux is the evaporation coefficient mentioned in Chapter 3. Feed is introduced into the Bottom and effects the enthalpy balance for the Bottom.

a. Free Surface and Pan Proper

$$DHDT_{ij}^n = -\Delta r \frac{\rho_{RB}^n A (H - H_i)}{\rho_{ij} V_{ij}} - \quad 4.2.4$$

$$\Delta z \frac{\rho_{RB}^n A (H - H_j)}{\rho_{ij} V_{ij}} + \alpha D_{rr}^n (T) + \alpha D_{zz}^n (T)$$

$$H_{ij}^n = H_{ij}^n + DHDT_{ij}^n \Delta t \quad 4.2.5$$

b. Calandria

$$\text{DHDT}_j^n = \frac{-\Delta_z^n (\rho_{wRB} (H - H_j))}{\rho_j \Delta z} + \text{ECOEFF POA} / \rho_j + \alpha D_{zz}^n (T) \quad 4.2.6$$

$$H_j^{n+1} = H_j^n + \text{DHDT}_j^n \Delta t \quad 4.2.7$$

c. Bottom

$$\text{DHDT}^n = ((-\rho wAH)_1 - (\rho wAH)_2 + F HF) / V$$

$$H^{n+1} = H^n + \text{DHDT}^n \Delta t \quad 4.2.8$$

Once the enthalpy is calculated, the density of the mixture is calculated by checking to see if the enthalpy is large enough to suggest that the vapor phase is present. This is done by calculating the mixture temperature, Equation 4.2.9.

$$T = H / CP \quad 4.2.9$$

If the temperature is greater than the boiling point of the mixture, given by Equation 3.4.16, then the vapor phase is present.

$$T_{BOIL} = f(P) + BPE \quad 3.4.16$$

Of course, if the vapor phase is present, then the temperature of the mixture is at the boiling point. The mass fraction of the vapor is then calculated by Equation 3.4.13.

$$XV = \frac{H - H_L}{H_V - H_L} \quad 3.4.13$$

The liquid enthalpy and vapor enthalpy functional relationships are given by Equations 3.4.10 and 3.4.11, respectively. The density of the mixture is then calculated by Equation 4.2.10.

$$\frac{1}{\rho} = \frac{1-XV}{\rho_V} + \frac{XV}{\rho_{LS}} \quad 4.2.10$$

The vapor density is given by Equation 3.4.3, which is corrected for changes in pressure relative to the reference pressure. The liquid and solid mixture density (ρ_{LS}) is given by Equation 3.4.6. The liquid density is given by Equation 3.4.5. The calculation of mixture enthalpy does not adjust the local mass fractions

when vaporization occurs, as discussed earlier.

$$\frac{1}{\rho_{LS}} = \frac{1-XCP}{\rho_L} + \frac{XCP}{\rho_C} \quad 3.4.6$$

4.2.3 DYNAMIC GRID

In order to track the volume change in the Pan and maintain a positive volume in the surface cells, for a fixed number of cells, it is necessary to adjust the grid positions. Adjustments are made only in the vertical direction. Figure 4.2.1 is an illustration of a typical grid arrangement. As is shown in the Figure, the inner cell vertical and radial cell widths are equal, but the surface cell heights may differ as a function of the fluid dynamics. The adjustments will be done by expanding or contracting the inner cell heights, as the average height of the fluid above the Calandria and Downtake changes. The average height is calculated by adding the average surface cell height to the sum of the inner cell heights. The rate of change of the inner cell heights are then calculated by Equation 4.2.11. Exponential smoothing is used to give a smooth rate of change.

$$\text{SURFDT} = \left((\bar{h} + j_{\max} \text{DZ})^n - (\bar{h} + j_{\max} \text{DZ})^{n-1} \right) / \Delta t / j_{\max} \quad 4.2.11$$

$$\text{DDZDT}^{n+1} = \text{DDZDT}^n - (\text{DDZDT}^n - \text{SURFDT}) \text{THETAS} \quad 4.2.12$$

$$0 \leq \text{THETAS} \leq 1$$

Once the rate of change of the inner cell heights is found, the cell height is updated by Equation 4.2.13.

$$DZ^{n+1} = DZ^n + DDZDT^{n+1}\Delta t \quad 4.2.13$$

The dynamic grid acts as a musical accordion, expanding or contracting according to the volume of fluid inside the Pan. Because the grid system is dynamic, each grid cell center may be moving. The continuity equation will be used to calculate the flux of mass in or out of the top cell boundary, but if the absolute value of the vertical component of the fluid velocity is to be extracted for this mass flux, given the fluid density, the vertical velocity of the cell boundary must be known. Likewise, if the vertical fluid velocity at the cell center is to be calculated, the velocity of the cell center must be known. Since the vertical velocity of the fluid at the cell center is needed for the vertical momentum equation, the cell center velocity will be calculated by Equation 4.2.14.

$$DPDT_j = DDZDT(2j-1)/2 \quad j=1,2\dots jmax \quad 4.2.14$$

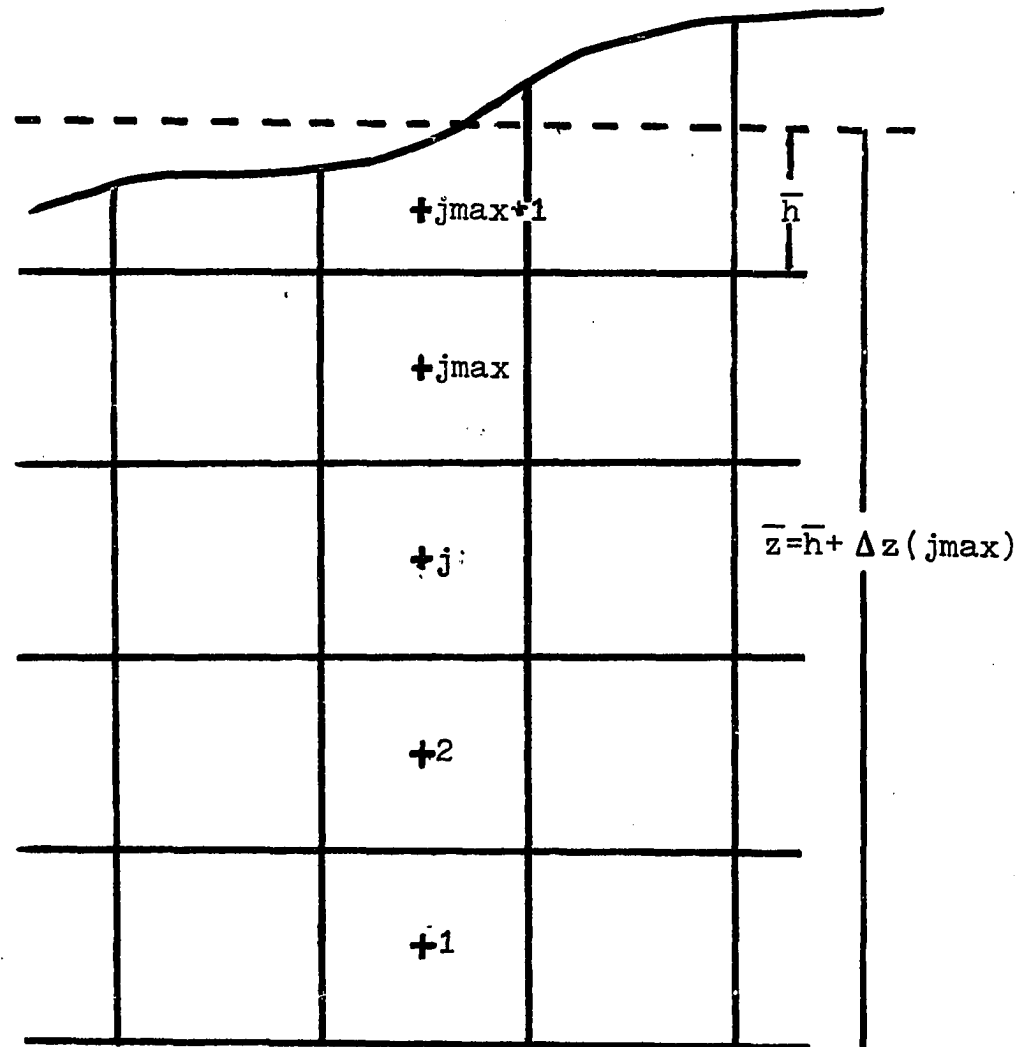


FIGURE 4.2.1 TYPICAL GRID ARRANGEMENT

4.2.4 OVERALL BALANCES

The mass fractions of the components in the Vacuum Pan are calculated via the overall mass balances. These mass fractions are then used to calculate physical properties needed for the other calculation steps. Those physical properties being the heat capacity, as given by Equation 3.4.9, the viscosity of the mixture, as given by Equation 3.4.17 and 3.4.18, the enthalpy of the vapor, Equation 3.4.11, and the density, Equation 3.4.1.

Because the dynamics of these equations are slow compared to the distributed balances of mass, momentum, and energy for each cell, the integration time step will be limited by the distributed balances. It would therefore, be possible to integrate the overall equation in the numerical code at a different time step. However, this was not done and the overall equations were integrated with a very small time step. Since such a small integration step is used, the integration method is not very important. The integration method that is used in the program is simply a one step forward time integration. The time derivative is calculated from the latest values of the inputs and outputs available. Again, whether the old or new inputs or outputs were used is not important, since the time step that will be used is very small.

4.2.5 VERTICAL VELOCITY AND MASS FLUX LEAVING THE CELL

The vertical velocity and mass flux leaving the cell are calculated algebraically by the continuity expression, once the volume, density, and radial velocity of each cell are known. Of course, these are given by the previous explicit calculations. The continuity relationship, also, applies at the top cell but, this is a special case by which the surface position is located, this will be discussed later. Once the pressure drop occurs across the Bottom, from the Downtake to the Calandria, the radial flow plus feed into the Bottom is converted into vertical flow in the Downtake and Calandria. Equation 4.2.15 is the continuity relationship for the top of the Downtake, Bottom of the Downtake, and radial flow at the Bottom, plus the feed into the Bottom. Figure 3.3.1 will help in the understanding of how the Downtake, Bottom, and Calandria is divided.

$$A_1 w_1 = A_2 w_2 = -A_7 u_7 \quad 4.2.15$$

Likewise, the continuity relationship for the Calandria entrance is given by Equation 4.2.16. Equations 4.2.15 and Equation 4.2.16 add together to give Equation 3.3.20, the overall continuity relationship for the Bottom and Downtake.

$$A_5 w_5 = A_7 u_7 + F/\rho_7 \quad 4.2.16$$

The direction of flow is always limited to be in the positive or counterclockwise direction, down the Downtake and up the Uptake (Calandria). Equation 4.2.16 is the boundary condition for the Calandria continuity relationship, which is Equation 3.3.5.

The mass flux at each cell boundary in the Calandria is given by Equation 4.2.17 and the velocity at the center of each cell is given by Equation 4.2.18.

$$(\rho w)_{j+\frac{1}{2}} = (\rho w)_{j-\frac{1}{2}} - \frac{\Delta \rho}{\Delta t} \Delta z \quad 4.2.17$$

$$w_j = 0.5 ((\rho w)_{j+\frac{1}{2}} + (\rho w)_{j-\frac{1}{2}}) / \rho_j \quad 4.2.18$$

With the mass flux up the Calandria and the mass flux down the Downtake calculated, the calculation proceeds into the two-dimensional Pan Proper. The mass flux relative to the cell boundary is calculated by Equation 4.2.19.

$$(\rho w)_{j+\frac{1}{2}} = (\rho w)_{j-\frac{1}{2}} - \frac{\Delta_r (\rho u_{RB} A)}{A_z(i)} + \frac{\Delta (\rho_i V_i)}{\Delta t A_z(i)} \quad 4.2.19$$

The velocity at the cell center is calculated by Equation 4.2.20. Notice that the velocity of the fluid at the cell center is adjusted by the velocity of the cell center. This is the result of the dynamic grid system.

$$w_j = 0.5 ((\rho w)_{j+\frac{1}{2}} + (\rho w)_{j-\frac{1}{2}}) / \rho_{i,j} + DPDT_j \quad 4.2.20$$

The calculation proceeds upward, increasing in vertical height, above the Calandria and Downtake, until the cell just below the surface cell is reached. The mass flux of vapor leaving, if any, from the top cell is then calculated by Equation 4.2.21.

$$E_i = \rho V(w_v - w_s) = W_v^* \gamma \quad 4.2.21$$

As discussed earlier, Equation 4.2.21 is the semi-theoretical relationship, describing the slip velocity of vapor relative to the liquid. However, because of lack of experimental data, Equation 4.2.21 is simply used as a method to remove the vapor present in top cell.

4.2.6 SURFACE POSITION

The height of each surface cell is calculated by a mass balance, therefore, the equation is just a continuity relationship. The surface equation is the same continuity relationship used in the grid cells below the surface to calculate the vertical velocity of the cell center and the mass flux leaving the top cell boundary. Because the mass flux of vapor has been already calculated by Equation 4.2.21 the equation can be used to calculate the rate of change of mass in the cell, and thus, with the density known, the surface height. Equation 4.2.22 is the Finite Difference Surface Continuity Equation. The last term in the equation is used to supply surface smoothing needed for stability.

$$(h\rho)_i^{n+1} = (h\rho)_i^n - \frac{\Delta_x^n (\rho u_{RB} A)}{A_z(i)} + (\rho w_{RB})_{j_{\max} + \frac{1}{2}} \quad 4.2.22$$

$$- E_i + \text{SFSMTH } D_{rr}(h)$$

As can be readily seen, Equation 4.2.22 is in tri-diagonal form, therefore, an implicit solution of the surface height is possible. This is a convenience afforded only to two-dimensional problems. If the model was three-dimensional, iterative solution techniques would have to be used. If the equation was solved explicitly, the equation without the diffusion term would

be unstable because central difference equations, like Equation 4.2.22, are unstable when integrated as demonstrated in Roache (1976). Surface diffusion or smoothing in the explicit formulation adds feedback between the grid points to stabilize the equation.

However, the amount of smoothing needed for stability of the explicit formulation is large and therefore, the free surface does not respond adequately to the fluid dynamics. Formulating an implicit solution eliminates the stability problems associated with the form of the difference equation but, because the other terms in the equation are affected by the surface position but are predicted explicitly, some surface smoothing is needed to insure stability. It was found by experiment, that for stability, the surface diffusivity needs to be greater than 0.1 FT./SEC.². The implicit surface diffusivity is at least a thousand times smaller than the surface diffusivity needed to stabilize the explicit calculation. A nominal surface diffusivity of 2.0 FT./SEC.² was used for all numerical calculations with the implicit surface calculation.

The tri-diagonal algorithm is presented in the computer code. Basically, it is the code developed by Roache (1976).

Once the new surface cell height has been calculated, the velocity of the center of the surface cell can be

calculated by Equation 4.2.23.

$$w_{jmax+1} = ((\rho w_{RB})_{jmax+\frac{1}{2}} - \frac{\Delta_r(\rho u_{RB}^A)}{2 A_z(i)} - \frac{\Delta \rho V_i}{2 \Delta t A_z(i)}) / \rho_{jmax+1} + DPDT_{jmax+1} \quad 4.2.23$$

$$DPDT_{jmax+1} = \frac{\Delta h}{2 \Delta t} + DDZDT(jmax+1)$$

The velocity of the surface may be calculated if needed for plotting by Equation 4.2.24.

$$w_s = \frac{\Delta h}{\Delta t} + DDZDT(jmax) \quad 4.2.24$$

4.2.7 PRESSURE CALCULATION

At this point, all the variables in the solution matrix have been calculated except the pressure profile. The pressure profile can be calculated from the vertical momentum equation. Although, the hydrostatic approximation is going to be used in the program, the full vertical momentum equation will be Finite Differenced in the same conservative fashion as the other equations for the sake of completeness. The hydrostatic head approximation can then be derived by eliminating all the terms except the body forces and the pressure gradient. The exceptions to this rule apply in the Downtake and Calandria where the friction pressure drop is also retained. The pressure calculation starts at the surface cell because the pressure at the surface is known. The difference equation allows the pressure on the lower boundary of the surface cell to be calculated. The pressure at the cell center is then the linear interpolation of the pressure difference from the top to the bottom boundary of the cell. Figure 4.2.2 illustrates this point. Once the pressure for all the cells along the surface has been calculated, the calculation can be proceeded to the next grid level below. Repetitively, the calculation then proceeds from the free surface to the Bottom of the Pan. The pertinent difference equations

for each section are presented below.

The pressure across the upper boundaries of the Downtake and Calandria are taken as the area average of the pressure forces on their surfaces. While the Calandria is treated in a distributed fashion, the Downtake is taken as one lump. The two pressures calculated at the lower boundary of the Downtake and Calandria are fed back into the Bottom Momentum Equation at the next time step. Likewise, the radial pressure profiles in the Pan Proper and Free Surface are used in their respective Radial Momentum Equations. Thus, the calculation sequence has been cycled.

a. Free Surface and Pan Proper

$$\rho_{ij} \frac{\Delta w_{ij}}{\Delta t} + \frac{\Delta_r (\rho u_{RB} (w - w_i))}{V_{ij}} + \frac{\Delta_z (\rho w_{RB} (w - w_j))}{V_{ij}} \quad 4.2.25$$

$$= -\frac{\Delta P}{\Delta z} + v D_{rr}(w) + v D_{zz}(w) + \rho_{ij}$$

$$P_c = P_u - \frac{\Delta P}{\Delta z} \cdot \Delta z / 2$$

b. Downtake

$$\begin{aligned} \text{PBIM1} &= \text{PNUP} + \text{DPFR} + \text{TUBEH} \rho \\ &+ \rho \frac{\Delta w}{\Delta t} \text{TUBEH} \end{aligned} \quad 4.2.26$$

$$\text{DPFR} = 8 \mu w_1 \text{TUBEH} / R_{\text{dwn}}^2 \quad 3.3.22$$

$$\text{PNUP} = \frac{\sum P_i A_i}{\sum A_i}$$

c. Calandria

$$\rho \frac{\Delta w_j}{\Delta t} + \Delta z \frac{(\rho w_{RB}(w - w_j))}{\Delta z} = - \frac{\Delta P}{\Delta z} + FR + \rho_j \quad 4.2.27$$

$$FR = 32 \rho_j v w / D_t^2 \quad 3.3.8$$

$$PNUP = \frac{\sum P_i A_i}{\sum A_i}$$

If desired, the action of a pump in the Downtake or Bottom may be simulated by simply increasing the pressure drop across the Downtake to the Calandria by the amount of head supplied by the pump.

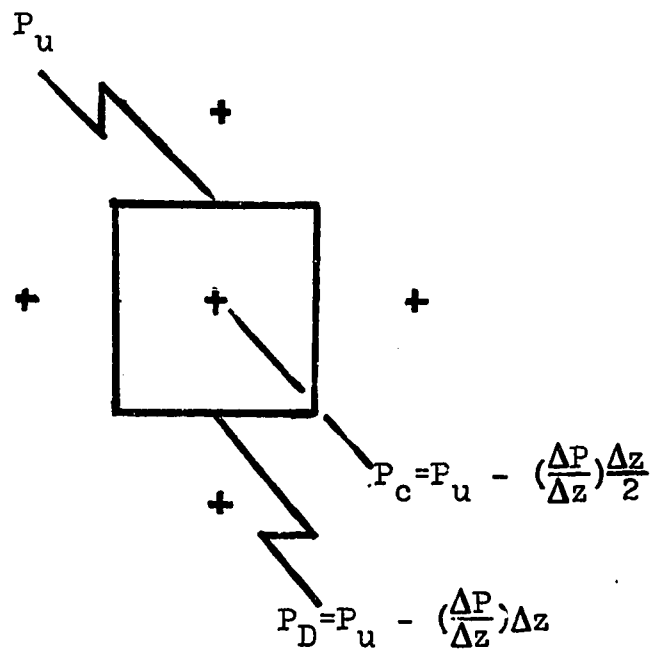


FIGURE 4.2.2 DIFFERENCING VERTICAL PRESSURE GRADIENT

CHAPTER 5

RESULTS

In the previous chapters a mathematical model of the Vacuum Pan Sugar Crystallizer was developed. The model includes overall material balances to simulate the effect of feed input, evaporation, and crystal growth on Pan operation. The distributed mass, momentum, and energy equations are included to simulate the distributed nature of the Pan operation. The model is capable of simulating the operation of a typical Industrial Calandria Vacuum Pan during the later periods of its operation, when vigorous boiling does not occur. This limitation results from instabilities in the numerical solution method when vigorous boiling occurs, vigorous boiling is characteristic of the early periods of the batch. In terms of the utility of the model this is not a severe limitation.

In the following pages, sensitivity of the numerical solution will be demonstrated to the thermal diffusivity and kinematic viscosity, and to Pan design and operating conditions. The sensitivity of the solution to the thermal diffusivity and kinematic viscosity demonstrates that convection is the most important mechanism to transport momentum and energy. The sensitivity of studies varying Pan design and operating conditions demonstrate the utility of the model as a research tool to aid in design

of Vacuum Pans, design of control systems for Vacuum Pans already existing or in the design stage. The significance of the model is its ability to calculate local supersaturation and growth rate profiles and velocity profiles in the Pan. The interaction of these velocity and growth rate profiles contributes to the increase of the variance of the crystal size distribution (CSD), and excessive local supersaturation contributes to unwanted nucleation occurring. In all cases, the model simulations demonstrated that significant growth rate profiles exist in the Vacuum Pan. The effect of these profiles quantitatively cannot be demonstrated until a distributed particle population balance is integrated with the fluid dynamics. These studies will also demonstrate how various designs and operating conditions affect these profiles as well as the velocity profiles and other pertinent Pan statistics. But since heat transfer correlations for the tubes do not exist that are sensitive to Pan design and the operating conditions, sweeping statements concerning Pan performance cannot be made. Future versions of the model will include more realistic heat transfer correlations. Comparisons of the predicted Calandria tube velocity from these studies against data in the literature shows favorable results.

Concluding this chapter, numerical difficulties with the solution method are discussed as well as the

applicability of the hydrostatic head assumption for modeling natural convection and boiling in the Vacuum Pan.

The methodology for performing the sensitivity studies mentioned above is as discussed below. The numerical integration is started at various operating points and the numerical model is allowed to come to a steady state. This steady state is accomplished by feeding water into the batch to match exactly the evaporation rate, maintaining constant heat input, and specifying the volume fraction of crystal and not allowing it to change, then integrating the dynamic model until the fluid dynamic transients disappear. The volume fraction crystal is maintained constant by artificially setting the calculated growth rate to be zero. Doing the simulation in this fashion causes the overall balances of sucrose, impurities, and water to maintain the same mass fractions as the initial conditions. This allows the perturbation of certain conditions while keeping others constant, thus, a true partial derivative is obtained. This type of analysis is justified for the crystallizer, when two-phase transients do not exist, because the fluid dynamics of the Pan are fast compared to the growth of crystals and the change of volume in the Pan.

5.1 SENSITIVITY OF CALCULATION TO THE KINEMATIC VISCOSITY AND THERMAL DIFFUSIVITY

One of the assumptions in the derivation of the model was the absence of excessive turbulence, that is, that laminar flow conditions exist. Thus, the need for turbulence models for this type of flow has not been explored. However, it is understood that in reality there is turbulent mixing in the Pan, especially when boiling occurs. During operation of the Pan, when boiling is not occurring, the laminar flow assumption is certainly valid because the viscosity of the mixture in the Pan is forty to five-hundred times the viscosity of water, while the velocities in the Pan are most of the time less than 1 FT./SEC.. Because of the uncertainty about the two-phase flow phenomena, experiments were run at various levels of viscosity and Prandtl number to test their effect on the profiles in the Pan Proper. The experiments demonstrate that the effects of the Thermal Diffusivity and Kinematic Viscosity over reasonable ranges of values are not significant. Table 5.1.1 is a log of the experimental runs. Velocity profiles for these runs are presented in Appendix II. These velocity profiles are plotted on one-half of an axisymmetrical cross-section of the Pan. The arrows indicate the magnitude and direction of the fluid velocity. For

convenience, the base of the arrow is located at the grid point and the radial and vertical velocity components are added to give the vector plotted.

Referring to Table 5.1.1, the first case and its corresponding figure presents typical conditions in the Vacuum Pan. All the other cases are perturbations of the first case to demonstrate the effect of the Thermal Diffusivity and the Kinematic Viscosity. In Cases 1 - 8 the effect on the velocity profiles is small. The last case, (case 9) is only included to indicate how large the diffusivities would have to be increased before the solution is effected. In fact, the Thermal and Momentum Diffusivity used in this case are in the range of liquid metals. Cases 2 and 3 in Table 5.1.2 also have special computational significance, since both the Thermal Diffusivity and the Kinematic Viscosity are zero. The significance of these cases will be discussed in Chapter 7. Therefore, as expected for the crystallizer, as in most industrial problems, the convective terms are the most important mechanism to transport momentum and energy. Extensive data about the experiment was omitted, because small changes in the velocity profiles presented in the figures are synonymous with small changes in all of the properties characterizing the experiment.

TABLE 5.1.1: LOG OF MODEL RUNS VARYING THE
THERMAL AND MOMENTUM DIFFUSIVITIES

CASE	THERMAL DIFF. (FT. ² /SEC.)	KINEMATIC VIS. (FT. ² /SEC.)	PRANDTL NO.
1	1.34×10^{-6}	2.68×10^{-3}	2000
2	0.0	2.68×10^{-3}	
3	0.0	0.0	
4	1.34×10^{-4}	1.34×10^{-2}	100
5	1.34×10^{-6}	1.34×10^{-6}	1
6	1.34×10^{-6}	1.34×10^{-4}	100
7	1.34×10^{-4}	1.34×10^{-4}	1
8	0.0	1.34×10^{-4}	
9	1.34×10^{-4}	2.68×10^{-1}	2000

5.2 EFFECT OF PAN DESIGN AND OPERATING CONDITIONS

The design and operating conditions, as pointed out in Hugot (1972) and Honig (1963), have a profound effect on the quality of the CSD produced and the batch time needed to produce a desired crystal size. The importance of a large downtake and large tube diameters is stressed in order to reduce the resistance to recirculating flow. However, increased tube diameter and downtake diameter cause decreased heat transfer area. The heat load is, of course, the forcing function causing the recirculation to occur. Hugot attempts an optimization to find the pan design that minimizes the resistance to flow. Although his method of analysis is correct, he was not able to include the effect of pan design on the fluid dynamics and assumed the recirculating flow rate was constant between pan designs. The model developed here, offers an alternative method of analysis which is more realistic. Obviously, considering the design variables in combination with the variety of operating conditions, finding an optimal Pan could be difficult. But, if judicious engineering constraints are applied the basic characteristics of a good circulating Pan can be determined. Good recirculation is synonymous with a good Pan because good recirculation promotes good heat transfer and a reduced effect of growth variation on

the CSD. The model offers an inexpensive way to accomplish such a characterization by studying the effect of varying Pan design and operating conditions. This leads into the discussion of the effects of the operating conditions and Pan design to demonstrate the model applicability for such studies.

Presented in Table 5.2.1 are a few typical design variations of industrial pans. Table 5.2.2 summarizes a series of experiments using the model to simulate these typical pans under various operating conditions. Table 5.2.3 summarizes the results of these experiments varying the design of the pan, volume fraction crystals, heat flux in the tubes, level of the pan, supersaturation, and pan pressure. As can be seen from Table 5.2.1, four different pans were simulated. Pan A and Case 1 will be used as the base case for discussion. In the following paragraphs the effect of pan design will be discussed first and then the operating conditions. Cases 1, 3, 8, and 10 will demonstrate the effect of pan design, comparing Pan A against Pans B, C, and D. Cases 1, 2, and 9 will demonstrate the effect of pan level. Cases 1 and 4 will demonstrate the effect of the presence of crystals. Cases 1, 4, 6, and 7 will demonstrate the effect of heat load and the interaction with crystal content. Cases 1, 5, and 11 will demonstrate the effect of pressure and the interaction with supersaturation. Case 12 against all the other cases will demonstrate the

effect of lower purity batch. Figures 5.2.1 (1) - (12) are the velocity profiles for the cases. Figures 5.2.2 (1) - (12) are the growth profiles for the cases.

The construction and meaning of the velocity profiles in Figure 5.2.1 are the same as discussed earlier. The growth rate profiles, Figure 5.2.2, are plotted on the same axisymmetrical half-section view of the Pan. For convenience, these profiles are indicated by an integer scale rather than an absolute magnitude. The integer representing the growth rate is calculated by the following formula after truncating the decimal.

$$\text{INTEGER} = (9) \left(\frac{\text{GROWTH RATE} - \text{MIN. GROWTH RATE}}{\text{MAX. GROWTH RATE} - \text{MIN. GROWTH RATE}} \right)$$

The scale thus includes the integers zero to nine.

Case 3 (Pan B), differs from Case 1 (Pan A), only in the diameter of the Downtake. Referring to Table 5.2.3, the effect of reducing the Downtake diameter was to slightly reduce the recirculation rate and increase the variance of the supersaturation. A reduction in recirculation can only be viewed as detrimental to CSD.

Case 8 (Pan C), is a variation of Case 1 (Pan A), in several aspects, Pan C's Calandria diameter is smaller than the Pan Proper diameter, and the tubes are shorter, three feet long, and smaller, four inches in diameter. The effect on the velocity profiles is drastic,

completely changing the circulation pattern. This is illustrated by comparing Figures 5.2.1 (1) and (8). The changing flow pattern is basically caused by the difference in Calandria diameter and the major diameter of the Pan. As shown in Table 5.2.3, the recirculation is lower and the variance of the supersaturation and the difference between maximum and minimum supersaturation are larger for Case 8. Therefore, Pan C is not superior to Pan A.

Case 10 (Pan D), is designed to demonstrate the effect of an extra large Downtake but at the expense of heat transfer area. The trade off is not a superior choice over Pan A for the same reason as the previous case.

The level at which a batch is terminated is often the concern of pan designers when considering optimization of the batch cycle time. The higher the level in the Pan, the more sugar can be produced. However, there are practical limits to this line of reasoning that are obvious, but there are other ones that may not be quantified without a model that is sensitive to the effects of the hydrostatic pressure or level of the Pan in reducing circulation through the tubes. Pressure in the tubes increases as the level rises, if the pressure is high enough no boiling will occur in the tubes. If no boiling occurs, the driving force for

recirculation is reduced to a low level. Referring to Tables 5.2.2 and 5.2.3, the break between fast recirculation and slow may be quick as the level rises, as evidenced by the abrupt change in recirculation between Cases 2 and 9, while little change in recirculation rate occurs between Cases 9 and 1. Oddly enough, Case 2, with lower level had a greater volume average variance of the supersaturation. The effect of this small increase in the volume averaged variance of Case 2 over Case 1 is not significant in itself except when one considers that the recirculation rate of Case 2 is twice that of Case 1. This result seems to be contrary to what the literature suggests should happen. This is another example of conditions in the Pan that cannot be predicted without a distributed model. Viewing Figures 5.2.1 (1) and (2), one can see that the velocity profiles are completely different. Likewise, the growth profiles Figures 5.2.2 (1) and (2), are also different. The effect of the level on the circulation and growth patterns in the Pan Proper is the result of more vapor in this section, caused by a higher heating rate per amount of material in the Pan at that time.

The effect of the volume fraction of crystals in the Pan is demonstrated between Cases 1 and 4. As can be seen by comparing the recirculation rates for each case in Table 5.2.3, the experiment with no crystals which is

characteristic of early time intervals of Pan operation has a much higher recirculation rate. The decreased recirculation caused by the presence of the crystals, Case 1, is caused primarily by three factors. The increase of the volume fraction crystals increases the pressure in the tubes due to a higher average density, displaces the liquid which thermally expands with increasing temperature by a crystal that does not expand with increased temperature, and increases the viscosity, all of which restricts recirculation.

Because correlations for heat transfer coefficients are not available for the local conditions in the tube of Vacuum Pan Sugar Crystallizers, as discussed earlier, typical values of the heat flux were calculated based on steam consumption per heat transfer area. To demonstrate the effect of heat load on the Pan, Cases 6 and 7, which are similar to Cases 1 and 4, were run, except, the heat flux was reduced by one-half. Refer to Table 5.2.3 to follow the discussion. The effect of reducing the heat load on a 90% full pan with crystals, Case 6, was to reduce recirculation by half as well as the volume averaged variance of the supersaturation in comparison to Case 1. The effect on the CSD would, therefore, be small. However, comparing Case 7 to Case 4, which have no crystals, the reduced heat load in Case 7 caused a 400% reduction in recirculation over Case 4, but, the

reduction in the variance is only by a half, suggesting the effect of the heat load is sensitive to the conditions in the Pan and its effect on the CSD is also. The heat load, besides affecting the fluid dynamics, also affects the batch time needed to produce a desired product.

During the course of the batch, the heat load must vary to match the program of evaporation needed to assure that the proper level of supersaturation is maintained for the growth of crystals. This suggests that the real effect, for example, of reduced steam pressure, cannot be evaluated without simulating the entire batch. But the experiment does demonstrate that there is a significant effect of the heat load on the Pan.

Changing the pressure in the Pan vapor space directly effects the boiling temperature in the Pan. Therefore, a Pan operating at an increased pressure, given everything else is equal, one would expect the recirculation to increase as a result of a reduced viscosity of the liquid. However, increasing the average temperature in the Pan also decreases the supersaturation in the Pan and hence, if one desires to maintain the supersaturation at a controlled set point, the brix in the Pan must be increased, which of course, increases the viscosity of the liquid. Therefore, two cases were run at an increased pressure to demonstrate the interaction between a change in supersaturation and a change in pressure. Maintaining

approximately the same supersaturation at a higher pressure, Case 5, the model predicted a higher recirculation but no change in profile. But, the model predicted something surprising for the run at higher pressure but lower supersaturation, Case 11, the recirculation increased as expected but the profile changed completely. This can be seen by comparing Figures 5.3.1 (5) and (11). This unexpected prediction results mainly from the interaction of the effect of temperature and brix on the viscosity of the fluid. At the lower brix the recirculation is fast enough that the fluid passing through the tubes does not boil in the tubes or just outside the tubes, therefore, the fluid simply rises to the surface to boil. But, in the other cases the recirculation is just low enough to cause some vapor to be formed in the tubes or just outside the tubes which in turn causes mixing at the tube exit, which then develops into the profile observed.

The previous cases discussed, Cases 1 thru 11, were all for high purity massecuite and therefore, the conditions and results are exemplary of high purity batch operation. Case 12 is exemplary of a typical low purity run. As can be seen in Table 5.2.3 and Figure 5.2.1 (1) - (12), the profile in the Pan Proper and pan statistics are similar to many others, but the recirculation is much slower. These effects are basically

due to the lower heat load and the increased viscosity of the fluid.

The experiments as a whole, demonstrate that there are significant supersaturation profiles in the Pan as shown by the volume average variance of the supersaturation and the maximum and minimum supersaturation, as shown in Table 5.3.3. Noting the growth profiles for each case, Figures 5.2.2 (1) - (12), one can observe that there are differences in the growth rates throughout the Pan. The differences throughout the Pan will cause a widening of the CSD as the batch proceeds. The extent of the widening of the CSD, as the result of growth variations and nucleation of new crystals, cannot be determined without a population balance in combination with the fluid dynamics. The model demonstrates that there is a large difference between the maximum and minimum supersaturation (growth rates), indicating that if a poor control system is used, excessive nucleation may occur or the average growth rate may be too low. This phenomenon may occur particularly when the level is low because the average Pan temperature is higher at this time resulting from the fact that a larger fraction of the total volume is contained in the tubes and because the heating rate per unit volume is larger. But, even though the Pan average temperature is higher, the temperature at the surface is limited by its boiling

point. Thus, to avoid nucleation at the surface the Pan average growth rate may need to be lower than expectations suggest, based on the average conditions in the Pan.

Figures 5.2.2 (1) - (12), of course, demonstrate the existence of the maximum growth rates occurring at the surface and the minimum in the tubes. The model offers an inexpensive method to study the various profiles in the Pan and qualitatively simulate the application of a control system.

Referring again to the velocity profiles, Figures 5.2.1 (1) - (12), and the growth rate profiles, Figures 5.2.2 (1) - (12), one can observe that if the velocity profiles are similar between the cases, the growth rate profiles are similar. This results from the fact that for no spatial differences in concentration in the Pan the growth rate profile is entirely dependent on the temperature profile. But, of course, the temperature profile, because the effect of diffusion is small, is greatly dependent on convection. This reinforces the importance of good circulation in the Pan. The more turbulence that is generated in the Pan Proper, the more uniform the growth profile. This point is typified in Figure 5.2.1 (1) and Figure 5.2.2 (1).. However, when the velocity profile is more streamlined (i.e., less turbulent), as in Figure 5.2.1 (11), the growth rate profiles, as in Figure 5.2.2 (11), are

less uniform in the Pan Proper.

TABLE 5.2.1: TYPICAL PAN DESIGNS

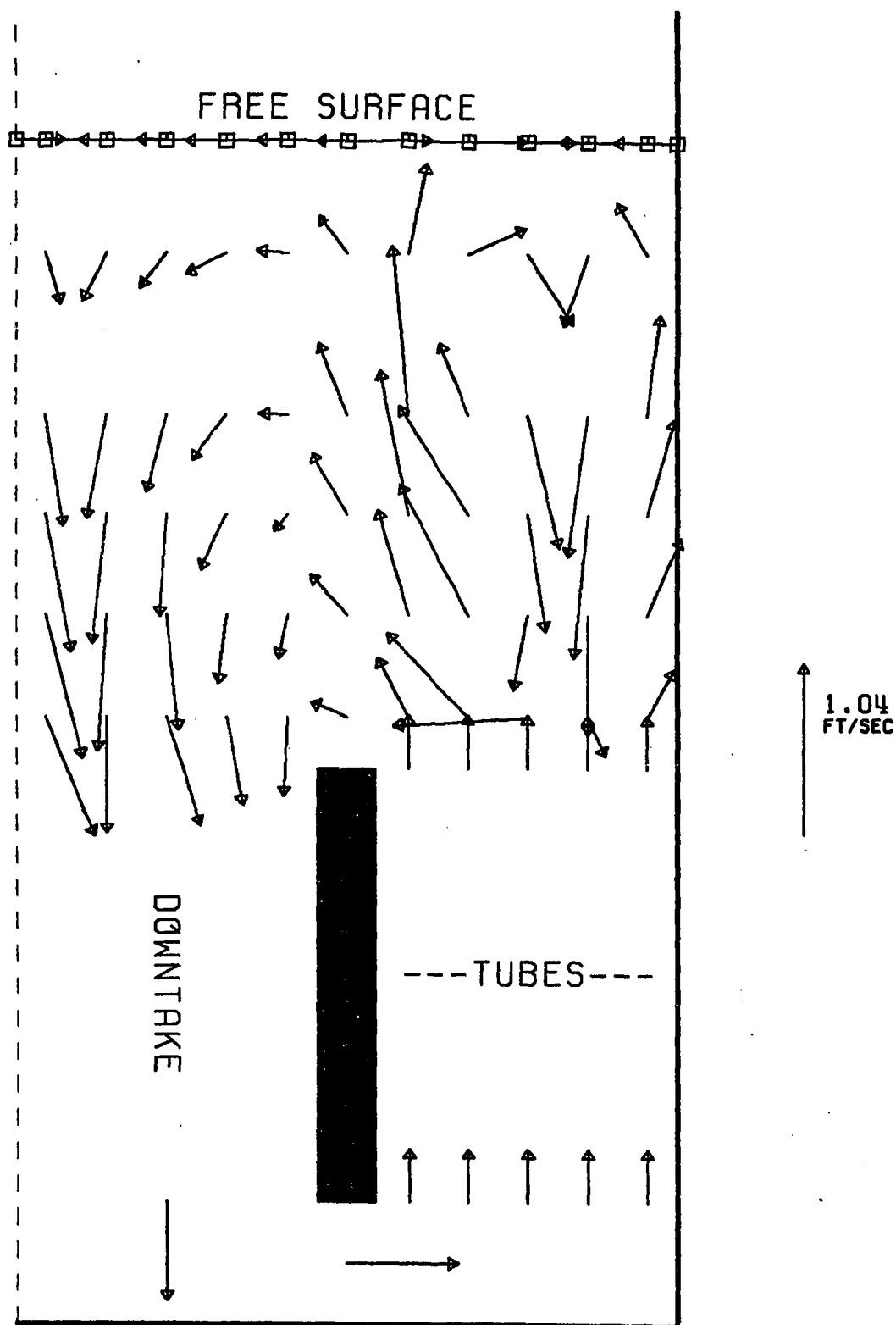
PAN	WVOL (FT ³)	HMAX (FT)	Dp (FT)	Dc (FT)	$\frac{Dd}{Dc}$ %	$\frac{AREAT}{WVOL}$	TUBES		
							NTUBES	TUBED (IN)	TUBEH (FT)
A	1200	12.1	12	12	45.5	1.5	343	5	4
B	1200	12.4	12	12	36.4	1.5	343	5	4
C	955	10.0	12	10.9	40.0	1.5	455	4	3
D	1200	12.2	12	12	50.0	1.4	356	4.5	4

TABLE 5.2.2: LOG OF MODEL RUNS VARYING
PAN DESIGN AND OPERATING CONDITIONS

CASE	PAN	BRIX	PURITY	HEAT RATE ($\frac{\text{BTU}}{\text{HR}}$) $\times 10^7$	P (PSIA)	CRYSTALS		LEVEL	
						γ_c	L (FT) $\times 10^{-4}$	% MAX	ABOVE CALANDRIA (FT)
1	A	.800	.94	2.69	2.00	.181	3.28	90	5.79
2	A	.800	.94	2.69	2.00	.181	3.28	75	3.98
3	B	.800	.94	2.69	2.00	.181	3.28	90	5.79
4	A	.800	.90	2.69	2.00	0	0	90	5.79
5	A	.824	.94	2.69	3.72	.181	3.28	90	5.79
6	A	.800	.94	1.35	2.00	.181	3.28	90	5.79
7	A	.800	.90	1.35	2.00	0	0	90	5.79
8	C	.800	.94	2.14	2.00	.181	3.28	90	5.00
9	C	.800	.94	2.14	2.00	.181	3.28	81	4.10
10	D	.800	.94	2.51	2.00	.181	3.28	90	5.79
11	A	.800	.94	2.69	3.72	.181	3.28	90	5.79
12	A	.824	.70	.553	2.00	.183	3.28	90	5.79

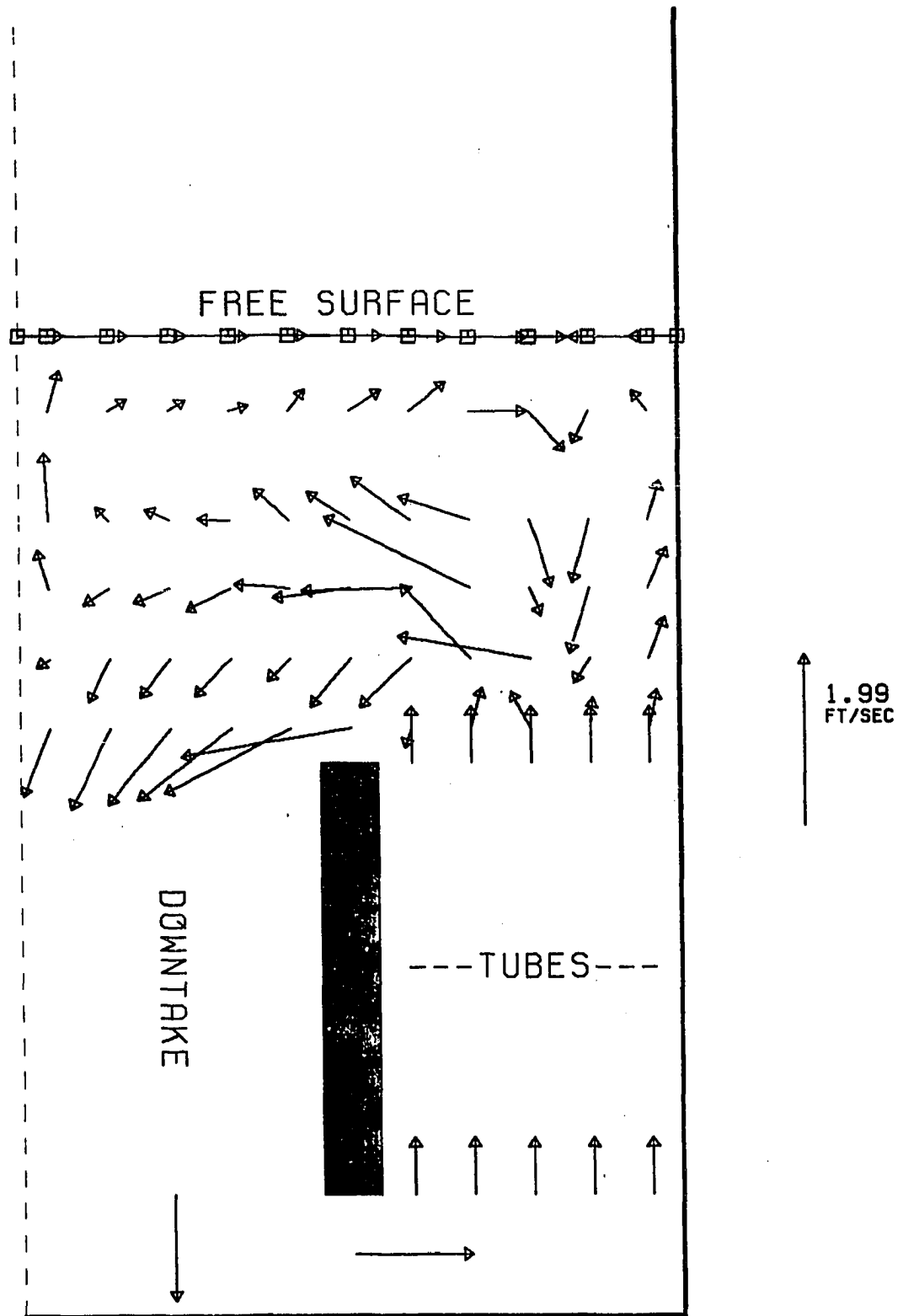
TABLE 5.2.3: SUMMARY OF MODEL RESULTS

CASE	PAN	SUPERSATURATION					VOL. AV. ρ ($\frac{LB}{FT^3}$)	VOL. AV. T ($^{\circ}F$)	RECIR. RATE ($\frac{LB}{HR}$) $\times 10^6$	AV. VEL. TUBES ($\frac{FT}{SEC}$)
		VOL. AV.	VOL. AV. σ^2 $\times 10^{-3}$	MAX.	MIN.					
1	A	1.300	1.13	1.339	1.241	89.83	139.6	4.47	.298	
2	A	1.284	1.18	1.339	1.231	89.79	141.6	9.21	.612	
3	B	1.299	1.20	1.339	1.237	89.83	139.7	4.18	.278	
4	A	1.305	.522	1.339	1.269	87.79	138.9	13.3	.976	
5	A	1.283	1.51	1.330	1.219	90.12	165.4	5.05	.335	
6	A	1.311	.651	1.339	1.264	89.86	138.3	2.95	.196	
7	A	1.315	.372	1.339	1.283	87.82	137.8	4.21	.286	
8	C	1.301	1.37	1.339	1.220	89.83	139.5	2.91	.229	
9	C	1.279	2.36	1.339	1.184	89.78	142.1	3.05	.240	
10	D	1.297	1.27	1.339	1.226	89.82	140.0	3.60	.286	
11	A	1.094	1.29	1.141	1.032	89.32	164.8	6.12	.409	
12	A	1.310	.300	1.326	1.275	90.67	138.5	1.47	.097	



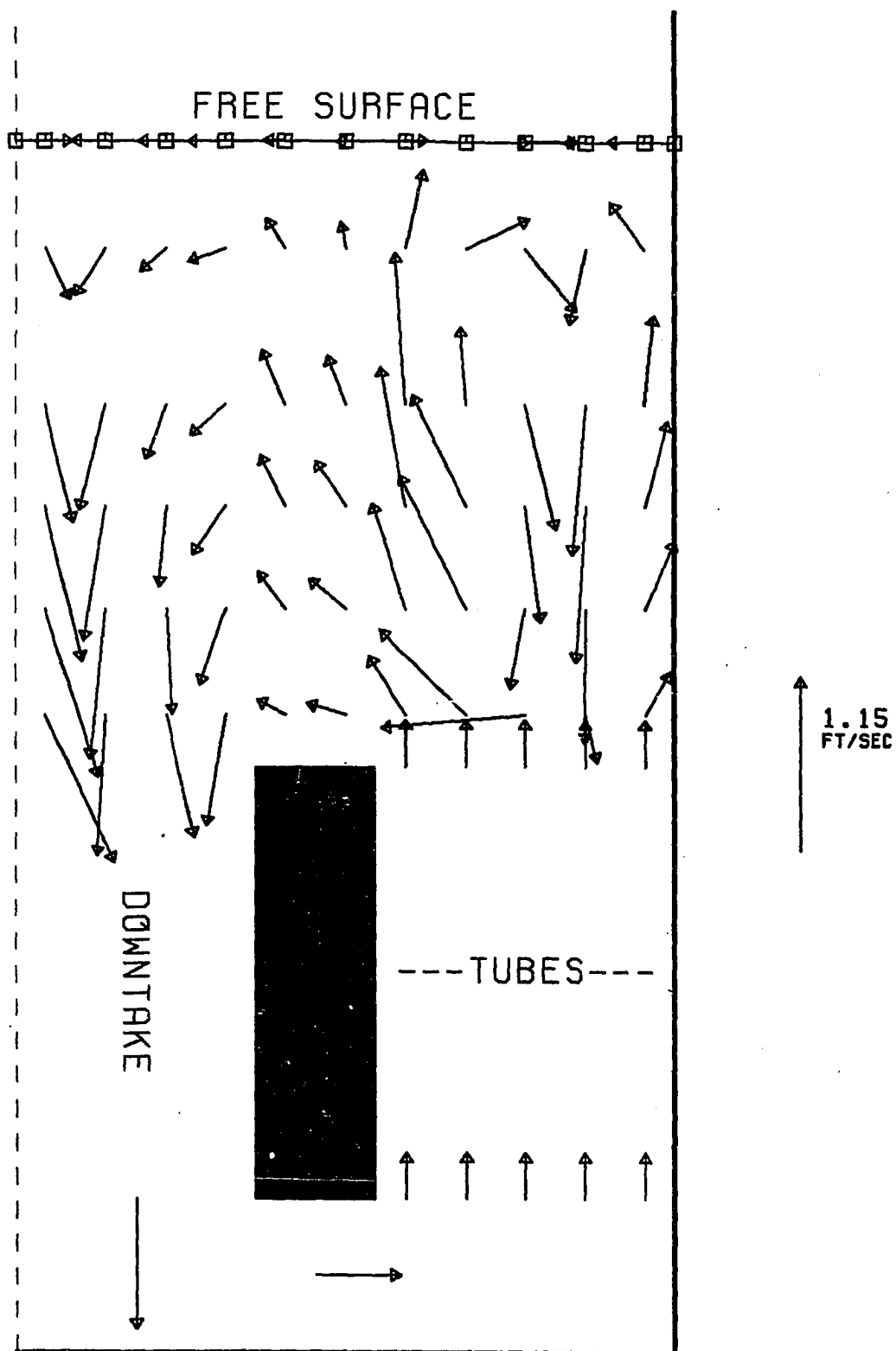
VELOCITY VECTORS
Base Case For Study

FIGURE 5.2.1 (1)

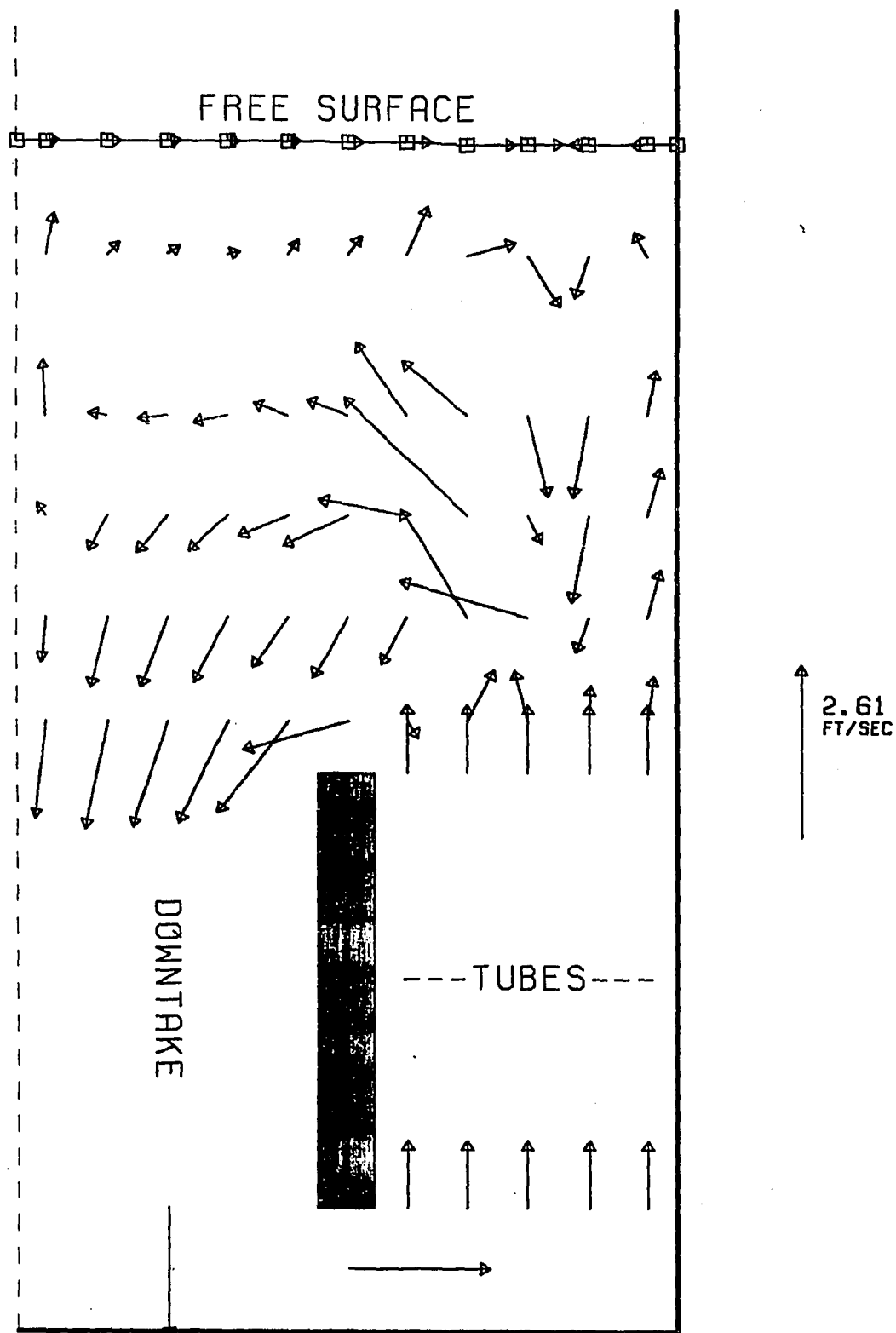


VELOCITY VECTORS
Effect of Reduced Level

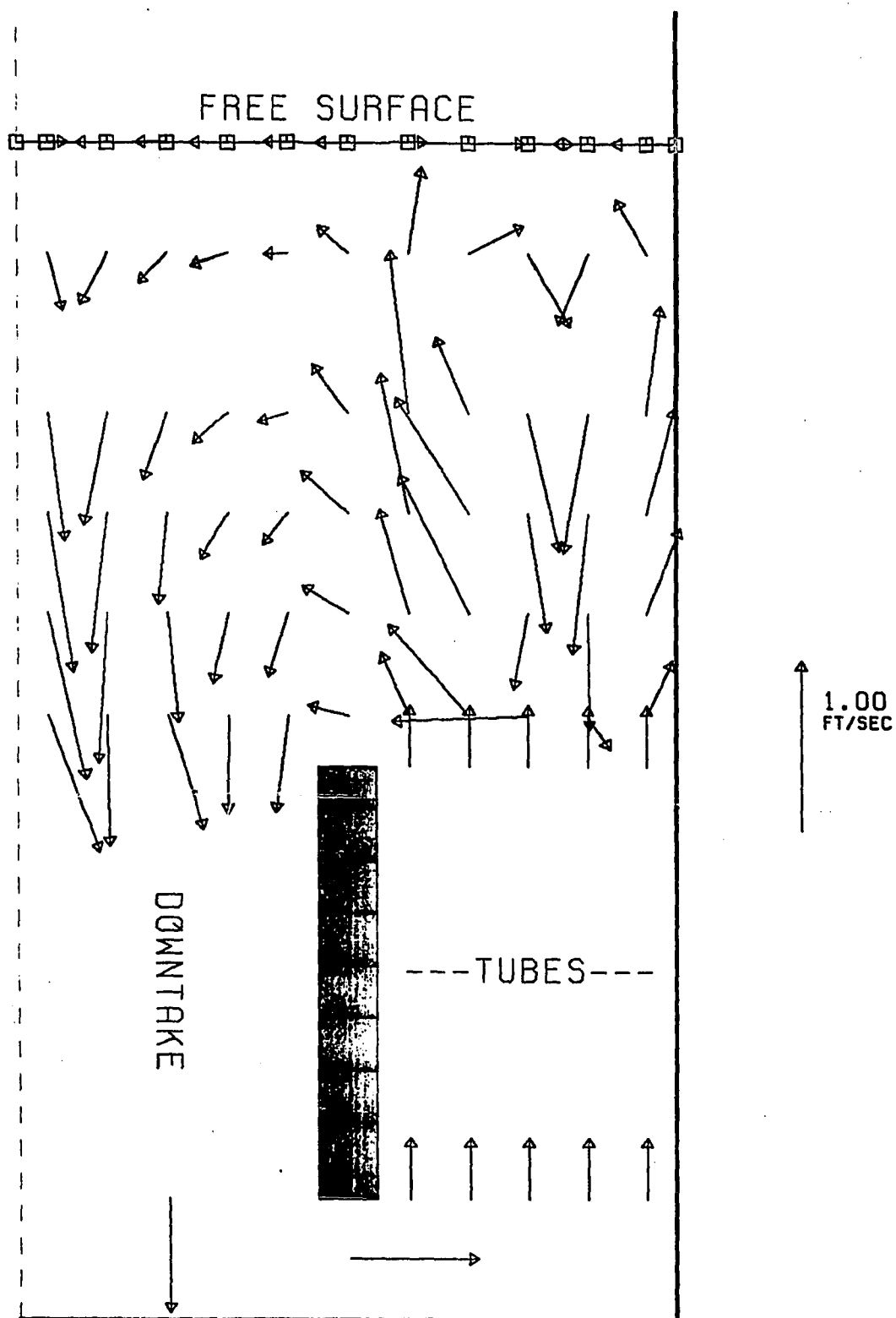
FIGURE 5.2.1 (2)



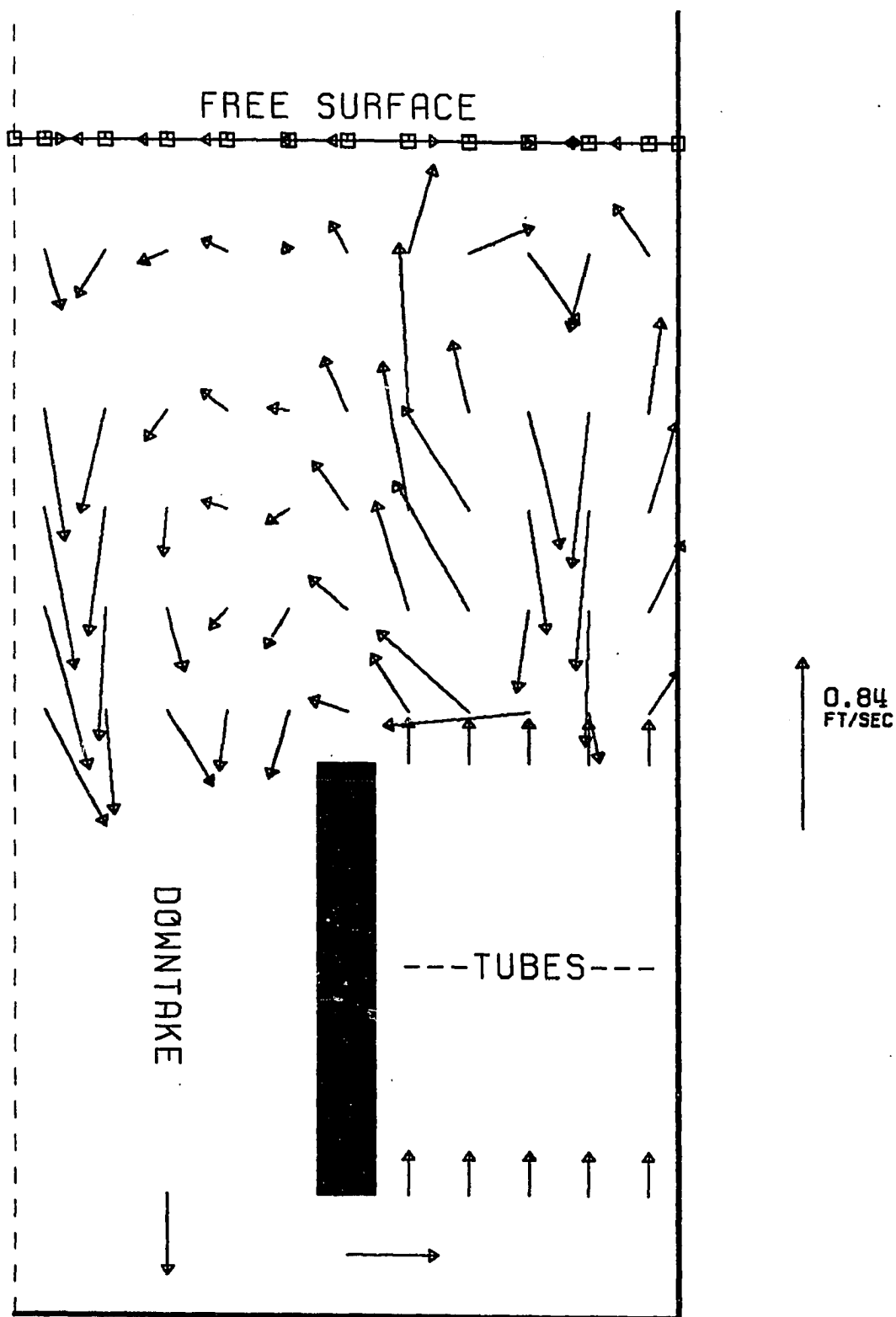
VELOCITY VECTORS FIGURE 5.2.1 (3)
Effect of Reduced Downtake Diameter



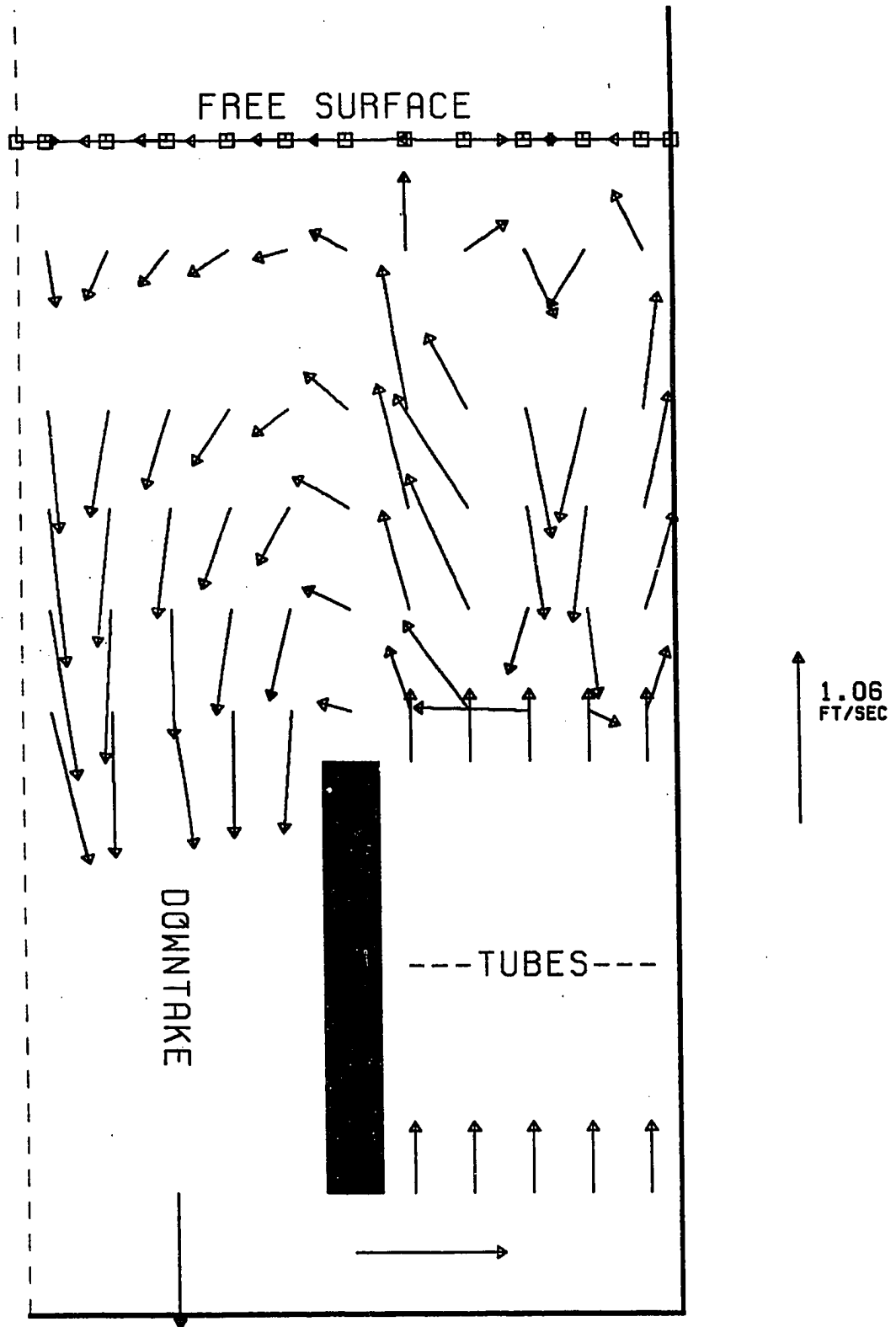
VELOCITY VECTORS FIGURE 5.2.1 (4)
Effect of Reduced Volume Fraction Crystals



VELOCITY VECTORS FIGURE 5.2.1 (5)
Effect of Increased Pressure and Increased Brix



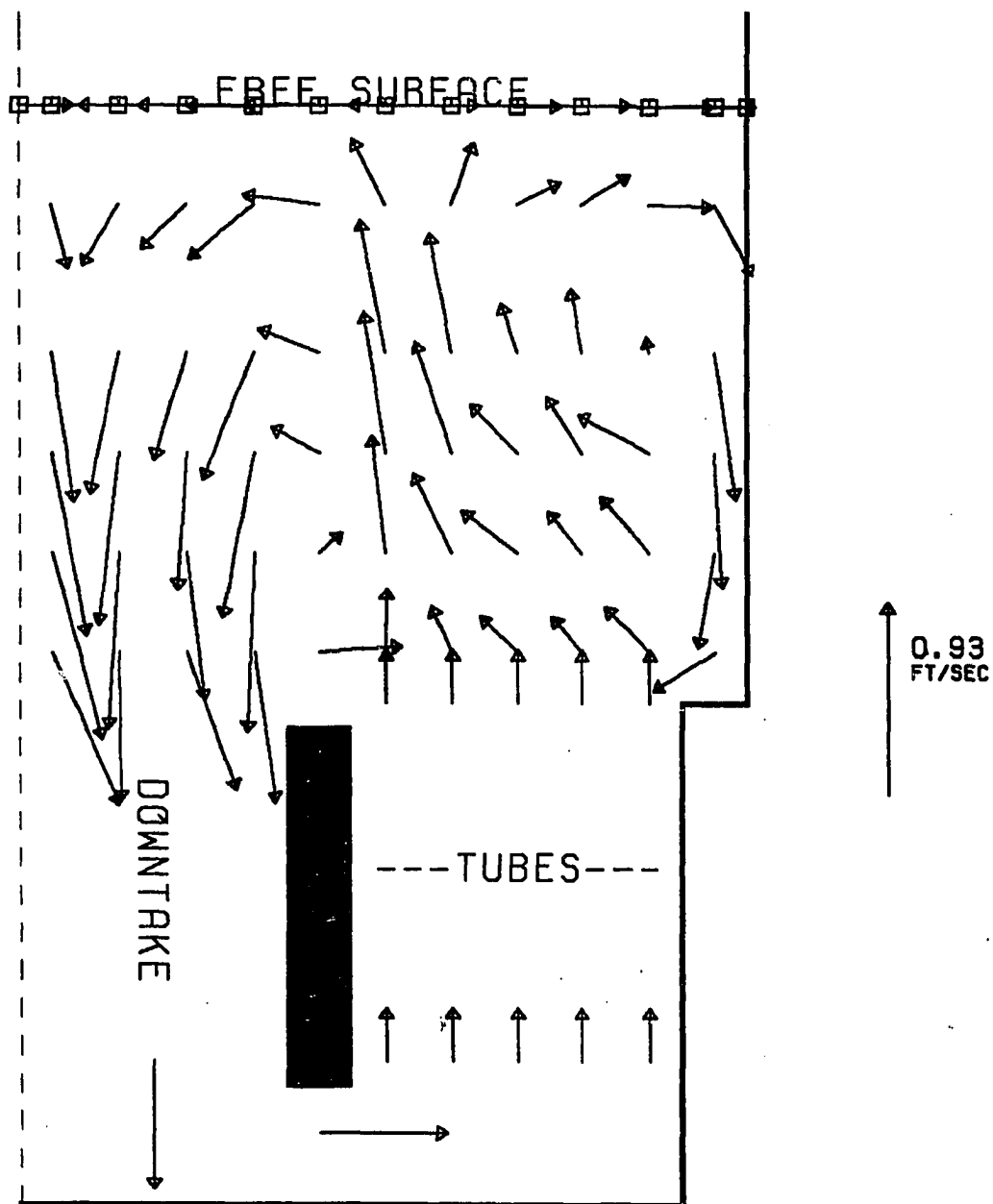
VELOCITY VECTORS FIGURE 5.2.1 (6)
Effect of Reduced Heat Input



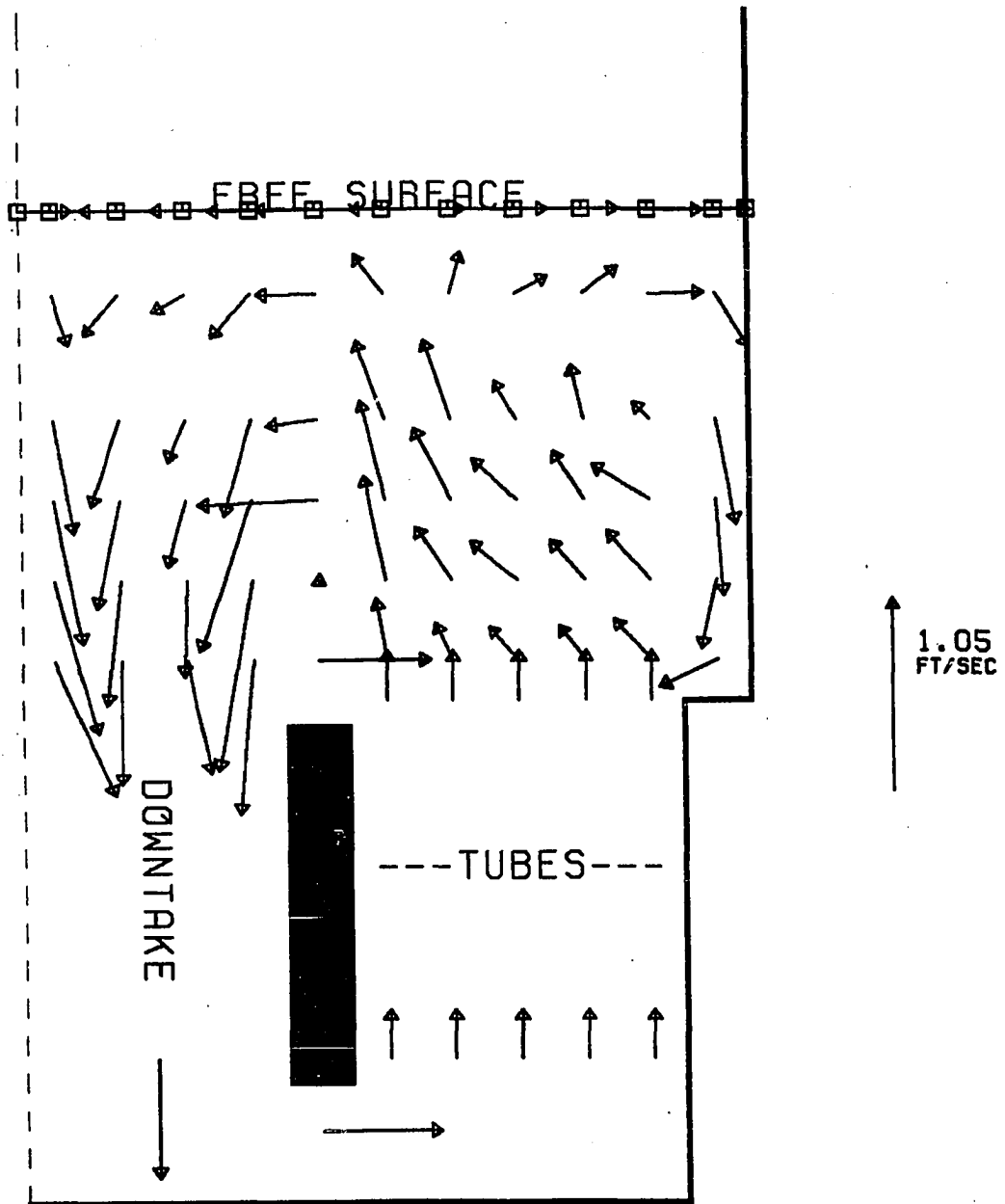
VELOCITY VECTORS

FIGURE 5.2.1 (7)

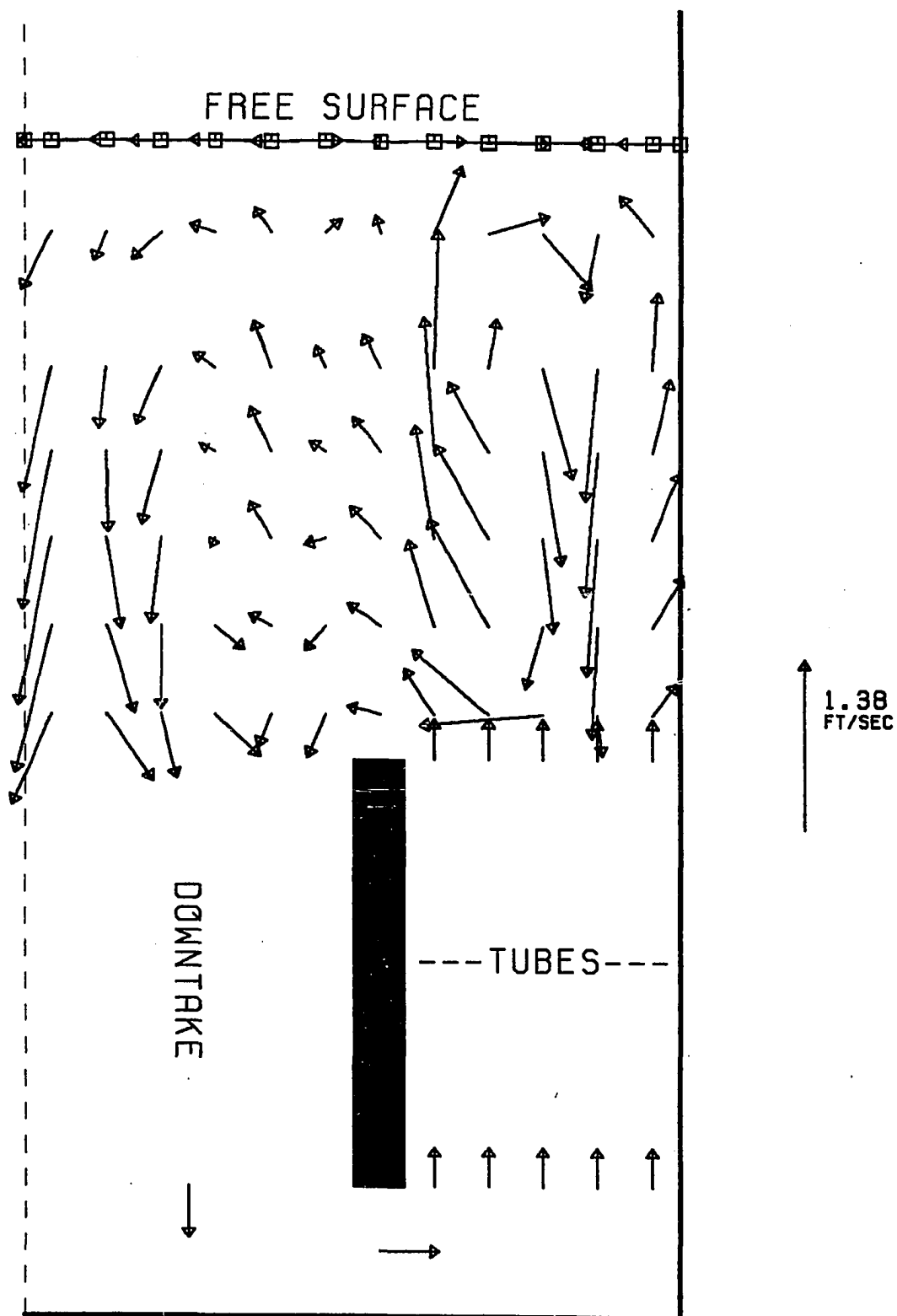
Effect of Reduced Heat Input and Reduced Volume
Fraction Crystals



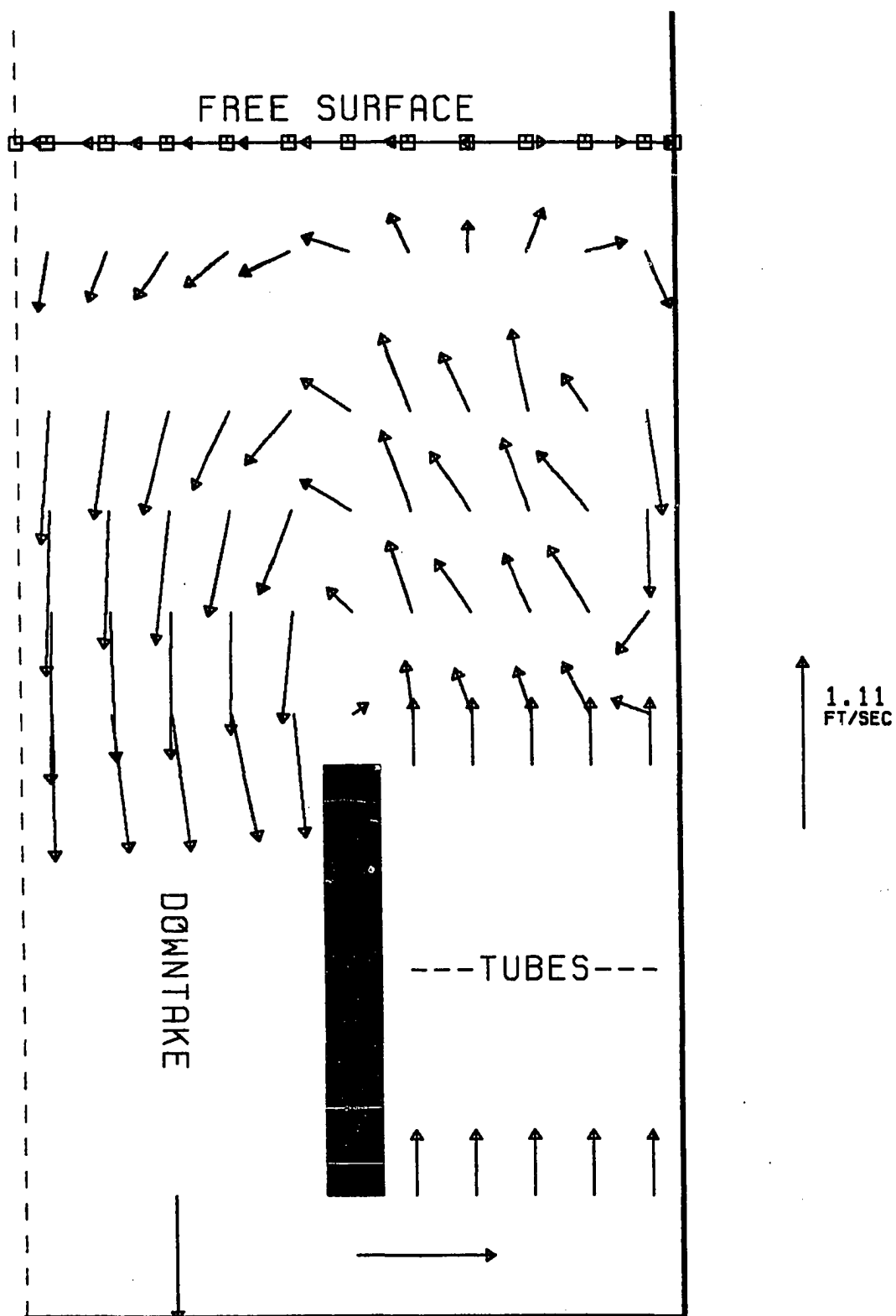
VELOCITY VECTORS FIGURE 5.2.1 (8)
Effect of Increased Major Pan Diameter



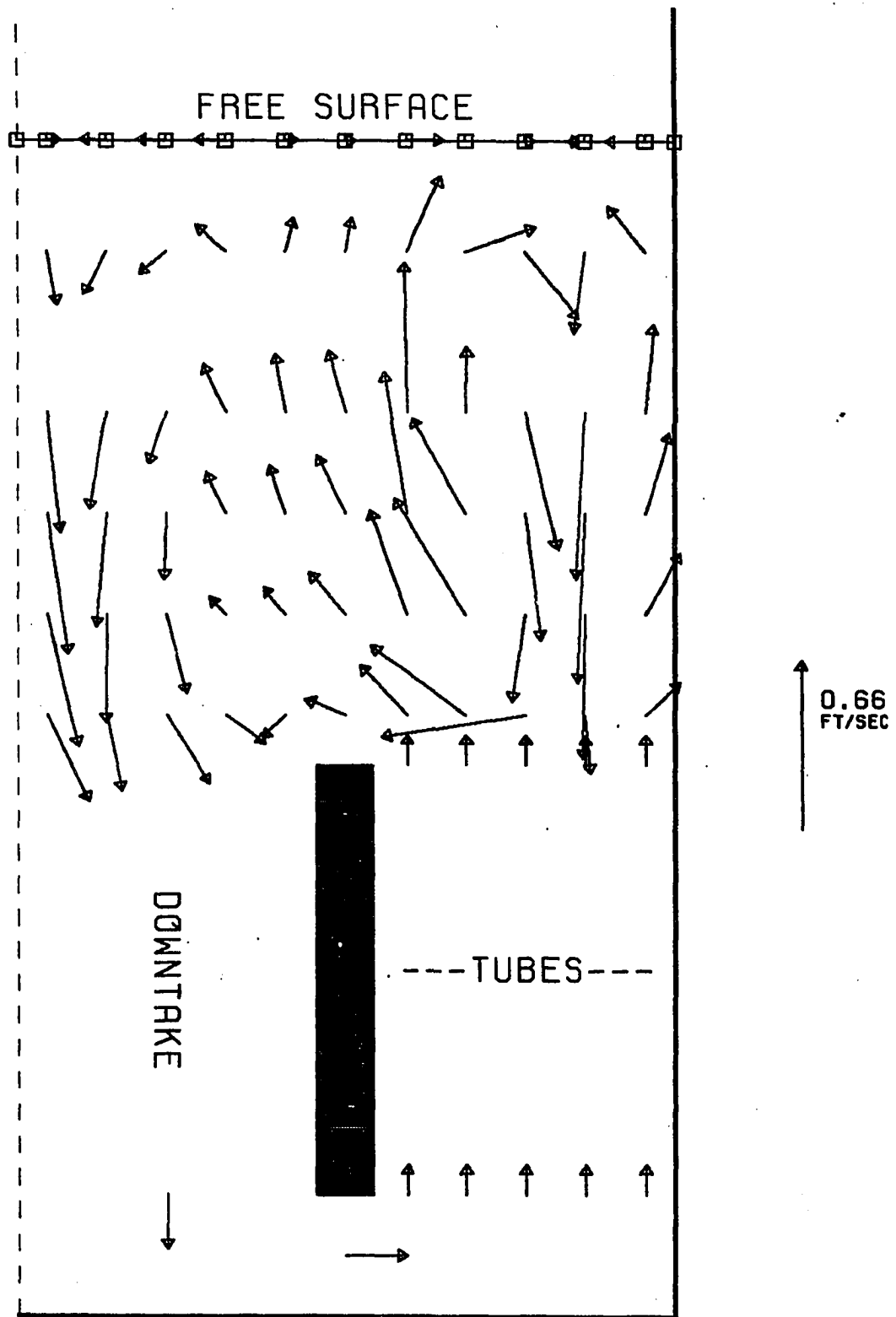
VELOCITY VECTORS FIGURE 5.2.1 (9)
Effect of Increased Major Pan Diameter and
Reduced Level



VELOCITY VECTORS FIGURE 5.2.1 (10)
Effect of Increased Downtake Diameter

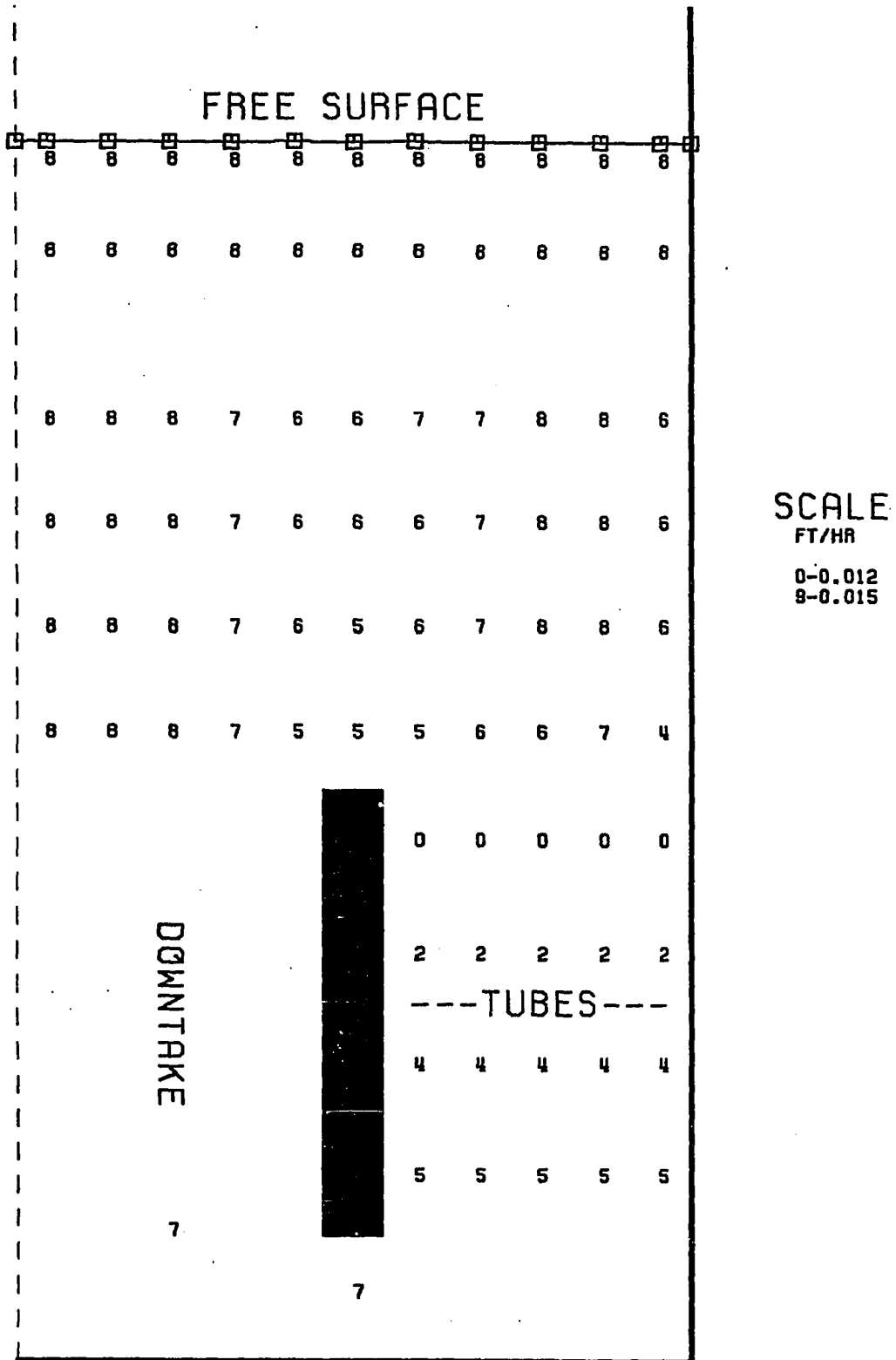


VELOCITY VECTORS FIGURE 5.2.1 (11)
 Effect of Increased Pressure and Reduced
 Supersaturation

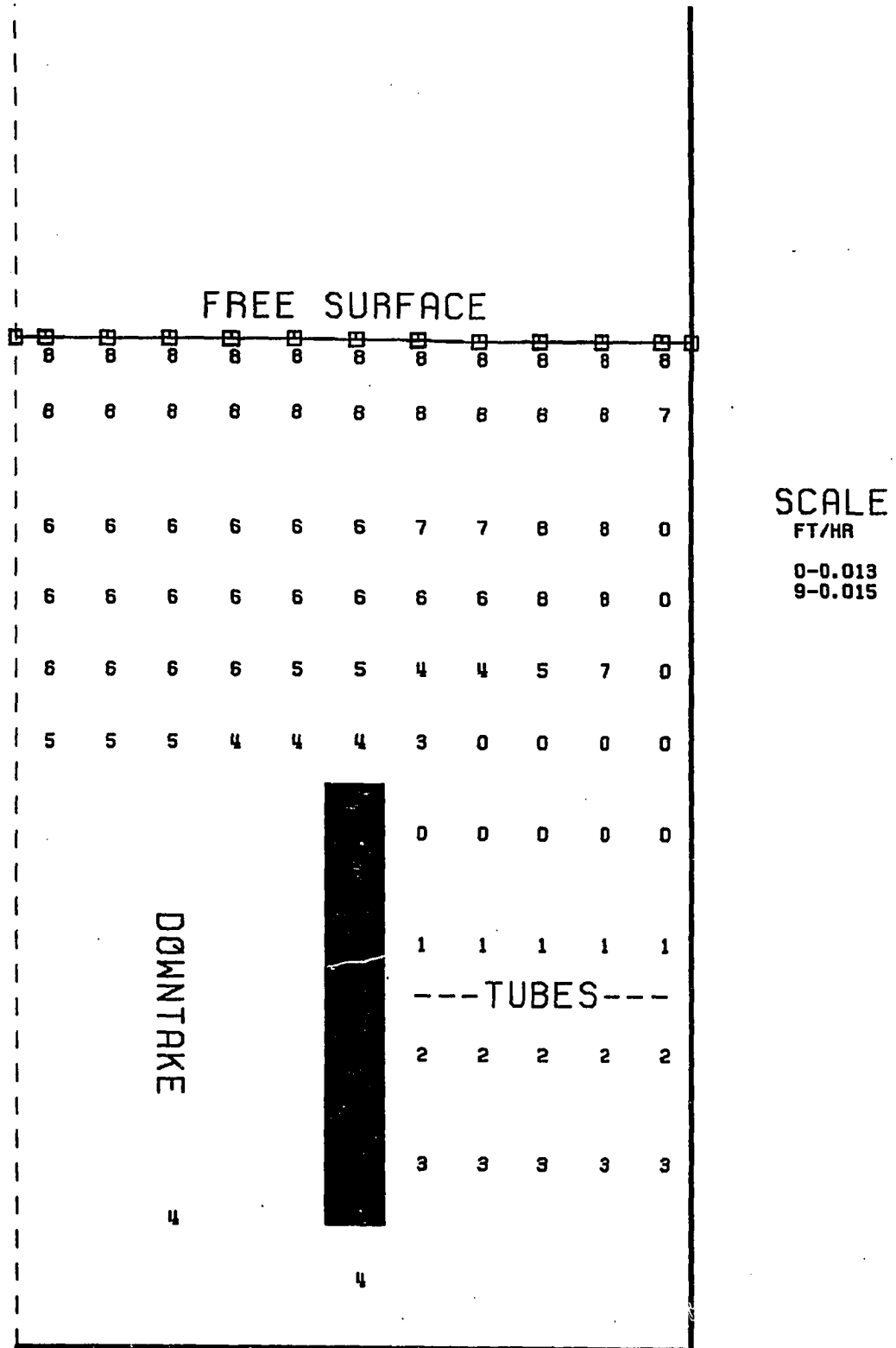


VELOCITY VECTORS
Effect of Low Purity

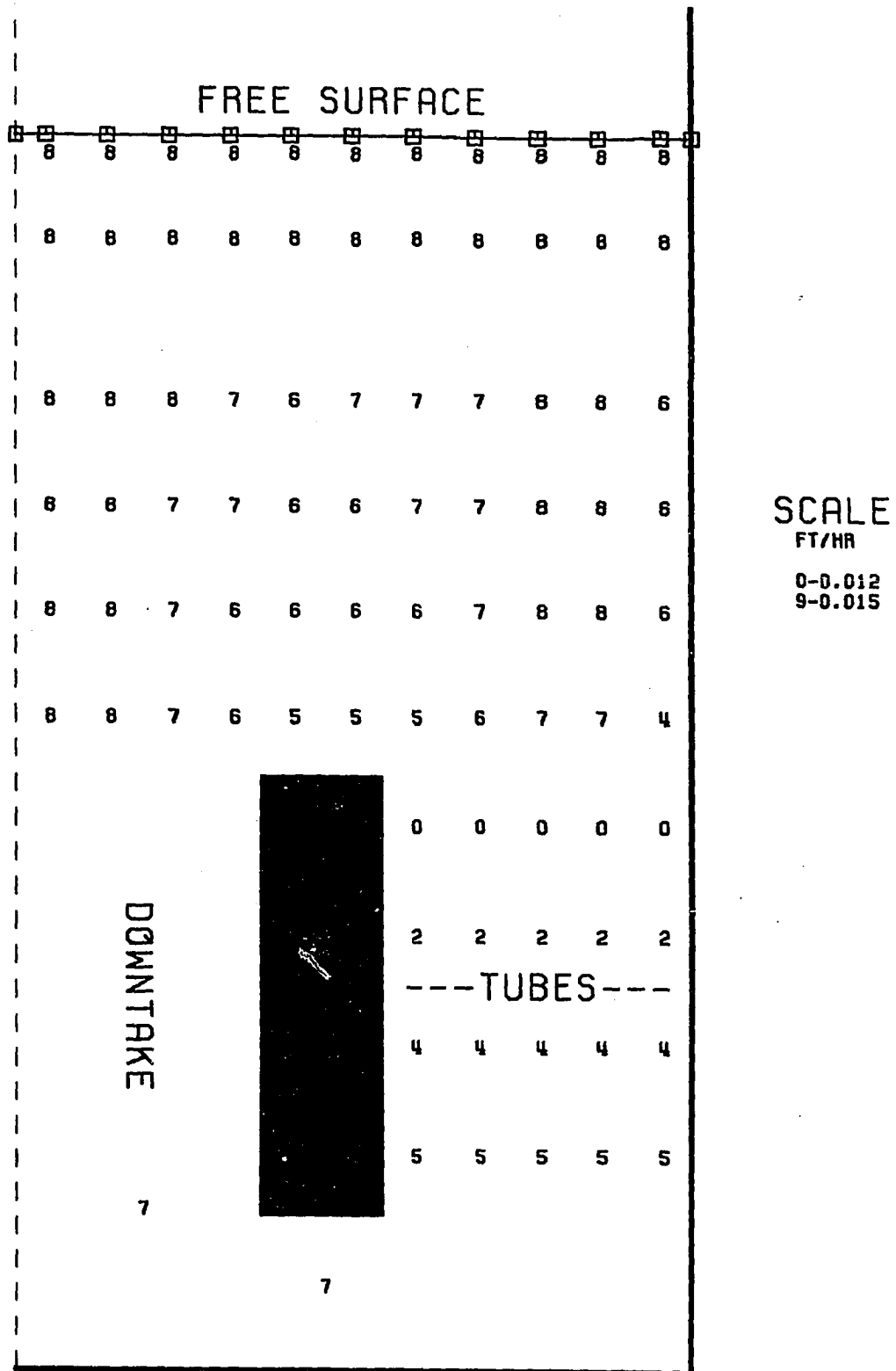
FIGURE 5.2.1 (12)



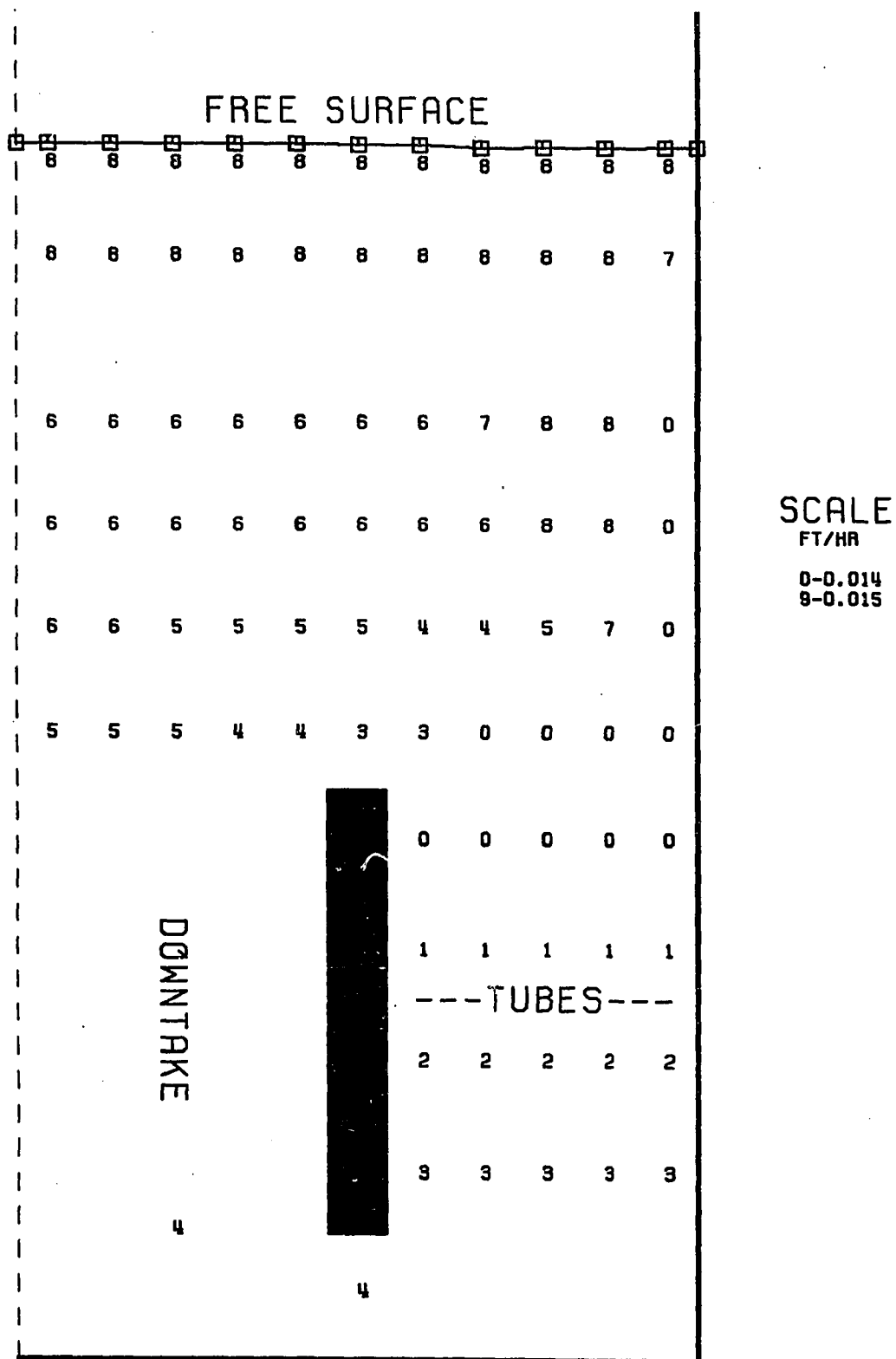
GROWTH PROFILE **FIGURE 5.2.2 (1)**
Base Case For Study



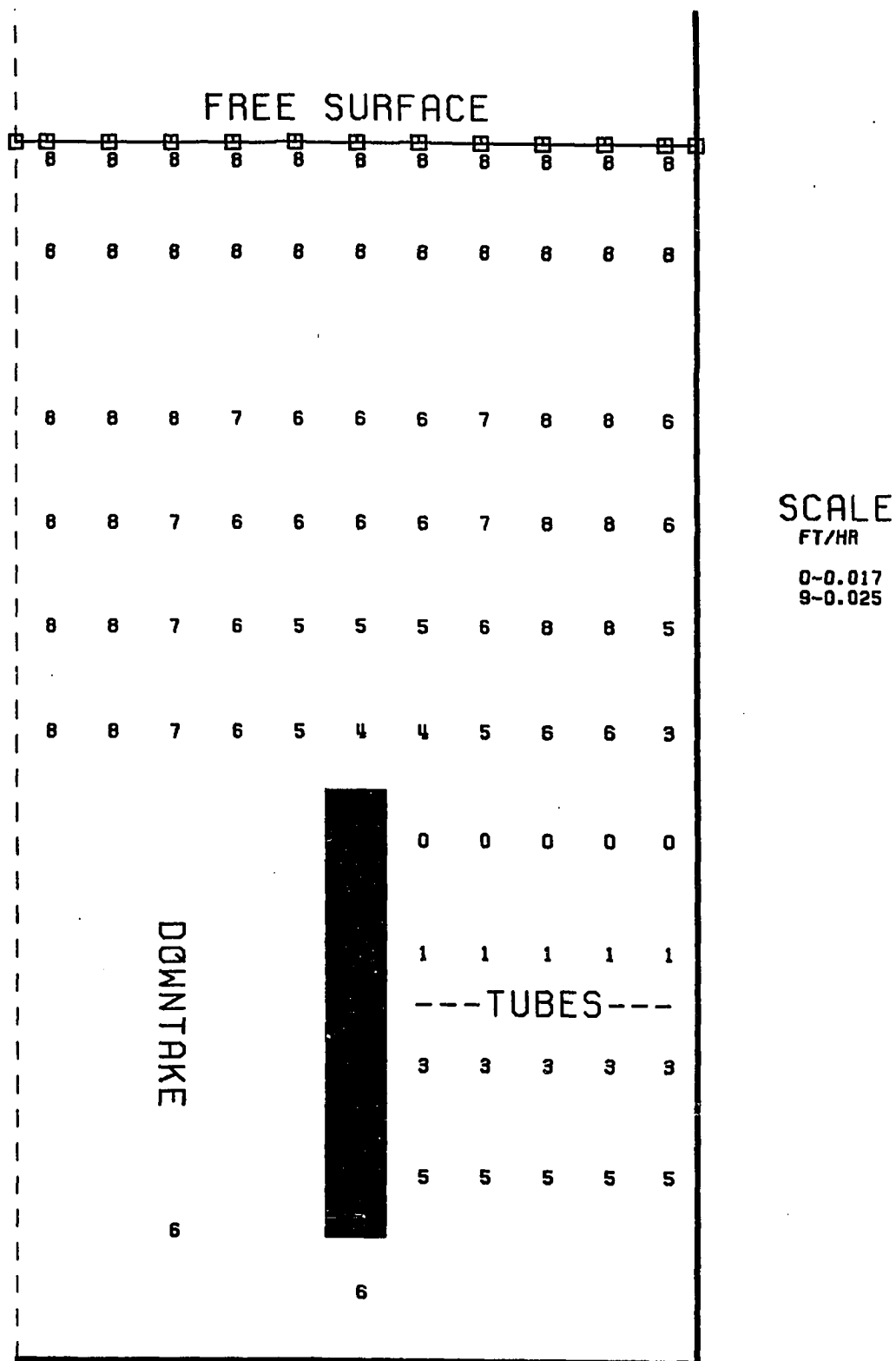
GROWTH PROFILE FIGURE 5.2.2 (2)
Effect of Reduced Level



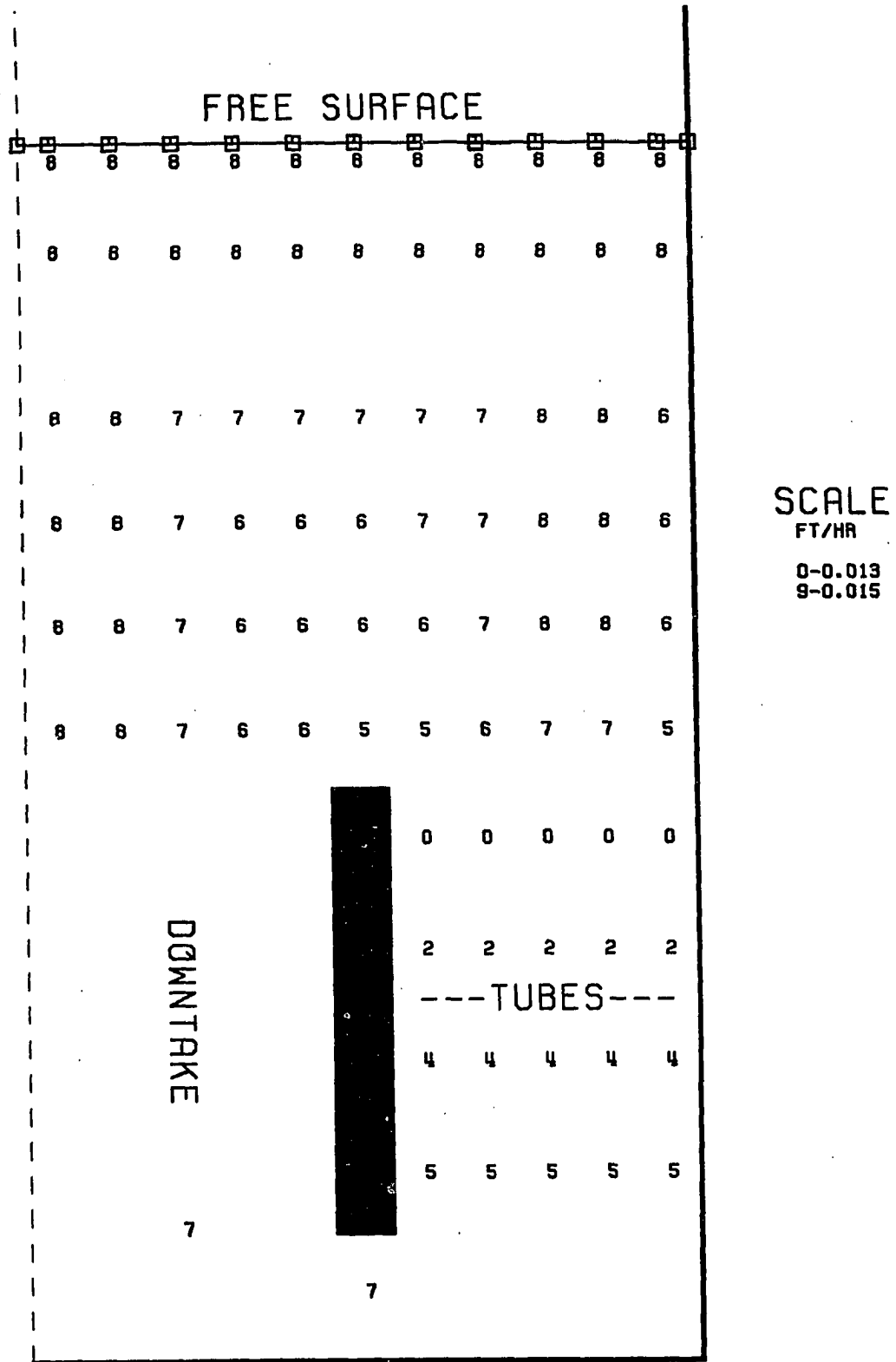
GROWTH PROFILE FIGURE 5.2.2 (3)
Effect of Reduced Downtake Diameter



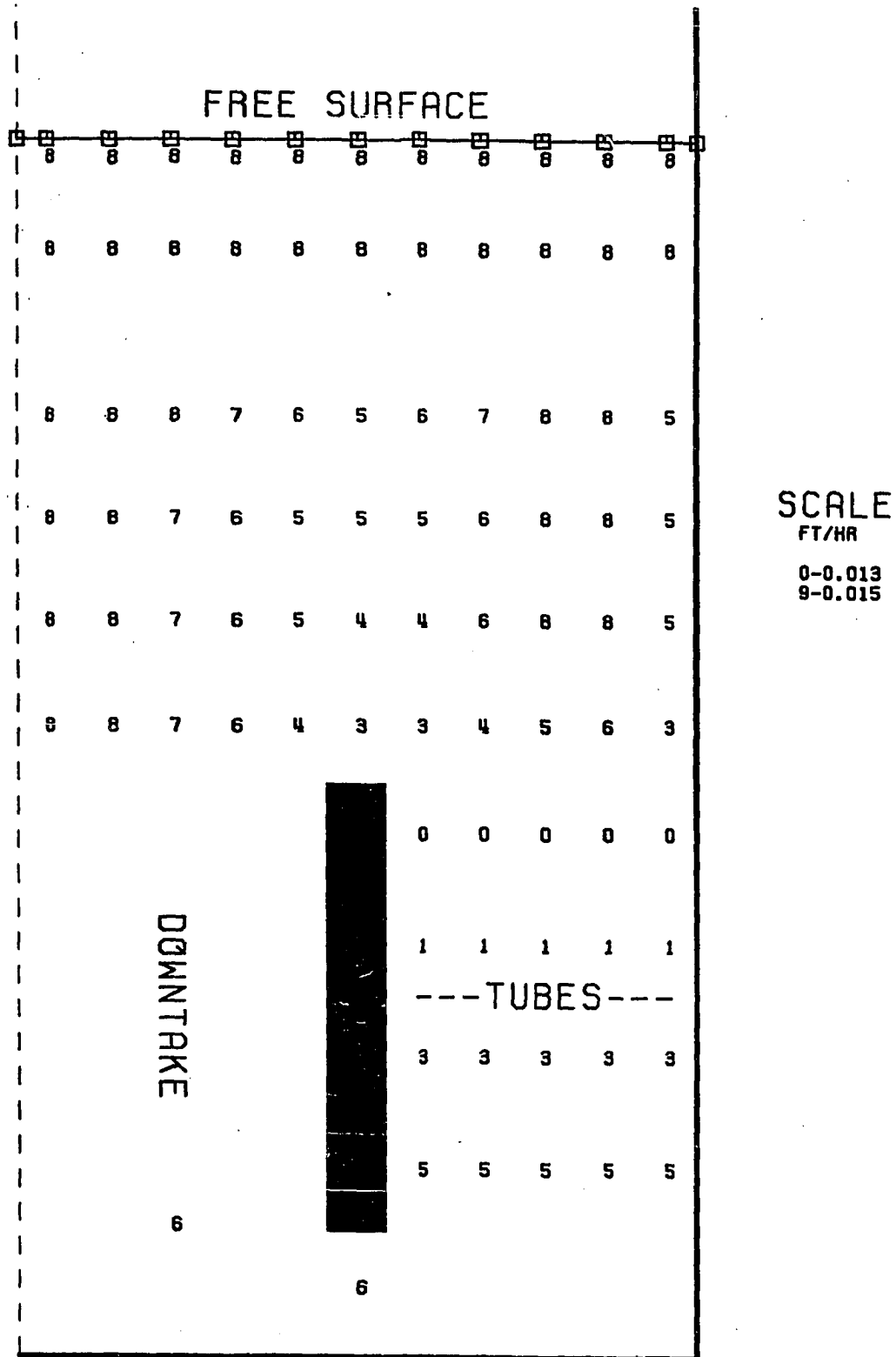
GROWTH PROFILE FIGURE 5.2.2 (4)
Effect of Reduced Volume Fraction Crystals



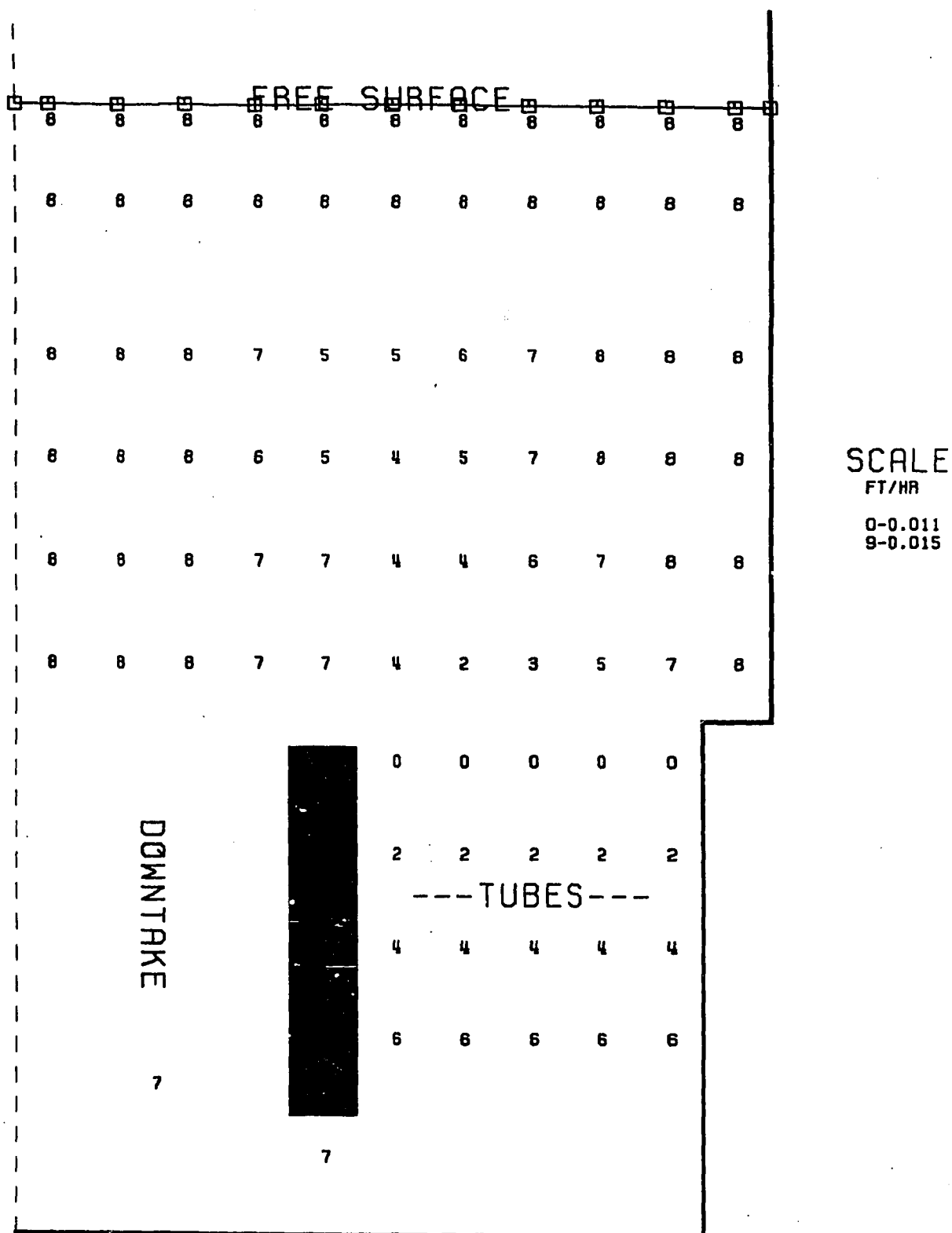
GROWTH PROFILE FIGURE 5.2.2 (5)
Effect of Increased Pressure and Increased Brix



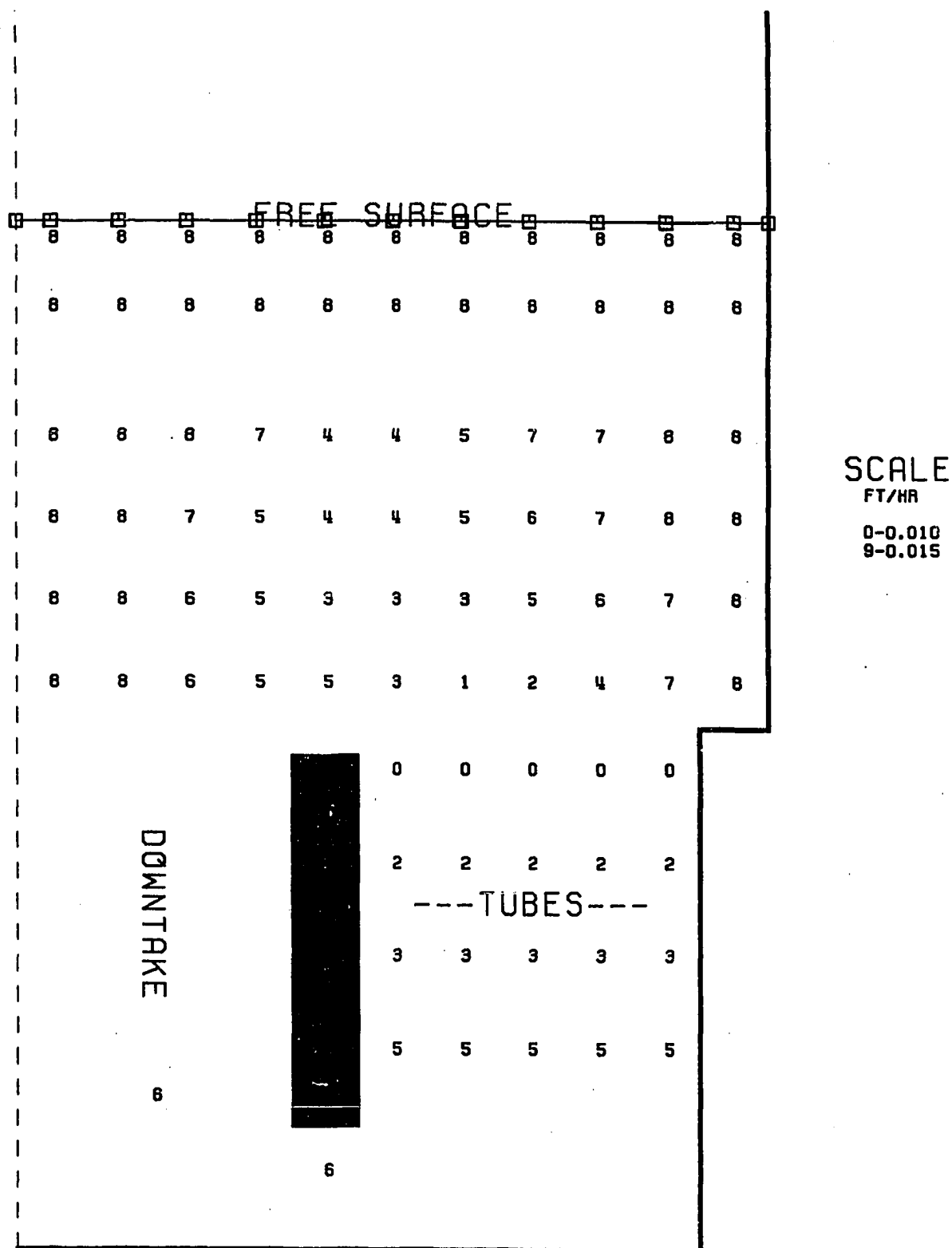
GROWTH PROFILE FIGURE 5.2.2 (6)
Effect of Reduced Heat Input



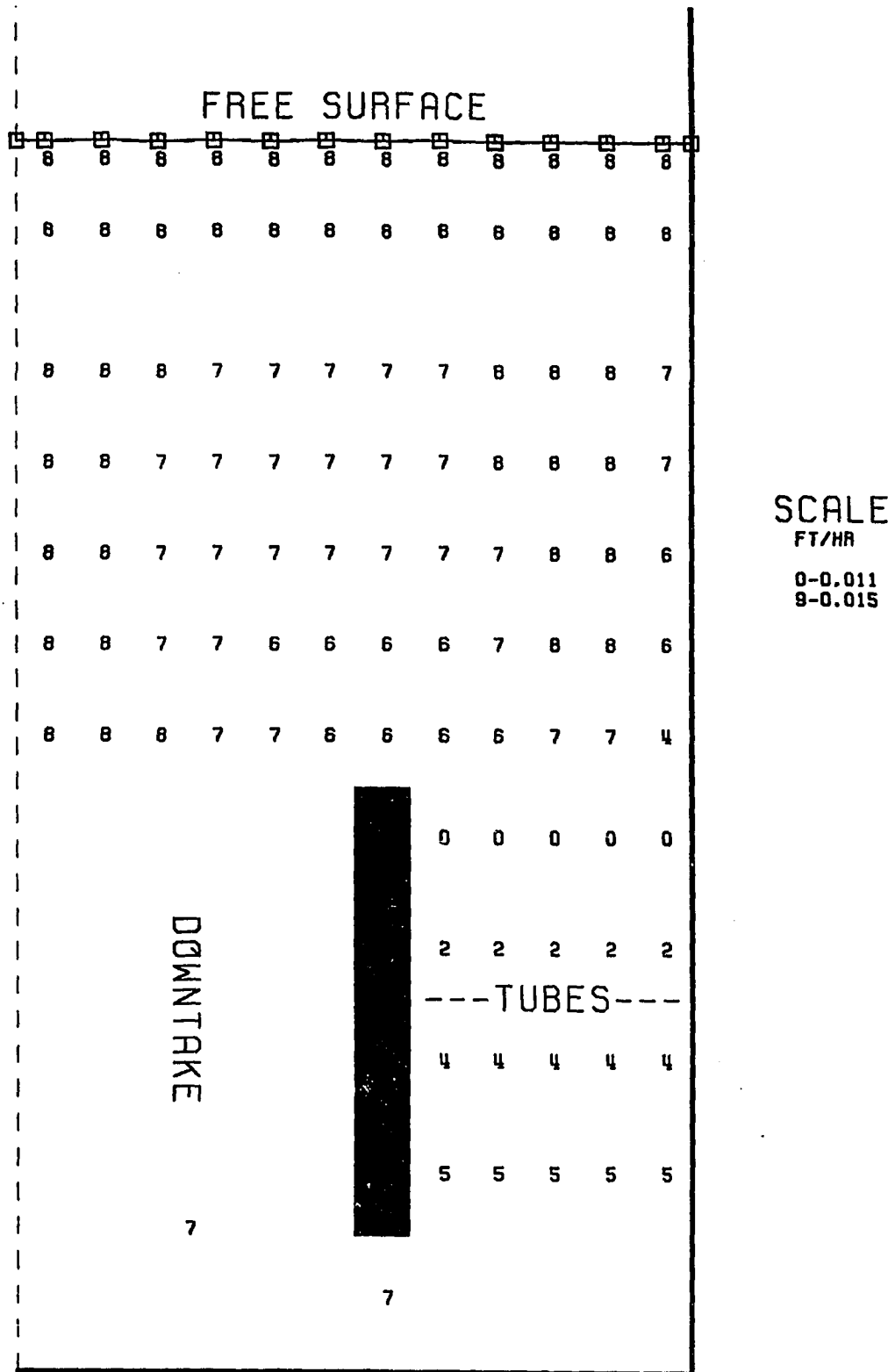
GROWTH PROFILE FIGURE 5.2.2 (7)
Effect of Reduced Heat Input and Reduced Volume
Fraction Crystals



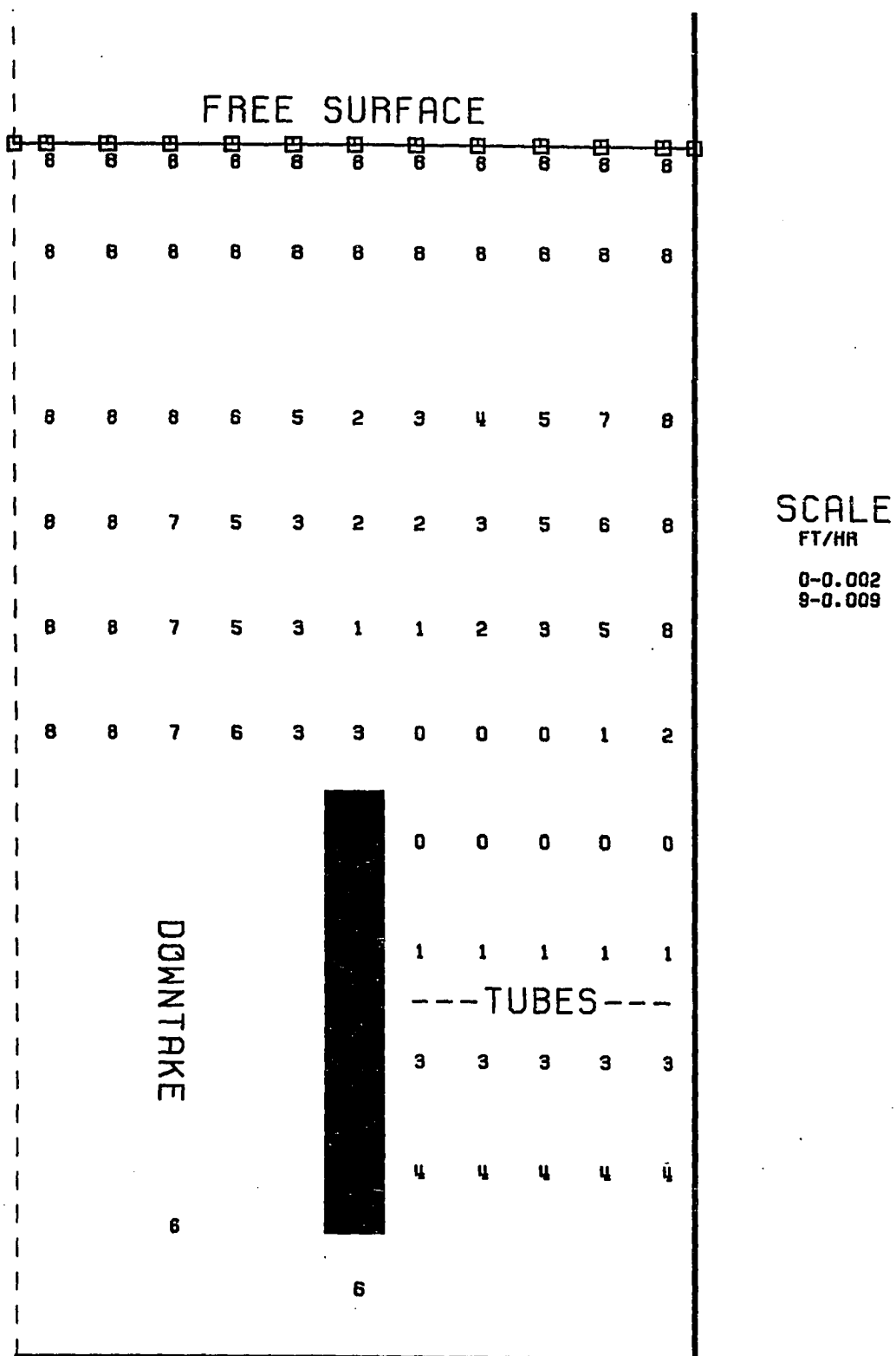
GROWTH PROFILE **FIGURE 5.2.2 (8)**
Effect of Increased Major Pan Diameter



GROWTH PROFILE **FIGURE 5.2.2 (9)**
Effect of Increased Major Pan Diameter and
Reduced Level

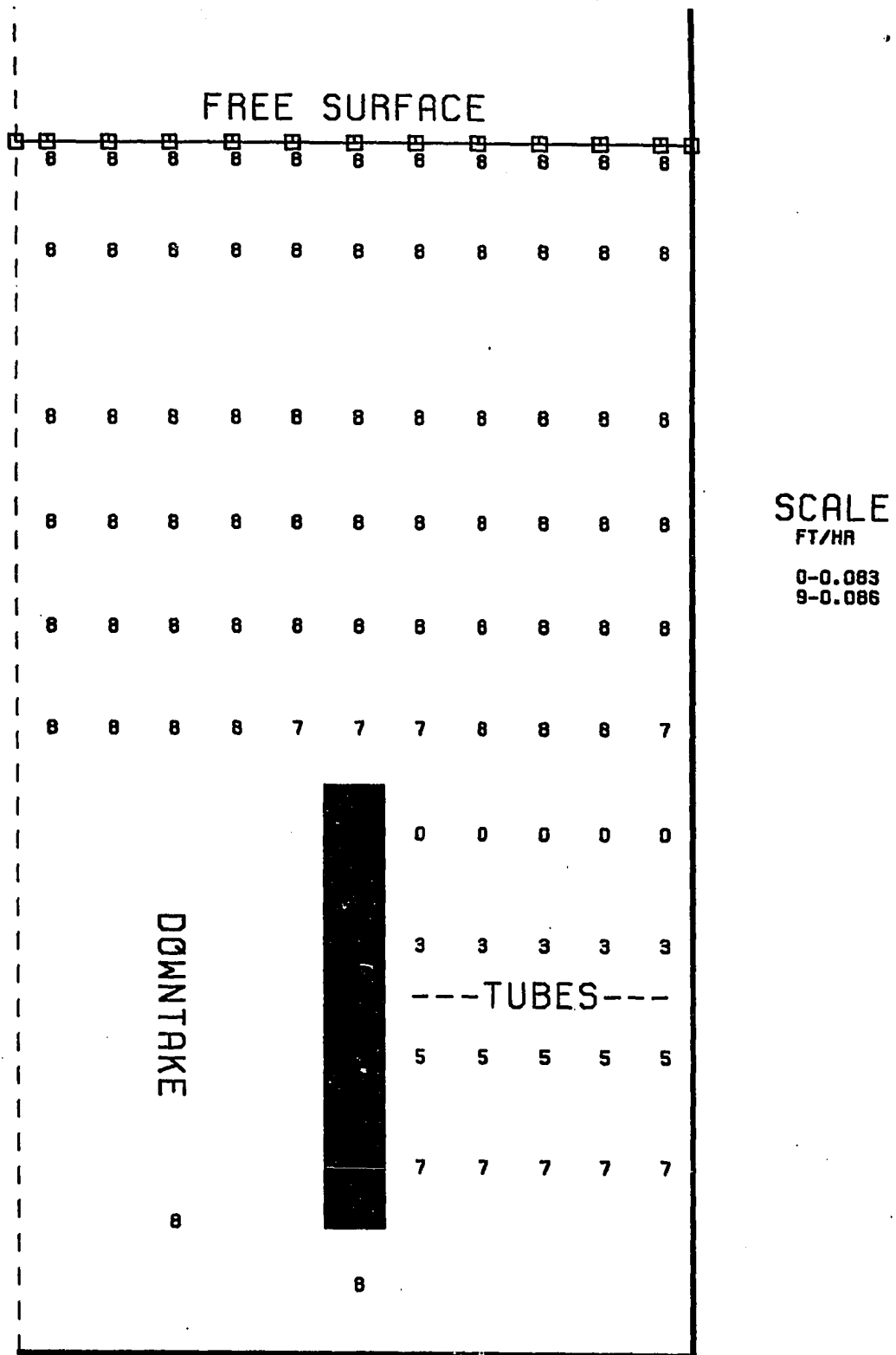


GROWTH PROFILE FIGURE 5.2.2 (10)
Effect of Increased Downtake Diameter



GROWTH PROFILE FIGURE 5.2.2 (11)

Effect of Increased Pressure and Reduced
Supersaturation



GROWTH PROFILE FIGURE 5.2.2 (12)
Effect of Low Purity

5.3 COMPARISON OF PREDICTED TUBE VELOCITIES AGAINST LITERATURE

Verification of the fluid mechanics at this point is important because Pan recirculation and flow patterns are determined by density differences, which in turn, are a function of the thermodynamic state, which in turn, is a function of the flow of momentum and energy. Thus, verification of the flow pattern inherently verifies the temperature profiles which are important for calculating supersaturation profiles. However, difficulty arises in the verification of the model because data in the literature are not in sufficient detail and are few in number. Most of the data in the literature concerning flow profiles and velocity in the tubes are summarized in Honig (1963) and also in Hugot (1972).

In 1934, Webre measured the velocity in the tubes as a function of time during a batch production of C raw cane sugar by using two sensitive thermometers and a heat balance. Webre's work is summarized in Table 5.3.1. Webre calculated the velocity in the tubes from only sensible heat changes in the massecuite rising up the tubes neglecting any vaporization. Thus, his calculation over estimates the velocity in tubes when boiling occurs. With this in mind, the criticism of Webre's pan in the literature as being extremely fast for C massecuite may be justified.

Nonetheless, Webre's data as an order of magnitude illustration of the velocity in the tubes are useful. His data should be reasonably accurate for the later time intervals when boiling is less probable.

Hugot also summarizes some of the tube velocities reported by Clausen, for beet sugar, using a hot wire anemometer. Table 5.3.2 summarizes those data. The data are presented as typical tube velocities that vary with batch time and purity of the massecuite.

Comparing the data presented in Tables 5.3.1 and 5.3.2, gives the reader an idea of the typical velocities expected in an operating pan. As shown in the tables, typical tube velocities in a Vacuum Pan may vary from 5.5 FT./SEC. in the early portions of a high grade A massecuite batch to almost zero at the end of the low grade C massecuite batch. Since the velocities are very dependent on the pan design and the operating conditions, especially heat load, which are not available in Hugot or the original articles, there is no real basis for comparison against a simulated case. Therefore, these data are not in sufficient detail to be used for a detailed verification of the model simulation. Nonetheless, Webre's and Clausen's data do illustrate the velocity in a typical natural convecting Vacuum Pan and since the cases presented earlier in Table 5.2.3 do also, there is a basis for comparison in terms of the order of magnitude.

Referring to Table 5.2.3, the predicted tube velocities vary from 1.0 FT./SEC. (Case 4), for a typical A or B grade massecuite to 0.1 FT./SEC. (Case 12), for a typical C massecuite. Since the model is not capable of simulating the early portions of the batch when the volume of massecuite is low and the volume fraction crystal is small, the velocities presented in Table 5.2.3 represent predictions resulting from conditions sometime after the first hour of operation of the Pan. This further restricts any comparisons of the predicted velocities against the literature. But, since the predicted velocities are within the correct range, this in itself is a favorable comparison. Reproducing the data in the literature is impossible without total specification of all the conditions concerning the experiment. Obviously, the data in the literature were not collected to verify a model such as this one because the essential information was omitted.

TABLE 5.3.1: WEBRE'S DATA

MASSECUITE PURITY		VELOCITY (FT/SEC)			
		1st hr.	2nd hr.	3rd hr.	6th hr.
C	60	1.53	0.63	0.15	0.01

TABLE 5.3.2: CLAUSEN'S DATA

MASSECUITE PURITY		VELOCITY (FT/SEC)	
		at the start	at the finish
A	96	3.3-5.5	0.72
B	82	1.08-0.72	0.02

5.4 NUMERICAL PROBLEMS AND HYDROSTATIC HEAD ASSUMPTION

As mentioned earlier, some numerical problems occurred that prevented the simulation of the Pan during the early time intervals. This problem resulted because the explicit formulation of the mathematical model was unable to maintain a stable calculation when the flow is vigorously boiling, which is characteristic of the early time intervals of the batch. At the same time, it was observed that the hydrostatic head assumption that reduces the vertical momentum equation to a very simple form was in error because the inertial and the convective terms were obviously important. Instead of attempting a serious reprogramming effort it was, at this point, decided to proceed with the demonstration of the use of the model, but limit its application to times where the stability problem did not occur. In essence, this limits the applicability of the model to the later time intervals of the batch. This limitation can be thought of as not a serious one, because problems associated with operation of the Vacuum Pan occur because of inadequate mixing and recirculation which are characteristic of the later time intervals. Thus, limiting the application of the model to the later time intervals is just where the model is needed the most.

As already mentioned above, the hydrostatic head

assumption may not adequately describe the pressure profiles in an operating Vacuum Pan. The possibility of this inadequacy was also discussed when the mathematical model was derived. In order to capitalize as much as possible on the experience developed to this point in working with the program, preliminary work was done with the explicit solution sequence and the full vertical momentum equation to see if a stable numerical solution can be obtained of flows where the inertial and convective terms are important. The crystallizer, of course, was used for the study. With the full momentum equation, the solution became immediately unstable at any time step. After taking out the inertial term the solution was initially stable, but as the Pan heating continued a rapidly accelerating vortex formed in the Pan not allowing much convection to the surface so the hot liquid could boil. Soon afterwards, sufficient heat had accumulated to cause vigorous boiling and the solution became unstable. The diffusion terms were also included in the vertical momentum equation but their effect was small as demonstrated earlier. It can only be concluded that the one-step explicit method is not sufficient as a solution method when the inertial terms and the convective terms are important as the result vigorous boiling. Multi-step or an implicit method should clear up the problem because this would allow the

pressure to affect the vertical and radial momentum at the same time. Implicit and mixed implicit-explicit methods are characteristic of most two-phase flow calculations in the literature because of the stiffness caused by sudden changes in density. Therefore, it should not be expected that the explicit method would work. However, fundamental research needs to be done to devise an implicit method that is efficient and convergent.

CHAPTER 6

DYNAMIC GRID

One of the distinguishing problems with numerically solving free surface problems, or generically speaking, time dependent moving boundary problems, is the need for a dynamic grid. A grid that is able to detect a need for a different grid formation and change to accomodate the flow and the present conditions. Numerical schemes have been devised that accomplish this and have been published in the literature.

The MAC method, discussed in Chapter 4, is after a fashion dynamic, since, grid cells are added or taken away from the surface as the fluid dynamics suggest. The floating surface cell method used by Waldrop and Pitts, discussed in Chapter 4, is also dynamic since the surface cell heights change in response to the fluid dynamics. However, much more general development of the dynamic grid concept is developed in the literature. Both Pracht (1974) and Chan (1974) develop a dynamic grid capable of arbitrary grid movements, movements according to the Lagrangian View Point, or stationary grid arrangements. The development of such dynamic grids are based on simple reasoning which will be discussed below. However, application of this reasoning in combination with complex generalized numerical codes is difficult.

Since the goal of this research is not the development of a generalized code for modeling free surface flows, but, simply a numerical code that meets the needs for modeling the Vacuum Pan, the development of the dynamic grid below will be based on this premise. Nonetheless, extensions and generalizations could be done in future research efforts based upon the principles presented below.

The development of the dynamic grid system is constrained by Equation 4.1.1, the general property equation discussed in Chapter 4. Equation 4.1.1 is presented below.

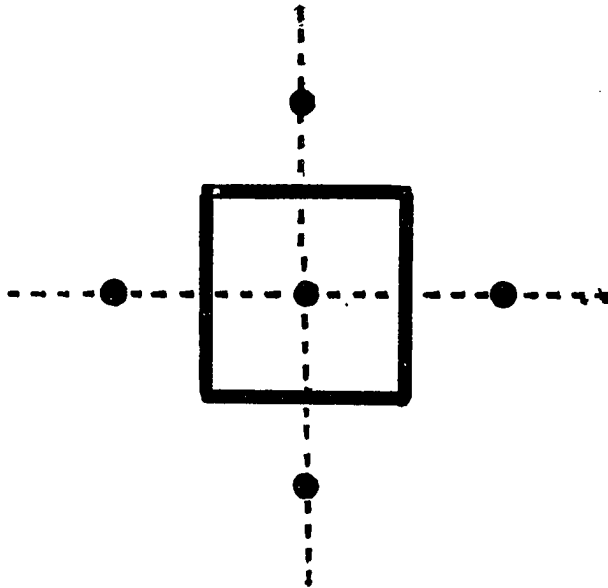
$$\frac{d}{dt} \int \rho \phi \, dV = - \oint \phi_F \cdot d\bar{A} + \int \phi_g \, dV \quad 4.1.1$$

$$\phi_F = \rho U_{RB} \phi + \bar{P}$$

In the development of the dynamic grid, the surface terms, compression forces and diffusion, are not effected or that is, do not change their form in Equation 4.1.1. These terms depend upon gradients that exist at the surface for the diffusion terms and the magnitude of the pressure for the compressive forces. However, translation of the cell boundaries does effect the convection of the general property into the volume. So the development of the dynamic grid must define this effect, as well as the effect of translation on cell volumes and boundary

areas.

Equation 4.1.1 expresses in a continuum sense, the conservation of ϕ in the volume of concern. The conservative principles do not restrict the size or shape of the volume in any way, therefore, Equation 4.1.1 also applies in a continuum sense to any arbitrary volume. Thus, Equation 4.1.1 also applies to the computation cell of the two-dimensional Pan Proper. The computation cell is presented below.



The computation center is located at the point (r_i, z_j) . The boundaries are located as prescribed for this rectangular grid cell by the grid increments Δr_i and Δz_j . The radial cross-sectional area is given as a function of radial position by Equation 6.0.1, its volume by Equation 6.0.2, vertical areas by Equation 6.0.3.

$$A_r(i) = 2\pi r_i \Delta z \quad 6.0.1$$

$$V(i) = 2\pi r_i \Delta r \Delta z \quad 6.0.2$$

$$A_z(i) = 2\pi r_i \Delta r \quad 6.0.3$$

Consider now that all the points in the computation cell are translated thru space at the same velocity, (\mathcal{U}_p). This velocity (\mathcal{U}_p) can be represented as the sum of its radial component (u_p) and vertical component (w_p). Because cell points in the cell are translating at the same velocity the boundary areas and volume of the cell do not change. But because of the translation, the convection of ϕ into the cell is effected by the relative motion of the cell boundaries to the fluid motion. The convection of the general properties is expressed by the integral below, Equation 6.0.4.

$$\int \rho U_{RB} \phi \cdot d\bar{A} \quad 6.0.4$$

Where U_{RB} expresses this relative motion. This relative motion is described mathematically below, by Equation 6.0.5.

$$U_{RB} = U - \mathcal{U}_p \quad 6.0.5$$

Equation 6.0.5 can be broken down into its radial component, Equation 6.0.6, and its vertical component, Equation 6.0.7.

$$u_{RB} = u - u_p \quad 6.0.6$$

$$w_{RB} = w - w_p \quad 6.0.7$$

Now consider the possibility of the distortion of the cell. In other words, each point within the cell may be moving at different velocities, therefore, the cell boundaries and volume may change as the result of this distortion. Nonetheless, Equation 4.1.1 still describes the conservation of the general property. Likewise, Equation 6.0.4 still represents the convection of the general property into the cell. Now in terms of the computation effort if U_p equals U then there is no convection of the general property into the cell, and Equation 4.1.1 is said to represent the Lagrangian point of view, i.e., the coordinate system moves the fluid. In contrast, if $U_p = 0$, then Equation 4.1.1 is said to represent the Eulerian point of view, i.e., the cell is fixed in space. However, the conservation principles do not limit the situation to these two cases. Therefore, U_p may be arbitrary specified to meet pertinent computation purposes.

The purpose of the dynamic grid system proposed here is to maintain, for a constant number of computational cells, a positive volume in all of the computational cells in the face of volume changes in the Pan Proper (the computational space). The methodology for adjusting the grid is based on the assumption that the average surface cell height is maintained constant and the average surface cell height is sufficient to prevent negative heights resulting from surface curvature. Furthermore, the surface is always assumed to be contained in the Pan Proper. Also, the radial grid increments remain constant for computation convenience and the inner vertical grid increment remains uniform for computation convenience but changes in response to volume changes in the Pan. This state is easily accomplished by letting (u_p) equal to zero but letting (w_p) change for the inner cells according to Equation 6.0.8.

$$w_p(z_j) = \frac{z_j}{z_{ic}} \frac{d\bar{z}}{dt} \quad 0 < z_j < z_{ic} \quad 6.0.8$$

Where (\bar{z}) is the average level in the Pan Proper, (z_{ic}) is the inner cells boundary height, and (z_j) is the vertical position in the Pan Proper. In terms of the computational grid for the Pan Proper, (z_j) is calculated via Equation 6.0.9, for the cell center and via Equation 6.0.10, for the vertical cell boundaries.

$$z_j = \Delta z(2j-1)/2 \quad j = 1, 2 \dots j_{\max} \quad 6.0.9$$

$$z_j = \Delta z j \quad j = 0, 1, 2 \dots j_{\max} \quad 6.0.10$$

The vertical grid increment is defined by Equation 6.0.11, where j_{\max} is the number of grid cells in the inner grid.

$$\Delta z = (\bar{z} - \bar{h})/j_{\max} \quad 6.0.11$$

Since the vertical grid increment (Δz) may change with time, but as mentioned earlier, the average surface height is to remain constant in time, therefore, upon differentiating Equation 6.0.11 with respect to time, Equation 6.0.12 results.

$$\frac{d \Delta z}{dt} = \frac{d \bar{z}}{dt} / j_{\max} \quad 6.0.12$$

Equation 6.0.12 can then be integrated with respect to time to give the vertical grid increment. Since the radial cross-sectional areas and the cell volume are related to the vertical increment, these quantities will change in time.

Although, to this point the discussion has been limited to the inner grid cell, the development also

applies to the surface cells. Equation 6.0.13 is the vertical velocity of each point in the surface cell.

$$w_p(z_j) = \frac{(z_j - z_{ic})}{h_i} \frac{dh_i}{dt} + \frac{dz}{dt} \quad 6.0.13$$

$$0 < z_j - z_{ic} < h_i$$

Where (h_i) is the surface cell height of the (i) radial position.

Since the discrete analog of the Equation 4.1.1, derived in Chapter 4, are derived specifically to include all the dynamic terms, applying the above equations in combination with the physics of the Pan, allows a computational set of equations to be specified that will adjust for volume changes in the Pan.

CHAPTER 7

SUMMARY AND CONCLUSIONS

In the preceding chapters, the reader has been introduced to the analysis of lumped particle systems and distributed particle systems. A distributed particle system as opposed to a lumped well mixed tank approach is needed when local disturbances or conditions have a significant effect on the resulting crystal size distribution (CSD). Such a circumstance might well describe the conditions in a Vacuum Pan Sugar Crystallizer. Of course, the distributed particle analysis has need of distributed velocity and growth profiles. Thus, the particle equation must be solved simultaneously with a distributed mathematical model of the fluid dynamics. The only recourse to this method is to use empiricism based on experimental data, this direction was taken by Wright (1974). But this approach does little in the way of helping to design control systems for Pans or in the design of Pans. This type of empiricism is dependent on the Pan and the operating conditions. The empiricism also lacks information that is needed to decide what kind of instrument to be used and how many and where it should be placed and what kind of effects Pan design and operating conditions have on the ability of the control system to meet a target CSD. The approach used here has

been to develop a mathematical model based on the fundamental laws of fluid dynamics to supply the needed information to a distributed particle balance. The distributed model would, by its nature, supply the essential information the empiricism lacks.

The derivation of the model introduces the reader to the basics of two-phase fluid flow. The later discussion of the numerical methods introduces the reader to the state of the art of numerical methods in two-phase flow and their applications. The numerical solution scheme for free surface problems was developed by Waldrop (1972), and is explicit in nature as opposed to mixed implicit-explicit methods used in the literature. The application of this solution scheme, presented in detail in Chapter 4, is completely new. This method was chosen over complicated methods because of its simplicity. The desire here was to use the most efficient code for the particular problem so the entire batch of several hours might be simulated. While previous work has been done by Pitts (1976) and Waldrop (1972) here at Louisiana State University on incompressible flow with a free surface, the finite difference methods used were very inconsistent and the surface cells were not treated properly. Therefore, quite a bit of fundamental research had to be done to make the finite difference equations consistent throughout the grid system and between

equations. This work is in addition to work done in designing the two-phase calculations and finding a method of removing the vapor from the Pan that is consistent with the homogeneous model. Additional work was done in the development of a much needed dynamic grid system without which an entire batch crystallization simulation cannot be attempted in a distributed system. The resulting numerical method is conservative and transportive and does not need a strong artificial diffusion to prevent numerical wandering of the numbers, in fact, needs no diffusion in the momentum and energy calculation to prevent numerical wandering of the numbers. This fact is demonstrated with a sensitivity analysis of the thermal diffusivity, Cases 2 and 3, in Table 5.1.1. The need for diffusion to prevent the wandering of the numbers is a sign that the finite differencing method does not satisfy all the equations simultaneously. Many times this numerical wandering of the numbers is mistaken for numerical instability. The differencing methods used by Pitts and Waldrop have this problem throughout the grid system and especially in the surface cells. The finite difference method developed in this work is conditionally stable as expected for explicit solution sequence, but its increased stability is characteristic over the methods in earlier works here at LSU. Also, the surface calculation is done with an implicit

tri-diagonal matrix solver. However, the model does have limitations associated with the assumptions made in the derivation of the mathematical model and when the numerical model was derived, these problems were discussed earlier.

Studies using the model to perform sensitivity analysis of the solution to the thermal diffusivity and demonstrate the use of the program to analyze pan design and operating conditions on pan performance are presented in the previous pages. The effect of pan design and operating conditions is seen to be significant, suggesting that the model could be used to aid in pan design and increasing the performance of existing pans. This type of analysis has never been attempted for a Vacuum Pan Sugar Crystallizer. The parameters used to measure the effect variations in pan design and operating conditions were changes in the growth and velocity profiles, the difference between the maximum and minimum supersaturation, and the recirculation rate. These of course, affect the product CSD tremendously. The most significant variations of the operating conditions studied were, the volume fraction crystals, pan level, heat load, and pan pressure. The most significant variations of pan designs studied were, the flare design over the straight walled pan and heat transfer area.

The sensitivity studies varying pan design demonstrate that contrary to some statements in the literature, large downtakes in excess of 40% of the Calandria diameter are not

needed, especially when heat transfer area is sacrificed. These studies also show that simple design changes such as the flare design may adversely effect the CSD because of the effect on the circulation patterns in the pan. The flare design causes a vortex zone or eddy near the wall that extends from the surface to the Calandria. This vortex may trap crystals for large enough periods of time to cause the crystals in this area to have a significantly different average size and thus, contribute to the variance of the product CSD.

The model demonstrates that the ability of the pan to transfer heat through its Calandria is one of the most important parameters to be considered when judging the performance of a Vacuum Pan. Good heat transfer is synonymous with good circulation, and good circulation is an indication that the pan will produce a uniform CSD. Therefore, it can only be concluded that development of a good correlation for the heat transfer coefficient in the pan would be a significant contribution to this research. The heat transfer correlation should be sensitive to the fluid dynamics as well as the physical properties.

The sensitivity studies show in all cases that there are significant growth profiles throughout the Pan. This fact suggests that the utility of multiple instrument probes to measure local supersaturation could prove great. Thus, the modern approach to use multiple instrument

probes in the Pan seems justified.

For the most part, the importance of the various pan designs and operating conditions mentioned above, at least to an experienced sugar boiler, is no revelation. However, the advantage the model offers is that quantitative effects of these design and operating conditions on the growth and velocity profiles and recirculation are calculated. These are essential parts of the analysis of the effects of pan design and operating conditions on the CSD based on a distributed population balance as discussed in Chapter 2. Thus, the model developed and demonstrated in this research must be looked upon as a stepping stone to bigger and better things. A model of this type is essential as a research tool and could aid in the development of a more efficient Vacuum Pan.

CHAPTER 8

RECOMMENDATIONS

To this point, the development of a mathematical model for a Vacuum Pan Sugar Crystallizer is not complete. The success of the present model in predicting natural convecting flows is evident. This success suggests that further research in modeling the Crystallizer should be continued. The recommendations for continued research are several fold and are experimental as well as computational. The recommendations are as follows:

(1) Basic computational research to develop multi-step or implicit numerical solution methods, to remedy the stability problems discussed earlier. The formulation of the mathematical model should not include the hydrostatic head assumption. Instead, the full vertical momentum equation should be programmed.

(2) Basic computational research to reduce the execution time for the dynamic flow model. This could be done by modifying the equations to reduce stiffness, thus, allowing bigger time steps to be taken. Elimination of all the diffusion terms might be considered to reduce the number of executions. Modification of the equations might be done by elimination of some of the dynamic terms, which tend to follow the oscillatory nature

of the two-phase flow transients, rather than the underlying quasi steady state nature of the Pan. The dynamics of which variables to be ignored and what method of converging the solution set, considering the free surface, should be part of the research.

(3) The particle equations should be included in the mathematical and numerical formulation, if the quantitative effects of Pan design and operation on the resulting CSD are desired.

(4) Experimental work to develop correlations for the local heat transfer coefficients and pressure drop in a crystallizer tube. This work could also involve modeling the crystallizer tube.

(5) Experimental measurement of velocity profiles and recirculation rates to aid in verification of future computational efforts in modeling the crystallizer.

The recommendations listed above directly extend the present work. However, the computation methods and literature cited in this dissertation are applicable to other industrially important problems. Further development of methods for two-phase flow would be beneficial because such methods are very marketable in industry today.

REFERENCES

Awang, M. and White E. T., "Effect of Crystal on the Viscosity of Masecutes", Queensland Society of Sugar Cane Technologists., 43Rd. Congress, (1976), pp. 263-270.

Batterham, R. J., Frew, J. A. and Wright, P. G., "Control of Vacuum Pans", International Society of Sugar Cane Technologists., XV. Congress, (1974), pp. 1326-1337.

Batterham, R. J. and Norgate, T. E., "Boiling Point Elevation and Superheat in Impure Cane Sugar Solutions", International Sugar Journal., December, (1975).

Bird, Stewart and Lightfoot, Transport Phenomena., John Wiley, (1960).

Bracco, Frediano V., "Unsteady Combustion of a Confined Spray", Heat Transfer: Research and Design, AICHE Symposium Series., Vol. 70. No. 138, (1974). pp. 48-56.

Brodley, R. S., Phenomena of Fluid Motion., Addison Wesley Inc., Reading, Mass., (1967).

Buchler, P., The Effect of Dextran on Sucrose Crystal Growth., Ph. D. Thesis, to be published, Louisiana State University.

Chan, Robert K.-C., "A Generalized Arbitrary Lagrangian-Eulerian Method for Incompressible Flows with Sharp Interfaces", Journal of Computational Physics., Vol. 17, (1975), pp. 311-331.

Doucet, J. and Giddey, C., "Automatic Control of Sucrose Crystallization", The International Sugar Journal., May, (1966), pp. 131-136.

Evans, L. B., Trearchis, G. P. and Jones, C., "Simulation Study of a Vacuum Pan Sugar Crystallizer", Part 1, Sugar y Azucar., October, (1970).

Frew, John A., "Optimal Control of Batch Raw Sugar Crystallization", Ind. Eng. Chem. Process Des. and Develop., Vol. 12, No. 4, (1973), pp. 460-466.

Grimmett, E. S., The Role of Seed Particles in the Prediction and Control of Product Particle Size in Fluid-Bed Dryers., Exxon Nuclear Idaho Company, Inc., April, (1980).

Hartel, Richard W., Berglund, Kris A. and Murphy, Vincent G., "Growth Kinetics for Sucrose Crystallization", Colorado State University, Presented at the 72nd Annual Meeting of AICHE., San Francisco, (1979).

Honig, P., Principles of Sugar Technology., Vol. I., Elsevier Publishing Co., London, (1963).

Hugot, E., Handbook of Cane Sugar Engineering., Second Edition, Elsevier Publishing Co., (1972).

Hulburt, H. M. and Katz, S., "Some Problems in Particle Technology: A Statistical Mechanical Formulation", Chemical Engineering Science., Vol. 19, (1964), pp. 555-574.

Ishii, M., Thermo-Fluid Dynamic Theory of Two-Phase Flow., Eyrolles, Paris, (1975).

Lyczkowski, Robert W., "Numerical Techniques for the Computation of Transient Unequal Phase Velocity, Unequal Phase Temperature, Two-Phase Flow and Heat Transfer", Two-Phase Transport and Reactor Safety, Vol. II., Proceedings of the Two-Phase Flow and Heat Transfer Symposium Workshop., Hemisphere Publishing Co., (1978), pp. 839-882.

MacCormack, Robert W., "An Efficient Explicit-Implicit Characteristic Method for Solving the Compressible Navier-Stokes Equations", SIAM-AMS Proceedings., Vol. 11, (1978), pp. 130-154.

Meade, George P., Cane Sugar Handbook., John Wiley and Sons, Inc., New York, (1963).

Miller, I. and Freund, J. E., Probability and Statistics for Engineers., Prentice-Hall Inc., Englewood Cliffs, N.J., (1965).

Mori, Masahiro and Umetani, Yoji, "Dynamic Characteristics of Vacuum Pan and Control Systems of Boiling Process", International Society of Sugar Cane Technologists., XIII. Congress, (1968), pp. 1641-1653.

Mukhopadhyay, Subhendra C. and Epstein, Mary Farrell, "Computer Modeling of a Semi-Batch Evaporative Crystallizer", Columbia University, Presented at the 72nd Annual Meeting of AIChE., San Francisco, (1979).

Mullin, J. W., Crystallization., Chemical Rubber Company, Cleveland, Ohio, (1972).

Park, J. E., Calculations of Fluid Circulation Patterns in the Vicinity of of Submerged Jets Using ORSMAC., Union Carbide Corp., Nuclear Division, January, (1980).

Patankar, S. V., Numerical Heat Transfer and Fluid Flow., McGraw-Hill Co., (1980).

Pitts, Fredericl H., A Three-Dimensional, Time-Dependent Model of Mobile Bay., Ph. D. Thesis, Louisiana State University, December, (1976).

Pracht, William E., "Calculating Three-Dimensional Fluid Flows at all Speeds With an Eulerian-Lagrangian Computing Mesh", Journal of Computational Physics., Vol. 17, (1975), pp. 132-159.

Randolph, A. D. and Tan, Chung-Sung, "Numerical Design Techniques for Classified Recycle Crystallizer: Examples of Continuous Alumina and Sucrose Crystallizers", Industrial and Engineering Chemistry Process Design and Development., Vol. 17, April, (1978), pp. 189-200.

Randolph, Alan D. and Larson, Maurice A., Theory of Particulate Processes: Analysis and Techniques in Continuous Crystallization., Academic Press, New York, (1971).

Roache, Patrick J., Computational Fluid Dynamics.,
Hermosa Publishers, Albuquerque, New Mexico, (1976).

Saranin, A. P. and Jenkins, G. H., "Heat Transfer
Co-Efficients in the Evaporators of Sugar Solutions",
Queensland Society of Sugar Cane Technologists Proceedings.,
(1954).

Smythe, B. M., "Sucrose Crystal Growth", Sugar Technology
Reviews., (1971), pp. 191-231.

Solbrig. Charles W. and Hughes, E. Daniel, "Governing
Equations for a Serrated Continuum: An Unequal Velocity
Model for Two-Phase Flow", Two-Phase Transport and
Reactor Safety, Vol. II., Proceedings of the Two-Phase
Flow and Heat Transfer Symposium Workshop., Hemisphere
Publishing Co., (1978), pp. 307-359.

Soo, S. L., Fluid Dynamics of Multi-Phase Systems.,
Blaisdell, Waltham, Mass., (1967).

Soo. S. L., "Multi-Phase Mechanics and Distinctions From
Continuum Mechanics", Two-Phase Transport and Reactor
Safety., Vol. I., Hemisphere Publishing Co., (1978),
pp. 267-281.

Sowul, L., Dynamics and Stability of Continuous Crystallization Systems: Evaporative Crystallization of Sucrose., Ph. D. Thesis, Columbia University, New York, (1977).

Sowul, L. and Epstein, Mary Anne Farrell, The Matrizant Approach to the Solution of the CMSMPR Evaporative Crystallizer System Equations., Ph. D. Thesis, Columbia University, New York, (1977).

Waldrop, William R., Three-Dimensional Flow and Sediment Transport at River Mouths., Ph. D. Thesis, Louisiana State University, December, (1972).

Wallis, Graham, One-Dimensional Two-Phase Flow., McGraw-Hill Co., New York, (1969).

Warming, R. F. and Beam, Richard M., "On the Construction and Application of Implicit Factored Schemes for Conservation Laws", SIAM-AMS Proceedings., Vol. 11, (1978), pp. 85-129.

Wey, Jong-Shinn and Estrin, Joseph, "Modeling the Batch Crystallization Process. The Ice-Brine System", Ind. Eng. Chem. Process Des. Develop., Vol. 12, No. 3, (1973), pp. 236-246.

Wright, P. G. and White, E. T., "A Mathematical Model of Vacuum Pan Crystallization", International Society of Sugar Cane Technologists., XV. Congress, June, (1974), pp. 13-29.

NOMENCLATURE

A	(FT. ²)	Area
A _r (i)	(FT. ²)	Area viewed from radial direction at the i position
A _z (i)	(FT. ²)	Area viewed from vertical direction at the i position
AREAT	(FT. ²)	Area for heat transfer
B	(NO./FT. ⁴)	Nucleation Rate Distribution Function
B _o	(NO./FT. ⁴)	Nucleation Rate
BPE	(F)	Boiling Point Elevation
BRIX		Mass fraction sucrose and impurities in massecuite
C	(LB.)	Mass of crystal
CP	(BTU/LB.-F)	Heat capacity of mixture
CPW	(BTU/LB.-F)	Heat capacity of water
CSD	(FT. ⁻¹)	Crystal Size Distribution
$\frac{D}{Dt}$		Substantial Derivative
D _c	(FT.)	Diameter of Calandria
D _{down}	(FT.)	Diameter of Downtake
D _t	(FT.)	Diameter of Tubes
DPDT	(FT./SEC.)	Velocity of Cell
E	(LB./SEC.-FT. ²)	Evaporation Rate Flux
EACT	$(\frac{KC}{g-MOLE})$	Activation Energy

ECOEFF	$(\text{LB.}/\text{FT.}^2\text{-SEC.})$	Evaporation Coefficient
ER	$(\text{LB.}/\text{SEC.})$	Evaporation Rate
F	$(\text{LB.}/\text{SEC.})$	Feed Rate
F_B	$(\text{LB.-FT.}/\text{SEC.}^2)$	Body Force
FR	$(\frac{\text{LB.-FT.}/\text{SEC.}^2}{\text{FT.}^3})$	Pressure drop due to friction
g	$(\text{FT.}/\text{SEC.}^2)$	Acceleration due to gravity
G	$(\text{FT.}/\text{SEC.})$	Growth Rate
h	(FT.)	Surface Cell Height
H	$(\text{BTU}/\text{LB.})$	Enthalpy
HF	$(\text{BTU}/\text{LB.})$	Enthalpy of Feed
HL	$(\text{BTU}/\text{LB.})$	Enthalpy of Liquid
HV	$(\text{BTU}/\text{LB.})$	Enthalpy of Vapor
IMP	(LB.)	Mass of impurities
k_G	$(\text{FT.}/\text{SEC.})$	Growth Rate Constant
k_G^0	$(\text{FT.}/\text{SEC.})$	Specific Growth Rate
L	(FT.)	Crystal Size
\bar{L}	(FT.)	Average Crystal Size
M_k		kth moment of η
N_c		Number of Crystals
NTUBES		Number of Tubes
OS		Oversaturation
P	$(\frac{\text{LB.-FT.}/\text{SEC.}^2}{\text{FT.}^2})$	Pressure

PR	$(\frac{\text{LB.-FT.}/\text{SEC.}^2}{\text{FT.}^2})$	Reference Pressure
P	(LB.-FT./SEC.)	Dynamic Momentum
POA	(FT. ⁻¹)	Perimeter of Tubes divided by the area for flow
Q	(FT. ³ /SEC.)	Volumetric Flow Rate
r	(FT.)	Radial Position
R _{dwn}	(FT.)	Radius of Downtake
R _g	(KC/g-MOLE-R)	Gas Law
S	(LB.)	Mass of Sucrose
SAT	(LB./LB.)	Saturation mass of sucrose per 100 pounds of water
SFSMTH	(FT. ² /SEC.)	Surface Diffusivity
SS		Supersaturation
t	(SEC.)	Time
T	(F)	Temperature
TMASS	(LB.)	Total Mass
TSTEAM	(F)	Temperature of Steam
TUBED	(FT.)	Tube Diameter
TUBEH	(FT.)	Tube Height
TW	(F)	Temperature of Water
u	(FT./SEC.)	Radial Velocity Component
u _{RB}	(FT./SEC.)	Radial Velocity relative to boundary of cell
U	(FT./SEC.)	Velocity Vector
U _{RB}	(FT./SEC.)	Velocity Vector relative to boundary motion

UPOA	(BTU/SEC.-FT. ³ -F)	Overall coefficient times perimeter divided by area for flow
UU	(BTU/SEC.-FT. ² -F)	Overall heat transfer coefficient
V	(FT. ³)	Volume
VCL		Volume Ratio of Crystal Volume to Liquid Volume
w	(FT./SEC.)	Vertical Velocity Component
w _{RB}	(FT./SEC.)	Vertical Velocity Relative to Cell Boundary
w _S	(FT./SEC.)	Velocity of Surface
w _V	(FT./SEC.)	Velocity of Vapor
W	(LB.)	Mass of Water
* W _V	(FT./SEC.)	Maximum Vapor Slip Velocity
x		Mass Fraction
XCP		Mass Fraction of Crystal in Pan
XIMP		Mass Fraction of Impurity in Pan
XIMF		Mass Fraction of Impurity in Feed
XL		Mass Fraction of Liquid
XSP		Mass Fraction of Sucrose in Pan
XSF		Mass Fraction of Sucrose in Feed
XWP		Mass Fraction of Water in Pan
XWF		Mass Fraction of Water in Feed
z	(FT.)	Vertical Position

GREEK

α	(FT. ² /SEC.)	Thermal Diffusivity
β	(F ⁻¹)	Coefficient of Thermal expansion
β_c	(BRIX ⁻¹)	Coefficient of Concentration
γ		Volume fraction
η	(NO./FT. ⁴)	Crystallizer Number Density Function
Δr	(FT.)	Radial increment
Δt	(SEC.)	Time increment
Δz	(FT.)	Vertical increment
κ	(BTU/SEC.-FT.-F)	Thermal Conductivity
μ	(LB./FT.-SEC.)	Viscosity
μ_L	(LB./FT.-SEC.)	Viscosity of molasses
ν	(FT. ² /SEC.)	Kinematic Viscosity
ρ	(LB./FT. ³)	Density
ρ_L	(LB./FT. ³)	Density of liquid
ρ_{LS}	(LB./FT. ³)	Density of liquid and solid mixture
ρ_R	(LB./FT. ³)	Reference Density
ρ_V	(LB./FT. ³)	Density of vapor
ρ_{VR}	(LB./FT. ³)	Reference density for vapor
σ^2	(FT. ²)	Variance of Crystal Size Distribution
τ	($\frac{\text{LB.-FT.}/\text{SEC.}^2}{\text{FT.}^2}$)	Stress Tensor
ϕ	(property/LB.)	General Property

ϕ_c	(BTU/SEC.)	Generation of energy due to Crystallization
ϕ_g	($\frac{\text{property}}{\text{SEC.-FT.}^3}$)	Generation of General Property

APPENDIX I

LISTING OF COMPUTER PROGRAM

This appendix presents a listing of computer program modeling the Vacuum Pan. The mathematical model and numerical methodology are presented in Chapters 4 and 5 of the main text. Comment cards are used throughout the listing to aid understanding. For as much as possible the symbols used in the computer programming are the same as used in the text.

All data needed for execution of the program are obtained upon execution of SUBROUTINE PRELIM. If a cold start is selected, initialization of the computational matrix is accomplished through statements in SUBROUTINE PRELIM. If a restart is selected, the computational matrix is initialized from a sequential file. Non-dimensionalization of the computational matrix is accomplished through statements in SUBROUTINE PRELIM.

At the completion of the run the computation matrix is dumped into a sequential file. This allows the restart feature to be executed.

After the program has executed the proper number of time steps, the program tabulates the computational matrix, as well as a brief summary of the run. Intermediate tabulation of the computational matrix is possible if desired, but, may also result if a

computation error occurs.

Separate programs are used when velocity or growth profiles are needed. These programs access the same sequential file needed to supply the restart capability to obtain the computation matrix. A listing of these programs are not included.

A listing of the computer program is now presented.

C----		00010001
C----	MAIN PROGRAM. MOTIVE FORCE FOR CALCULATION.	00010002
C----		00010003
	IMPLICIT REAL*8 (A-H, O-Z)	00010004
	DIMENSION ZZZZ (2,20), ZZZC (10,2,5)	00020000
	DIMENSION ZPARS (5), ZPARV (4), ZPARH (8), ZPARG (9), ZPART (3)	00030000
	DIMENSION ZPARCP (4), ZPARBP (2), ZRATIO (3)	00040000
	REAL*8 IMP (2)	00050000
	COMMON/ BLOCK / ERIFFF, PURFF, TEMPPF,	00060000
1	VART, PRECMX, AHTOV, HK, TINTAL, HV, JJMAX	00070000
	COMMON/JOBRUN/ IRUN (3)	00080000
	COMMON/CONC /DELDDB, DELRH, BRIXR, CONST1, CONST2, EPE, VRATIO	00090000
	COMMON/ CONECT/ HBND (30), DBND (30), TBND (30), QJCAL	00100000
	COMMON/MOVE / DPDT (30)	00110000
	COMMON/FORCE/ PUMPDP	00120000
	COMMON/INOUT/ IN, IOUT	00130000
	COMMON/WSTRT/ EM (2), S (2), IMP, C (2), Q (2), AVERT (2), HHM (2), HH (2)	00140000
1,	F, XWF, XSF, XIF, G (2), HF, AVERD (2), TMASS (2), WATER (2)	00150012
2,	TOTALH (2), XSP (2), XIF (2), XCP (2), XWP (2), AVERH (2)	00160000
3,	SSMAX, SSMIN	00170000
	COMMON/OVERAL/ E (2), HHH (2), EVINTO, ENVINT, AQFLUX	00180011
	COMMON/FLAG/ IWSTRT, IFLAG1, IFLAG2	00190000
	COMMON/REAL/ RTIME, TCONST	00200000
	COMMON/PAN/ VOLSCH, RADSQ, VOLC, WVCL, WHEIG	00210000
	COMMON/DIMEM/ U (2,30,30), W (2,30,30), T (2,30,30), WW (30,30)	00220000
	COMMON/DIMEN1/ P (30,30), PBIP1, PBIM1	00230000
	COMMON/TPHASE/ ENTH (2,30,30), DEN (2,30,30)	00240000
	COMMON/GRID/ DR, DZ, DT, DTOZSQ, DTODZ, DZODR, DZO2DR, DTO2DR, DTO2DZ	00250000
1,	DT2DRZ, DTODRZ, DTODR, FOURMD, DZORSQ, DZODT, DTORSQ	00260000
2,	DZO2, CALFC2, CALFC3, DDZDT, SURFDT, DRT2, DZO, DDZDTO	00270000
3,	DZODTO	00280000
	COMMON/PROPTY/ RHO, RHOINV, RHOO2, VISC, ALPHA, VORHO, BETA	00290000
1,	FOURMR, FMO2DR, FMODR, CP, FOURMC, TZERO	00300000
2,	HVIN, DELHLV, DENSTY	00310000
	COMMON/COORD/ R (30), Z (30), RINV (30), RH (30)	00320000
	COMMON/LIMITS/ INAX, INAXN1, INAXN2, JMAX, JMAXN1, JMAXN2, NMAX, NPRINT	00330000


```

1,      COMMON/STEP/ MN,MO,N      00340000
COMMON/SIZE/ H,RAD,HMAX          00350000
COMMON /AREAP/ DV(30),DVOA(30)   00360000
COMMON/BOUND/ IRIGHT,IRIGP1,ILEFT,ILEFP1,ILEFM1,IDOWN 00370000
1,      IDWNP1,IDOWN1             00380000
COMMON/CHEST/ UU,UA,TUBEH,AREAT,POA,UPOA,DTOTH,THODT,UAOA,CALANH 00390000
1,BOTH,TUBED,FMCN,CDZ,ETOCDDZ,TSTREAM,NTUBES,NCAL,NCALM1 00400000
2,NCALP1                          00410000
COMMON/FLOW1/ DUDT(30,30),DEDT(30,30),HCDT(10),BTDUDT,BTDEDT 00420000
1,      DCDZDT(30,30),DDCDT(10)   00430000
COMMON/AVPART/AVERN(2),AVERLL(2) 00440000
COMMON/TOP/ SURFAC(30),SSURF(30),SVFRV(30),HVAP 00450000
1,      SPSMTH,THETAZ,THETAS,FRAT(30),DHDT(30) 00460000
COMMON/ENTLIN/ XVLIN             00470000
COMMON/VAPDEN/ PRESRF,RHOVR      00480000
COMMON/LUMBT/ WDNWJP(2),TDWNJP(2),DDWNJP(2),HDWNJP(2) 00490000
1,      WDNWJM(2),TBOTT(2),DBOTT(2),HBOTT(2) 00500000
2,      UBOTT(2),UONFB(2),WCALAV(2),TCALAV(2),DCALAV(2) 00510000
3,      HCALAV(2),WCALJM(2),TCALJM(2),DCALJM(2),HICALJM(2) 00520000
COMMON/LUMCAL/ CALW(10,2),CALH(10,2),CALT(10,2),CALD(10,2) 00530000
1,      CALP(10,2)                 00540000
COMMON/BOTTOM/ VOLUP,AFLWU,AFLWD,ABOAFD,ABOAFU 00550000
1,      VOLBT,DTAUOV,CONST6,CONST7,CONST8 00560000
1,      ENTHFR,FFLUXU             00570000
COMMON/ ENPEQ/ SLIPV,EXPV        00580000
COMMON/ CHECK/ DELHIO(30),DELHT(30),DELHDT(30),DELWIO(30) 00590000
COMMON/ EQUON / RATCR            00600000
COMMON / PARS/ PARS1, PARS2, PARS3, PARS4, PARS5 00610000
COMMON / SPARS/ SPARS1, SPARS2, SPARS3, SPARS4, SPARS5 00620000
COMMON / PARV/ PARV1, PARV2, PARV3, PARV4 00630000
COMMON / SPARV/ SPARV1, SPARV2, SPARV3, SPARV4 00640000
COMMON / PARH/ PARH1, PARH2, PARH3, PARH4, 00650000
PARH5, PARH6, PARH7, PARH8 00660000
COMMON / SPARH/ SPARH1, SPARH2, SPARH3, SPARH4, 00670000
SPARH5, SPARH6, SPARH7, SPARH8, SPARH9 00680000
8      00690000

```

```

COMMON / PARG/ PARG1, PARG2, PARG3, PARG4,
      & PARG5, PARG6, PARG7, PARG8, PARG9
COMMON / SPARG/ SPARG1, SPARG2, SPARG3, SPARG4,
      & SPARG5, SPARG6
COMMON / PART/ PART1, PART2, PART3
COMMON / SPART/ SPART1, SPART2, SPART3
COMMON / PRATIO/ PARR1, PARR2, PARR3
COMMON / PARCP/ PRCP1, PRCP2, PRCP3, PRCP4
COMMON / PARBP/ PRBP1, PRBP2
COMMON / SPRATO/ SPARR1, SPARR2, SPARR3
COMMON / SPARCP/ SPRCP1, SPRCP2, SPRCP3, SPRCP4
COMMON / SPARBP/ SPRBP1, SPRBP2
DATA PIE, COEFFV, RHOC, GR/3.14159D0, 0.5236D0, 99.1D0, 32.2D0/
EQUIVALENCE (ZZZZ, WDNWJP)
EQUIVALENCE (ZZZC, CALW)
EQUIVALENCE (ZPARS, PARS1)
EQUIVALENCE (ZPARV, PARV1)
EQUIVALENCE (ZPARH, PARH1)
EQUIVALENCE (ZPARG, PARG1)
EQUIVALENCE (ZPART, PART1)
EQUIVALENCE (ZPARCP, PRCP1)
EQUIVALENCE (ZPARBP, PRBP1)
EQUIVALENCE (ZRATIO, PARR1)

C
CALL PRELIM
CALL OUTPUT
CALL OUTALL
CALL EOUNDY

C
BIG LOOP STARTS HERE

MOO=MO
NO=MN
NN=MOO
DO 999 N=1, NMAX
RTIME=RTIME+TCONST*DT

00700000
00710000
00720000
00730000
00740000
00750000
00760000
00770000
00780000
00790000
00800000
00810000
00820015
00830000
00840000
00850000
00860000
00870000
00880000
00890000
00900000
00910000
00920000
00930000
00940000
00950000
00960000
00970000
00980000
00990000
01000000
01010000
01020000
01030000
01040000
01050000

```

C		01060000
C	CALCULATE NEW RADIAL VELOCITIES, ENTHALPIES, DENSITIES	01070000
C	AND TEMPERATURES ABOVE THE CALANDRIA	01080000
C		01090000
	CALL HUNEW	01100000
C		01110000
C	CALCULATION OF NEW ENTHALPIES, DENSITIES, TEMPERATURES,	01120000
C	AND VELOCITIES FOR CALANDRIA AND BOTTOM	01130000
C		01140000
	CALL LOOP	01150000
C		01160000
C	SET BOUNDARY CONDITIONS BETWEEN CALANDRIA AND PAN PROPER	01170000
C		01180000
	CALL BOUNDY	01190000
C		01200000
C	CALCULATION OF AVERAGE CONDITIONS IN PAN	01210000
C		01220000
	CALL AVERAGE	01230000
C		01240000
C	CALCULATE VAPOR RATES FROM FREE SURFACE	01250000
C		01260000
	CALL CALVAP	01270000
C		01280000
C	USE TO CHANGE MANIPULATED AND LOAD VARIABLES	01290010
C		01300010
	CALL CNTRL	01310010
C		01320010
C	WELL MIXED TANK CALCULATIONS	01330010
C		01340010
	IF(INSTRT.GT.0) CALL WMIXT	01350010
C		01360000
C	MOVE GRID POINTS	01370000
C		01380000
	CALL REZONE	01390000
C		01400000
C	CALCULATE NEW VERTICAL VELOCITIES	01410000

```

C          CALL CONTIN
C
C          CALACULATE RATE OF CHANGE OF FREE SURFACE POSITION
C          AND LOCATE FREE SURFACE POSITION
C
C          CALL CCNVSF
C
C          CALCULATE PRESSURE PROFILE
C
C          CALL PRES
C
C          ONE-D PRESSURE CALCULATIONS THROUGH CALANDRIA
C          AND DOWNTAKE
C
C          CALL PRESSC
C
C          IF (N/NSTART.EQ.0) GO TO 91
C          IF (N/NPRINT*NPRINT.EQ.N) CALL OUTPUT
C          IF (N/NEAR*NEAR.EQ.N) CALL OUTALL
C
C          91  CONTINUE
C              MOO=MO
C              MO=MN
C              MN=MOO
C          999  CONTINUE
C
C          BIG LOOP ENDS HERE
C
C              MOO=MO
C              MO=MN
C              MN=MOO

```

01420000
01430000
01440000
01450000
01460000
01470000
01480000
01490000
01500000
01510000
01520000
01530000
01540000
01550000
01560000
01570000
01580000
01590000
01600000
01610000
01620000
01630000
01640000
01650000
01660000
01730000
01740000
01750000
01760000
01770000
01780000
01790000
01800000
01810000
01820000

[illegible]

02160000
02170000
02180000
02190000

1,133A8)
1113 FORMAT(19A4)
STOP
END

```

C-----
C-----
C-----
SUBROUTINE AVERAGE
  PREFORMS AVERAGEING OF PERTINENT VARIABLES
  IMPLICIT REAL*8 (A-H,O-Z)
  DIMENSION ZZZZ(2,20),ZZZC(10,2,5)
  REAL*8 IMP(2)
  COMMON/BOTTOM/ VOLUP, AFIWU, AFLWD, ABOAFD, ABOAFU
  1, VOLBT, DTAUOV, CONST6, CONST7, CONST8
  1, ENTHFR, FFLUXU
  COMMON/WSIRT/EM(2),S(2),IMP,C(2),Q(2),AVERT(2),HHM(2),HH(2)
  1,F,XWF,XSF,XIF,G(2),HF,AVERD(2),TMASS(2),WATER(2)
  2,TOTALH(2),XSP(2),XIP(2),XCP(2),XWP(2),AVERH(2)
  3,SSMAX,SSMIN
  COMMON/OVERAL/ E(2), HHH(2), EVINTO, ENVINT, AQFLUX
  COMMON/PAN/ VOLSCH, RADSQ, VOLC, NVOL, WHEIG
  COMMON/DIMEN/U(2,30,30),W(2,30,30),T(2,30,30),WH(30,30)
  COMMON/DIMEN1/P(30,30),PBIP1,EBIN1
  COMMON/TPHASE/ENTH(2,30,30),DEN(2,30,30)
  COMMON/GRID/DR,DZ,DT,DTOZSQ,DTODZ,DZODR,DZO2DR,DTO2DR,DTO2DZ
  1,DT2DRZ,DTODRZ,DTODR,FOURND,DZORSQ,DZODT,DTORSQ
  2,DZO2,CALPC2,CALPC3,DDZDT,SURFDT,DRT2,DZO,DDZPTO
  3,DZODTO
  COMMON/PROPTY/RHO,KHOINV,RHOO2,VISC,ALPHA,VORHO,BETA
  1,FOURMR,FMO2DR,FMODR,CP,FOURMC,TZERO
  2,HVINV,DELHLV,DENSTY
  COMMON/COORD/K(30),Z(30),RINV(30),RH(30)
  COMMON/LIMITS/IMAX,IMAXM1,IMAXM2,JMAX,JMAXM1,JMAXM2,NMAX,NPRINT
  1,NBAR,NPRINT,JHAXP1,NSTART,JMAXP2,IMAXP1
  COMMON/STEP/MN,MO,N
  COMMON/SIZE/H,RAD,HMAX
  COMMON /AREAP/DV(30),DVOA(30)
  COMMON/ENTHAL/DHNEW,DHOLD,DHIF1,DHIM1,DHJP1,DHJM1
  COMMON/BOUND/IRIGHT,IRIGP1,ILEFT,ILEFP1,ILEFN1,IDOWN
  1,IDWNP1,IDOWN1
  COMMON/CHEST/UU,UA,TUBEH,AREAT,POA,UPOA,DTOTH,THODT,UAOA,CALANH
  02190003
  02190004
  02190005
  02190006
  02190007
  02190008
  02190009
  02190010
  02190011
  02190012
  02190013
  02190014
  02190015
  02190016
  02190017
  02190018
  02190019
  02190020
  02190021
  02190022
  02190023
  02190024
  02190025
  02190026
  02190027
  02190028
  02190029
  02190030
  02190031
  02190032
  02190033
  02190034
  02190035
  02190036
  02190037
  02190038

```

1,BOTTH,TUBED,FMCN,CDZ,DTCODZ,ISTEAM,NTUBES,NCAL,NCALM1	02190039
2,NCALP1	02190040
COMMON /FLOW/DWT	02190041
COMMON/FLOW1/DUDT (30,30),DEDT (30,30),HCDT (10),BTUDT,BTDEDT	02190042
1,DDDZDT (30,30),DDCDT (10)	02190043
COMMON/AVPART/AVERN (2),AVERLL (2)	02190044
COMMON/TOP/ SURFAC (30),SSURF (30),SVFRV (30),HVAP	02190045
1, SFSMTH,THETAZ,THETAS,FRAT (30),DHDT (30)	02190046
COMMON/ENTLIM/XVLIM	02190047
COMMON/VAPDEN/PRESRF,RHOVR	02190048
COMMON/LUMBT/WDWNJP (2),TDWNJP (2),DDWNJP (2),HDWNJP (2)	02190049
1,WDWNJM (2),TBOTT (2),DBOTT (2),HBOTT (2)	02190050
2,UBOTT (2),UONEB (2),WCALAV (2),TCALAV (2),DCALAV (2),HCALAV (2)	02190051
3,WCALJM (2),TCALJM (2),DCALJM (2),HCALJM (2)	02190052
COMMON/LUMCAL/ CALW (10,2),CALH (10,2),CALT (10,2),CALD (10,2)	02190053
1,CALP (10,2)	02190054
COMMON/ EMPEQ/ SLIPV, EXPV	02190055
COMMON/ CHECK/ DELHIO (30),DELHT (30),DELHDT (30),DELWIO (30)	02190056
DATA PIE,COEFFV,RHOC,GR/3.14159D0,0.5236D0,99.1D0,32.2D0/	02190057
EQUIVALENCE (ZZZZ,WDWNJP)	02190058
EQUIVALENCE (ZZZC,CALW)	02190059
DELT=0.0	02190060
RNEW=0.0	02190061
COMP2=0.0	02190062
HNEW=0.0	02190063
SUMG=0.0	02190064
SSMIN=100.0	02190065
SSMAX=0.0	02190066
DO 80 I=2,IMAX	02190067
DDVI=DV (I)	02190068
SURFI=SURFAC (I)	02190069
DDDVI=DDVI*SURFI/DZ	02190070
TNEW=T (MN,I,JMAXP1)	02190071
SS = SUPERS (TNEW,XSP (MO),XIF (MO),XWP (MO))	02190072
IF (SS.GT.SSMAX) SSMAX=SS	02190073
IF (SS.LT.SSMIN) SSMIN=SS	02190074


```

SUMG = SUNG+GROWTH(TNEW,SS,XIE(MO),XWP(MO))*DDDDVI
DNEW=DEN(MN,I,JMAXP1)
DOLD=DEH(MO,I,JMAXP1)
DHNEW=ENTH(MN,I,JMAXP1)
DHOLD=ENTH(MO,I,JMAXP1)
COMP2=CCMP2+DDDDVI
DELT=DELT+TNEW*DDDDVI
HNEW=HNEW+DHNEW*DDDDVI
RNEW=RNEW+DNEW*DDDDVI
DO 80 JJ=1,JMAX
J=JMAXP1-JJ
DHNEW=ENTH(MN,I,J)
DHOLD=ENTH(MO,I,J)
TNEW=T(MN,I,J)
SS = SUPERS(TNEW,XSP(MN),XIE(MN),XWP(MN))
IP(SS.GT.SSMAX) SSMAX=SS
IP(SS.LT.SSMIN) SSMIN=SS
SUMG = SUNG+GROWTH(TNEW,SS,XIP(MN),XWP(MN))*DDVI
DNEW=DEN(MN,I,J)
DOLD=DEN(MO,I,J)
DELT=DELT+TNEW*DDVI
HNEW=HNEW+DHNEW*DDVI
RNEW=RNEW+DNEW*DDVI
COMP2=CCMP2+DDVI
CONTINUE
VOLOZU=VOLUP/DZ
VOLOZB=VOLBT/DZ
COMP2=COMP2+VOLOZU+VOLOZB
SS = SUPERS(TBOTT(MN),XSP(MN),XIP(MN),XWP(MN))
IP(SS.GT.SSMAX) SSMAX=SS
IP(SS.LT.SSMIN) SSMIN=SS
SUMG = SUNG+GROWTH(TBOTT(MN),SS,XIP(MN),XWP(MN))*VOLOZB
SS = SUPERS(TCALAV(MN),XSP(MN),XIP(MN),XWP(MN))
IF(SS.GT.SSMAX) SSMAX=SS
IF(SS.LT.SSMIN) SSMIN=SS
SUMG = SUNG+GROWTH(TCALAV(MN),SS,XIP(MN),XWP(MN))*VOLOZB

```

80

	DELT=DELT+VOLOZB*TBOTT(MN)	02190111
	RNEW=RNEW+VOLOZB*DBOTT(MN)	02190112
	HNEW=HNEW+VOLOZB*HBOTT(MN)	02190113
	DELT=DELT+VOLOZU*TCALAV(MN)	02190114
	RNEW=RNEW+VOLOZU*DCALAV(MN)	02190115
	HNEW=HNEW+VOLOZU*HCALAV(MN)	02190116
	DHNEW=PIE*DZ*HMAX*HMAX*HMAX*DENSTY*HNEW/BETA	02190117
	TOTALH(MN)=DHNEW	02190118
	DELT=DELT/COMP2	02190119
	RNEW=RNEW/COMP2	02190120
	AVERD(MN)=RNEW	02190121
	AVERT(MN)=DELT	02190122
C	AVERH(MN)=HNEW/RNEW/COMP2	02190123
	AVERH(MN)=HNEW/COMP2	02190124
	G(MN)=SUMG/COMP2	02190125
	DELT=DELT-AVERT(MO)	02190126
C		02190127
C	CALCULATION OF EVAPORATION RATE	02190128
C		02190129
	QQ=AQFLUX*AREAT/BETA*DENSTY	02190130
	Q(MN)=QQ	02190131
	E(MN)=0.0	02190132
	DHOLD=TOTALH(MO)	02190133
	DELH= ((AVERH(MN)-AVERH(MO)) * (HH(MO)+VOLC/RADSQ) *AVERD(MO)	02190134
	1+ (HH(MO)*AVERD(MO)-HH(MN)*AVERD(MN)) *AVERH(MO)) *RADSQ*DENSTY/BETA	02190135
	DELHV=(QQ+HF*F)*DT-DELH	02190136
C	*****	02190137
C	*** THIS IS REALLY AN ERROR TEST *****	02190138
C	*****	02190139
	E(MN)=DELHV/DT*BETA/HVAP	02190140
C	*****	02190141
C	*****	02190142
	IF(E(MN).LT.0) E(MN)=0.0	02190143


```

BLOCK DATA
IMPLICIT REAL*8 (A-H,O-Z)
REAL*8 IMP(2)
DIMENSION ZZZZ(2,20),ZZZC(10,2,5)
DIMENSION ZPARS(5),ZPARV(4),ZPARH(8),ZPARG(9),ZPART(3)
DIMENSION ZPARCP(4),ZPARBP(2),ZRATIO(3)
COMMON/ CHECK/ DELHIO(30),DELHT(30),DELHDT(30),DELWIO(30)
COMMON/ OVERAL/ E(2),HHH(2),EVINTO,EMVINT,AQFIUX
COMMON/ REAL/ RTIME, TCONST
COMMON/ DIMEN/ U(2,30,30),W(2,30,30),T(2,30,30),NW(30,30)
COMMON/ DIMEN1/ P(30,30),PBIP1,PBIM1
COMMON/ TPHASE/ ENTH(2,30,30),DEN(2,30,30)
COMMON/ COORD/ R(30),Z(30),RINV(30),RH(30)
COMMON/ STEP/ MN,MO,N
COMMON/ FLOW1/ DUDT(30,30),DEDT(30,30),HCDT(10),BTUDT,BTDEDT
1,DDDDZDT(30,30),DDCDT(10)
COMMON/ CONC /DELDEB,DELRH,BRIKX,CCNST1,CONST2,BPE,VRATIO
COMMON/ FORCE/ PUMPDP
COMMON/ INOUT/ IN,IOUT
COMMON/ WSTRT/ EM(2),S(2),IMP,C(2),Q(2),AVERT(2),HHM(2),HH(2)
1,F,XWF,XSF,XIF,G(2),HF,AVERD(2),TMASS(2),WATER(2)
2,TOTALH(2),XSP(2),XIP(2),XCP(2),XWP(2),AVERH(2)
3,SSMAX,SSMIN
COMMON/ FLAG/ IWSTRT,IFLAG1,IFLAG2
COMMON/ PAN/ VOLSCH,RADSQ,VOLC,WVOL,WHEIG
COMMON/ GRID/ DR,DZ,DT,DTOSQ,DTODZ,DZODR,DZO2DR,DTO2DR,DTO2DZ
1,DT2DRZ,DTODEZ,DTODR,FOURMD,DZORSQ,DZODT,DTORSQ
2,DZO2,CALFC2,CALFC3,DDZDT,SURFDT,DEI2,DZO,DDZDZO
3,DZODTO
COMMON/ PROPTY/ RHO,RHOINV,RHO2,VISC,ALPHA,VORHO,BETA
1,FOURMR,FMO2DR,FMODR,CP,FOURMC,TZERO
2,HVINV,DELHLV,DENSTY
COMMON/ LIMITS/ IMAX,IMAXM1,IMAXM2,JMAX,JMAXM1,JMAXM2,NMAX,NPRINT
1,NEAR,NPRINT,JMAXP1,NSTART,JMAXP2,IMAXP1
COMMON/ SIZE/ H,RAD,HMAX
COMMON/ CHEST/ UU,UA,TUBEH,AREAT,POA,UPOA,DTOTH,THODT,UAOA,CALANH
02190150
02190151
02190152
02190153
02190154
02190155
02190156
02190157
02190158
02190159
02190160
02190161
02190162
02190163
02190164
02190165
02190166
02190167
02190168
02190169
02190170
02190171
02190172
02190173
02190174
02190175
02190176
02190177
02190178
02190179
02190180
02190181
02190182
02190183
02190184
02190185

```

```

1,BOTTH,TUBED,FMCN,CDZ,DTOCDZ,TSTEAM,NTUBES,NCAL,NCALM1
2,NCALP1
COMMON/BOUND/IRIGHT,IRIGP1,ILEFT,ILEFP1,ILEFM1,IDOWN
1,IDWNP1,IDOWN1
COMMON/AVPART/AVERN(2),AVERL1(2)
COMMON/TOP/ SURFAC(30),SSURF(30),SVFRV(30),HVAP
1,SPSMTH,THETAZ,THETAS,FRAT(30),DHDT(30)
COMMON/ENTLIM/XVLIM
COMMON/VAPDEN/PRESRF,RHOVR
COMMON/EMPEQ/SLIPV,EXPV
COMMON/ITTER/NSITER
COMMON/EQUON/RATCR
COMMON/LUBT/WDWNP(2),TDWNP(2),DDWNP(2),HDWNP(2)
1,WDWNP(2),TBOTT(2),DBOTT(2),HBOTT(2)
2,UBOTT(2),UONEB(2),WCALV(2),TCALV(2),DCALV(2),HCALV(2)
3,WCALJ(2),TCALJ(2),DCALJ(2),HCALJ(2)
COMMON/LUNCAL/CALW(10,2),CALH(10,2),CALT(10,2),CALD(10,2)
1,CALP(10,2)
COMMON/BLOCK / BRIKFF, PURFF,TEMPFF,
1 VART, PRECNX, AHTOV, HR, TINTAL, HV, JJMAX
COMMON / NMIJ/ N1, N2, N3
COMMON / PARS/ PARS1, PARS2, PARS3, PARS4, PARS5
COMMON / PARV/ PARV1, PARV2, PARV3, PARV4
COMMON / PARH/ PARH1, PARH2, PARH3, PARH4,
8 PARH5, PARH6, PARH7, PARH8
COMMON / PARG/ PARG1, PARG2, PARG3, PARG4,
8 PARG5, PARG6, PARG7, PARG8, PARG9
COMMON / PART/ PART1, PART2, PART3
COMMON / PRATIO/ PARR1, PARR2, PARR3
COMMON / PARCP/ PRCP1, PRCP2, PRCP3, PRCP4
COMMON / PARBP/ PRBP1, PRBP2
EQUIVALENCE (ZZZZ,WDWNP)
EQUIVALENCE (ZZZC,CALW)
EQUIVALENCE (ZPARS,PARS1)
EQUIVALENCE (ZPARV,PARV1)
EQUIVALENCE (ZPARH,PARH1)
02190186
02190187
02190188
02190189
02190190
02190191
02190192
02190193
02190194
02190195
02190196
02190197
02190198
02190199
02190200
02190201
02190202
02190203
02190204
02190205
02190206
02190207
02190208
02190209
02190210
02190211
02190212
02190213
02190214
02190215
02190216
02190217
02190218
02190219
02190220
02190221

```

EQUIVALENCE (ZPARG,PARG1)	02190222
EQUIVALENCE (ZPART,PART1)	02190223
EQUIVALENCE (ZPARCP,PRCP1)	02190224
EQUIVALENCE (ZPARBP,PRBP1)	02190225
EQUIVALENCE (ZRATIO,PARR1)	02190226
DATA PARR1/8.959873D0/, PARR2/0.15D0/, PARR3/0.0D0/	02190227
DATA PRCP1/1.0D0/, PRCP2/-0.1D0/, PRCP3/6.0D0/, PRCP4/0.6D0/	02190228
DATA PRBP1/2.2D0/, PRBP2/1.1D0/	02190229
DATA PARS1/63.8188D0/, PARS2/-5.1082D-3/, PARS3/7.8360D-4/	02190230
& PARS4/-1.5492D-6/, PARS5/0.089D0/	02190231
DATA PARV1/10195.02D0/, PARV2/460.0D0/, PARV3/18.860D0/	02190232
& PARV4/-26.523D0/	02190233
DATA PARH1/1075.84D0/, PARH2/0.434659D0/, PARH3/1.4877D-5/	02190234
& PARH4/-7.0548D-7/, PARH5/3.756599D-3/, PARH6/0.44973521D0/	02190235
& PARH7/-6.9478D-5/, PARH8/-6.959D-6/	02190236
DATA PARG1/11.0D0/, PARG2/-0.011D0/, PARG3/-140.0D0/	02190237
& PARG4/8.0D0/, PARG5/0.004577D0/, PARG6/1.8D0/	02190238
& PARG7/460.0D0/, PARG8/333.0D0/, PARG9/1.75D0/	02190239
DATA PART1/3061.596D0/, PART2/6.306699D0/, PART3/-383.7148D0/	02190240
DATA RAD/ 6.0D0/,PRECMX/0.90D0/,WVOL/1200.0D0/, WHEIG/7.0D0/	02190241
1 AHTOV/1.50D0/, TUBEH/4.0D0/, TUBED/5.0D0/	02190242
2 IMAX/12/, JJMAX/15/, IDCWN/6/	02190243
3 ILEFT/8/, IRIGHT/12/, NCAL/5/	02190244
DATA BETA/0.277D-3/, DELddb/C.4635D0/, BRIXR/0.8D0/	02190245
1 RHOVR/0.576D-2/, DENSTY/88.1088D0/, TZERO/126.069D0/	02190246
2 HV/1127.3D0/, DELHLV/1006.38D0/, HR/94.03D0/	02190247
DATA F/0.00D+0/, BRIxFF/0.0D0/, PUFFF/0.9D0/	02190248
1 TSTEAM/280.0D0/, UU/90.0D0/, PRESRF/2.0D0/	02190249
2 TEMPF/105.0D0/	02190250
DATA XSP/2*0.576D0/, XIF/2*0.064D0/, XCP/2*0.2D0/	02190251
1 XWP/2*0.16D0/, AVERN/2*0.1D+13/, AVERLL/2*3.281D-4/	02190252
2 RATCR/0.00D0/, TINTAL/134.979D0/	02190253
DATA NSITER/5/, SPSMTH/2.0D0/, THETAZ/0.5D0/, THETAS/0.75D0/	02190254
1 XVLIM/0.99999D0/, SLIPV/ 30.0D0/, EXPV/ 0.0D0/	02190255
2 PUMPDP/0.0D0/, VART/0.0D0/,ALPHA/1.339D-6/	02190256
3 IWSTRT/1/, DT/0.1D-1/	02190257

```

3      N1/2/, N2/30/, N3/30/
DATA  MN/1/, MO/2/, N/0/, JMAX/0/,
1      RTIME/0.0D0/, BTDUOT/0.0D0/, BTDEDT/0.0D0/,
2      DDZDT/0.0D0/, SURFDT/0.0D0/, EVINTG/0.0D0/,
3      EMVINT/0.0D0/, IFLAG1/0/, IFLAG2/0/
DATA  S/2*-0.9D+27/, C/2*-0.9D+27/, IMP/2*-0.9D+27/,
1      EM/2*-0.9D+27/, Q/2*-0.9D+27/, AVERT/2*-0.9D+27/,
2      AVERH/2*-0.9D+27/, AVERD/2*-0.9D+27/, TOTALH/2*-0.9D+27/
DATA  ZZZZ/40*-0.9D+27/, ZZZC/100*-0.9D+27/
      END
02190258
02190259
02190260
02190261
02190262
02190263
02190264
02190265
02190266
02190267

```

	SUBROUTINE BOUNDY	02190270
C----		02190271
C----	SETS UP BOUNDARY CONDITIONS BETWEEN	02190272
C----	PAN PROPER AND THE LOWER PART OF PAN	02190273
C----	I. E. DOWNTAKE AND CALANDRIA.	02190274
C----		02190275
	IMPLICIT REAL*8 (A-H,O-Z)	02190276
	REAL*8 IMP(2)	02190277
	COMMON/WSTRT/EM(2),S(2),IMP,C(2),Q(2),AVERT(2),HHM(2),HH(2)	02190278
	1,F,XWP,XSF,XIP,G(2),HF,AVERD(2),TMASS(2),WATER(2)	02190279
	2,TOTALH(2),XSP(2),XIP(2),XCP(2),XWF(2),AVERH(2)	02190280
	3,SSMAX,SSMIN	02190281
	COMMON/OVERAL/E(2),HHH(2),EVINTO,ENVINT,AQFLUX	02190282
	COMMON/FLAG/IWSTRT,IFLAG1,IFLAG2	02190283
	COMMON/REAL/RTIME,TCONST	02190284
	COMMON/PAN/VOLSCH,RADSQ,VCIC,WVCL,WHEIG	02190285
	COMMON/DIMEM/U(2,30,30),W(2,30,30),T(2,30,30),WW(30,30)	02190286
	COMMON/DIMEN1/P(30,30),PBIP1,PBIM1	02190287
	COMMON/TPHASE/ENTH(2,30,30),DEN(2,30,30)	02190288
	COMMON/GRID/DR,DZ,DT,DTOZSQ,DTODZ,DZODR,DZO2DR,DTO2DR,DTO2DZ	02190289
	1,DT2DRZ,DTODRZ,DTODR,FOURMD,DZORSQ,DZODT,DTORSQ	02190290
	2,DZO2,CALFC2,CALFC3,DDZDT,SURFDT,DRT2,DZO,DDZDZO	02190291
	3,DZODTO	02190292
	COMMON/PROPTY/RHO,RHOINV,RHOO2,VISC,ALPHA,VORHO,BETA	02190293
	1,FOURMR,FMO2DR,FMODR,CP,FOURMC,TZERO	02190294
	2,HVINV,DELHIV,DENSTY	02190295
	COMMON/COORD/R(30),Z(30),RINV(30),RH(30)	02190296
	COMMON/LIMITS/IMAX,IMAXM1,IMAXM2,JMAX,JMAXM1,JMAXM2,NMAX,NPRINT	02190297
	1,NBAR,NPRNT,JMAXP1,NSTART,JMAXP2,IMAXP1	02190298
	COMMON/STEP/MN,MO,N	02190299
	COMMON/SIZE/H,RAD,HMAX	02190300
	COMMON/AREAP/DV(30),DVOA(30)	02190301
	COMMON/ENTHAL/DHNEW,DHOLD,DHIF1,DHIM1,DHJP1,DHJM1	02190302
	COMMON/BOUND/IRIGHT,IRIGP1,ILEFT,ILEFP1,ILEFM1,ICOWN	02190303
	1,IDWNP1,IDOWN1	02190304


```

COMMON/CHEST/UA,UA,TUBEH,AREAT,EOA,UPOA,DTOTH,THODT,UAOA,CALANH
1,BOTTH,TUBED,FMCH,CDZ,DTOCDZ,TSTEAM,NTUBES,NCAL,NCALM1
2,NCALP1
COMMON/LUMBT/WDWNJP(2),TDWNJP(2),DDWNJP(2),HDWNJP(2)
1,WDWNJM(2),TROTT(2),DBOTT(2),HECTT(2)
2,UBOTT(2),UONEB(2),WCALAV(2),TCALAV(2),DCALAV(2),HCALAV(2)
3,WCALJM(2),TCALJM(2),DCALJM(2),HCALJM(2)
COMMON/LUMCAL/CALW(10,2),CALH(10,2),CALT(10,2),CALD(10,2)
1,CALP(10,2)
COMMON/ CONECT/ HBND(30),DBNDS(30),TBNDS(30),QJCAL
COMMON/ EMPEQ/ SLIPV, EXPV
COMMON/ CHECK/ DELHIO(30),DELHT(30),DELHDT(30),DELWIO(30)
COMMON/BOTTOM/ VOLUP, AFLWU, AFLWD, ABOAFD, ABOAFU
1, VCLBT, DTAUOV, CONST6, CONST7, CONST8
1, ENTHFR, FFLUXU
DATA PIE, COEFFV, RHOC, GR/3.14159D0, 0.5236D0, 99.1D0, 32.2D0/
QJ=0.0
TJM1=CALT(NCAL,MC)
DJM1=CALD(NCAL,MC)
DO 391 I=1,LEFT,IRIGHT
391 QJ=QJ+DV(I)*(T(MO,I,1)-TJM1)*(DEN(MO,I,1)*DZ+DJM1*CDZ)
QJCAL=QJ/AFLWU/(DZ+CDZ)
COMP11=0.0
HJJ1=0.0
DJJ1=0.0
TJJ1=0.0
DO 12 I=2,IDOWN
DDVI=DV(I)
HJJ1=HJJ1+DDVI*ENTH(MN,I,1)
TJJ1=TJJ1+DDVI*T(MN,I,1)
DJJ1=DJJ1+DDVI*DEN(MN,I,1)
COMP11=COMP11+DDVI
12 CONTINUE
02190305
02190306
02190307
02190308
02190309
02190310
02190311
02190312
02190313
02190314
02190315
02190316
02190317
02190318
02190319
02190320
02190321
02190322
02190323
02190324
02190325
02190326
02190327
02190328
02190329
02190330
02190331
02190332
02190333
02190334
02190335
02190336
02190337

```

```

DHJP1=HJJP1/COMP11
DJP1=DJJP1/COMP11
TJP1=TJJP1/COMP11
TDHNP(MN)=TJP1
DDHNP(MN)=DJJP1
HGHNP(MN)=DHJP1
WJD=WDHNP(MN)
DO 2227 I=2, IDOWN
HBND(I)=HBPOT(MN)
DBND(I)=DBPOT(MN)
TBND(I)=T(MN, I, 1)
WW(I, 1)=WJD
2227 CONTINUE
DO 2228 I=IDWNP1, ILEFM1
HBND(I)=ENTH(MN, I, 1)
DBND(I)=DEN(MN, I, 1)
TBND(I)=T(MN, I, 1)
2228 CONTINUE
DO 2230 I=IRIGP1, IMAX
HBND(I)=ENTH(MN, I, 1)
DBND(I)=DEN(MN, I, 1)
TBND(I)=T(MN, I, 1)
2230 CONTINUE
HJM1=CALH(NCAL, MN)
DJM1=CALD(NCAL, MN)
TJM1=CALT(NCAL, MN)
WJM1=CALE(NCAL, MN)/PHOM
DO 2229 I=ILEFT, IRIGHT
HBND(I)=HJM1
DBND(I)=DJM1
TBND(I)=T(MN, I, 1)
WW(I, 1)=WJM1
2229 CONTINUE
RETURN
END

```

```

02190338
02190339
02190340
02190341
02190342
02190343
02190344
02190345
02190346
02190347
02190348
02190349
02190350
02190351
02190352
02190353
02190354
02190355
02190356
02190357
02190358
02190359
02190360
02190361
02190362
02190363
02190364
02190365
02190366
02190367
02190368
02190369
02190370
02190371
02190372

```

```

C----- 02190375
C----- 02190376
C----- 02190377
C----- 02190378
C----- 02190379
C----- 02190380
C----- 02190381
C----- 02190382
C----- 02190383
C----- 02190384
C----- 02190385
C----- 02190386
C----- 02190387
C----- 02190388
C----- 02190389
C----- 02190390
C----- 02190391
C----- 02190392
C----- 02190393
C----- 02190394
C----- 02190395
C----- 02190396
C----- 02190397
C----- 02190398
C----- 02190399
C----- 02190400
C----- 02190401
C----- 02190402
C----- 02190403
C----- 02190404
C----- 02190405
C----- 02190406
C----- 02190407
C----- 02190408
C----- 02190409

SUBROUTINE CALDEN(DD,DHNEW,TNEW,XV,XL,PJ,XVLIM)
      CALCULATES MIXTURE DENSITY GIVEN ENTHALPY
      AND PRESSURE, CORRECTS FOR PRESENCES OF
      CRYSTALS.
      IMPLICIT REAL*8(A-H,O-Z)
      COMMON/VAPDEN/PRESRF,RHCVR
      COMMON/PROPTI/RHO,RHOINV,RHOO2,VISC,ALPHA,VORHO,BETA
      1, FOURME,FMO2DR,FMODR,CP,FOURMC,TZERO
      2, HVINV,DELHLV,DENSTY
      COMMON/CONC /DELDDE,DELRH,BRIXR,CONST1,CONST2,EPE,VRATIO
      TNEW=DHNEW/CP
      TTSAT=TSAT(PJ)
      TBOIL=TTSAT+BPE
      IF(TNEW.LT.TBOIL) GO TO 99
      TNEW=TBOIL
      HL=CP*TBOIL
      RHOL=1.0D0-TNEW+DELRH
      RHOL=CONST1/RHOL+CONST2
      RHOL=1.0D0/RHOL
      RHOV=RHOVR*(1.0D0+PJ/PRESRF)
      DELHLV=ENTHV(TTSAT,PJ,EPE)-HL
      XV=DHNEW/DELHLV-HL/DELHLV
      IF(XV.LI.XVLIM) GO TO 1
      DHNEW=HL+DELHLV*XVLIM
      XV=XVLIM
      CONTINUE
      XL=1.0D0-XV
      DD=XL/RHOL+XV/RHOV
      DD=1.0D0/DD
      RETURN
      99
      XV=0.0
      XL=1.0D0
      DD=1.0D0-TNEW+DELRH

```

02190410
02190411
02190412
02190413

DD=CONST 1/DD+CONST 2
DD=1.0DD/DD
RETURN
END

	SUBROUTINE CALHTD	02190416
C----		02190417
C----	CALCULATES ENTHALPY AND TEMPERATURE FOR CALANDRIA	02190418
C----		02190419
	IMPLICIT REAL*8 (A-H,O-Z)	02190420
	REAL*8 IMP(2)	02190421
	DIMENSION ZZZZ(2,20),ZZZC(10,2,5), QFLUX(10)	02190422
	COMMON/ CONECT/ HBND(30),DBND(30),TRND(30),QJCAL	02190423
	COMMON/ OVERAL/ E(2), HHH(2), EVINTO, EMVINT, AQFLUX	02190424
	COMMON/ENTLIM/XVLIM	02190425
	COMMON/FLOW1/DUDT(30,30),DEDT(30,30),HCDT(10),BTUDT,BTDED	02190426
	1,DDZDT(30,30),DDCDT(10)	02190427
	COMMON/LUMBT/WDWNJP(2),TDWNJP(2),DDWNJP(2),HDWNJP(2)	02190428
	1,WDWNJM(2),TBOTT(2),DBOTT(2),HBOTT(2)	02190429
	2,UBOTT(2),UBONEB(2),WCALAV(2),ICALAV(2),DCALAV(2),HCALAV(2)	02190430
	3,WCALJM(2),TCALJM(2),DCALJM(2),HCALJM(2)	02190431
	COMMON/WSTRT/EM(2),S(2),IMP,C(2),Q(2),AVERT(2),HHM(2),HH(2)	02190432
	1,F,XWF,XSF,XIF,G(2),HF,AVERD(2),TMASS(2),WATER(2)	02190433
	2,TOTALH(2),XSP(2),XIP(2),XCP(2),XWP(2),AVERH(2)	02190434
	3,SSMAX,SSMIN	02190435
	COMMON/PAN/ VOLSCH, RADSQ, VOLC, WVOL, WHEIG	02190436
	COMMON/PROPTY/RHC,RHOINV,RHOC2,VISC,ALPHA,VORHO,BETA	02190437
	1,FOURMR,FMO2DR,FMODR,CP,FOURMC,TZERO	02190438
	2,HVINV,DELHLV,DENSTY	02190439
	COMMON/COORD/R(30),Z(30),RINV(30),RH(30)	02190440
	COMMON/LIMITS/IMAX,IMAXM1,IMAXM2,JMAX,JMAXM1,JMAXM2,NMAX,NPRINT	02190441
	1,NBAR,NPRNT,JMAXP1,NSTART,JMAXP2,IMAXP1	02190442
	COMMON/STEP/MN,MO,N	02190443
	COMMON/LUMCAL/ CALW(10,2),CALH(10,2),CALT(10,2),CALD(10,2)	02190444
	1,CALP(10,2)	02190445
	COMMON/GRID/DR,DZ,DT,DZOZSQ,DZOLZ,DZODR,DZO2DR,DZO2DR,DZO2DZ	02190446
	1,DT2DRZ,DTODRZ,DTODR,FOURMD,DZORSQ,DZODT,DTORSQ	02190447
	2,DZO2,CALFC2,CALFC3,DDZDT,SURFDT,DRT2,DZO,DDZDT	02190448

3,	DZCDTO	02190449-
	COMMON/CHEST/UU,UA,TUBEH,AREAT,POA,UPOA,DTOTH,THODT,UAOA,CALANH	02190450
1,	BOTTH,TUBED,PMGM,CDZ,DTOCDZ,TSTEAM,NTUBES,NCAL,NCALM1	02190451
2,	NCALP1	02190452
	COMMON/ENTHAL/DHNEW,DHOLD,DHIP1,DHIM1,DHJP1,DHJM1	02190453
	COMMON/VAPDEN/PRESRF,RHOVR	02190454
	EQUIVALENCE (ZZZZ,WDWNJP)	02190455
	EQUIVALENCE (ZZZC,CALW)	02190456
C		02190457
C	USE TO CHANGE HFAT LOAD (BY SPECIFYING CONSTANT QFLUX	02190458
C	,CHANGING TSTEAM, OR CALCULATING HEAT TRANSFER COEFF.)	02190459
C		02190460
	CALL HEATIN(CALT, QFLUX, AQFLUX)	02190461
C		02190462
	SSUMT=0.0	02190463
	SSUMH=0.0	02190464
	SSUMD=0.0	02190465
	QJ=QJCAL/CALFC2*CDZ	02190466
	CALT (1,MO)=CALT (2,MO)	02190467
	DJM1=CALD (NCAL,MO)	02190468
	DO 2 JJ=1,NCALM1	02190469
	J=NCAL-JJ	02190470
	JP1=J+1	02190471
	DHOLD=CALH (JP1,MO)	02190472
	TOLD=CALT (JP1,MO)	02190473
	DOLD=DJM1	02190474
	DJM1=CALD (J,MO)	02190475
	QJP1=QJ	02190476
	QJ= (TOLD-CALT (J,MO)) *(DJM1+DOLD) *0.5D0	02190477
	HCODT= (QFLUX (JP1) *POA- (DHOLD-CALH (J,MO)) /CDZ	02190478
	1*CALW (J,MO) *DJM1+ (QJP1-QJ) *FCURMC/DT) /DOLD	02190479
	DHNEW=DHOLD+HCODT*DT	02190480
	HCDT (JP1) =HCODT	02190481
C	-----	02190482
C	----- PRESSURE NOT ON STANDARD GRID INCREMENT ---	02190483
	PJ=CALP (J,MO)	02190484

```

C-----
  CALL CALDEN(DD,DHNEW,TNEW,XV,XL,PJ,XV LIM)
  CALH(JP1,MN)=DHNEW
  CALD(JP1,MN)=DD
  CALI(JP1,MN)=TNEW
  SSUMT=SSUMT+TNEW
  SSUMD=SSUMD+DD
  SSUMH=SSUMH+DHNEW
2  CONTINUE
  COMP1=DFLOAT(NCALM1)
  TCALAV(MN)=SSUMT/COMP1
  HCALAV(MN)=SSUMH/COMP1
  DCALAV(MN)=SSUMD/COMP1
  RETURN
  END

```

```

02190485
02190486
02190487
02190488
02190489
02190490
02190491
02190492
02190493
02190494
02190495
02190496
02190497
02190498
02190499

```

```

C-----
C-----
C-----
SUBROUTINE CALPP(PBIP1)
      CALCULATES PRESSURE PROFILE IN CALANDRIA
      IMPLICIT REAL*8(A-H,O-Z)
      REAL*8 IMP(2)
      DIMENSION ZZZC(10,2,5)
      COMMON/LUMBT/ WDNJJP(2),TDWNJP(2),DDWNJP(2),HDDWNJP(2)
1,      WDNJJP(2),TBOTT(2),DBOTT(2),HBOTT(2)
2,      UBOTT(2),UCNEB(2),WCALAV(2),TCALAV(2),DCALAV(2)
3,      HCALAV(2),WCALJJP(2),TCALJJP(2),DCALJJP(2),HDCALJJP(2)
      COMMON/CONC /DELDDP,DELRH,BRHXF,CONST1,CONST2,BPE,VRATIO
      COMMON/PROPTY/ RHO,RHOINV,RHCC2,VISC,ALPHA,VORHO,BETA
1,      FOURMR,FMO2DR,FMODR,CP,FOURMC,TZERO
2,      HVINV,DELHLV,DENSTY
      COMMON/WSTRT/EM(2),S(2),IMP,C(2),Q(2),AVERT(2),HHM(2),HH(2)
1,      F,XWF,XSF,XIF,G(2),HF,AVERD(2),TMASS(2),KATER(2)
2,      TOTALH(2),XSP(2),XIP(2),XCF(2),XWP(2),AVERH(2)
3,      SSMAX,SSMIN
      COMMON/STEP/MN,MC,N
      COMMON/LUMCAL/ CALW(10,2),CALH(10,2),CALT(10,2),CALD(10,2)
1,CALP(10,2)
      COMMON/CHEST/UA,TUBEH,AREAT,FOA,UPOA,DTOTH,THODT,UAOA,CALANH
1,BOTTH,TUBED,FMCN,CDZ,DTOCDZ,TSTEAM,NTUBES,NCAL,NCALM1
2,NCALP1
      EQUIVALENCE (ZZZC,CALW)
C
      DPFRP= 8.0D0/TUBED/TUBED*VRATIO/DBOTT(MN)
      BB = (XIP(MN) + XSP(MN))/CCNST1
      PJ=CALP(NCAL,MN)
      DPDCJ = 0.0
      DO 2 JJ=1,NCALM1
        J = NCAL-JJ
        JP1 = J + 1

```

C


```

C----- PRESSURE IS OFF THE STANDARD GRID INCREMENT ----
C----- BECAUSE CALP(NCAL,MN) IS PRESS. AT TOP OF -----
C----- CALANDEIA INSTEAD OF GRID POINT ABOVE THE CAL. -
      DPDCJP = DPDCJ
      DJ      = CALD(JP1,MN)
      DPDCJ   = DPDEF*VISCTY( CALT(JP1,MN), BE )*(CALW(JP1,MN)*DJ
      &      + CALW(JP1,MO)*CALD(JP1,MO)) + DJ
      PJ      = PJ+(DPDCJP+DPDCJ)*CDZ*0.5D0
      2 CALP(J,MN)=PJ
C-----
C----- PRESSURE FOR BOTTOM MOMENTUM BALANCE ----
      PBIP1 = PJ + DPDCJ*0.5D0*CDZ
C-----
      RETURN
      END
02190536
02190537
02190538
02190539
02190540
02190541
02190542
02190543
02190544
02190545
02190546
02190547
02190548
02190549
02190550

```

```

C-----
C-----
C-----
C-----
SUBROUTINE CALVAE
      CALCULATES MASS FLUX CF VAPOR
      LEAVING FREE SURFACE.

      IMPLICIT REAL*8 (A-H,O-Z)
      REAL*8 IMP(2)
      COMMON/CVERAL/ E(2), HHH(2), EVINTO, EMVINT, AQFLUX
      COMMON/WSTRT/EM(2), S(2), IMP,C(2), C(2), AVERT(2), HHM(2), HH(2)
      1,F,XWF,XSF,XLF,G(2),HF,AVERT(2),TMASS(2),WATER(2)
      2,TOTALH(2),XSP(2),XIP(2),XCP(2),XWF(2),AVERH(2)
      3,SSMAX,SSMIN
      COMMON/PAN/ VOLSCH, RALSQ, VOLC, KVOL, WHEIG
      COMMON/GRID/DE,DZ,DT,DZESQ,DTODZ,DZODR,DZODR,DTODZ,DTODZ,DTODZ
      1,DT2DRZ,DTODRZ,DTODR,FOURMD,DZORSQ,DZODT,DTORSQ
      2,DZO2,CALFC2,CALFC3,DDZDT,SURFDT,DEI2,DZO,DDZDT
      3,DZODTO
      COMMON/PROPTY/RHO,RHOINV,RHOC2,VISC,ALPHA,VORHO,BETA
      1,FOURMR,FMO2DR,FMODR,CP,FOURMC,TZERO
      2,HVINV,DELHLV,DENSTY
      COMMON/COORD/R(30),Z(30),RINV(30),RH(30)
      COMMON/LIMITS/IMAX,IMAXM1,IMAXM2,JMAX,JMAXM1,JMAXM2,NMAX,NPRINT
      1,NEAR,NPRINT,JMAXP1,NSTART,JMAXP2,IMAXP1
      COMMON/STFP/MN,MQ,N
      COMMON/SIZE/H,RAD,HMAX
      COMMON /AREAP/DV(30),DVOA(30)
      COMMON/TOP/ SURFAC(30),SSURF(30),SVFRV(30),HVAP
      1,SFSMTH,THETAZ,THETAS,FRAT(30),DHDT(30)
      COMMON/VAPDEN/PRESF,RHOVR
      COMMON/ EMPEQ/ SLIPV, EXPV
      DATA PIE,COEFFV,RHOC,GE/3.14159D0,0.5236D0,99.1D0,32.2D0/
      COMP1=0.0
      DO 32 I=2,IMAX
      COMP2=RHOVR*SLIPV*SVFRV(I)*(1.0D0-SVFRV(I))**EXPV
      COMP1=COMP1+DV(I)*COMP2

```

02190588
02190589
02190590
02190591
02190592
02190593

PRAT(I)=CCMP2
CONTINUE
FM(XN)=COMP1*DENSITY*HMAX**3*PIE
ENVINT=FM(MH)*DT+ENVINT
RETURN
END

82

```

C-----
C-----
C-----
C-----
C-----
SUBROUTINE CALW
      CALCULATES MASS FLUX OF VAPOR LEAVING
      ONE-E CELL IN CALANDRIA, AND VELOCITY OF
      CELL CENTER.
      IMPLICIT REAL*8 (A-H,C-Z)
      REAL*8 IMP(2)
      DIMENSION ZZZZ(2,20),ZZZC(10,2,5)
      COMMON/GRID/ DP,DZ,DT,DTCSQ,DTCDZ,DZODR,DZO2DF,DTO2DE,DTO2DZ
      1, DT2ERZ,DTOLEZ,DTODR,FOURMD,DZOFSC,DZODT,DTORSQ
      2, DZO2,CALFC2,CALFC3,DDZDT,SURFDT,DTI2,DZC,DDZDTO
      3, DZODT
      COMMON/PROPT/ RHO,RHOINV,RHOC2,VISC,ALPHA,VORHO,BETA
      1, FOURMR,FMO2DR,FMODR,CP,FOURMC,TZERO
      2, HVINV,DELHLV,DENSTY
      COMMON/FLOW1/UDT(30,30),DEDT(30,30),HCDT(10),ETEUDT,BTDEPT
      1,DDZDT(30,30),DECDT(10)
      COMMON/LUMBT/WDWNJP(2),TDWNJP(2),DDWNJP(2),HDWNJP(2)
      1,WDWNJM(2),TECT(2),DEOT(2),HBOIT(2)
      2,UBOTT(2),UONER(2),WCALAV(2),TCALAV(2),DCALAV(2),HCALAV(2)
      3,WCALJM(2),TCALJM(2),DCALJM(2),HCALJM(2)
      COMMON/WSTRT/EX(2),S(2),IMP,C(2),Q(2),AVERT(2),HHM(2),HH(2)
      1,F,XWF,XSF,XIF,G(2),HF,AVERD(2),TMASS(2),WATER(2)
      2,TOTALH(2),XSP(2),XIP(2),XCP(2),XWP(2),AVERH(2)
      3,SSMAX,SSMIN
      COMMON/STEP/IN,MC,N
      COMMON/LUMCAL/ CALW(10,2),CALH(10,2),CALT(10,2),CALD(10,2)
      1,CALP(10,2)
      COMMON/CHEST/UA,UA,TUBEH,AREAT,FOA,UPOA,DTOTH,THODT,UAOA,CALANH
      1,BOTH,TUEED,FMON,CDZ,DTOCDZ,ISTEAM,NTUBES,NCAL,NCALM1
      2,NCALF1
      EQUIVALENCE (ZZZZ,WDWNJP)
      EQUIVALENCE (ZZZC,CALW)
      C
      SSUMW = 0.0

```

C

02190632
 02190633
 02190634
 02190635
 02190636
 02190637
 02190638
 02190639
 02190640
 02190641
 02190642
 02190643
 02190644

```

REWNEW      = WCALJN(MN)*DBOTT(MN)*FNOM
CALF(1,MN) = REWNEW/CALD(1,MN)
DC 1 J=2,NCAL
DD=CALD(J,MN)
REWNEW=REWNEW-CDZ*(DD-CALD(J,MO))/DT
KNEW=REWNEW/ED
SSUMW=SSUMW+KNEW
CALW(J,MN)=KNEW
CONTINUE
COMP1=DFLOAT(NCALM1)
WCALAV(MN)=SSUMW/COMP1
RETURN
END

```

1

```

C-----
C-----
C-----
C-----
C-----
SUBROUTINE CONTIN
      CALCULATES VERTICAL MASS FLUX LEAVING CELL
      IN PAN PROFILE, AND THE VELOCITY OF EACH CELL
      CENTER.
      IMPLICIT REAL*8 (A-H,O-Z)
      REAL*8 IMP(2)
      COMMON/MOVE / DEDT(30)
      COMMON/CONNECT/ HBXDS(30), DBXDS(30), TBXDS(30), QJCAL
      COMMON/INOUT/IN,IOUT
      COMMON/DIMEN/U(2,30,30), W(2,30,30), T(2,30,30), RW(30,30)
      COMMON/TPHASE/ENTH(2,30,30), DEN(2,30,30)
      COMMON/GRID/DR,DZ,DT,DTCZSQ,DTODE,DZODR,DZODT,DZODR,DTODR,DTODZ
      COMMON/TPHASE/ENTH(2,30,30), DEN(2,30,30)
      COMMON/GRID/DR,DZ,DT,DTCZSQ,DTODE,DZODR,DZODT,DZODR,DTODR,DTODZ
      1,DT2DRZ,DTODEZ,DTODR,FOURMD,DZORSQ,DZODT,DTORSQ
      2,DZO2,CALFC2,CALFC3,DDZDT,SURFDT,DET2,DZO,DDZDTO
      3,DZOTC
      COMMON/PROPT/ RHO,REOLNV,RHCU2,VISC,ALPHA,VORHO,BETA
      1,FOURMR,FMG2DR,FMODR,CP,FOURMC,TZERO
      2,HVINV,DELHLV,DENSTY
      COMMON/COORD/R(30),Z(30),RINV(30),RH(30)
      COMMON/LIMITS/IMAX,IMAXM1,IMAXM2,JMAX,JMAXM1,JMAXM2,NMAX,NPRINT
      1,NBAR,NPRINT,JMAXF1,NSTART,JMAXP2,IMAXP1
      COMMON/STEP/MN,MC,N
      COMMON/SIZE/H,RAD,HMAX
      COMMON/AREAP/DV(30),DVCA(30)
      COMMON/BOUND/IRIGHT,IRIGP1,ILEFT,ILEFP1,ILEFM1,IDOWN
      1,IDWNP1,IDWNM1
      COMMON/CHEST/UD,UA,TUREH,AREAT,POA,UPOA,DTOT,THCDT,UAOA,CAIANH
      1,BOTTH,TUBED,FMCN,CDZ,DTCCDZ,TSTEAM,NTUBES,NCAL,NCALM1
      2,NCALF1
      COMMON/FLOW1/DUDT(30,30),DEDT(30,30),HCDT(10),HIDUDT,HTDEDT
      1,DDZDZDT(30,30),EDCDT(10)
      COMMON/CHECK/ DELHIO(30),DELHT(30),DELHDT(30),DELWIO(30)
02190647
02190648
02190649
02190650
02190651
02190652
02190653
02190654
02190655
02190656
02190657
02190658
02190659
02190660
02190661
02190662
02190663
02190664
02190665
02190666
02190667
02190668
02190669
02190670
02190671
02190672
02190673
02190674
02190675
02190676
02190677
02190678
02190679
02190680

```

```

C
DO 34 I=2,IMAX
  IP1=I+1
  IM1=I-1
  IF (I.EQ.2) IM1=I
  IF (I.EQ.IMAX) IP1=IMAX
  RIP1=R(IP1)
  RIM1=R(IM1)
  DJ=DBNDS(I)
  WWW=WW(I,1)
DO 34 J=1,JMAX
  JP1=J+1
  DJM1=DJ
  DJ=DEN(MN,I,J)
  DIP1=DEN(MN,IP1,J)
  DIM1=DEN(MN,IM1,J)
  COMP1=RIM1*DIM1*U(MN,IM1,J)-RIP1*DIP1*U(MN,IP1,J)
C
  IF (I.EQ.2) COMP1=-RIP1*DIP1*U(MN,IP1,J)
  1-R(I)*DJ*U(MN,I,J)
  IF (I.EQ.IMAX) COMP1=R(I)*DJ*U(MN,I,J)
  1+RIM1*DIM1*U(MN,IM1,J)
C
  AVDMDT=(DZ*DJ-DZO*DEN(MO,I,J))/DJ/DT
  COMP1=0.5D0*DZO2DR*RIINV(I)*COMP1/DJ-AVDMDT*0.5D0
  WWW=WWW+DJM1/DJ+CCMP1
  W(MN,I,J)=WWW+DPDT(J)
C
  WWW=WWW+COMP1
  WW(I,JP1)=WWW
  CONTINUE
  RETURN
  END
34

```

```

02190681
02190682
02190683
02190684
02190685
02190686
02190687
02190688
02190689
02190690
02190691
02190692
02190693
02190694
02190695
02190696
02190697
02190698
02190699
02190700
02190701
02190702
02190703
02190704
02190705
02190706
02190707
02190708
02190709
02190710
02190711
02190712
02190713

```

	SUBROUTINE CONTRL	02190716
C----		02190717
C----	IMPOSES CONSTRAINTS CN CALCULATION,	02190718
C----	PREFORMS CONTRCL CALCULATIONS.	02190719
C----	PRESENT USE- MAINTAIN TOTAL MASS CONSTANT.	02190720
C----	FEED CONTAINS NO SUGAR AND MATCHS EVAPORATION RATE	02190721
C----		02190722
	IMPLICIT REAL*8 (A-I,O-Z)	02190723
	REAL*8 IMP(2)	02190724
	COMMON/BOTTOM/ VOLUP, AFLWU, AFLWC, ABOAFD, ABOAFU	02190725
1,	VOLBT, DTAUOV, CONST6, CONST7, CONST8	02190726
1,	ENTHFR, FFLUXU	02190727
	COMMON/PROPTY/RHO,RHOINV,RHCO2,VISC,ALPHA,VORHO,BETA	02190728
1,	FOURMR,FMO2DR,FMODR,CP,FOURMC,TZERO	02190729
2,	HVINV,DELHLV,DENSTY	02190730
	COMMON/WSTRT/EM(2),S(2),IMP,C(2),Q(2),AVERT(2),HHM(2),HH(2)	02190731
1,F,XWF,XSF,XIF,G(2),HF,AVERD(2),TMASS(2),WATER(2)		02190732
2,TOTALH(2),XSP(2),XIP(2),XCP(2),XWP(2),AVERH(2)		02190733
3,	SSMAX,SSMIN	02190734
	COMMON/GRID/DR,DZ,DT,DZOZSQ,DTODZ,DZODR,DZO2DR,DTO2DR,DTO2DZ	02190735
1,DT2DRZ,DTODRZ,DTODR,FOURMD,DZORSQ,DZODT,DTORSQ		02190736
2,DZO2,CALFC2,CALFC3,DDZDT,SURFDT,DRT2,DZO,DDZDZO		02190737
3,	DZODTO	02190738
	COMMON/STEP/MN,MO,N	02190739
	COMMON/SIZE/ H, RAD, HMAX	02190740
	COMMON/PAN/ VOLSCH, RADSQ, VOLC, WVOL, WHEIG	02190741
	COMMON/CHEST/UU,UA,TUBEH,AREAT,POA,UPOA,DTOTH,THODT,UAOA,CALANH	02190742
1,BOTTH,TUBED,FMCN,CDZ,DTOCDZ,ISTEAM,NTUBES,NCAL,NCALM1		02190743
2,NCALP1		02190744
	COMMON/ VAPDEN / PRESRF,RHOVR	02190745
	COMMON/ AVPART / AVERN(2), AVERLL(2)	02190746
	COMMON/ BLOCK / BRIFFF,PURFF,TEMPFF,	02190747
1	VART,PRECMX,AHTOV,HR,TINTAL,HV,JJMAX	02190748
	DATA RHOC,COEFFV,PIE / 99.1D0,0.5236D0,3.14159D0 /	02190749
		02190750
		02190751

C
C


```

F      = EH(MN)
ENTHER = F/DENSTY/HMAX**3/VOLBT/PIE
FLOUW  = F/DENSTY/HMAX**3/AFLWU/PIE
RETURN
ENTRY ECNTRL
AVERN(MN) = XCP(MN)*THASS(MN)/RHOC/AVERLL(MN)**3/COEFFV
AVERN(MO) = AVERN(MN)
RETURN
END
02190752
02190753
02190754
02190755
02190756
02190757
02190758
02190759
02190760

```

```

C-----
C-----
C-----
C-----

SUBROUTINE CONVSP
      TRILIAGONAL IMPLICIT CALCUIATION TO
      LOCATE FREE SURFACE.

      IMPLICIT REAL*8 (A-H,O-Z)
      REAL*8 IMP(2)
      DIMENSION AA(30),CC(30),DD(30),EE(30),FF(30),WH(30)
      DIMENSION AF(30),CP(30),BB(30),DDD(30)
      COMMON/ ITTER/ NSITER
      COMMON/GRID/DR,DZ,DT,DZQSQ,DTODZ,DZODR,DZO2DR,DTO2DR,DTO2DZ
      1, DT2DRZ,DTODRZ,DTODR,FOURND,DZORSQ,DZOLT,DTORSQ
      2, DZO2,CALFC2,CALFC3,DDZDT,SURFDT,DRT2,DZO,DDZDTO
      3, DZODTO
      COMMON/LIMITS/IMAX,IMAXM1,IMAXM2,JMAX,JMAXM1,JMAXM2,NMAX,NPRINT
      1, NEAR,NPRINT,JHAXP1,NSTART,JHAXP2,IMAXP1
      COMMON/WSTRT/EM(2),S(2),IMP,C(2),Q(2),AVERT(2),HHM(2),HH(2)
      1,F,XWF,XSF,XIF,G(2),HF,AVERD(2),THASS(2),WATER(2)
      2,TOTALH(2),XSP(2),XIP(2),XCP(2),XWP(2),AVERH(2)
      3, SSMAX,SSMIN
      COMMON/OVERAL/ E(2), HHH(2), EVINTO, EMVINT, AQFLUX
      COMMON/REAL/ RTIME, TCONST
      COMMON/EAN/ VOLSCH, RADSQ, VOIC, HVCL, WHEIG
      COMMON/AVPART/AVERN(2),AVERLL(2)
      COMMON/DIMEN/U(2,30,30),W(2,30,30),T(2,30,30),FW(30,30)
      COMMON/DIMEN1/P(30,30),PBIP1,PBIM1
      COMMON/TPHASE/ENTH(2,30,30),DEN(2,30,30)
      COMMON/PROPTY/RHC,RHOINV,RHO2,VISC,ALPHA,VORHO,BETA
      1, FOURMR,FMO2DR,FMODR,CP,FOURMC,TZERO
      2, HVINV,DELHLV,DENSTY
      COMMON/COORD/R(30),Z(30),RINV(30),RH(30)
      COMMON/STEP/MN,MO,N
      COMMON/SIZE/H,RAD,HMAX
      COMMON /AREAP/DV(30),DVOA(30)
      COMMON/TOP/ SURFAC(30),SSURF(30),SVFV(30),HVAP
      1, SFSMTH,THETAZ,THETAS,FRAT(30),DHDT(30)

```

```

02190763
02190764
02190765
02190766
02190767
02190768
02190769
02190770
02190771
02190772
02190773
02190774
02190775
02190776
02190777
02190778
02190779
02190780
02190781
02190782
02190783
02190784
02190785
02190786
02190787
02190788
02190789
02190790
02190791
02190792
02190793
02190794
02190795
02190796
02190797
02190798

```

```

COMMON/CHEST/UU,UA,TUBEH,AREAT,POA,UPOA,DTOTH,THODT,UAOA,CALANH
1,BOITH,TUDED,FMCN,CDZ,DTCDDZ,TSTEAM,NTUBES,NCAI,NCAIM1
2,NCALP1
DATA EE(1)/1.0D0/, FF(1)/0.0D0/

C
DO 1 I=3,IMAXM1
IM1 = I - 1
IP1 = I + 1
DDD(I) = HW(I,JMAXP1)*DEN(MN,I,JMAX)-FRAT(I)
DD(I) = DDD(I)*DT
E + SURFAC(I)*DEN(MO,I,JMAXP1)
AA(I) = -R(IP1)*U(MN,IP1,JMAXP1) * RINV(I) * LTO2DR
E + AF(I)
1 CC(I) = R(IM1)*U(MN,IM1,JMAXP1) * RINV(I) * DTO2DR
E + CF(I)
C----- BOUNDARY CONDITIONS -----
DDD(2) = HW(2,JMAXP1)*DEN(MN,2,JMAX)-FRAT(2)
DD(2) = DDD(2)*DT
E + SURFAC(2)*DEN(MO,2,JMAXP1)
AA(2) = -R(3)*U(MN,3,JMAXP1) * RINV(2) * DTO2DR
E + AF(2)
CC(2) = -U(MN,2,JMAXP1) * DTO2DR
E + CF(2)
DDD(IMAX) = HW(IMAX,JMAXP1)*DEN(MN,IMAX,JMAX)-FRAT(IMAX)
DD(IMAX) = DDD(IMAX)*DT
E + SURFAC(IMAX)*DEN(MO,IMAX,JMAXP1)
AA(IMAX) = U(MN,IMAX,JMAXP1) * DTC2DR
E + AF(IMAX)
CC(IMAX) = R(IMAXM1)*U(MN,IMAXM1,JMAXP1)*RINV(IMAX)*DTO2DR
E + CF(IMAX)
C-----
DO 2 I=2,IMAX
COMP1 = BB(I) - CC(I) * EE(I-1)
EE(I) = AA(I)/COMP1
2 FF(I) = (DD(I) + CC(I) * FF(I-1))/COMP1

```

02190799

02190800

02190801

02190802

02190803

02190804

02190805

02190806

02190807

02190808

02190809

02190810

02190811

02190812

02190813

02190814

02190815

02190816

02190817

02190818

02190819

02190820

02190821

02190822

02190823

02190824

02190825

02190826

02190827

02190828

02190829

02190830

02190831

02190832

02190833

02190834

02190835

02190836

02190837

02190838

02190839

02190840

02190841

02190842

02190843

02190844

02190845

02190846

02190847

02190848

02190849

02190850

02190851

02190852

02190853

02190854

02190855

02190856

02190857

02190858

02190859

02190860

02190861

02190862

02190863

02190864

02190865

02190866

02190867

02190868

02190869

02190870

02190871

02190872

02190873

02190874

02190875

02190876

02190877

02190878

02190879

02190880

02190881

02190882

02190883

02190884

02190885

02190886

02190887

02190888

02190889

02190890

02190891

02190892

02190893

02190894

02190895

02190896

02190897

02190898

02190899

02190900

02190901

02190902

02190903

02190904

02190905

02190906

02190907

02190908

02190909

02190910

02190911

02190912

02190913

02190914

02190915

02190916

02190917

02190918

02190919

02190920

02190921

02190922

02190923

02190924

02190925

02190926

02190927

02190928

02190929

02190930

02190931

02190932

02190933

02190934

02190935

02190936

02190937

02190938

02190939

02190940

02190941

02190942

02190943

02190944

02190945

02190946

02190947

02190948

02190949

02190950

02190951

02190952

02190953

02190954

02190955

02190956

02190957

02190958

02190959

02190960

02190961

02190962

02190963

02190964

02190965

02190966

02190967

02190968

02190969

02190970

02190971

02190972

02190973

02190974

02190975

02190976

02190977

02190978

02190979

02190980

02190981

02190982

02190983

02190984

02190985

02190986

02190987

02190988

02190989

02190990

02190991

02190992

02190993

02190994

02190995

02190996

02190997

02190998

02190999

02191000

02191001

02191002

02191003

02191004

02191005

02191006

02191007

02191008

02191009

02191010

02191011

02191012

02191013

02191014

02191015

02191016

02191017

02191018

02191019

02191020

02191021

02191022

02191023

02191024

02191025

02191026

02191027

02191028

02191029

02191030

02191031

02191032

02191033

02191034

02191035

02191036

02191037

02191038

02191039

02191040

02191041

02191042

02191043

02191044

02191045

02191046

02191047

02191048

02191049

02191050

02191051

02191052

02191053

02191054

02191055

02191056

02191057

02191058

02191059

02191060

02191061

02191062

02191063

02191064

02191065

02191066

02191067

02191068

02191069

02191070

02191071

02191072

02191073

02191074

02191075

02191076

02191077

02191078

02191079

02191080

02191081

02191082

02191083

02191084

02191085

02191086

02191087

02191088

02191089

02191090

02191091

02191092

02191093

02191094

02191095

02191096

02191097

02191098

02191099

02191100

02191101

02191102

02191103

02191104

02191105

02191106

02191107

```

02190834      WH(IMAXP1) = PF(IMAX)/(1.0D0 - EE(IMAX))
02190835      SMIN = 1000.0
02190836      SURFHN = 0.0
02190837      RATZ = DDZDT*DFLOAT(JMAX)
02190838      DO 3 II=1,IMAXM1
02190839      I = IMAXP1 - II
02190840      DNEW = DEN(MN,I,JMAXP1)
02190841      WH(I) = EE(I) * WH(I+1) + PF(I)
02190842      SURFI = WH(I)/DNEW
02190843      SURFHN = SURFHN+DVOA(I)*SURFI
02190844      IF(SURFI.LT.SMIN) SMIN=SURFI
02190845      RATH = (SURFI-SURFAC(I))/DT
02190846      W(MN,I,JMAXP2) = RATH + RATZ
02190847      W(MN,I,JMAXP1) = 0.5D0*(RATH + DDD(I)/DNEW) + RATZ
02190848      SSURF(I) = SURFI
02190849      SURFAC(I) = SURFI
02190850      WH(1) = WH(2)
02190851      C----- DO 4 I=2,IMAX
02190852      C4----- DHDT(I) = ( (AA(I)-AF(I))*WH(I+1) + (CC(I)-CF(I))*WH(I-1) )/DT
02190853      C----- 8 + DDD(I) )/DEN(MN,I,JMAXP1)
02190854      C
02190855      HH(MN) = (SURFHN+JMAX*DZ)*HMAX+CALANH
02190856      SMIN=SMIN-0.10D0*DZ
02190857      IF(SMIN.GT.0.0) GO TO 50
02190858      CALL OUTPUT
02190859      CALL CUTALL
02190860      STOP 50
02190861      50 CONTINUE
02190862      RETURN
02190863      ENTRY INCONV
02190864      DO 10 I=2,IMAXM1
02190865      BB(I) = 1.0D0 + 2.0D0*SFSMTH*DTORSQ
02190866      AF(I) = SFSMTH*DTORSQ*RH(I)*RINV(I)
02190867      CF(I) = SFSMTH*DTORSQ*RH(I-1)*RINV(I)
02190868      BB(2) = 1.0D0 + SFSMTH*DTORSQ*RH(2)*RINV(2)

```

```

AF(2)      = SFSMTH*DTORSQ*RH(2)*RINV(2)
CF(2)      = 0.0D0
EB(IMAX)   = 1.0D0 + SFSMTH*DTORSQ*RH(IMAXM1)*RINV(IMAX)
AF(IMAX)   = 0.0D0
CF(IMAX)   = SFSMTH*DTORSQ*RH(IMAXM1)*RINV(IMAX)
RETURN
END
02190869
02190870
02190871
02190872
02190873
02190874
02190875

```

```

C-----
C-----
C-----
SUEROUTINE ENERGY
      02190878
      02190879
      02190880
      02190881
      02190882
      02190883
      02190884
      02190885
      02190886
      02190887
      02190888
      02190889
      02190890
      02190891
      02190892
      02190893
      02190894
      02190895
      02190896
      02190897
      02190898
      02190899
      02190900
      02190901
      02190902
      02190903
      02190904
      02190905
      02190906
      02190907
      02190908
      02190909
      02190910
      02190911
      02190912
      02190913

      INTEGRATION OF ENERGY EQUATION

      IMPLICIT REAL*8 (A-H,O-Z)
      COMMON/ CHECK/ DELHIO(30), DELHT(30), DELHDT(30), DELWIO(30)
      COMMON/ AREAP/DV(30), DVOA(30)
      COMMON/DIMEN/U(2,30,30), W(2,30,30), T(2,30,30), WW(30,30)
      COMMON/DIMEN1/P(30,30), PBIP1, PBIM1
      COMMON/GRID/DR,DZ,DT,DZDSQ,DTODZ,DZODR,DZODR,DTODR,DTODZ
      1,DT2DRZ,DTODRZ,DTODR,FCURMD,DZORSQ,DZODT,DTORSQ
      2,DZOD2,CALFC2,CALFC3,DDZDT,SURFDT,DRT2,DZO,DDZDZTO
      3,DZODTO
      COMMON/PROPTY/EHC,RHOINV,RHO02,VISC,ALPHA,VORHO,BETA
      1,FOURMR,FMO2DR,FMODR,CP,FOURMC,TZERO
      2,HVINV,DELHLV,DENSTY
      COMMON/COORD/R(30),Z(30),RINV(30),RH(30)
      COMMON/LIMITS/INAX,INAXM1,INAXM2,JMAX,JMAXM1,JMAXM2,NMAX,NPRINT
      1,NEAR,NPRNT,JHAXP1,NSTART,JMAXP2,INAXP1
      COMMON/BOUND/IRIGHT,IRIGP1,ILEFT,ILEFP1,ILEFM1,IDOWN
      1,IDWNP1,IDOWN1
      COMMON/STEP/MN,HO,N
      COMMON/SUBDER/DPDTI
      COMMON/FLOW1/DUDT(30,30),DEDT(30,30),HCDT(10),BTDUDT,BTDEDT
      1,DDZDZDT(30,30),DECDT(10)
      COMMON/CHEST/UU,UA,TUBEH,AREAT,POA,UPOA,DTOTH,THODT,UAOA,CALANH
      1,BOTTH,TUBED,FMCN,CDZ,DTCCDZ,ISTEAM,NTUBES,NCAL,NCALM1
      2,NCALF1
      COMMON/TEMP/TNEW,TOLD,TIP1,TIM1,TJP1,TJM1
      COMMON/CONSER/DIP1,DIM1,DJP1,DJM1,RIPI1,RI,RIPI1,RHIM1
      1,ADIP1,ADIM1,ADJP1,ADJM1
      COMMON/VELCTY/UNEH,UOLD,WNEW,WOLD,UIP1,UIM1,UJP1,UJM1,WIP1,WIM1
      1,WJPI1,WJM1,UF,UB,Wf,WB
      COMMON/INDEX/I,J
      COMMON/ENTHAL/DHNEW,DHOLD,DHIE1,DHIN1,DHJP1,DHJM1

```

C

```

HUF=0.0
IF (UF.LT.0.0) HUF=DHIP1-DHOLD
HUB=DHIM1-DHOLD
IF (UB.LT.0.0) HUB=0.0
HWF=0.0
IF (WF.LT.0.0) HWF=DHJP1-DHOLD
HNB=DHJM1-DHOLD
IF (NB.LT.0.0) HNB=0.0

C
C
C
COMP1=DTODZ*(WF*HWF-NB*HNB)
COMP2=DTODR*RINV(I)*(UF*HUF-UB*HUB)
CCMP3=FOURMD*((TJP1-TOLD)*ADJF1-(TOLD-TJM1)*ADJM1)
IF (J.EQ.1.AND.I.GT.ILEFN1) COMP3=FOURMD*((TJP1-TOLD)*ADJF1
1-(TOLD-TJM1)/FMCH/CALFC2*DZ*ADJM1)
COMP4=FOURMR*RINV(I)*(RHIP1*(TIP1-TOLD)*ADIP1
1-RHIM1*(TOLD-TIM1)*ADIM1)
DEODT=(-COMP1-COMP2+COMP3+COMP4)*RHOINV
DHNEW=DHOLD+DEODT
DEDT(I,J)=DEODT/DT
C----- QJ=FOURMD*DZODT*(TOLD-TJM1)*ADJM1
C----- IF (J.EQ.1.AND.I.GT.ILEFN1) QJ=ALPHA*ADJM1/FMCH*(TOLD-TJM1)/CALFC2

02190914
02190915
02190916
02190917
02190918
02190919
02190920
02190921
02190922
02190923
02190924
02190925
02190926
02190927
02190928
02190929
02190930
02190931
02190932
02190933
02190934
02190935
02190936

02190937
02190938
02190939
RETURN
END

```

REAL FUNCTION VISCTY*8(T,B)	02190941
C---- VISCOSITY	02190942
IMPLICIT REAL*8 (A-H,O-Z)	02190943
COMMON / SPARV/ SPARV1, SPARV2, SPARV3, SPARV4	02190944
VISCTY=DEXP (SPARV1/(T+SPARV2) +SPARV3*B+SPARV4)	02190945
RETURN	02190946
END	02190947
CCC	02190948
CCC	02190949
REAL FUNCTION HEATC*8(XCP,B)	02190950
C---- HEAT CAPACITY	02190951
IMPLICIT REAL*8 (A-H,O-Z)	02190952
COMMON / SPARCP/ SPRCP1, SPRCP2, SPRCP3, SPRCP4	02190953
HEATC = SPRCP1 + (SPRCP2 + SPRCP3*XCP) *B	02190954
RETURN	02190955
END	02190956
CCC	02190957
CCC	02190958
REAL FUNCTION BOILPE*8(XIP,XWP,B)	02190959
C---- BOILING PCINT ELEVATION	02190960
IMPLICIT REAL*8 (A-H,O-Z)	02190961
COMMON / SPARBP/ SPRBP1, SPRBP2	02190962
BOILPE = SPRBP1*(B/XWP) +SPRBP2*(XIP/B)	02190963
RETURN	02190964
END	02190965
CCC	02190966
CCC	02190967
REAL FUNCTION SUPERS*8(T,XSP,XIP,XWP)	02190968
C---- SUPERSATURATION	02190969
IMPLICIT REAL*8 (A-H,O-Z)	02190970
COMMON / SPARS/ SPARS1, SPARS2, SPARS3, SPARS4, SPARS5	02190971
SAT=SPARS1 + (SPARS2 + SPARS3*T + SPARS4*T*T) *T	02190972
SUPERS=(100.0-SAT)/SAT*XSP/XWP* (1.0/ (1.0-SPARS5*XIP/XWP))	02190973
RETURN	02190974
END	02190975

```

C-----
      REAL FUNCTION GRCWTH*8(T,SS,XIP,XWP)
      GROWTH RATE
      IMPLICIT REAL*8 (A-H,O-Z)
      COMMON / SPARG / SPARG1, SPARG2, SPARG3, SPARG4,
      & SPARG5, SPARG6
      COMMON/ EQUON / KATCR
      EACT=SPARG1 + SPARG2*T + SPARG3*XIP/XWP
      RATC=RATCR*DEXP(-EACT*(1.0D0/(T+SPARG4)-SPARG5)+SPARG6*XIP/XWP)
      CS=SS-1.0
      GROWTH=RATC*OS
      IF(OS.LT.0.0) GROWTH=5.0*GRCWTH
      RETURN
      END
      CCC
      CCC
C-----
      REAL FUNCTION RATIO*8(V,X)
      EFFECT OF CRYSTALS ON VISCOSITY
      IMPLICIT REAL*8 (A-H,O-Z)
      COMMON / SPARTO/ SPARR1, SPARR2, SPARR3
      RATIO = DEXP(SPARR1*V*X**SPARR2)
      RETURN
      END
      CCC
      CCC
C-----
      REAL FUNCTION TSAT*8(PJ)
      BOILING POINT OF PURE WATER
      IMPLICIT REAL*8 (A-H,O-Z)
      COMMON/VAPDEN/PRESRF,RHOVR
      COMMON / SPART/ SPART1, SPART2, SPART3
      TSAT=SPART1/(SPART2-DLOG10(PJ+PRESRF))+ SPART3
      RETURN
      END

```

```

02190978
02190979
02190980
02190981
02190982
02190983
02190984
02190985
02190986
02190987
02190988
02190989
02190990
02190991
02190992
02190993
02190994
02190995
02190996
02190997
02190998
02190999
02191000
02191001
02191002
02191003
02191004
02191005
02191006
02191007
02191008
02191009

```

```

C-----
REAL FUNCTION ENTHV*8(TT,PP,DDT)
  ENTHALPY OF VAPOR
  IMPLICIT REAL*8 (A-H,O-Z)
  COMMON/ BLOCK / BRIXFF, PURFF, TEMPPF,
1    VART, PRECHX, AHTOV, HR, TINTAL, HV, JJMAX
  COMMON / SPARH/ SPARH1, SPARH2, SPARH3, SPARH4,
  &    SPARH5, SPARH6, SPARH7, SPARH8, SPARH9
  ENTHV= SPARH1 + (SPARH2 + SPARH3*TT + SPARH4*TT*TT)*TT
1    + (PP*SPARH5 + SPARH6 + SPARH7*PP*PP
1    + SPARH8*DDT*PP + SPARH9*DDT ) *DDT
  RETURN
END
CCC
CCC
C-----
C-----
REAL FUNCTION VKINEM*8(TT,BB)
  CALCULATE KINEMATIC VISCOSITY
  (VART IS ARTIFICIAL VISCOSITY = 0)
  IMPLICIT REAL*8 (A-H,O-Z)
  REAL*8 IMP(2)
  COMMON/INSTRT/EM(2),S(2),IMP,C(2),Q(2),AVERT(2),HHM(2),HH(2)
1,    F,XRF,XSF,XIF,G(2),HF,AVERD(2),TMASS(2),WATER(2)
2,    TOTALH(2),XSP(2),XIP(2),XCP(2),XWP(2),AVERH(2)
3,    SSMAX,SSMIN
  COMMON/ BLOCK / ERIXFF, PURFF, TEMPPF,
1    VART, PRECHX, AHTOV, HR, TINTAL, HV, JJMAX
  COMMON/CONC /DELDDDB,DELRH,BRIXR,CONST1,CONST2,BPE,VRATIO
  COMMON/STEP /MN,MO,N
  VKINEM = VART + VISCITY(TT,BB) *VRATIO/AVERD(MN)
  VKINEM = VART
  RETURN
END
C
-----

```

```

02191012
02191013
02191014
02191015
02191016
02191017
02191018
02191019
02191020
02191021
02191022
02191023
02191024
02191025
02191026
02191027
02191028
02191029
02191030
02191031
02191032
02191033
02191034
02191035
02191036
02191037
02191038
02191039
02191040
02191041
02191042

```

```

C----- SUBROUTINE HEATIN( CALT, QFLUX, AQFLUX )
          CALCULATES OR IMPOSES HEAT FLUX IN CALANDRIA
          IMPLICIT REAL*8 (A-H,O-Z)
          DIMENSION CALT(10,2), QFLUX(10)
          COMMON/TOP/ SURFAC(30), SSURF(30), SVFRV(30), HVAP
1,        SPSETH, THETAZ, THETAS, PRAT(30), DHDT(30)
          COMMON/REAL/ RTIME, TCONST
          COMMON/PROPT/ RHO, RHOINV, RHOO2, VISC, ALPHA, VORHO, BETA
1,        FOURMR, FMO2DR, FMODR, CP, FOURMC, TZERO
2,        HVINV, DELHLV, DENSTY
          COMMON/STEP/ MN, MO, N
          COMMON/SIZE/ H, RAD, HMAX
          COMMON/CHEST/ UU, UA, TUBEH, AREAT, POA, UEOA, DTOH, THODT, UAOA, CALANH
1,        BOTTH, TUBED, FMOM, CDZ, DTOCDZ, TSTEAM, NTUBES, NCAL, NCALM1
2,        AQFLUX = FLUX
          DO 1 J = 2, NCAL
1        QFLUX(J) = FLUX
          RETURN
          ENTRY INHEAT(EVAP)
C----- ENTRY EVAPORATION COEFFICIENT -----
          FLUX = EVAP*HVAP/3600.0*TCONST/DENSTY
          RETURN
          END
02191045
02191046
02191047
02191048
02191049
02191050
02191051
02191052
02191053
02191054
02191055
02191056
02191057
02191058
02191059
02191060
02191061
02191062
02191063
02191064
02191065
02191066
02191067
02191068

```

```

C-----
C-----
C-----
      SUBROUTINE HUNEW
      SET UP FOR INTEGRATION OF ENERGY AND MOMENTUM EQUATIONS
      IMPLICIT REAL*8(A-H,O-Z)
      DIMENSION ZZZZ(2,20),ZZZC(10,2,5)
      REAL*8 IMP(2)
      COMMON/CONNECT/ HBND(30),DBND(30),TBND(30),QJCAL
      COMMON/MOVE / DPDT(30)
      COMMON/FORCE/ PUMPD
      COMMON/INOUT/IN,IOUT
      COMMON/WSTRT/EM(2),S(2),IMP,C(2),Q(2),AVERT(2),HHM(2),HH(2)
      1,F,XWP,XSP,XIF,G(2),HF,AVERT(2),TMASS(2),WATER(2)
      2,TOTALH(2),XSP(2),XIP(2),XCP(2),XWP(2),AVERH(2)
      3,SSMAX,SSMIN
      COMMON/OVERALL/ E(2),HHH(2),EVINTO,EMVINT,AQFLUX
      COMMON/FLAG/ INSTRT,IFLAG1,IFLAG2
      COMMON/REAL/ RTIME,TCONST
      COMMON/PAN/ VOLSCH,RADSQ,VOLC,HVOL,WHEIG
      COMMON/DIMEN/U(2,30,30),W(2,30,30),T(2,30,30),WW(30,30)
      COMMON/DIMEN1/P(30,30),PBIP1,PBIM1
      COMMON/TPHASE/ENTH(2,30,30),DEN(2,30,30)
      COMMON/GRID/DR,DZ,DT,DZDSQ,DTODZ,DZODR,DZO2DR,DTO2DR,DTO2DZ
      1,DT2DRZ,DTODRZ,DTODR,FOURMD,DZORSQ,DZODT,DTORSQ
      2,DZO2,CALFC2,CALFC3,DDZDT,SURFDT,DEFT2,DZO,DDZDT
      3,DZODT
      COMMON/PROPTY/RHO,RHOINV,RHOC2,VISC,ALPHA,VORHO,BETA
      1,FOURMR,FMO2DR,FNODR,CP,FOURNC,TZERO
      2,HVINV,DELHLV,DENSTY
      COMMON/COORD/R(30),Z(30),RINV(30),RH(30)
      COMMON/LIMITS/INAX,IMAXM1,IMAXM2,JMAX,JMAXM1,JMAXM2,NMAX,NPRINT
      1,NBAR,NPRINT,JMAXP1,NSTART,JMAXP2,IMAXP1
      COMMON/STEP/MN,NO,N
      COMMON/TEMP/TNEW,TOLD,TIP1,TIM1,TJP1,TJM1
      COMMON/CONSER/DIP1,DIM1,DJP1,DJM1,RIP1,RIM1,RI,RHIP1,RHIM1

```

```

02191071
02191072
02191073
02191074
02191075
02191076
02191077
02191078
02191079
02191080
02191081
02191082
02191083
02191084
02191085
02191086
02191087
02191088
02191089
02191090
02191091
02191092
02191093
02191094
02191095
02191096
02191097
02191098
02191099
02191100
02191101
02191102
02191103
02191104
02191105

```

1,ADIP1,ADIM1,ADJP1,ADJM1	02191106
COMMON/VELCTY/UNEW,WOLD,WNEW,WOLD,UIP1,UIM1,UJP1,UJM1,WIP1,WIM1	02191107
1,WJP1,WJM1,UF,UB,WF,WB	02191108
COMMON/PRESS/PIP1,PIM1,PJ,PJP1	02191109
COMMON/SIZE/H,RAD,HMAX	02191110
COMMON/INDEX/I,J	02191111
COMMON /AREAP/DV(30),DVOA(30)	02191112
COMMON/ENTHAL/DHNEW,DHOLD,DHIF1,DHIM1,DHJF1,DHJM1	02191113
COMMON/BOUND/IRIGHT,IRIGP1,ILEFT,ILEFP1,ILEFM1,IDOWN	02191114
1,IDWNP1,IDOWN1	02191115
COMMON/CHEST/UU,UA,TUBEH,AREAT,POA,UPOA,DTOTH,THODT,UAOA,CALANH	02191116
1,BOTTH,TUBED,FMCH,CDZ,DTOCDZ,TSTEAM,NTUBES,NCAL,NCALM1	02191117
2,NCALF1	02191118
COMMON /FLOW/DWT	02191119
COMMON/FLOW1/DUDT(30,30),DEDT(30,30),HCDT(10),BTDUET,BTDEDT	02191120
1,DDDZDT(30,30),DDCDT(10)	02191121
COMMON/AVPART/AVERN(2),AVERLL(2)	02191122
COMMON/TOE/ SURFAC(30),SSURF(30),SVFRV(30),HVAP	02191123
1, SFSMTH,THETAZ,THETAS,FRAT(30),DHDT(30)	02191124
COMMON/SUBDER/DPDTI	02191125
COMMON/ENTLIN/XVLIN	02191126
COMMON/VAPDEN/PRESRF,RHOVR	02191127
COMMON/LUMBT/WDWNJP(2),TDWNJF(2),DDWNJP(2),HDWNJP(2)	02191128
1,WDWNJM(2),TBOTT(2),DBOTT(2),HBOTT(2)	02191129
2,UBOTT(2),UONEB(2),WCALAV(2),TCALAV(2),LCALAV(2),HCALAV(2)	02191130
3,WCALJM(2),TCALJM(2),DCALJM(2),HCALJM(2)	02191131
COMMON/LUMCAL/ CALW(10,2),CALH(10,2),CALT(10,2),CALD(10,2)	02191132
1,CALP(10,2)	02191133
COMMON/ EMPEQ/ SLIPV, EXPV	02191134
COMMON/ CHECK/ DELHIO(30),DELHT(30),DELHDT(30),DELWIO(30)	02191135
DATA PIF,COEFFV,RHOC,GR/3.14159D0,0.5236D0,99.1D0,32.2D0/	02191136
EQUIVALENCE (ZZZZ,WDWNJP)	02191137
EQUIVALENCE (ZZZC,CALW)	02191138
	02191139

C

```

DO 11 I=2,IMAX
  IM1=I-1
  IP1=I+1
  IF (I.EQ.2) IM1=I
  IF (I.EQ.IMAX) IP1=IMAX
  RHIP1=R(IP1)
  RIM1=R(IM1)
  RI=R(I)
  RHIP1=RH(I)
  RHIM1=RH(IM1)
  HI=SURFAC(I)
  HIP1=SURFAC(IP1)
  HIM1=SURFAC(IM1)
  SURFI=(HI+DZ)*0.5D0
  PIM1=P(IM1,JMAXP1)
  PIP1=P(IP1,JMAXP1)
  PJ=P(I,JMAXP1)
  UCOLD=U(MO,I,JMAXP1)
  UJP1=UCLD
  UJM1=U(MO,I,JMAX)
  UIM1=U(MO,IM1,JMAXP1)
  UIP1=U(MO,IP1,JMAXP1)
  RHO=DEN(MO,I,JMAXP1)
  DJM1=DEN(MO,I,JMAX)
  DJP1=RHO
  DIP1=DEN(MO,IP1,JMAXP1)
  DIM1=DEN(MO,IM1,JMAXP1)
  ADIP1=(DIP1+RHO)/2.0D0
  ADIM1=(RHO+DIM1)/2.0D0
  ADJM1=(RHO*HI+DJM1*DZ)/(HI+DZ)
  RHOINV=1.0D0/RHO
  HHIP1=(HIP1+HI)/2.0D0
  HHIM1=(HIM1+HI)/2.0D0
  DTOHI=D1/HI
02191140
02191141
02191142
02191143
02191144
02191145
02191146
02191147
02191148
02191149
02191150
02191151
02191152
02191153
02191154
02191155
02191156
02191157
02191158
02191159
02191160
02191161
02191162
02191163
02191164
02191165
02191166
02191167
02191168
02191169
02191170
02191171
02191172
02191173

```

```

UF=RIP1*HIP1*DIP1*UIP1+RI*HI*RRHO*UOLD
UB=RIM1*HIM1*DIM1*UIM1+RI*HI*RRHO*UOLD
IF(I.EQ.2) UB=0.0
IP(I.EQ.IMAX) UF=0.0
UUF=0.0
IF(UF.LT.0.0) UUF=UIP1-UOLD
UUB=UIM1-UOLD
IF(UB.LT.0.0) UUB=0.0
WB=WB(I,JMAXP1)*DJM1
UWB=UJM1-UOLD
IF(WB.LT.0.0) UWB=0.0

COMP1=DTODR*RINV(I)*(UF*UUF-UB*UUB)/HI
COMP2=DTODI*UWB*WB
COMP3=VORHO*DTORSQ*RINV(I)*(RHIP1*(UIP1-UOLD)*HHIP1*ADIP1
1-RHIM1*(UOLD-UIM1)*HHIM1*ADIM1)/HI
COMP5=VORHO*DTODI*(UJM1-UOLD)/SURFI*ADJM1
COMP6=DTODR*((PIM1+PJ)*HHIM1-(PIP1+PJ)*HHIP1)/HI
COMP7=-VORHO*DT*RINV(I)*RINV(I)*UOLD
DUODT=(-COMP1+COMP2+COMP3+COMP5+COMP6)*BHOINV+COMP7
UNEW=UOLD+(DUODT(I,JMAXP1)*DT+DUODT)*0.5D0
DUDT(I,JMAXP1)=DUODT/DT
U(MN,I,JMAXP1)=UNEW

TJM1=T(MO,I,JMAX)
TOLD=T(MO,I,JMAXP1)
TJP1=TOLD
TIP1=T(MO,IP1,JMAXP1)
TIM1=T(MO,IM1,JMAXP1)
DHJM1=ENTH(MO,I,JMAX)
DHCLD=ENTH(MO,I,JMAXP1)
DHJP1=DHOLD
DHIP1=ENTH(MO,IP1,JMAXP1)
DHIM1=ENTH(MO,IM1,JMAXP1)

```

C
C
C

C

C	HUF=0.0	02191211
	IF(UF.LT.0.0) HUF=DHIP1-DHOLD	02191212
	HUB=DHIM1-DHOLD	02191213
	IF(UB.LT.0.0) HUE=0.0	02191214
	HWE=DHJM1-DHOLD	02191215
	IF(WB.LT.0.0) HWB=0.0	02191216
C		02191217
C		02191218
C		02191219
	COMP1=DT02DR*RINV(I)*(HUF*UF-HUB*UB)/HI	02191220
	COMP2=DT0HI*(FRAT(I)*(HVAP-DHOLD)-WB*HWB)	02191221
	COMP3=FOURNE*RINV(I)*(RHIP1*(TIP1-TOLD)*HHIP1*ADIP1	02191222
	1-RHIM1*(TOLD-TIM1)*HHIM1*ADIM1)/HI	02191223
	COMP4=ALPHA*DT0HI*(TJM1-TOLD)/SURFI*ADJM1	02191224
	DEODT=(-COMP1-COMP2+COMP3+COMP4)*RHOINV	02191225
C	DHNEW=DHOLD+(DEDT(I,JMAXP1)*DT+DEODT)*0.5D0	02191226
	DHNEW=DHOLD+DEODT	02191227
	DEDT(I,JMAXP1)=DEODT/DT	02191228
C		02191229
	CALL CALDEN(DD,DHNEW,TNEW,XV,XL,PJ,XVLI1M)	02191230
	ENTH(MN,I,JMAXP1)=DHNEW	02191231
	T(MN,I,JMAXP1)=TNEW	02191232
	DEN(MN,I,JMAXP1)=DD	02191233
C		02191234
	CALL CALDEN(DD,DHNEW,TNEW,XV,XL,0.0D0,0.999999D+00)	02191235
	SVFRV(I)=XV*DD/RHOVR	02191236
	T(MN,I,JMAXP2)=TNEW	02191237
	DEN(MN,I,JMAXP2)=DD	02191238
	ENTH(MN,I,JMAXP2)=DHNEW	02191239
C		02191240
		02191241


```

C
C
C
TJP1=TCOLD
TOLD=TJM1
UJP1=UCLD
UOLD=UJM1
DHJP1=DHOLD
DHOLD=DHJM1
DJP1=RHQ
RHO=DJM1
UJM1=U(MO,I,JMAXM1)
UIP1=U(MO,IP1,JMAX)
UIM1=U(MC,IM1,JMAX)
PIP1=P(IP1,JMAX)
PIM1=P(IM1,JMAX)
PJ=P(I,JMAX)
DIP1=DEN(MO,IP1,JMAX)
DIH1=DEN(MO,IM1,JMAX)
DJM1=DEN(MO,I,JMAXM1)
ADIP1=(DIP1+RHO)/2.0D0
ADIM1=(RHO+DIM1)/2.0D0
ADJP1=ADJM1
ADJM1=(RHO+DJM1)/2.0D0
RHOINV=1.0D0/RHO
C
UF=RIP1*DIP1+UIP1+RI*RHO*UOLD
UB=RIM1*DIM1+UIM1+RI*RHO*UOLD
IF(I.EQ.2) UB=0.0
IF(I.EQ.IMAX) UF=0.0
UUF=0.0
IF(UF.LT.0.0) UUF=UIP1-UOLD
UUB=UIM1-UOLD
IF(UB.LT.0.0) UUB=0.0
WF=WB
WB=DJM1*WB(I,JMAX)
02191242
02191243
02191244
02191245
02191246
02191247
02191248
02191249
02191250
02191251
02191252
02191253
02191254
02191255
02191256
02191257
02191258
02191259
02191260
02191261
02191262
02191263
02191264
02191265
02191266
02191267
02191268
02191269
02191270
02191271
02191272
02191273
02191274
02191275
02191276
02191277

```

```

UWF=0.0
IF (WF.LT.0.0) UWF=UJP1-UOLD
UWB=UJM1-UOLD
IF (WB.LT.0.0) UWB=0.0

```

```

02191278
02191279
02191280
02191281
02191282
02191283
02191284
02191285
02191286
02191287
02200000
02210000
02220000
02230000
02240000
02250000
02260000
02270000
02280000
02290000
02300000
02310000
02320000
02330000
02340000
02350000
02360000
02370000
02380000
02390000
02400000
02410000
02420000
02430000

```

C

```

CCMP1=DTODR*RINV(I)*(UWF*UF-UWB*UB)
COMP2=DTODZ*(UWF*WF-UWB*WB)
COMP3=VORHO*DTORSQ*RINV(I)*(RHIP1*(UIP1-UOLD)*ALIP1
1-RHIM1*(UOLD-UIM1)*ADIM1)
COMP5=VORHO*DTODZ*(ADJP1*(UJP1-UOLD)/SURFI-ADJM1*(UOLD-UJM1)/DZ)
COMP6=DTODR*(FIM1-PIPI)
COMP7=-VORHO*RINV(I)*RINV(I)*UOLD*DT
DUODT=(-CCMP1-COMP2+COMP3+COMP5+COMP6)*RHOINV+COMP7
UNEW=UOLD+0.5D0*(DUOT(I,JMAX)*DT+DUODT)
DUOT(I,JMAX)=DUODT/DT
U(W,I,JMAX)=UNEW

```

C

```

DHJM1=ENTH(MO,I,JMAXM1)
DHIP1=ENTH(MO,IP1,JMAX)
DHIM1=ENTH(MO,IM1,JMAX)
TIP1=T(MO,IP1,JMAX)
TIM1=T(MO,IE1,JMAX)
TJM1=T(MO,T,JMAXM1)

```

C

```

HUF=0.0
IF (UF.LT.0.0) HUF=DHIP1-DHOLD
HUB=DHIM1-DHOLD
IF (UB.LT.0.0) HUB=0.0
HWF=0.0
IF (WF.LT.0.0) HWF=DHJP1-DHOLD
HWB=DHJM1-DHOLD
IF (WB.LT.0.0) HWB=0.0

```

```

02191278
02191279
02191280
02191281
02191282
02191283
02191284
02191285
02191286
02191287
02200000
02210000
02220000
02230000
02240000
02250000
02260000
02270000
02280000
02290000
02300000
02310000
02320000
02330000
02340000
02350000
02360000
02370000
02380000
02390000
02400000
02410000
02420000
02430000

```

```

02440000
02450000
02460000
02470000
02480000
02490000
02500000
02510000
02520000
02540000
02550000
02580000
02590000
02600000
02610000
02620000
02630000
02640000
02650000
02660000
02670000
02680000
02690000
02700000
02710000
02720000
02730000
02740000
02750000
02760000
02770000
02780000
02790000
02800000
02810000
02820000

COMP1=DIO2DR*RINV(I)*(HUF*UF-HUB*UB)
COMP2=DTODZ*(HWF*WF-HWB*WB)
COMP3=FOURMR*RINV(I)*(RHIP1*(TIP1-TOLD)*ACIP1
1-RHIM1*(TOLD-TIM1)*ADIM1)
COMP4=DTODZ*ALPHA*((TJP1-TOLD)/SURFI*ADJP1-(TOLD-TJM1)/DZ*ADJM1)
DEODT=(-COMP1-COMP2+COMP3+COMP4)*RHOINV
DHNEW=DHOLD+DEODT
DEDT(I,JMAX)=DEODT/DT
CALL CALCFN(DD,DHNEW,TNEW,XV,XL,PJ,XVLIH)
ENTH(MN,I,JMAX)=DHNEW
DEN(MN,I,JMAX)=DD
T(MN,I,JMAX)=TNEW

DO 10 JJ=1,JMAXM2
J=JMAX-JJ
JP1=J+1
JM1=J-1
TJP1=TCOLD
TOLD=TJM1
UJP1=UOLD
UOLD=UJM1
DHJP1=DHOLD
DHOLD=DHJM1
DJP1=RHO
RHO=DJM1
TJM1=T(MO,I,JM1)
TIP1=T(MO,IP1,J)
TIM1=T(MO,IM1,J)
UIP1=U(MO,IP1,J)
UIM1=U(MO,IM1,J)
UJM1=U(MO,I,JM1)
RIP1=P(IP1,J)

```

```

PIM1=P(IM1,J)
PJ=P(I,J)
DHJM1=ENTH(MO,I,JM1)
DHLPI=ENTH(MO,IP1,J)
DHIM1=ENTH(MO,IM1,J)
DJM1=DEN(MO,I,JM1)
DIP1=DEN(MO,IP1,J)
DIM1=DEN(MO,IM1,J)
ADIP1=(DIP1+RHO)/2.0D0
ADIM1=(RHO+DIM1)/2.0D0
ADJP1=ADJM1
ADJM1=(EHO+DJM1)/2.0D0
RHOINV=1.0D0/RHO
UF=RIP1*DIP1*UIP1+RI*RHO*UOLD
UB=EIM1*DIM1*UIM1+RI*RHO*UOLD
IF(I.EQ.2) UB=0.0
IF(I.EQ.IMAX) UF=0.0
WP=WB
WB=DJM1*WR(I,J)
D=DTI=DDDZDT(I,J)*DTODZ
CALL RMCMEQ
U(MN,I,J)=UNEW
CALL ENERGY
CALL CALDEN(DD,DHNEW,TNEW,XV,XL,PJ,XVLIM)
ENTH(MN,I,J)=DHNEW
DEN(MN,I,J)=DD
T(MN,I,J)=TNEW
CONTINUE
J=1
TJP1=TCID
TOLD=TJM1
UJP1=UOLD
UOLD=UJM1
DHJP1=DHOLD
DHOLD=DHJM1
DJP1=RHQ

```

10

C

```

02830000
02840000
02850000
02860000
02870000
02880000
02890000
02900000
02910000
02920000
02930000
02940000
02950000
02960000
02970000
02980000
02990000
03000000
03010000
03020000
03030000
03040000
03050000
03060000
03070000
03080000
03090000
03100000
03110000
03120000
03130000
03140000
03150000
03160000
03170000
03180000

```

```

RHO=DJM1
TJM1=TBNDS(I)
TIP1=T(MO,IP1,1)
TIM1=T(MO,IM1,1)
UIP1=U(MO,IP1,1)
UIM1=U(MO,IM1,1)
UJM1=-UOLD
PIP1=P(IP1,1)
PIM1=P(IM1,1)
PJ=P(I,1)
DHJM1=HBNDS(I)
DHI21=ENTH(MO,IP1,1)
DHIM1=ENTH(MO,IM1,1)
DJM1=LEND(I)
DIP1=DEN(MO,IP1,1)
DIM1=DEN(MO,IM1,1)
ADIP1=(DIP1+RHO)/2.0D0
ADIM1=(RHO+DIM1)/2.0D0
ADJP1=ADJM1
ADJM1=(RHO*DZ+DJM1*CDZ)/(DZ+CDZ)
RHOINV=1.0D0/RHO
UF=RIP1*DIP1*UIP1+RI*RHO*UCID
UB=RIM1*DIM1*UIM1+RI*RHO*UOLD
IF(I.EQ.2) UB=0.0
IF(I.EQ.IMAX) UF=0.0
WF=WB
WB=DJM1*WW(I,1)
DPDTI=DDDZDT(I,1)*DTCDZ
CALL BMCMEQ
U(MN,I,1)=UNEW

```

C

```

03190000
03200000
03210000
03220000
03230000
03240000
03250000
03260000
03270000
03280000
03290000
03300000
03310000
03320000
03330000
03340000
03350000
03360000
03370000
03380000
03390000
03400000
03410000
03420000
03430000
03440000
03450000
03460000
03470000
03480000

```

03490000
03500000
03510000
03520000
03530000
03540000
03550000
03560000

CALL ENERGY
CALL CALDEN(DD,DHNEW,TNEW,XV,XL,PJ,XVLIX)
ENTH(MN,I,1)=DHNEW
DEN(MN,I,1)=DD
T(MN,I,1)=TNEW
CONTINUE
RETURN
END

11

```

C-----
C-----
C-----
C-----
SUPEROUTINE LOOP
      LOOP THRU DOWNTAKE AND CALANDRIA.
      CALCULATIONS FOR BOTTOM
      IMPLICIT REAL*8(A-H,O-Z)
      DIMENSION ZZZZ(2,20),ZZZC(10,2,5)
      REAL*8 IMP(2)
      COMMON/BOTTOM/ VOLUP, AFLWD, ABOAFD, ABOAFU
      1, VOLBT, DTAUOV, CONST6, CCNST7, CONST8
      1, ENTHFR, FFLUXU
      COMMON/FLAG/ INSTRT, IFLAG1, IFLAG2
      COMMON/ENTLIM/ IVLIM
      COMMON/FORCE/ PUMPPD
      COMMON/MOVE / DPDT(30)
      COMMON/INSTRT/EM(2),S(2),IMP,C(2),Q(2),AVERT(2),HHM(2),HH(2)
      1,F,XFP,XSF,XIF,G(2),HF,AVERD(2),TMASS(2),WATER(2)
      2,TOTALH(2),XSP(2),XIP(2),XCP(2),XWP(2),AVERH(2)
      3,SSMAX,SSMIN
      COMMON/PAN/ VOLSCH, RADSQ, VCIC, HVCL, WHEIG
      COMMON/DIMEN1/P(30,30),PBIP1,EBIM1
      COMMON/TPHASE/ENTH(2,30,30),DEN(2,30,30)
      COMMON/GRID/DR,DZ,DT,DZOSQ,DTODZ,DZODR,DZO2DR,DTO2DR,DTO2DZ
      1,DT2DRZ,DTODRZ,DTODR,FOURMD,DZORSQ,DZODT,DTORSQ
      2,DZO2,CALFC2,CALFC3,DDZDT,SURFDT,DRT2,DZO,DDZDZO
      3,DZODTO
      COMMON/PROPTY/RHO,RHOINV,RHO02,VISC,ALPHA,VORHO,BETA
      1,FOURMR,FMO2DR,FMODR,CP,FOURMC,TZERO
      2,HVINV,DELHLV,DENSTY
      COMMON/COORD/R(30),Z(30),RINV(30),RH(30)
      COMMON/LIMITS/IMAX,IMAXN1,IMAXM2,JMAX,JMAXM1,JMAXM2,NMAX,NPRINT
      1,NEAR,NPRINT,JMAXP1,NSTART,JMAXP2,IMAXP1
      COMMON/STEP/MN,MO,N
      COMMON/SIZE/H,RAD,HMAX
      COMMON /AREAP/DV(30),DVOA(30)
03560003
03560004
03560005
03560006
03560007
03560008
03560009
03560010
03560011
03560012
03560013
03560014
03560015
03560016
03560017
03560018
03560019
03560020
03560021
03560022
03560023
03560024
03560025
03560026
03560027
03560028
03560029
03560030
03560031
03560032
03560033
03560034
03560035
03560036
03560037

```

C
C
C

COMMON/BOUND/IRIGHT,IRIGP1,ILEFT,ILEFP1,ILEFM1,IDOWN
1,IDWNP1,IDWNM1
COMMON/CHEST/UU,UA,TUBEH,AREAT,POA,UPOA,DTOTH,THODT,UAOA,CALANH
1,BOTTH,TUBED,FMCN,CDZ,DTOCDZ,ISTEAM,NTUBES,NCAL,NCALM1
2,NCALP1
COMMON/FLOW1/DUDT(30,30),DEDT(30,30),HCDT(10),BIDUDT,BTDEDT
1,DDDZDT(30,30),DDCDT(10)
COMMON/VAPDEN/PRESRF,RHOVR
COMMON/LUMBT/WDWNJP(2),TDWNJP(2),DDWNJP(2),HDWNJP(2)
1,WDWNJM(2),TBOTT(2),DBOTT(2),HBOTT(2)
2,UBOTT(2),UCNFB(2),WCALAV(2),TCALAV(2),LCALAV(2),HCALAV(2)
3,WCALJM(2),TCALJM(2),DCALJM(2),HCALJM(2)
COMMON/LUMCAL/CALW(10,2),CALH(10,2),CALT(10,2),CALD(10,2)
1,CALP(10,2)
COMMON/CHECK/DELHIO(30),DELHT(30),DELHDT(30),DELWIO(30)
DATA PIE,COEFFV,RHOC,GR/3.14159D0,0.5236D0,99.1D0,32.2D0/
EQUIVALENCE (ZZZZ,WDWNJP)
EQUIVALENCE (ZZZC,CALW)

RADIAL MOM. EQUATION LUMPED

RHO=DBOTT(MO)
RHOINV=1.0D0/RHO
UCNE=UCNFB(MO)
UOLD=UBOTT(MO)
COMP1=RHOINV*(PBIN1-PBIP1+PUMFEP)*CCNST7
COMP2=1.0D0/DT+CONST8*UOLD
UNEW = UOLD + COMP1/COMP2*DT
UBOTT(MN)=UNEW

C
C
C

LUMPED ENERGY EQUATIONS

DHJP1=HDWNJP(MO)
DHOLD=HBOTT(MO)
HJM1=WCALJM(MO)
DOLD=DEOTT(MO)

03560038
03560039
03560040
03560041
03560042
03560043
03560044
03560045
03560046
03560047
03560048
03560049
03560050
03560051
03560052
03560053
03560054
03560055
03560056
03560057
03560058
03560059
03560060
03560061
03560062
03560063
03560064
03560065
03560066
03560067
03560068
03560069
03560070
03560071
03560072
03560073


```

1022 FORMAT(1X,'FLOW TENDING IN WRONG DIRECTION OCCURANCE = '
1,I3,'VEL. SET TO ZERO EXEC. CCNTINJING',I,N=I,I6)
3232 CONTINUE
      WJU=WJU*DNEW
      WJU=WJU+FFLUXU
      WDWNJH(MN)=WJD
      WDWNJE(MN)=WJD
      WCAIJH(MN)=WJU/DNEW

      CALANDRIA
      CALCULATE VELOCITY IN TUBES

      CALI CALRW
      RETURN
      END

```

C
C
C
C
C
C
C

03560110
03560111
03560112
03560113
03560114
03560115
03560116
03560117
03560118
03560119
03560120
03560121
03560122
03560123
03560124
03560125
03560126
03560127

SUBROUTINE OUTPUT	03560130
IMPLICIT REAL*8 (A-H,O-Z)	03560131
REAL*8 IMP(2)	03560132
DIMENSION ZZZZ(2,20),ZZZC(10,2,5), RATH(30)	03560133
COMMON/EOTOM/ VOLUP, AFLWU, AFLWD, ABOAFD, ABOAFU	03560134
1, VOLBT, DTAUV, CONST6, CONST7, CONST8	03560135
1, ENTHFR, FFLUXU	03560136
COMMON/SIZE/ H,RAD,HMAX	03560137
COMMON /AREAP/ DV(30),DVOA(30)	03560138
COMMON/OVERAL/ E(2), HHH(2), EVINTO, ENVINT, AQFLUX	03560139
COMMON/ CHECK/ DELHIC(30),DELHT(30),DELEDT(30),DELWIO(30)	03560140
COMMON/INOUT/IN,IOUT	03560141
COMMON/LUMBT/WDWNJP(2),TDWNJP(2),DDWNJP(2),HDWNJP(2)	03560142
1,WDWNJM(2),TBOIT(2),DBOTT(2),HBOTT(2)	03560143
2,UBOTT(2),UONEE(2),WCALAV(2),TCALAV(2),DCALAV(2),HCALAV(2)	03560144
3,WCALJM(2),TCALJM(2),DCALJM(2),HCALJM(2)	03560145
COMMON/WSTRT/EM(2),S(2),IMP,C(2),Q(2),AVERT(2),HHM(2),HH(2)	03560146
1,F,XWF,XSF,XIP,G(2),HF,AVERD(2),TMASS(2),WATER(2)	03560147
2,TOTALH(2),XSP(2),XIP(2),XCP(2),XWP(2),AVERH(2)	03560148
3, SSMAX, SSMIN	03560149
COMMON/GRID/ DR,DZ,DT,DTOZSQ,DTODZ,DZODR,EZO2DR,DTO2DR,DTO2DZ	03560150
1, DT2DRZ,DTODRZ,DTCDR,FOUFMD,DZORSQ,IZODT,DTORSQ	03560151
2, DZO2,CALFC2,CALFC3,DDZDT,SURFDT,DRT2,DZO,DDZDZO	03560152
3, DZODTO	03560153
COMMON/REAL/ RTIME,TCONST	03560154
COMMON/PAN/ VOLSCH, RADSQ, VOLC, WVOL, WHEIG	03560155
COMMON/DIMEN/U(2,30,30),W(2,30,30),T(2,30,30),WW(30,30)	03560156
COMMON/DIMEN1/P(30,30),PBIP1,PBIM1	03560157
COMMON/TPHASE/ENTH(2,30,30),DEN(2,30,30)	03560158
COMMON/PROPTY/RHO,RHOINV,RHO02,VISC,ALPHA,VORHO,BETA	03560159
1, FOURMR,FMO2DR,FNODR,CP,FOURMC,TZERO	03560160
2, HVINV,DELHLV,DENSTY	03560161
COMMON/COORD/R(30),Z(30),RINV(30),RH(30)	03560162
COMMON/LIMITS/IMAX,IMAXM1,IMAXM2,JMAX,JMAXM1,JMAXM2,NMAX,NPRINT	03560163
1, NBAR,NPRINT,JNAXP1,NSTART,JNAXP2,INAXP1	03560164

```

COMMON/STEP/MN,MO,N
COMMON/AVPART/AVERN(2),AVERLL(2)
COMMON/CHEST/UD,UA,TUBEH,AREAT,FOA,UPOA,DTOTH,THODT,UAGA,CALANH
1,BOTTH,TUBED,FMGH,CDZ,DFOCDZ,TSTEAM,NTUBES,NCAL,NCALM1
2,NCALP1
COMMON/TOP/ SURFAC(30),SSURF(30),SVFV(30),HVAP
1,SFSMTH,THETAZ,THETAS,FRAT(30),DHDT(30)
COMMON/LUMCAL/ CALW(10,2),CALH(10,2),CALT(10,2),CALD(10,2)
1,CALP(10,2)
EQUIVALENCE (ZZZZ,WDWNJP)
EQUIVALENCE (ZZZC,CALW)
WRITE(6,1000) N,RTIME
WRITE(6,1020)
WRITE(6,1013)
DO 1 JJ=1,JMAXP1
J=JMAXP2-JJ
WRITE(6,1001) (U(MN,I,J),I=2,IMAX)
WRITE(6,1014)
WRITE(6,1001) (W(MN,I,JMAXP2),I=2,IMAX)
DO 2 JJ=1,JMAXP1
J=JMAXP2-JJ
WRITE(6,1001) (W(MN,I,J),I=2,IMAX)
WRITE(6,1015)
WRITE(6,1001) (FRAT(I),I=2,IMAX)
DO 22 JJ=1,JMAXP1
J=JMAXP2-JJ
WRITE(6,1001) (WH(I,J),I=2,IMAX)
WRITE(6,1016)
DO 3 JJ=1,JMAXP2
J=JMAXP2-JJ+1
WRITE(6,1001) (P(I,J),I=2,IMAX)
WRITE(6,1017)
DO 4 JJ=1,JMAXP2
J=JMAXP2-JJ+1
WRITE(6,1001) (T(MN,I,J),I=2,IMAX)
WRITE(6,1018)

```

03560165
03560166
03560167
03560168
03560169
03560170
03560171
03560172
03560173
03560174
03560175
03560176
03560177
03560178
03560179
03560180
03560181
03560182
03560183
03560184
03560185
03560186
03560187
03560188
03560189
03560190
03560191
03560192
03560193
03560194
03560195
03560196
03560197
03560198
03560199
03560200

```

DO 5 JJ=1,JMAXP2
J=JMAXP2-JJ+1
WRITE(6,1001) (ENTH(MN,I,J),I=2,IMAX)
WRITE(6,1019)
DO 6 JJ=1,JMAXP2
J=JMAXP2-JJ+1
WRITE(6,1001) (DEN(MN,I,J),I=2,IMAX)
WRITE(6,1004)
WRITE(6,1008)
WRITE(6,1005) (ZZZZ(MN,I),I=1,4)
WRITE(6,1009)
WRITE(6,1005) ZZZZ(MN,5)
WRITE(6,1010)
WRITE(6,1005) ZZZZ(MN,9), (ZZZZ(MN,I),I=6,8)
WRITE(6,1007) ZZZZ(MN,10)
WRITE(6,1011)
WRITE(6,1005) (ZZZZ(MN,I),I=11,14)
WRITE(6,1012)
WRITE(6,1005) (ZZZZ(MN,I),I=15,18)
WRITE(6,1002)
WRITE(6,1006) PBIM1,PBIP1
WRITE(6,1003)
WRITE(6,1021)
WRITE(6,1014)
WRITE(6,1001) (CALW(J,MN),J=1,NCAL)
WRITE(6,1016)
WRITE(6,1001) (CALP(J,MN),J=1,NCAL)
WRITE(6,1017)
WRITE(6,1001) (CALT(J,MN),J=1,NCAL)
WRITE(6,1018)
WRITE(6,1001) (CALH(J,MN),J=1,NCAL)
WRITE(6,1019)
WRITE(6,1001) (CALD(J,MN),J=1,NCAL)
RETURN

```

ENTRY OUTALL	03560236
WBAR=0.0	03560237
UBAR=0.0	03560238
RATZ = DDZDT*DFLOAT(JMAX)	03560239
DO 90 I=2,IMAX	03560240
RATH(I) = W(MN,I,JMAXP2) - RATZ	03560241
DO 90 J=1,JMAXP1	03560242
UBAR=UBAR+DABS(U(MN,I,J)-U(MO,I,J))	03560243
WBAR=WBAR+DABS(W(MN,I,J)-W(MO,I,J))	03560244
90 CONTINUE	03560245
FRACH=HH(MN)/HMAX	03560246
WRITE(6,1003)	03560247
WRITE(6,1029)	03560248
WRITE(6,1001) (SURFAC(I),I=2,IMAX)	03560249
WRITE(6,1031)	03560250
WRITE(6,1001) (RATH(I),I=2,IMAX)	03560251
WRITE(6,1003)	03560252
WRITE(6,1023) TMASS(MN),XSP(MN),XIP(MN),XCP(MN),XWP(MN)	03560253
WRITE(6,1024) AVERT(MN),AVERH(MN),AVERD(MN)	03560254
WRITE(6,1025) AVERN(MN),AVERLL(MN)	03560255
WRITE(6,1030) G(MN),SSMAX,SSMIN	03560256
WRITE(6,1026) HH(MN),FRACH,FM(MN),Q(MN),EMVINT	03560257
WRITE(6,1027) UBAR,WBAR,DZ,DDZDT	03560258
WRITE(6,1028) HHH(MN),HHM(MN),E(MN),EVINTO	03560259
CFORMATS	03560260
1000 FORMAT(1H1,' N= ',I10,2X,'REAL TIME = ',F10.2,' SEC.',/)	03560261
1001 FORMAT(11(1X,G11.4),/)	03560262
1002 FORMAT(/)	03560263
1003 FORMAT(/)	03560264
1004 FORMAT(/,10X,'CONDITIONS IN BOTTOM',/)	03560265
1005 FORMAT(6X,'VEL=',G11.4,1X,'TEMP=',G11.4,1X,'DEN=',G11.4	03560266
1,1X,'ENTHAL=',G11.4,/)	03560267
1006 FORMAT(1X,'PRESSURE AT DWNTAKE=',G11.4,'PRESSURE AT UP'	03560268
1,'TAKE=',G11.4)	03560269
1007 FORMAT(6X,'VEL*=',G11.4)	03560270
1008 FORMAT(4X,'TOP OF DOWNTAKE',/)	03560271

1009	FORMAT(4X,'BOTTCM OF DOWNTAKE',/)	03560272
1010	FORMAT(4X,'BOTTCM OF PAN',/)	03560273
1011	FORMAT(4X,'AVERAGE CONDITIONS IN STEAM CHEST',/)	03560274
1012	FORMAT(4X,'BOTTCM OF STEAM CHEST',/)	03560275
1013	FORMAT(/,8X,'SPATIAL DISTRIBUTION OF RADIAL VELOCITY',/)	03560276
1014	FORMAT(/,8X,'SPATIAL DISTRIBUTION OF VERTICAL VELOCITY',/)	03560277
1015	FORMAT(/,8X,'SPATIAL DISTRIBUTION OF VERTICAL VELOCITY INTO'	03560278
	1,' EACH MOVING CELL',/)	03560279
1016	FORMAT(/,8X,'SPATIAL DISTRIBUTION OF PRESSURE',/)	03560280
1017	FORMAT(/,8X,'SPATIAL DISTRIBUTION OF TEMPERATURE',/)	03560281
1018	FORMAT(/,8X,'SPATIAL DISTRIBUTION OF ENTHALPY',/)	03560282
1019	FORMAT(/,8X,'SPATIAL DISTRIBUTION OF DENSITY',/)	03560283
1020	FORMAT(/,10X,'CONDITIONS ABOVE THE CALANDRIA',/)	03560284
1021	FORMAT(10X,'CONDITIONS IN TUBES BOTTCM TO TOP',/)	03560285
1022	FORMAT(10X,'AVERAGE CONDITIONS IN PAN',/)	03560286
1023	FORMAT(5X,'TOTAL MASS =',G12.5,/	03560287
	1,5X,'MASS FRACTIONS:',2X,'SOLUT. SUGAR=',E10.3,2X,'IMPURITY='	03560288
	2,E10.3,2X,'CRYSTAL=',E10.3,2X,'WATER=',E10.3,/)	03560289
1024	FORMAT(5X,'TEMPERATURE=',E14.7,' ENTHALPY=',E14.7	03560290
	1,' DENSTIY=',E14.7,/)	03560291
1025	FORMAT(5X,'NUMBER OF CRYSTALS=',E14.7,2X,'AVERAGE LENGHT=',E14.7	03560292
	1,' FEET'/)	03560293
1026	FORMAT(5X,'LEVEL=',F5.2,' FT.', ' PREC.MAX=',F5.2,' EVAP. RATE='	03560294
	1,G11.4,' HEAT IN=',G11.4,' TOTAL EVAP.=',G11.4,/)	03560295
1027	FORMAT(10X,'UBAR=',G11.4,' WEAR=',G11.5,' DZ=',G11.4	03560296
	1,' DDZDT=',G11.4,/)	03560297
1028	FORMAT(10X,'DOUBLE CHECK FORM OVERALL BALANCES'/	03560298
	1,6X,'HHH=',G11.4,' HHM=',G11.4,' E=',G11.4	03560299
	2,6X,'TOTAL E =',G11.4)	03560300
1029	FORMAT(10X,'SURFACE HEIGHTS',/)	03560301
1030	FORMAT(5X,'AV. GROWTH RATE= ',E9.2,' MAX. SUPERSAT.= ',F4.2	03560302
	1,' MIN. SUPERSAT.= ',F4.2,/)	03560303
1031	FORMAT(/,10X,'RATE OF CHANGE OF SURFACE HEIGHTS',/)	03560304
	RETURN	03560305
	END	03560306

SUBROUTINE PARMEQ	03560309
C-----	03560310
C----- PROFORMS NON-DIMENSIONALIZATION OF ANY	03560311
C----- DIMENSIONAL PARAMETERS OR REDEFINES PARAMETERS TO	03560312
C----- CONSISTENT WITH CALCULATIONS.	03560313
C-----	03560314
IMPLICIT REAL*8 (A-H,O-Z)	03560315
COMMON/ BLOCK / BRIXFF, PURFF,TEMPFF,	03560316
1 VART, PRECNX, AHTOV, HR, TINTAL, HV, JJMAX	03560317
COMMON / SIZE/ H , RAD, HMAX	03560318
COMMON / PARS/ PARS1, PARS2, PARS3, PARS4, PARS5	03560319
COMMON / SPARS/ SPARS1, SPARS2, SPARS3, SPARS4, SPARS5	03560320
COMMON / PARV/ PARV1, PARV2, PARV3, PARV4	03560321
COMMON / SPARV/ SPARV1, SPARV2, SPARV3, SPARV4	03560322
COMMON / PARH/ PARH1, PARH2, PARH3, PARH4,	03560323
& PARH5, PARH6, PARH7, PARH8	03560324
COMMON / SPARH/ SPARH1, SPARH2, SPARH3, SPARH4,	03560325
& SPARH5, SPARH6, SPARH7, SPARH8, SPARH9	03560326
COMMON / PARG/ PARG1, PARG2, PARG3, PARG4,	03560327
& PARG5, PARG6, PARG7, PARG8, PARG9	03560328
COMMON / SPARG/ SPARG1, SPARG2, SPARG3, SPARG4,	03560329
& SPARG5, SPARG6	03560330
COMMON / PART/ PART1, PART2, PART3	03560331
COMMON / SPART/ SPART1, SPART2, SPART3	03560332
COMMON / FRATIO/ PARR1, PARR2, PARR3	03560333
COMMON / PARCP/ PRCP1, PRCP2, PRCP3, PRCP4	03560334
COMMON / PARBP/ PRBP1, PRBP2	03560335
COMMON / SPBATO/ SPARR1, SPARR2, SPARR3	03560336
COMMON / SPARCP/ SPRCP1, SPRCP2, SPRCP3, SPRCP4	03560337
COMMON / SPARBP/ SPREP1, SPREP2	03560338
COMMON / VAPDEN / PRESRF, RHOVR	03560339
COMMON / UNITS/ DIEVIS, DIMPRS	03560340
COMMON/PROPTY/ RHO, RHOINV, RHOC2, VISC, ALPHA, VORHO, BETA	03560341
1, FOURMR, FMO2DR, FMODR, CP, FOURMC, TZERO	03560342
2, HVINV, DELHLV, DENSTY	03560343
NAMelist /SUPST/ PARS1, PARS2, PARS3, PARS4, PARS5	03560344

NAMelist /SUPSTS/ SPARS1, SPARS2, SPARS3, SPARS3, SPARS5	03560345
NAMelist /GROW / PARG1, PARG2, PARG3, PARG4, PARG5,	03560346
& PARG6, PARG7, PARG8, PARG9	03560347
NAMelist /GROWS / SPARG1, SPARG2, SPARG3, SPARG3, SPARG5,	03560348
& SPARG6	03560349
NAMelist /VAPOR/ PARH1, PARH2, PARH3, PARH4, PARH5,	03560350
& PARH6, PARH7, PARH8, PARH9	03560351
NAMelist /VAPORS/ SPARH1, SPARH2, SPARH3, SPARH3, SPARH5,	03560352
& SPARH6, SPARH7, SPARH8, SPARH9	03560353
NAMelist /VISTY/ PARV1, PARV2, PARV3, PARV4	03560354
NAMelist /VISTYS/ SPARV1, SPARV2, SPARV3, SPARV4	03560355
NAMelist /SATTM/ PART1, PART2, PART3	03560356
NAMelist /SATTMS/ SPART1, SPART2, SPART3	03560357
NAMelist /CONSTS/ DIMPRS, DIMVIS, PRESRF, HMAX	03560358
NAMelist /VRATO/ PARR1, PARR2, PARR3	03560359
NAMelist / SUGCP/ PRCP1, PRCP2, PRCP3, PRCP4	03560360
NAMelist / SUGEPE/ PRBP1, PRBP2	03560361
NAMelist /SVRATO/ SPARR1, SPARR2, SPARR3	03560362
NAMelist /SSUGCP/ SPRCP1, SPRCP2, SPRCP3, SPRCP4	03560363
NAMelist /SSUGBP/ SPRBP1, SPRBP2	03560364
	03560365
WRITE (6,CONSTS)	03560366
	03560367
	03560368
SPARS1 = PARS1 + (PARS2+TZERO*PARS3+TZERO*TZERO*PARS4)*TZERO	03560369
SPARS2 = (PARS2 + 2.0D0*TZERO*PARS3+3.0D0*TZERO**2*PARS4)/BETA	03560370
SPARS3 = (PARS3 + 3.0D0*TZERO*PARS4)/BETA/BETA	03560371
SPARS4 = PARS4/BETA/BETA/BETA	03560372
SPARS5 = PARS5	03560373
	03560374
DDLOG = DLOG (DIMVIS)	03560375
SPARV1 = PARV1*BETA	03560376
SPARV2 = (PARV2 + TZERO)*BETA	03560377
SPARV3 = PARV3	03560378
SPARV4 = PARV4 - DDLOG	03560379

```

C
DELTAZ = TZERO-32.0D0
SPARH1 = (PARH1 - HR +
& (PARH2 + PARH3*DELTAZ + PARH4*DELTAZ**2) *DELTAZ) *BETA
SPARH2 = PARH2 + ( 2.0D0*PARH3 + 3.0D0*DELTAZ*PARH4) *DELTAZ
SPARH3 = (PARH3 + 3.0D0*DELTAZ*PARH4)/BETA
SPARH4 = PARH4/BETA/BETA
SPARH5 = DIMPRS*(PARH5 + 2.0D0*DIMPERS*PRESRF*PARH7)
SPARH6 = PARH6 +
& (PARH5 + PARH7*DIMPERS*PRESRF) *DIMPERS*PRESRF
SPARH7 = PARH7*DIMPERS*DIMPERS
SPARH8 = PARH8*DIMPERS/BETA
SPARH9 = PARH8/BETA*DIMPERS*PRESRF

C
SPARG1 = (PARG1 + TZERO*PARG2 + PARG3*PARG2)/PARG5*BETA*PARG6
SPARG2 = PARG2 /PARG5 * PARG6
SPARG3 = PARG4 /PARG5 * BETA*PARG6
SPARG4 = (PARG7 + TZERO) *BETA
SPARG5 = 1.0D0/PARG8/BETA/PARG6
SPARG6 = PARG9

C
SPART1 = PART1*BETA
SPART2 = PART2 - DLOG10 (DIMPERS)
SPART3 = (PART3 - TZERO) *BETA

C
SPRCP1 = PRCP1
SPRCP2 = PRCP2*PRCP3
SPRCP3 = PRCP2/PRCP4

C
SPARR1 = PARR1
SPARR2 = PARR2
SPARR3 = PARR3

C
SPRBP1 = PRBP1
SPRBP2 = PRBP2
WRITE(6,SUPST)
03560380
03560381
03560382
03560383
03560384
03560385
03560386
03560387
03560388
03560389
03560390
03560391
03560392
03560393
03560394
03560395
03560396
03560397
03560398
03560399
03560400
03560401
03560402
03560403
03560404
03560405
03560406
03560407
03560408
03560409
03560410
03560411
03560412
03560413
03560414
03560415

```

03560416
03560417
03560418
03560419
03560420
03560421
03560422
03560423
03560424
03560425
03560426
03560427
03560428
03560429
03560430
03560431
03560432

WRITE(6,SUPSTS)
WRITE(6,GROW)
WRITE(6,GROWS)
WRITE(6,VAPOR)
WRITE(6,VAPORS)
WRITE(6,VISTY)
WRITE(6,VISTYS)
WRITE(6,SATTM)
WRITE(6,SATTMS)
WRITE(6,SUGPE)
WRITE(6,SSUGBP)
WRITE(6,SUGCP)
WRITE(6,SSUGCP)
WRITE(6,VRATO)
WRITE(6,SVRATO)
RETURN
END

```

SUBROUTINE PRELIM
C-----
C----- PREFORMS ANY INITIALIZATION OR PRELIMINARY CALCULATIONS.
C----- READS IN DATA FOR RUN.
C-----
      IMPLICIT REAL*8(A-H,O-Z)
      INTEGER STMODE
      DIMENSION ZZZZ(2,20),ZZZC(10,2,5),QFLUX(10)
      DIMENSION ZPARS(5),ZPARV(4),ZPARH(8),ZPARG(9),ZPART(3)
      DIMENSION ZPARCP(4),ZPARBP(2),ZRATIO(3)
      REAL*8 IMP(2)
      COMMON/JOERUN/ IRUN(3)
      COMMON/UNITS / DIMVIS, DIMPRS
      COMMON/CHECK/ DELHIO(30),DELHT(30),DELHDT(30),DELWIO(30)
      COMMON/BOTTOM/ VOLUP, AFLWU, AFLWD, ABOAFD, ABOAFU
1,          VOLBT, DTAUOV, CONST6, CONST7, CONST8
1,          ENTHFR, PFLUXU
      COMMON/MOVE / LPDT(30)
      COMMON/OVERAL/ E(2), HHH(2), EVINTO, EMVINT, AQFLUX
      COMMON/LUMBT/WDWNJP(2),TDWNJP(2),DDWNJP(2),HDWNJP(2)
1,WDWNJM(2),TBOTT(2),DBOTT(2),HBOTT(2)
2,UBOTT(2),UONEB(2),WCALAV(2),TCALAV(2),DCALAV(2),HCALAV(2)
3,WCALJM(2),TCALJM(2),ECALJM(2),HCALJM(2)
      COMMON/LUMCAL/ CALW(10,2),CALH(10,2),CALT(10,2),CALD(10,2)
1,CALP(10,2)
      COMMON/REAL/ RTIME, TCONST
      COMMON/DIMEM/U(2,30,30),W(2,30,30),T(2,30,30),WW(30,30)
      COMMON/DIMEN1/P(30,30),PBIP1,FBIM1
      COMMON/TPHASE/ENTH(2,30,30),DEN(2,30,30)
      COMMON/COORD/R(30),Z(30),RINV(30),RH(30)
      COMMON/STEP/MN,MC,N
      COMMON/FLOW1/DUDT(30,30),DEDT(30,30),HCDT(10),BTUDT,BTDEDT
1,DDDZDT(30,30),DDCDT(10)
      COMMON /AREAP/DV(30),DVOA(30)
      COMMON/CONC /DELDEB,DELRH,BRIXR,CONST1,CONST2,BPE,VRATIO
      COMMON/FORCE/ PUMPDP

```

```

03560435
03560436
03560437
03560438
03560439
03560440
03560441
03560442
03560443
03560444
03560445
03560446
03560447
03560448
03560449
03560450
03560451
03560452
03560453
03560454
03560455
03560456
03560457
03560458
03560459
03560460
03560461
03560462
03560463
03560464
03560465
03560466
03560467
03560468
03560469
03560470

```

COMMON/INOUT/IN,IOUT	03560471
COMMON/ESTRT/EM(2),S(2),IMP,C(2),Q(2),AVERT(2),HEM(2),HH(2)	03560472
1,F,XWF,XSF,XIP,G(2),HF,AVERD(2),TMASS(2),WATER(2)	03560473
2,TOTALH(2),XSP(2),XIP(2),XCP(2),XWP(2),AVERH(2)	03560474
3,SSMAX,SSMIN	03560475
COMMON/FLAG/IWSTRT,IFLAG1,IFLAG2	03560476
COMMON/PAN/VOLSCH,RADSQ,VOLC,WVOL,WHEIG	03560477
COMMON/GRID/DR,DZ,DT,DTOZSQ,DTODZ,DZODR,DZO2DR,DTO2DR,DTO2DZ	03560478
1,DT2DRZ,DTODRZ,ETODE,FOURMD,DZORSQ,DZODT,DTORSQ	03560479
2,DZO2,CALFC2,CALFC3,DDZDT,SURFDT,DET2,DZO,DDZDTO	03560480
3,DZODT	03560481
COMMON/PROPT/RHO,RHOINV,RHOC2,VISC,ALPHA,VORHO,PETA	03560482
1,FOURMR,FMO2DR,FMODR,CP,FOURMC,TZERO	03560483
2,HVINV,DELHLV,DENSTY	03560484
COMMON/LIMITS/IMAX,IMAXM1,IMAXM2,JMAX,JMAXM1,JMAXM2,NMAX,NPRINT	03560485
1,NEAR,NPRNT,JMAXP1,NSTART,JMAXP2,IMAXP1	03560486
COMMON/SIZE/H,RAD,HMAX	03560487
COMMON/CHEST/UU,UA,TUBEH,AREAT,POA,UPOA,DTOTH,THODT,UAOA,CALANH	03560488
1,BOTTH,TUBED,FMCM,CDZ,DTOCDZ,TSTEAM,NTUBES,NCAI,NCALM1	03560489
2,NCALP1	03560490
COMMON/BOUND/IRIGHT,IRIGP1,ILEFT,ILEFP1,ILEPH1,IDOWN	03560491
1,IDWHP1,IDOWN1	03560492
COMMON/AVPART/AVERN(2),AVERLL(2)	03560493
COMMON/TOP/SURFAC(30),SSURF(30),SVFHV(30),HVAP	03560494
1,SFSMTH,THETAZ,THETAS,FRAT(30),DHDT(30)	03560495
COMMON/ENTLIM/XVLIM	03560496
COMMON/VAPDEN/PRESRF,RHOVR	03560497
COMMON/EMPEQ/SLIPV,EXPV	03560498
COMMON/ITTER/NSITER	03560499
COMMON/EQUON/RATCH	03560500
COMMON/BLOCK/BRIXFF,PURFF,TEMPFF,	03560501
1,VART,PRECMX,AHTOV,HR,TINTAL,HV,JJMAX	03560502
COMMON/PARS/PARS1,PARS2,PARS3,PARS4,PARS5	03560503
COMMON/PARV/PARV1,PARV2,PARV3,PARV4	03560504
COMMON/PARH/PARH1,PARH2,PARH3,PARH4,	03560505
8,PARH5,PARH6,PARH7,PARH8	03560506

COMMON / PARG/ PARG1, PARG2, PARG3, PARG4,	03560507
8 PARG5, PARG6, PARG7, PARG8, PARG9	03560508
COMMON / PART/ PART1, PART2, PART3	03560509
COMMON / PRATIO/ PARR1, PARR2, PARR3	03560510
COMMON / PARCP/ PRCP1, PRCP2, PRCP3, PRCP4	03560511
COMMON / PARBP/ PRBP1, PRBP2	03560512
DATA GR,PIE,RHOC/32.2D0,3.14159D0,99.1D0/	03560513
EQUIVALENCE (ZZZZ,WDWNJP)	03560514
EQUIVALENCE (ZZZC,CALW)	03560515
EQUIVALENCE (ZPARS,PARS1)	03560516
EQUIVALENCE (ZPARV,PARV1)	03560517
EQUIVALENCE (ZPARH,PARH1)	03560518
EQUIVALENCE (ZPARG,PARG1)	03560519
EQUIVALENCE (ZPART,PART1)	03560520
EQUIVALENCE (ZPARCP,PRCP1)	03560521
EQUIVALENCE (ZPARBP,PRBP1)	03560522
EQUIVALENCE (ZRATIO,PARR1)	03560523
C----- DEFINE THE PAN	03560524
NAMelist /DDPAN/ RAD, PRECMX, WVOL, WHEIG,	03560525
1 AHTOV, TUBEH, TUBED,	03560526
2 IMAX, JJMAX, IDOWN,	03560527
3 ILEFT, IRIGHT, NCAL	03560528
C----- REFERENCE PHYSICAL PROPERTIES	03560529
NAMelist /PHYSP/ BETA, DELDDB, BRIXR,	03560530
1 RHOVR, DENSTY, TZERO,	03560531
2 HV, DELHLV, HR	03560532
C----- LOAD VARIABLES - THINGS THAT CHANGE	03560533
NAMelist /LOADV/ F, BRIXFF, FURFF,	03560534
1 TEMPFF, TSTEAM, UU, PRESRF, EVAP	03560535
C----- INITIALIZATION VARIABLES	03560536
NAMelist /INTIAL/ XSP, XIP, XCE, XWP,	03560537
1 AVERLL, AVERNIN,	03560538
2 RATCR, TINTAL	03560539
C----- VARIABLES NEEDED FOR COMPUTATIONAL PURPOSES	03560540
NAMelist /STABLE/ NSITER, SFSMTH, THETAZ, THETAS,	03560541

1	XVLIM, SLIPV, EXPV,	03560542
2	PUMPDP, VART, ALPHA,	03560543
3	IWSTRT, DT	03560544
C-----	PARAMETERS FOR FUNCTIONS	03560545
	NAMelist /SUPST/ PARS1, PARS2, PARS3, PARS4, PARS5	03560546
	NAMelist /GROW / PARG1, PARG2, PARG3, PARG4, PARG5,	03560547
6	PARG6, PARG7, PARG8, PARG9	03560548
	NAMelist /VAPOR/ PARH1, PARH2, PARH3, PARH4, PARH5,	03560549
6	PARH6, PARH7, PARH8, PARH9	03560550
	NAMelist /VISTY/ PARV1, PARV2, PARV3, PARV4	03560551
	NAMelist /SATM/ PART1, PART2, PART3	03560552
	NAMelist /VRATO/ PARR1, PARR2, PARR3	03560553
	NAMelist / SUGCP/ PRCP1, PRCP2, PRCP3, PRCP4	03560554
	NAMelist / SUGBPE/ PRBP1, PRBP2	03560555
C		03560556
C-----	RUN IDENTIFICATION	03560557
	READ(5,1006) IRUN	03560558
	1006 FORMAT(3A4)	03560559
C-----	IN- INPUT UNIT NO. IOUT- CUTPUT UNIT NO.	03560560
	READ(5,*) IN,IOUT	03560561
	WRITE(6,1002) IN,IOUT	03560562
C-----	STMODE- STARTING MODE	03560563
C-----	.EQ. 1 COLD START	03560564
C-----	.NE. 1 RESTART	03560565
	READ(5,*) STMODE	03560566
	WRITE(6,1002) STMODE	03560567
C-----	NMAX - MAX. NO. OF TIME STEPS	03560568
C-----	NPRINT- PRINT INTERVAL FOR BIG PRINTOUT	03560569
C-----	NEAR - PRINT INTERVAL FOR SMALL PRINTOUT	03560570
C-----	NSTART - TIME STEP WHEN PRINTOUTS START	03560571
	READ(5,*) NMAX,NPRINT,NEAR,NSTART	03560572
	WRITE(6,1002) NMAX,NPRINT,NEAR,NSTART	03560573
	IF(STMODE.EQ.1) GO TO 600	03560574
	REWIND IN	03560575

[illegible]

C-----	E, (EM)	- EVAPORATION RATE	03560612
C-----	S	- TOTAL MASS OF DISSOLVED SUGAR	03560613
C-----	IMP	- TOTAL MASS OF IMPURITY	03560614
C-----	C	- TOTAL MASS OF CRYSTALS	03560615
C-----	Q	- HEAT INPUT RATE	03560616
C-----	AVERT	- AVERAGE TEMPERATURE IN PAN	03560617
C-----	F	- FEED RATE	03560618
C-----	BRIXXF	- BRIX OF FEED	03560619
C-----	PURPF	- PURITY OF FEED	03560620
C-----	TEMPFF	- TEMPERATURE OF FEED	03560621
C-----	G	- GROWTH RATE	03560622
C-----	TMASS	- TOTAL MASS IN PAN	03560623
C-----	WATER	- TOTAL MASS OF WATER	03560624
C-----	AVERD	- AVERAGE DENSITY IN PAN	03560625
C-----	AVERH	- AVERAGE ENTHALPY IN PAN	03560626
C-----	RTIME	- REAL TIME	03560627
C-----	VOLSCH	- VOLUME OF THE STEAM CHEST (CALANDRIA)	03560628
C-----	RADSQ	- RADIUS SQUARED	03560629
C-----	VOLC	- VOLUME OF PAN BELOW PAN PROPER	03560630
C-----	WVOL	- WORKING VOLUME OF PAN	03560631
C-----	WFEIG	- WORKING HEIGHT OF PAN	03560632
C-----	PRECMX	- PERCENT OF MAX. HEIGHT OF PAN	03560633
C-----	AREAT	- HEAT TRANSFER AREA	03560634
C-----	AHTOV	- RATIO OF THE HEAT TRANSFER AREA TO VOLUME	03560635
C-----	DT	- TIME STEP	03560636
C-----	DR	- RADIAL INCREMENT	03560637
C-----	DZ	- VERTICAL INCREMENT	03560638
C-----	CDZ	- VERTICAL INCREMENT IN THE CALANDRIA	03560639
C-----	DDZDT, (SURFDT)	- RATE OF CHANGE VERTICAL INCREMENT	03560640
C-----	BETA	- COEFFICIENT OF THERMAL EXPANSION	03560641
C-----	AVERN	- AVERAGE NO. DENSITY OF CRYSTALS	03560642
C-----	AVERLL	- AVERAGE CRYSTAL SIZE	03560643
C-----	DENSTY	- REFERENCE DENSITY	03560644
C-----	SLIPV	- PARAMETER FOR SLIP VELOCITY OF VAPOR AT SURFACE	03560645
C-----	EXPV	- PARAMETER FOR SLIP VELOCITY OF VAPOR AT SURFACE	03560646
C-----	VART	- ARTIFICIAL VISCOSITY (=0)	03560647

C-----	HR	- REFERENCE ENTHALPY OF LIQUID	03560648
C-----	ALPHA	- THERMAL DIFFUSIVITY	03560649
C-----	SFSMTH	- SURFACE DIFFUSIVITY (SMOOTH FACTER)	03560650
C-----	UU	- HEAT TRANSFER COEFFICIENT	03560651
C-----	TSTEAM	- STEAM TEMPERATURE	03560652
C-----	TZERO	- INITIAL TEMPERATURE IN PAN	03560653
C-----	BATCR	- GROWTH RATE CCNSTANT	03560654
C-----	RHOVR	- REFERENCE DENSITY OF VAPOR	03560655
C-----	PRESRF	- PRESSURE IN VAPOR SPACE	03560656
C-----	DELDDB	- COEFFICIENT OF CCNCENTRATION	03560657
C-----	BRIXR	- REFERENCE BRIX	03560658
C-----	XSP	- MASS FRACTION SUGAR	03560659
C-----	XIP	- MASS FRACTICN IMPURITY	03560660
C-----	XCP	- MASS FRACTION CRYSTAL	03560661
C-----	XWP	- MASS FRACTION WATER	03560662
C-----	INSTRT	- EQ. 1 DO WSTRT CALCULATIONS	03560663
C-----		- GT. 1 DO NOT DO WSTRT CALCULATIONS	03560664
C-----	IMAX	- NO. RADIAL GRID POINTS	03560665
C-----	JMAX	- NO. OF SUBSURFACE CELLS	03560666
C-----	IRIGHT	- RIGHT MOST RADIAL GRID POINT CONTAINING CALANDRIA	03560667
C-----	ILEFT	- LEFT MOST RADIAL GRID POINT CONTAINING CALANDRIA	03560668
C-----	IDOWN	- RIGHT MOST RADIAL GRID POINT IN DOWNTAKE	03560669
C-----	NCAL	- NO. OF GRID POINTS IN CALANDRIA	03560670
C-----	TUBEH	- HEIGHT OF TUBES	03560671
C-----	TUBED	- DIAMETER OF TUBES	03560672
C-----	NTUBES	- NO. OF TUBES	03560673
C-----	BOTTH	- HEIGHT OF THE BOTTOM OF PAN TO CALANDRIA	03560674
600	CONTINUE		03560675
C			03560676
	READ (5,DDPAN)		03560677
	READ (5,PHYSP)		03560678
	READ (5,LOADV)		03560679
	READ (5,INTIAL)		03560680
	READ (5,STABLE)		03560681
	READ (5,SUPST)		03560682
	READ (5,GROW)		03560683

	READ (5,VAPOR)	03560684
	READ (5,VISTY)	03560685
	READ (5,SAITM)	03560686
	READ (5,VRATO)	03560687
	READ (5,SUGCP)	03560688
	READ (5,SUGBPE)	03560689
	WRITE (6,DDPAN)	03560690
	WRITE (6,PHYSP)	03560691
	WRITE (6,LOADV)	03560692
	WRITE (6,INTIAL)	03560693
	WRITE (6,STABLE)	03560694
C		03560695
	ILEFM1=ILEFT-1	03560696
	ILEFP1=ILEFT+1	03560697
	IDWNP1=IDOWN+1	03560698
	IDOWN1=IDOWN-1	03560699
	IRIGP1=IRIGHT+1	03560700
	IF (IRIGHT.EQ.IMAX) IRIGP1=IMAX	03560701
	IMAXP1=IMAX+1	03560702
	IMAXM1=IMAX-1	03560703
	IMAXM2=IMAX-2	03560704
	NCALM1=NCAL-1	03560705
	NCALP1=NCAL+1	03560706
	JMAXM1=JMAX-1	03560707
	JMAXM2=JMAX-2	03560708
	JMAXP1=JMAX+1	03560709
	JMAXP2=JMAX+2	03560710
C		03560711
	IF (STMODE.EQ.1) GO TO 6000	03560712
	TCCNST = DSQRT (HMAX/GR)	03560713
	RATCR = RATCR*TCONST/3600.0	03560714
	DIMPRS = DENSITY*HMAX/144.0DO	03560715
	PRESRF = PRESRF/DIMPRS	03560716
	DIMVIS = DENSITY*HMAX*DSQRT (HMAX*GR) /6.72E-04	03560717
	CALL PARMEQ	03560718
B	= XIP(MN) +XSP(MN)	03560719

	BPE = BOILPE(XIP(MN) , XWP(MN) , B) *BETA	03560720
	CONST1 = 1.000-XCP(MN)	03560721
	CONST2 = XCP(MN)/RHOC*DENSTY	03560722
	BB = B/CONST1	03560723
	DELRH = DELDEB*(BB-BR1XR)	03560724
	CP = HEATC(XCP(MN) , BB)	03560725
6000	CONTINUE	03560726
	RHOVR = RHOVR/DENSTY	03560727
	TSTEAM = (TSTEAM-TZERO) *BETA	03560728
	TINTAL = (TINTAL-TZERO) *BETA	03560729
C		03560730
	IF (STMODE.NE.1) GO TO 999	03560731
C		03560732
C	CALCULATE HEAT TRANSFER AREA AND NO. TUBES	03560733
C		03560734
	TUBED = TUBED/12.000	03560735
	A = WVOL*AHTOV	03560736
	COMP2 = TUBED*TUBED/4.000*PIE	03560737
	COMP3 = TUBED*TUBEH*PIE	03560738
	NTUBES = A/COMP3	03560739
	AREAT = NTUBES*COMP3	03560740
	VOLSCH = NTUBES*COMP2*TUBEH	03560741
	DELR = RAD/DFLCAT(IMAXM1)	03560742
	RIDWN = DFLOAT(IDOWN1) *DELR	03560743
	VOLDWN = RIDWN**2*TUBEH*PIE	03560744
	BOTTH = (WVOL-VOLSCH-VOLDWN)/RAD/RAD/PIE-WHEIG	03560745
	HMAX = BOTTH+TUBEH+WHEIG	03560746
	H = PRECMX*HMAX	03560747
	POA = AREAT/VOLSCH	03560748
	RADSQ = RAD*RAD*PIE	03560749
C		03560750
	DR = RAD/HMAX/DFLOAT(IMAXM1)	03560751
	DZ = 1.000/DFLOAT(JJMAX)	03560752
	CDZ = TUBEH/DFLOAT(NCALM1) /HMAX	03560753
C		03560754
	TUBEH = TUBEH/HMAX	03560755

TUBED = TUBED/HMAX	03560756
BOTTH = BOTTH/HMAX	03560757
CALANH = (TUBEH+BOTTH)*HMAX	03560758
TCONST = DSQRT(HMAX/GR)	03560759
RATCR = RATCR*TCONST/3600.0D0	03560760
DIMPRS = DENSTY*HMAX/144.0D0	03560761
PRESRF = PRESRF/DIMPRS	03560762
DIMVIS = DENSTY*HMAX*DSQRT(HMAX*GR)/6.72E-04	03560763
CALL FARMFQ	03560764
B = XIP(MN)+XSP(MN)	03560765
BPE = BOILPE(XIP(MN) , XWP(MN) , B)*BETA	03560766
CCNST1 = 1.0D0-XCP(MN)	03560767
CONST2 = XCP(MN)/RHOC*DENSTY	03560768
BB = B/CONST1	03560769
DELRH = DELDDB*(BB-BR1XR)	03560770
CP = HEATC(XCP(MN) , BB)	03560771
DHNEW = CP*TINTAL	03560772
CALL CALDEN(DD,DHNEW,TNEW,XV,XL,0.0D0,XVLIM)	03560773
RHO=DD	03560774
DH=H-CALANH	03560775
DH=DH/HMAX	03560776
JMAX=DH/DZ-2	03560777
C**** *****	03560778
IF(JMAX.GT.2) GO TO 5122	03560779
WRITE(6,1009)	03560780
STOP 53	03560781
1009 FORMAT(1X,'TRY AGAIN - NOT ENOUGH GRID POINTS')	03560782
5122 IF(JMAX.LT.29) GO TO 5123	03560783
WRITE(6,1010)	03560784
STOP 54	03560785
1010 FORMAT(1X,'TRY AGAIN - TOO MANY GRID POINTS')	03560786
C**** *****	03560787
5123 JMAX=DH/DZ-2	03560788
JMAXP2=JMAX+2	03560789
JMAXP1=JMAX+1	03560790
JMAXM1=JMAX-1	03560791

```

JMAXM2=JMAX-2
SURFI=DH-JMAX*DZ
XXXX=0.0
S(MN)=XXXX
S(MO)=S(MN)
C(MN)=XXXX
C(MO)=C(MN)
IMP(MN)=XXXX
IMP(MO)=IMP(MN)
EM(MN)=XXXX
EM(MO)=EM(MN)
Q(MN)=XXXX
Q(MO)=Q(MN)
DO 5111 I=1,IMAX
FRAT(I)=XXXX
DHDT(I)=XXXX
W(MN,I,JMAXP2) = XXXX
W(MO,I,JMAXP2) = XXXX
DO 5111 J=1,JMAXP1
U(MN,I,J)=XXXX
W(MN,I,J)=XXXX
DUDT(I,J)=XXXX
DEDT(I,J)=XXXX
DDDZDT(I,J)=XXXX
U(MO,I,J)=U(MN,I,J)
W(MO,I,J)=W(MN,I,J)
WW(I,J)=XXXX
5111 CONTINUE
DO 5121 J=1,NCAL
HCDT(J)=XXXX
DDCDT(J)=XXXX
DO 5121 K=1,2
DO 5121 I=1,5
5121 ZZZC(J,K,I)=XXXX
DO 52 I=1,IMAX

```

```

03560792
03560793
03560794
03560795
03560796
03560797
03560798
03560799
03560800
03560801
03560802
03560803
03560804
03560805
03560806
03560807
03560808
03560809
03560810
03560811
03560812
03560813
03560814
03560815
03560816
03560817
03560818
03560819
03560820
03560821
03560822
03560823
03560824
03560825
03560826

```

```

P(I,JMAXP2)=0.0
P(I,JMAXP1)=0.5*SURFI*RHO
P(I,JMAX)=SURFI*RHO
SURFAC(I)=SURFI
52 CONTINUE
SURFAC(IMAX+1)=SURFI
DO 53 I=1,IMAX
DO 53 JJ=1,JMAXM1
J=JMAX-JJ
JP1=J+1
P(I,J)=P(I,JP1)+DZ*RHO
53 CONTINUE
PBIP1=P(1,1)+TUBEH*RHO
PBIM1=P(1,1)+TUEEH*RHO
DO 533 I=1,IMAX
DO 533 J=1,JMAXP2
T(MN,I,J)=TINTAL
DEN(MN,I,J)=RHO
ENTH(MN,I,J)=CP*TINTAL
T(MO,I,J)=TINTAL
DEN(MO,I,J)=RHO
ENTH(MO,I,J)=CP*TINTAL
533 CONTINUE
AVERT(MN)=TINTAL
AVERT(MO)=AVERT(MN)
AVERH(MN)=CP*TINTAL
AVERH(MO)=AVERH(MN)
AVERD(MN)=RHO
AVERD(MO)=AVERD(MN)
TDHNP(MN)=TINTAL
TDHNP(MO)=TINTAL
TBOTT(MN)=TINTAL
TBOTT(MO)=TINTAL
TCALJM(MN)=TINTAL
TCALJM(MO)=TINTAL
DDHNP(MN)=RHO
DBOTT(MN)=RHO
03560827
03560828
03560829
03560830
03560831
03560832
03560833
03560834
03560835
03560836
03560837
03560838
03560839
03560840
03560841
03560842
03560843
03560844
03560845
03560846
03560847
03560848
03560849
03560850
03560851
03560852
03560853
03560854
03560855
03560856
03560857
03560858
03560859
03560860
03560861

```

DCALJM (MN) = EHO	03560862
DCALAV (MN) = EHO	03560863
HDWNJP (MN) = CP*TINTAL	03560864
HBOTT (MN) = CP*TINTAL	03560865
HCALJM (MN) = CP*TINTAL	03560866
HCALAV (MN) = CP*TINTAL	03560867
TDWNJP (MO) = TINTAL	03560868
TBOTT (MO) = TINTAL	03560869
TCALJM (MO) = TINTAL	03560870
TCALAV (MO) = TINTAL	03560871
DDWNJP (MO) = EHO	03560872
DBOTT (MO) = RHO	03560873
DCALJM (MO) = EHO	03560874
DCALAV (MO) = RHO	03560875
HDWNJP (MO) = CP*TINTAL	03560876
HBOTT (MO) = CP*TINTAL	03560877
HCALJM (MO) = CP*TINTAL	03560878
HCALAV (MO) = CP*TINTAL	03560879
WCALAV (MN) = 0.0	03560880
WCALAV (MO) = 0.0	03560881
WDWNJP (MN) = 0.0	03560882
WDWNJP (MO) = 0.0	03560883
WDWNJM (MN) = 0.0	03560884
WDWNJM (MO) = 0.0	03560885
WCALJM (MN) = 0.0	03560886
WCALJM (MO) = 0.0	03560887
UBOTT (MN) = 0.0	03570000
UBOTT (MO) = 0.0	03580000
KHM (MN) = H	03590000
HHM (NO) = HHM (MN)	03600000
HH (MN) = H	03610000
HH (MO) = HH (MN)	03620000
VOLC = VOLSCH + BOTTH*HMAX*RADSQ + VCOLDWN	03630000
DH = HHM (MN) - CALANH	03640000
VOLP = VOLC + DH*RADSQ	03650000
THASS (MN) = DENSTY*AVRD (MN)*VCIP	03660000


```

TOTALH(MN)=THASS(MN)*AVERH(MN)
TOTALH(MO)=TOTALH(MN)
WATER(MN)=XWP(MN)*THASS(MN)
S(MN)=XSP(MN)*THASS(MN)
IMP(MN)=XIP(MN)*THASS(MN)
C(MN)=XCP(MN)*THASS(MN)
WATER(MO)=WATER(MN)
S(MO)=S(MN)
IMP(MO)=IMP(MN)
C(MO)=C(MN)
THASS(MO)=THASS(MN)
SS = SUPERS(AVERT(MN),XSP(MN),XIP(MN),XWP(MN))
G(MN) = GROWTH(AVERT(MN),SS,XIP(MN),XWP(MN))
G(MO) = G(MN)
DO 5331 J=1,NCAL
  CALT(J,MN)=TINTAL
  CALH(J,MN)=TINTAL*CP
  CALD(J,MN)=RHO
  CALT(J,MO)=TINTAL
  CALH(J,MO)=TINTAL*CP
  CALD(J,MO)=RHO
  CALN(J,MN)=0.0
  CALW(J,MO)=0.0
5331 CONTINUE
  CALP(NCAL,MN)=P(1,1)
  CALP(NCAL,MO)=P(1,1)
  DO 5332 JJ=1,NCALM1
    J=NCAL-JJ
    CALP(J,MN)=CALP(J+1,MN)+CDZ*RHO
    CALP(J,MO)=CALP(J,MN)
5332 CONTINUE
C
999 CONTINUE
C
UU = UU*TCNST/3600.0D0
03670000
03680000
03690000
03700000
03710000
03720000
03730000
03740000
03750000
03760000
03770000
03780000
03790000
03800000
03810000
03820000
03830000
03840000
03850000
03860000
03870000
03880000
03890000
03900000
03910000
03920000
03930000
03940000
03950000
03960000
03970000
03980000
03990000
04000000
04010011

```

```

100
      UA      = UU*AREAT
      UPOA    = POA*UU/DENSTY
      DINKV   = HMAX*DSQRT(HMAX*GR)
      VART    = VART/DINKV
      SPSMTH  = SPSMTH/DINKV
      ALPHA   = ALPHA/DINKV
      R(1)    = 0.0
      R(2)    = 0.5D0*DE
      RH(1)   = 0.0
      RH(2)   = DR
      DO 100 I=3,IMAX
      IM1=I-1
      R(I)    = R(IM1)+DR
      RH(I)   = RH(IM1)+DR
      CONTINUE
      R(IMAX+1)=0.0
      DO 3 I=2,IMAX
      RI      = R(I)
      RINV(I) = 1.0D0/RI
      RIE1    = RI+DR*0.5D0
      RIM1    = RI-DR*0.5D0
      DV(I)   = RIP1*RIP1-RIM1*RIM1
      CONTINUE
      RINV(1) = 9.99E+70
      DV(1)   = 9.99E+70
      COMP1   = (R(IMAX)+0.5D0*DR)*(R(IMAX)+0.5D0*DR)
      DO 5 I=1,IMAX
      DVOA(I) = DV(I)/COMP1
      CONTINUE
      Z(1)    = 0.0
      DO 2 J=2,JMAXP1
      Z(J)    = Z(J-1)+DZ
      DRT2    = ER*2.0D0
      SLIPV   = SLIPV/DSQRT(GR*HMAX)
      DTOH    = DT/TUBEH
      THODT   = TUBEH/DT
      04200000
      04300000
      04040001
      04050001
      04060001
      04070001
      04080000
      04090000
      04100000
      04110000
      04120000
      04130000
      04140000
      04150000
      04160000
      04170000
      04180000
      04190000
      04200000
      04210000
      04220300
      04230000
      04240000
      04250000
      04260000
      04270000
      04280000
      04290000
      04300000
      04310000
      04320000
      04330000
      04340000
      04350000
      04360000
      04370000

```

```

DTOCDZ = DT/CDZ
FOURMC = DTOCDZ/CDZ*ALPHA
DT02DR = DT/(2.0D0*DR)
DT0DR = DT/DR
FOURME = DT*ALPHA/DR**2
DTORSQ = DT/(DR*DR)
FM02DR = DT*ALPHA/DR*0.5D0
FM0DR = DT0DR*ALPHA
FM02DR = DT02DR*ALPHA

C
CALL SETUPP
CALL INCONV

RIP1 = R(IRIGHT)+0.5D0*DR
RIM1 = R(ILEFT)-0.5D0*DR
COMP2 = RIP1*RIP1-RIM1*RIM1
FMOM = COMP2/(DFLOAT(NTUBES)*TUBED**2/4.0D0)
VOLUP = VOLSCH/PIE/HMAX**3
AFLWD = R(IDOWN)+0.5D0*DR
AFLWD = AFLWD*AFLWD
RIM1 = R(ILEFT)-0.5D0*DR
RIP1 = R(IRIGHT)+0.5D0*DR
AFLWU = RIP1*RIP1-RIM1*RIM1
COMP2 = 2.0D0*BOTH*(R(IDOWN)+0.5D0*DR)
ABOAFD = COMP2/AFLWD
ABOAFU = COMP2/AFLWU
RIM1 = R(IDOWN)+0.5D0*DR
V1 = AFLWD*TUBEH+BOTH*RIM1*RIM1
RIP1 = R(IMAX)+0.5D0*DR
V2 = BOTH*(RIP1*RIP1-RIM1*RIM1)
VOLET = V1+V2
DTAUOV = DT*AFLWU/VCLBT
F = F*TCNST/3600.0D0
XIF = BRXFF*(1.0-PURFF)
XSF = BRXFF*PURFF

```

```

04380000
04390000
04400000
04410000
04420000
04430000
04440000
04450000
04460000
04470000
04480000
04490000
04500000
04510000
04520000
04530000
04540000
04550000
04560000
04570000
04580000
04590000
04600000
04610000
04620000
04630000
04640000
04650000
04660000
04670000
04680000
04690000
04700011
04710000
04720000

```

C

C

```

XWF      = 1.0-XSP-XIP
HF        = HEATC(0.0D0,BRIXFF)*(TEMPFF-TZERO)

C
C
RIP1     = R(ILEPT)-0.5D0*DR
RIM1     = K(IDOWN)+0.5D0*DR
BAV      = (RIP1+RIM1)/2.0D0
DELTAR  = RIP1-RIM1
DELRSQ  = RIP1*RIP1-RIM1*RIM1
DNVR     = 1.0D0/RIP1-1.0D0/RIM1
IF(DELTAR.LE.0.0) STOP 60
CONST8   = -(1.0D0/RIP1)**3*BAV LIMITING VALUE
GO TO 2222

CONST8   = 2.0D0*DNVR/DELRSQ*BAV**2
CONST6   = BAV/RIM1
CONST7   = 1.0D0/DELTAR
HHH(MN) = HH(MN)
HHH(MO) = HH(MN)
HHM(MN) = HH(MN)
HHM(MO) = HH(MO)

C----- INITIALIZE VARIABLES THAT ARE CONTRAINTED BY CONTROL ---
C----- OR BY MATERIAL AND ENERGY BALANCES -----
CALL ECNTRL
CALL CNTRL

C-----
BB       = (XIP(MN) + XSP(MN))/CONST1
V        = CONST2*AVERD(MN)/(1.0D0-CONST2*AVERD(MN))
VRATIO  = RATIO( V , AVERLL(MN) )
VORHO   = VKINEM(AVERT(MN),BB)
HVAP    = ENTHV(0.0D0,0.0D0,BPE)

C----- INITIALIZE HEAT FLUX ACCORDING TO PROBLEM -----
CALL INHEAT(EVAP)
CALL HEATIN( CALT, QFLUX, AQFLUX )

C-----

```

04730000
04740000
04750000
04760000
04770000
04780000
04790000
04800000
04810000
04820000
04830000
04840000
04850000
04860000
04870000
04880000
04890000
04900000
04910000
04920000
04930009
04940009
04950010
04960009
04970009
04980009
04990000
05000000
05010000
05020000
05030009
05040013
05050008
05060009

05070000
05080000
05090000
05100000
05110000
05180000
05190000
05200000

```
DO 2225 I=2,IMAX
  2225 SSURP(I)=SURFAC(I)
  DO 2226 J=1,JMAX
    JJJ=2*J-1
    2226 DPDT(J)=DDZDT*DFLOAT(JJJ)*0.5D0
  1002 FORMAT(1X,6I6)
  RETURN
END
```

```

C-----
C-----
C-----
C-----
SUBROUTINE PRES
      MOTIVE SUBROUTINE FOR PRESSURE CALCULATION IN
      PAN PROPER
      IMPLICIT REAL*8 (A-H,O-Z)
      COMMON/PROPTY/RHO,RHOINV,RHOO2,VISC,ALPHA,VORHO,BETA
      FOURMR,FMO2DR,FMO2DR,CP,FOURMC,TZERO
      HVINV,DELHLV,DENSTY
      COMMON/COORD/R(30),Z(30),RINV(30),RH(30)
      COMMON/LIMITS/IMAX,IMAXM1,IMAXM2,JMAX,JMAXM1,JMAXM2,NMAX,NPRINT
      1, NBAR,NPRINT,JMAXP1,NSTART,JMAXP2,IMAXP1
      COMMON/STEP/MN,MO,N
      COMMON/SIZE/H,RAD,HMAX
      COMMON /AREAP/DV(30),DVOA(30)
      COMMON/BOUND/IRIGHT,IRIGP1,ILEFT,ILEFP1,ILEFM1,IDOWN
      1,IDWNP1,IDOWN1
      COMMON/TOP/ SURFAC(30),SSURF(30),SVFEV(30),HVAP
      1, SPSMTH,THETAZ,THETAS,FRAT(30),DHDT(30)
      COMMON/DIMEN1/P(30,30),PBIP1,PBIM1
      COMMON/TPHASE/ENTH(2,30,30),DEN(2,30,30)
      COMMON/GRID/DR,DZ,DT,DZDSQ,DTODZ,DZODF,DZODR,DTODR,DTODZ
      1,DT2DRZ,DTODRZ,DTODR,FOURMD,DZORSQ,DZOD1,DTORSQ
      2,DZO2,CALFC2,CALFC3,DDZDT,SURFDT,DEFT2,DZO,DDZDT
      3, DZODTO
      DO 60 I=2,IMAX
      SURFI=0.5D0*SURFAC(I)
      DJP1=DEN(MN,I,JMAXP1)
      DNEW=DEN(MN,I,JMAX)
      P(I,JMAXP1)=SURFI*DJP1
      P(I,JMAX)=2.0D0*SURFI*DJP1+DZO2*DNEW
      DO 60 JJ=1,JMAXM1
      J=JMAX-JJ
      JP1=J+1

```

C

05200038
05200039
05200040
05200041
05200042
05200043

DJP1=DNEW
DNEW=DN(MN,I,J)
P(I,J)=DZO2*(DNEW+DJP1)+P(I,JE1)
CONTINUE
RETURN
END

60

```

SUBROUTINE PRESSC
C-----
C----- CALCULATION OF ONE-D PRESSURE PROFILE IN CALANGLIA
C-----
IMPLICIT REAL*8(A-H,O-Z)
DIMENSION ZZZZ(2,20),ZZZC(10,2,5)
REAL*8 IMP(2)
COMMON/CONC /DELDDB,DELRH,BKXR,CONST1,CONST2,BPE,VRATIO
COMMON/WSIRT/EM(2),S(2),IMP,C(2),Q(2),AVERD(2),HH(2),HH(2)
1,F,XWF,XSF,XIF,G(2),HF,AVERD(2),THASS(2),WATER(2)
2,TOTALH(2),KSP(2),XIP(2),KCP(2),IMP(2),AVERH(2)
3,SSMAX,SSMIN
COMMON/PAN/ VOLSCH,RADSQ,VCIC,WVCL,RHEIG
COMMON/DIMEN1/P(30,30),PBIP1,PBIM1
COMMON/TPHASE/ENTH(2,30,30),DEN(2,30,30)
COMMON/GRID/DK,DZ,DT,DTOZSQ,DTODZ,DZODR,DZO2DR,DTO2DR,DTO2DZ
1,DT2DRZ,DTODRZ,PTODR,POURMD,DZORSQ,DZODT,DTORSQ
2,DZO2,CALFC2,CALFC3,DDZDT,SURFDT,DEFT2,DZO,DDZDZTO
3,DZODTO
COMMON/PROPTY/RHO,RHOINV,RHOC2,VISC,ALPHA,VORHO,BETA
1,POURMR,FMO2DR,FMODR,CP,POURMC,TZERO
2,HVINV,DELHLV,DENSITY
COMMON/COORD/R(30),Z(30),RINV(30),RH(30)
COMMON/LIMITS/IMAX,IMAXM1,IMAXM2,JMAX,JMAXM1,JMAXM2,NMAX,NPRINT
1,NBAR,NPRINT,JMAXP1,NSTART,JMAXP2,IMAXP1
COMMON/STEP/NN,NC,N
COMMON/SIZE/H,RAD,HMAX
COMMON /ABEAF/DV(30),DVOA(30)
COMMON/BOUND/IRIGHT,IRIGP1,ILEFT,ILEFP1,ILEFM1,IDOWN
1,IDNFP1,IDOWN1
COMMON/CHEST/UV,UA,TUBEH,AREAT,POA,UPOA,DTOTH,THODT,UAOA,CALANH
1,BOTTH,TUBED,FMC,CDZ,LTCCDZ,TSTFAM,NTUBES,NCAL,NCALM1
2,NCALP1
COMMON/LUMBT/MDMNP(2),TDMNP(2),DDMNP(2),HDMNP(2)
1,MDMNH(2),TBOIT(2),DBOIT(2),HBOIT(2)

```

```

05200046
05200047
05200048
05200049
05200050
05200051
05200052
05200053
05200054
05200055
05200056
05200057
05200058
05200059
05200060
05200061
05200062
05200063
05200064
05200065
05200066
05200067
05200068
05200069
05200070
05200071
05200072
05200073
05200074
05200075
05200076
05200077
05200078
05200079
05200080

```


2,UBOTT(2),UONEB(2),WCALAV(2),TCALAV(2),DCALAV(2),HCALAV(2)	05200081
3,WCALJM(2),TCALJM(2),DCALJM(2),HCALJM(2)	05200082
COMMON/LUMCAL/ CALW(10,2),CALH(10,2),CALI(10,2),CALD(10,2)	05200083
1,CALP(10,2)	05200084
DATA PIE,COEFFV,RHOC,GR/3.14159D0,0.5236D0,99.1D0,32.2D0/	05200085
EQUIVALENCE (ZZZZ,WDWNJP)	05200086
EQUIVALENCE (ZZZC,CALW)	05200087
C	05200088
C----- CALCULATE PRESSURE AT TCP OF CALANDRIA ---	05200089
C	05200090
PNUP=0.0	05200091
CCMP1=0.0	05200092
DO 63 I=1LEFT,IRIGHT	05200093
DDVI=DV(I)	05200094
PNUP=PNUP+DDVI*(P(1,1)+DZO2*DEN(MN,I,1))	05200095
COMP1=CCMP1+DDVI	05200096
63 CONTINUE	05200097
PNUP=PNUP/COMP1	05200098
C	05200099
C----- CALCULATE PRESSURE PROFILE IN CALANDRIA	05200100
C	05200101
CALP(NCAL,MN)=PNUP	05200102
CALL CALPP(PBIP1)	05200103
C	05200104
C----- CALCULATE PRESSURE AT TOP OF DOWNTAKE	05200105
C	05200106
PNUP=0.0	05200107
COMP1=0.0	05200108
DO 61 I=2,IDOWN	05200109
DDVI=DV(I)	05200110
PNUP=PNUP+DDVI*(P(1,1)+DZO2*DEN(MN,I,1))	05200111
COMP1=CCMP1+DDVI	05200112
61 CONTINUE	05200113
PNUP=PNUP/COMP1	05200114
C	05200115
C----- CALCULATE PRESSURE AT BOTTOM OF DOWNTAKE ----	05200116

05200118
 05200119
 05200120
 05200121
 05200122
 05200123
 05200124
 05200125
 05200126
 05200127
 05200128
 05200129
 05200130

```

      B = (XSP(MN) + XIP(MN))/(1.0D0 - XCP(MN) )
      DNEW=LECTT(MN)
      WAV=WDWNJM(MN)+WDWNJM(MO)
      RIP1=R(IDOWN)+0.5D0*DR
      DPFR=4.0D0*TUBEH*VISCTY(TBOT(MN),B)*WAV/RIP1*VRATIO

      PBIM1=ENUP+DNEW*TUBEH+DPFR

      RETURN
      END

```

C C
 C C

SUBROUTINE REZONE

— —

CALCULATIONS FOR DYNAMIC GRID

1

IMPLICIT REAL*3(A-H,O-Z)

REAL*8 IMP(2)

COMMON/WHSTRT/EM(2),S(2),IMP,C(2),C(2),AVERT(2),HEM(2),DH(2)

1, F, XMF, XSF, XIF, G(2), HF, AVERD(2), TMASS(2), WATER(2)

TOTALH(2),XSP(2),XIP(2),XCP(2),XMP(2),AVERH(2)

3, SSMAX, SSMIN

COMMON/OVERALL/ E(2), HHH(2), EVINTO, EVVINT, AQFLUX

COMMON/PAN/ VOLSCH, RADS2, VOLC, WVOL, WHEIG

COMMON/MOVE / DPDT(30)

COMMON/TOP/ SURFAC(30),SSURF(30),SVFRV(30),HVAP

1, SFSMT, THETAZ, THETAS, FRAT(30), DHD(30)

COMMON/GRID/DR,DZ,DT,DT0ZSQ,DTCDZ,DZQDK,DZ02DR,DT02DR,DT02DZ

1,DT2DRZ,D1ODRZ,D1ODR,FCU FMD,DZORSQ,DZODT,D1ORSQ

2,DZ02,CALFC2,CALFC3,DDZDT,SURFDT,DR T2,DZO,DDZDTC

3, DZODTO

COMMON/PROPERTY/RHO, RHOINV, RHO02, VISC, ALPHA, VORHO, BETA

1, FOURMR, FMO2DR, FMODR, CP, FO DRMC, TZERO

2. HVINV, DELHLV, DENSITY

COMMON/COORD/R(30),Z(30),RINV(30),RH(30)

COMMON/LIMITS/IMAX,IMAXM1,IMAXM2,JMAX,JMAXM1,JMAXM2,NMAX,NPRINT

1, NEAR, NPRINT, JMAXP1, NSTART, JMAXP2, JMAXP1

COMMON/STEP/MN,HO,N

COMMON/SIZE/H, RAD, HMAX

COMMON /AREAP/DV(30), DVOA(30)

COMMON/BOUND/IRIGHT,IRIGP1,ILEFT,ILFFP1,ILEFM1,IDOWN

1, IDWNE1, IDOHE1

9

$$SURFDT = (HH(MO) - HH(MN)) / DT$$

DDZDT0=DDZDT

$$DNDZDT = (SURFDT / DFL0AT(JMAX)) / HMAX - DDZDT) * THETAZ + DDZDT$$

CALL STOP

05200133
05200134
05200135
05200136
05200137
05200138
05200139
05200140
05200141
05200142
05200143
05200144
05200145
05200146
05200147
05200148
05200149
05200150
05200151
05200152
05200153
05200154
05200155
05200156
05200157
05200158
05200159
05200160
05200161
05200162
05200163
05200164
05200165
05200166

05200167
05200168
05200169
05200170
05200171
05200172

DO 8555 J=1,JMAX
JJJ=2*J-1
8555 DPDT(J)=DDZ DT*DFLOAT(JJJ)*0.5D0
RETURN
END

```
C-----
SUBROUTINE RMOMEQ
C-----
      INTEGRATION RADIAL MOMENTUM PAN PEOPER
C-----
      IMPLICIT REAL*8(A-H,O-Z)
      COMMON/DIMEN/U(2,30,30),W(2,30,30),T(2,30,30),WW(30,30)
      COMMON/DIMEN1/P(30,30),PEIP1,PBIM1
      COMMON/GRID/DR,DZ,DT,DZOZSQ,DTODZ,DZODR,DZO2DR,DTO2DR,DTO2DZ
      1,DT2DRZ,DTODRZ,DTODR,FOURMD,DZORSQ,DZODT,DTORSQ
      2,DZO2,CALFC2,CALFC3,DEZDT,SUREFT,DRT2,DDZO,DDZDTO
      3,DZODTO
      COMMON/PROPTY/RHO,RHOINV,RHCC2,VISC,ALPHA,VORHO,EETA
      1,FOURMR,FMO2DR,FMODR,CP,FOURMC,TZERO
      2,HVINV,DELHLV,DENSTY
      COMMON/COORD/R(30),Z(30),RINV(30),RH(30)
      COMMON/LIMITS/IMAX,IMAXM1,IMAXM2,JMAX,JMAXM1,JMAXM2,NMAX,NPRINT
      1,NEAR,NPRNT,JMAXP1,NSTART,JMAXP2,IMAXP1
      COMMON/STEP/MN,NO,N
      COMMON/TEMP/TNEW,TOLD,TIP1,TIM1,TJP1,TJM1
      COMMON/CNSER/LIP1,DIM1,DJP1,DJM1,RIP1,RI,RHIP1,RHM1
      1,ADIP1,ADIM1,ACJP1,ADJM1
      COMMON/VELCTY/UNEW,UOLD,WNEW,WOLD,UIP1,UIM1,UJP1,WIP1,WIM1
      1,WJP1,WJM1,UF,UB,WF,WB
      COMMON/PRESS/PIPI,PII1,PJ,PJP1
      COMMON/INDEX/I,J
      COMMON/FLOW1/DUDT(30,30),DEDT(30,30),HCDDT(10),BTEDUT,BTDEDT
      1,DDZDZDT(30,30),EDCDT(10)
      COMMON/SUBDER/DPDTI
      UUF=0.0
      IF(UF.LT.0.0) UUF=UIP1-UOLD
      UUB=UIM1-UOLD
      IF(UE.LT.0.0) UUE=0.0
      UWF=0.0
      IF(WF.LT.0.0) UWF=UJP1-UOLD
```

C
C
C
C

UWE=UJM1-UOLD
IF (WB.LT.0.0) UWE=0.0

COMP1=DT02DR*RINV(I)*(UF*UUF-UB*UUF)
COMP2=DT0DZ*(WF*UWF-WB*UWB)
COMP3=VCRHO*DTORSQ*RINV(I)*(RHIP1*(UIP1-UOLD)*ALIP1
1-RHIM1*(UOLD-UIM1)*ADIM1)
COMP5=VORHO*DT0ZSQ*(ADJP1*(UJP1-UOLD)-ADJM1*(UOLD-UJM1))
COMP6=DT02DR*(FIM1-PIF1)
COMP7=-VORHO*DT*RINV(I)*RINV(I)*UOLD
DUODT=(-COMP1-COMP2+COMP3+COMP5+COMP6)*RHOINV+COMP7
UNEW=UCID+(DUOT(I,J)*DT+DUODT)*0.5D0
DUOT(I,J)=DUODT/DT
RETURN
END

05200209
05200210
05200211
05200212
05200213
05200214
05200215
05200216
05200217
05200218
05200219
05200220
05200221
05200222
05200223
05200224
05200225
05200226

```

C-----
C-----
C-----
SUBROUTINE SETUP
      CALCULATION OF NEW GRID CONSTANTS (DZ)

      IMPLICIT REAL*8 (A-H,O-Z)
      COMMON/GRID/DR,DZ,DT,DTODZ,DZODZ,DZODR,DTODR,DTODZ
      1,DT2DRZ,DTODRZ,DTODE,FOURMD,DZORSQ,DZODT,DTORSQ
      2,DZODZ,CALFC2,CALFC3,DDZDT,SURFDT,DRF2,DZO,DDZDT
      3,DZODT
      COMMON/PROPTY/RHO,KHOLNV,RHOO2,VISC,ALPHA,VORHO,BETA
      1,FOURMR,FMO2DR,FMODR,CP,FOURMC,TZERO
      2,HVIN,DEHLV,DENSTY
      COMMON/CHEST/UA,UA,TUBEH,AREAT,FOA,UFOA,DTOTH,THODT,UAOA,CALANH
      1,BOTTH,TUBED,FACH,CZ,DTODCZ,TSTEAM,NTUBES,NCAI,NCAIH1
      2,NCALP1

      DZO=DZ
      DZODT=DZODT
      DZ=DZO+DDZDT*DT
      ENBY SETUP
      CALFC2=(DZ+CDZ)*0.5D0
      DZODZ=DZ/2.0D0
      DTCDZ=DT/DZ
      DZODR=DZ/DR
      DZODR=DZ/(2.0D0*DR)
      DZORSQ=DZ/DR**2
      DZODT=DZ/DT
      DTODZ=DT/(2.0D0*DZ)
      DT2DRZ=DT/(2.0D0*DR*DZ)
      DTODRZ=DT/(DR*DZ)
      FOURMD=DT*ALPHA/DZ**2
      RETURN
      END

```

```

05200229
05200230
05200231
05200232
05200233
05200234
05200235
05200236
05200237
05200238
05200239
05200240
05200241
05200242
05200243
05200244
05200245
05200246
05200247
05200248
05200249
05200250
05200251
05200252
05200253
05200254
05200255
05200256
05200257
05200258
05200259
05200260
05200261

```

C

	SUBROUTINE WMIKT	05200264
C-----		05200265
C-----	WELL MIX TANK CALCULATIONS.	05200266
C-----	OVERALL MATERIAL BALANCES, CRYSTAL GROWTH.	05200267
C-----	CALCULATION OF PRETINIENT AVERAGE PHYSICAL PROPERTIES	05200268
C-----	(VISCOSITY).	05200269
C-----		05200270
	IMPLICIT REAL*8(A-I,O-Z)	05200271
	REAL*8 IMP(2)	05200272
	COMMON/TOP/ SURFAC(30), SSURF(30), SVFRV(30), HVAP	05200273
1,	SFSMTH, THETAZ, THETAS, FRAT(30), DHDT(30)	05200274
	COMMON/CONC /DELDDB, DELBH, BRIXR, CONST1, CONST2, BPE, VRATIO	05200275
	COMMON/AVPART/AVERN(2), AVERLI(2)	05200276
	COMMON/PROPTY/RHO, RHOINV, RHOO2, VISC, ALPHA, VORHO, BETA	05200277
1,	FOURMR, FMO2DR, FMODR, CP, FOURMC, TZERO	05200278
2,	HVINV, DELHLV, DENSTY	05200279
	COMMON/WSTRT/EM(2), S(2), IMP, C(2), Q(2), AVERT(2), HHM(2), HH(2)	05200280
1,	F, XWF, YSF, XIF, G(2), HF, AVERD(2), TMASS(2), WATER(2)	05200281
2,	TOTALH(2), XSP(2), XIP(2), XCP(2), XWP(2), AVERH(2)	05200282
3,	SSMAX, SSMIN	05200283
	COMMON/OVERAL/ E(2), HHH(2), EVINTO, ENVINT, AQFLUX	05200284
	COMMON/GRID/DR, DZ, DT, DTOZSQ, DTODZ, DZODR, DZO2DR, DTO2DR, DTO2DZ	05200285
1,	DT2DRZ, DTODEZ, DTODR, FOURMD, DZORSQ, DZODT, DTORSQ	05200286
2,	DZO2, CALFC2, CALFC3, DDZDT, SURFDT, DRT2, DZO, DDZDZO	05200287
3,	DZODTO	05200288
	COMMON/STEP/MN, MO, N	05200289
	COMMON/PAN/ VOLSCH, RADSQ, VOLC, WVOL, WHEIG	05200290
	COMMON/ENTHAL/DHNEW, DHOLD, DHIP1, DHIM1, DHJP1, DHJM1	05200291
	COMMON/CHEST/UU, UA, TUBEH, AREAT, POA, UPOA, DTOH, THODT, UAOA, CALANH	05200292
1,	BOTTH, TUBED, FMOM, CDZ, DTOCDZ, TSTEAM, NTUBES, NCAL, NCALM1	05200293
2,	NCALP1	05200294
	COMMON/VAPDEN/PRESRF, RHOVR	05200295
	COMMON/ BLOCK / BRIKFF, PURFF, TEMPPF,	05200296
1	VART, PRECMX, AHTOV, HF, TINTAL, HV, JJMAX	05200297
	DATA RHOC, COEFFV / 99.1D0, 0.5236D0 /	05200298
		05200299
		05200300

C


```

05200301
05200302
05200303
05200304
05200305
05200306
05200307
05200308
05200309
05200310
05200311
05200312
05200313
05200314
05200315
05200316
05200317
05200318
05200319
05200320
05200321
05200322
05200323
05200324
05200325
05200326
05200327
05200328
05200329
05200330
05200331
05200332
05200333
05200334
05200335

C
AVERLL(MN) = AVERLL(MO) + (G(MN)+G(MO)) * DT*0.5D0
IF (AVERLL(MN).LT.0.0) AVERLL(MN)=0.0
DELC = (AVERLL(MN)**3-AVERLL(MO)**3)*RHOC*COEFFV*AVERNN(MN)
WATER(MN)=WATER(MO) + (P*XWP- EM(MN)) *DT
S(MN) =S(MO) + P*XS*DT - DELC
IMP(MN) =IMP(MO) + F*XIP*DT
C(MN) =C(MO) + DELC
THASS(MN)=THASS(MO) + (F - EM(MN) ) *DT

C
CALCULATION OF MASS FRACTION
C
COMP1=TMASS(MN)
COMP2=S(MN)/COMP1
COMP3=IMP(MN)/CCMP1
COMP4=C(MN)/COMP1
COMP5=WATER(MN)/COMP1
SUM=COMP2+COMP3+COMP4+COMP5
XSP(MN)=COMP2/SUM
XIP(MN)=CCMP3/SUM
XCP(MN)=COMP4/SUM
XWP(MN)=COMP5/SUM

C
CALCULATION AVERAGE PAN HEIGHT
C
VOLP=TMASS(MN)/DENSTY/AVERD(MN)
VOLP=VOLP-VOLC
HHM(MN)=VOLP/RADSQ+CALANH

C
CALCULATION AVERAGE PROPERTY
C
B=XIP(MN)+XSP(MN)
BPE = BOILPE( XIP(MN) , XWP(MN) , B ) *BETA
CONST1 = 1.0D0-XCP(MN)
CONST2 = XCP(MN)/RHOC+DENSTY

```

05200336
 05200337
 05200338
 05200339
 05200340
 05200341
 05200342
 05200343
 05200344
 05200345

```

EE=E/CONST1
CP = HEATC( XCP(MN) , BB )
DELRH = DELDDB*(BB-BRIXR)
V=CONST2*AVERD(MN)/(1.0DO-CONST2*AVERD(MN))
VRATIO = RATIO( V , AVERLL(MN) )
VORHO = VKINEM(AVERT(MN),BB)
HVAP = ENTHV(0.0DO,0.0DO,BPE)

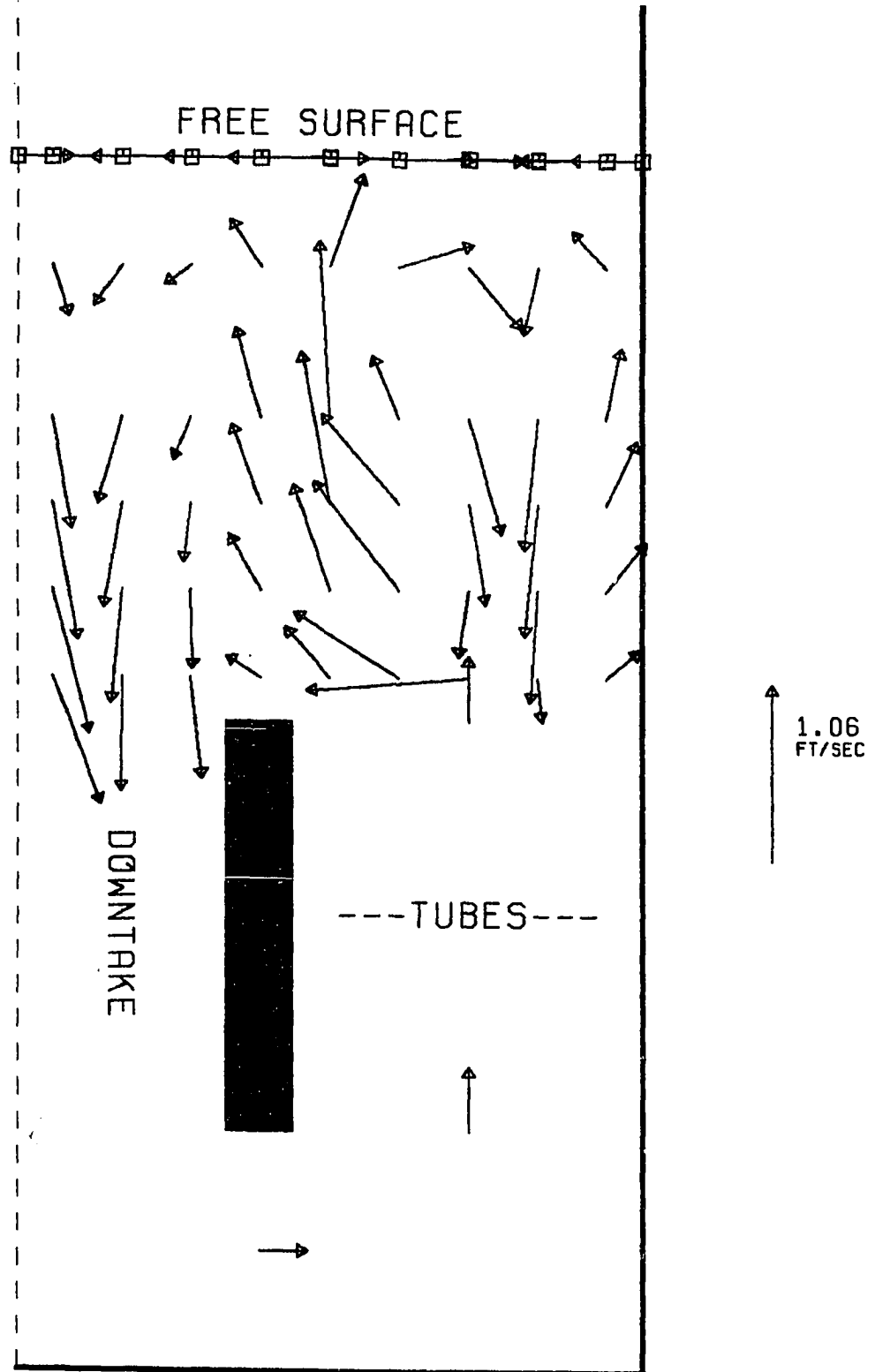
      RETURN
      END

```

C

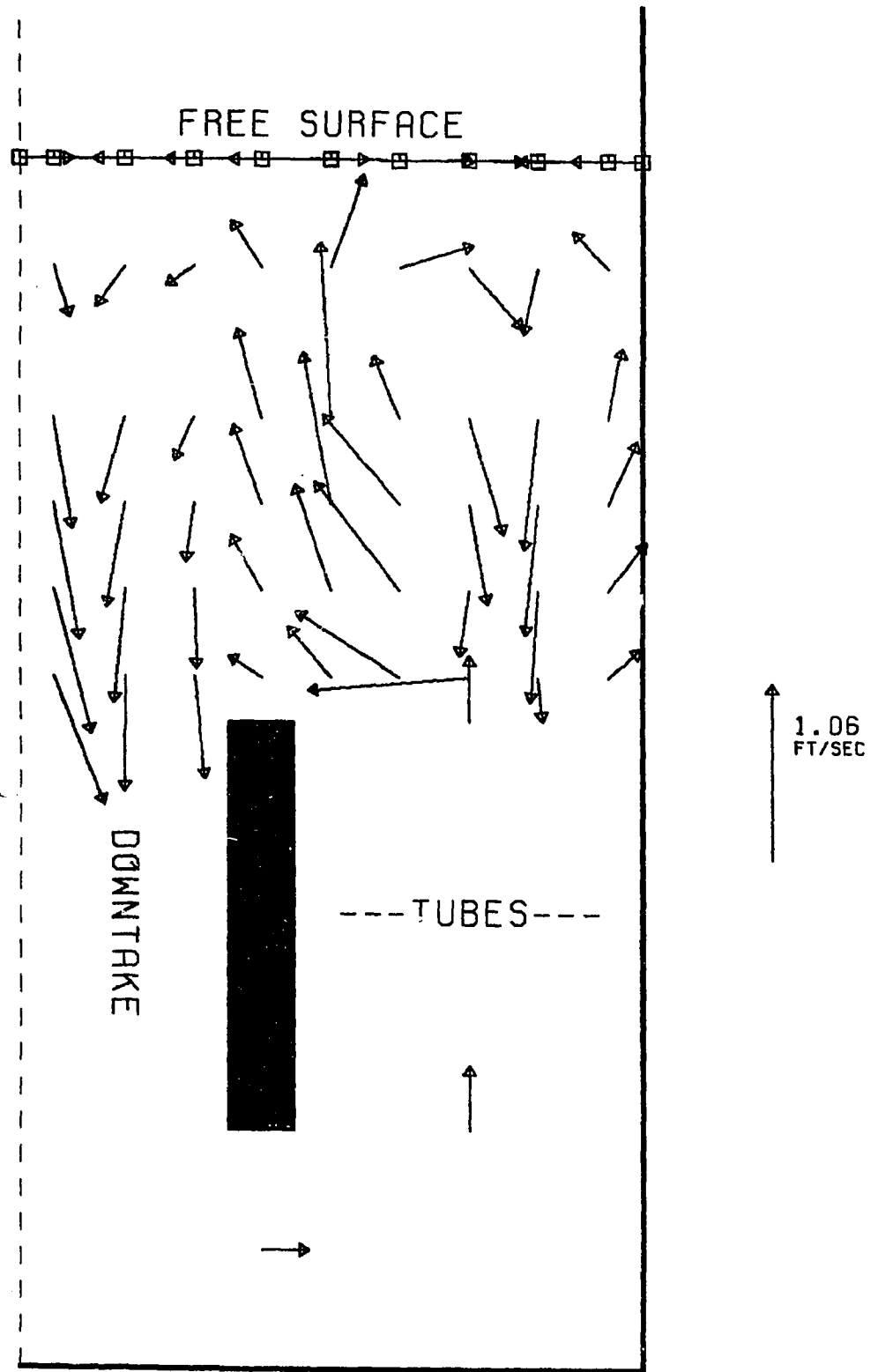
APPENDIX II

EFFECT OF THERMAL DIFFUSIVITY AND KINEMATIC VISCOSITY



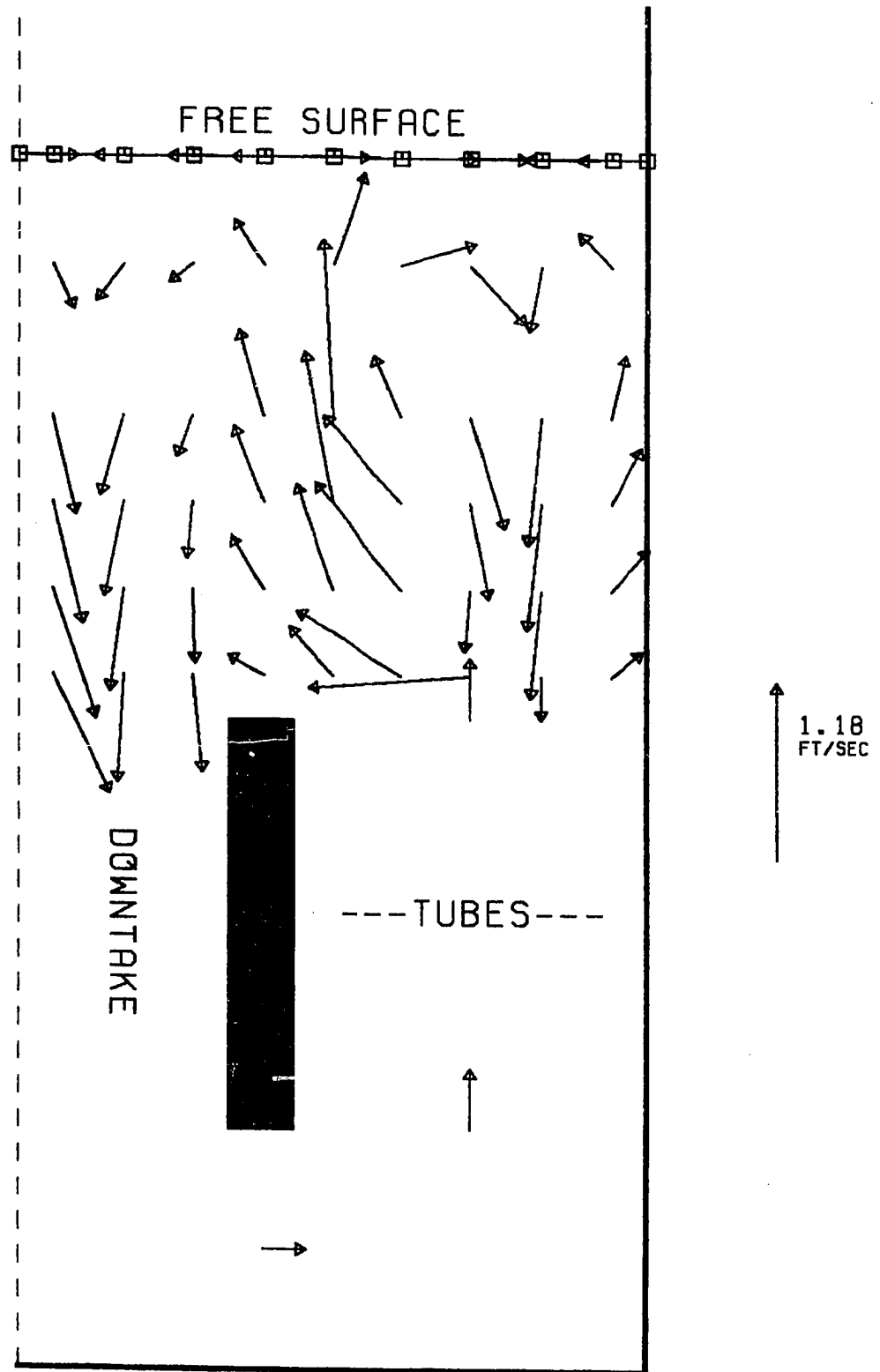
VELOCITY VECTORS

FIGURE II.1 CASE 1



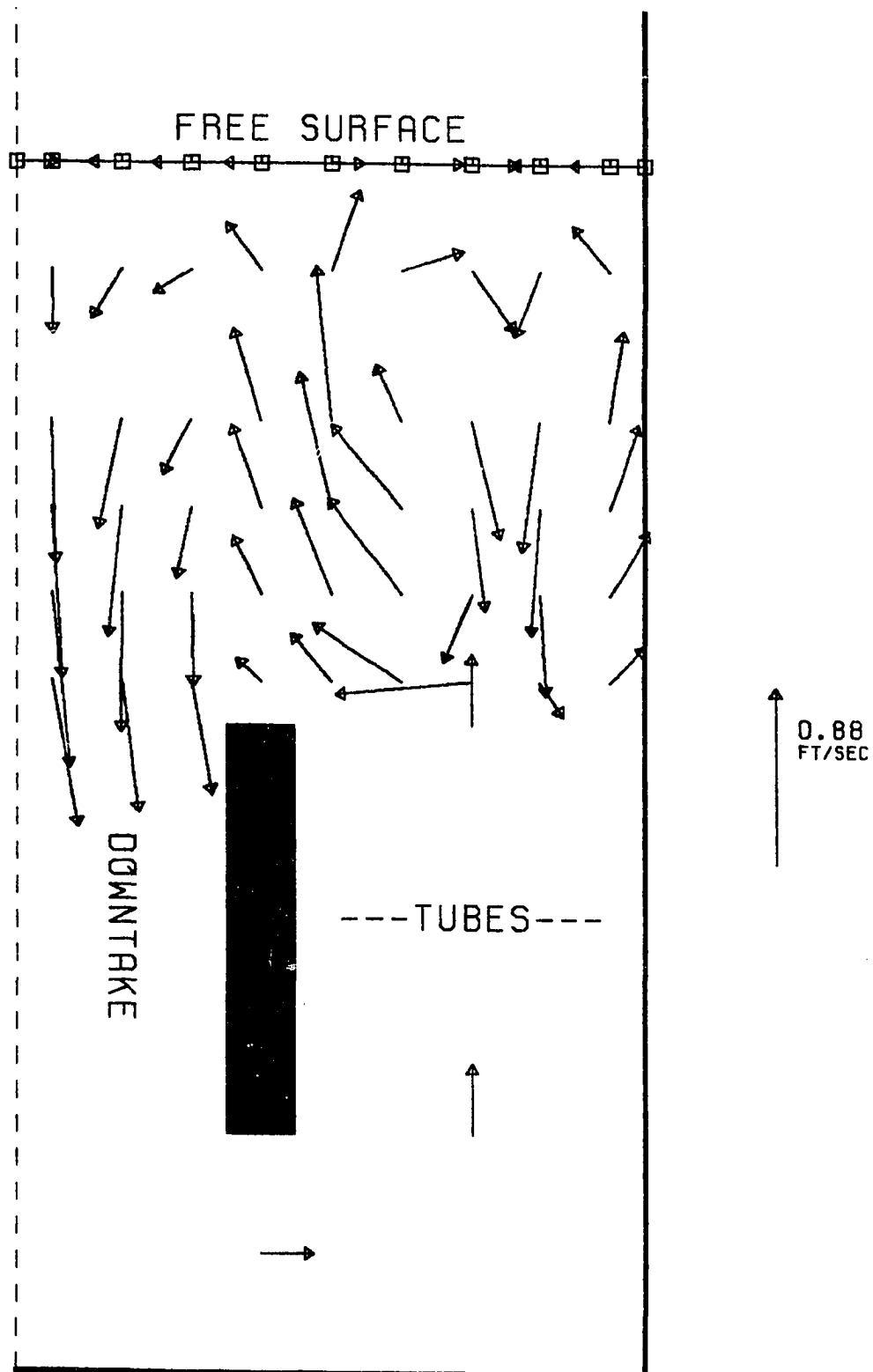
VELOCITY VECTORS

FIGURE II. 2 CASE 2



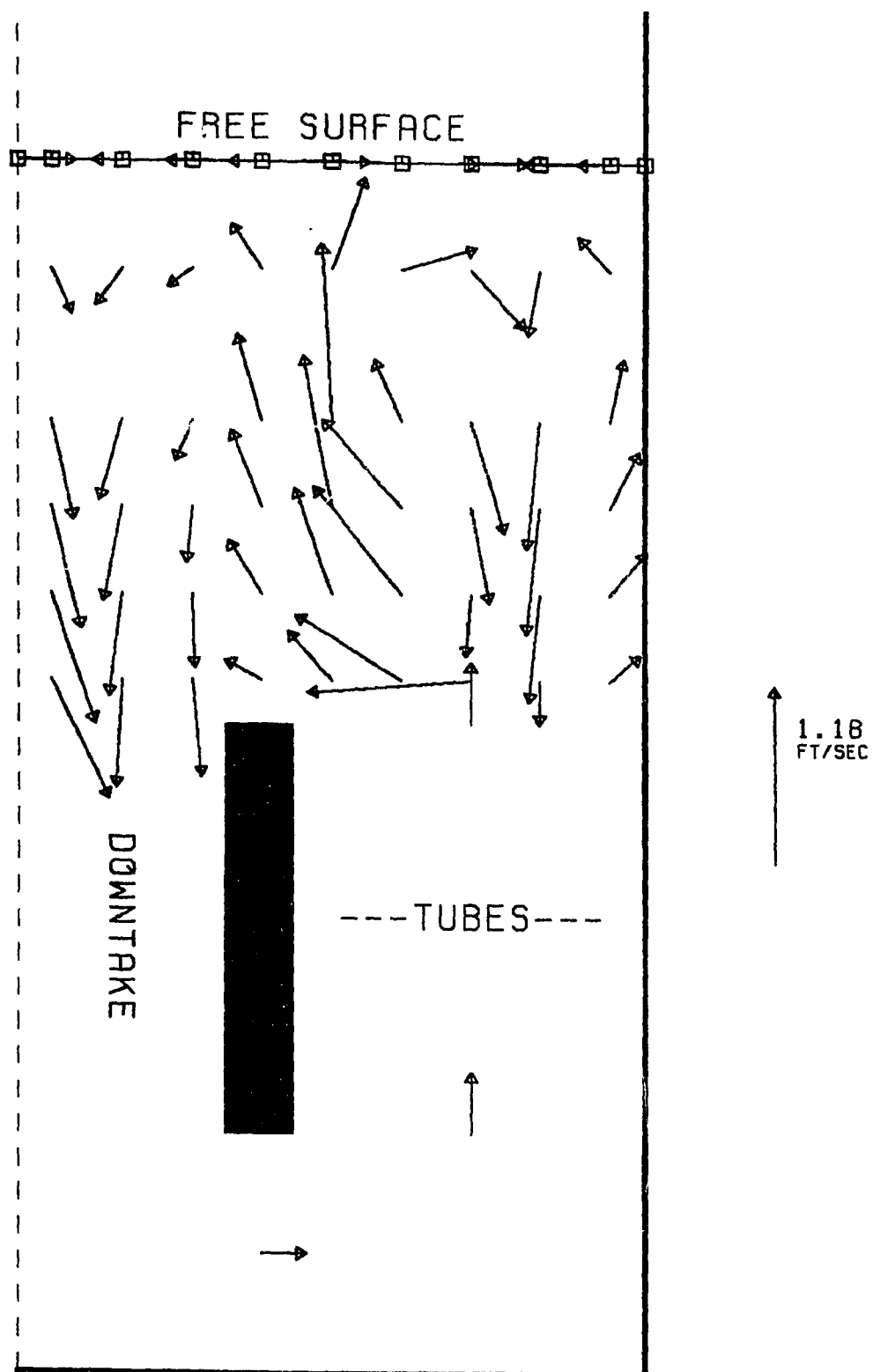
VELOCITY VECTORS

FIGURE II. 3 CASE 3



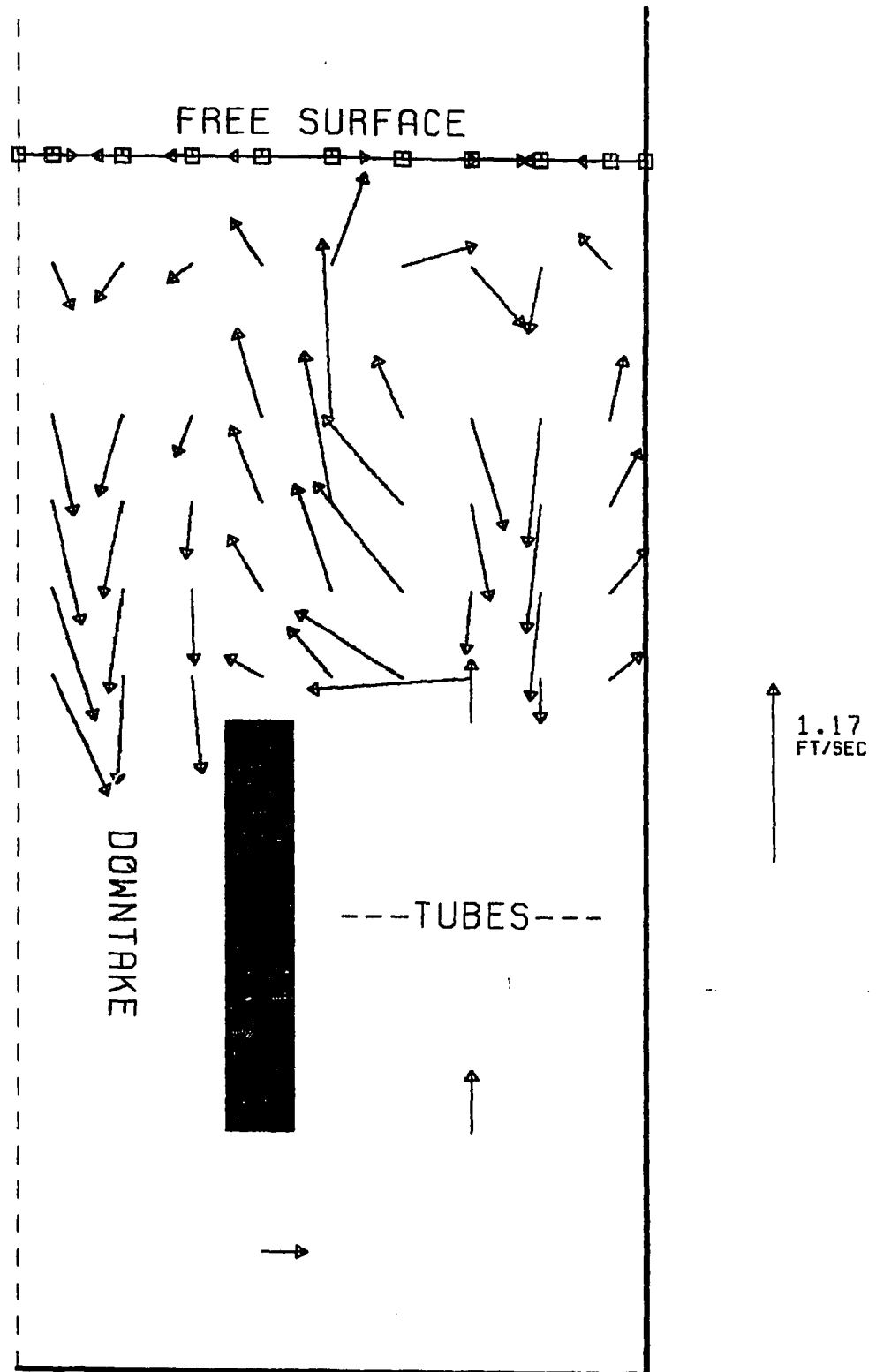
VELOCITY VECTORS

FIGURE II. 4 CASE 4



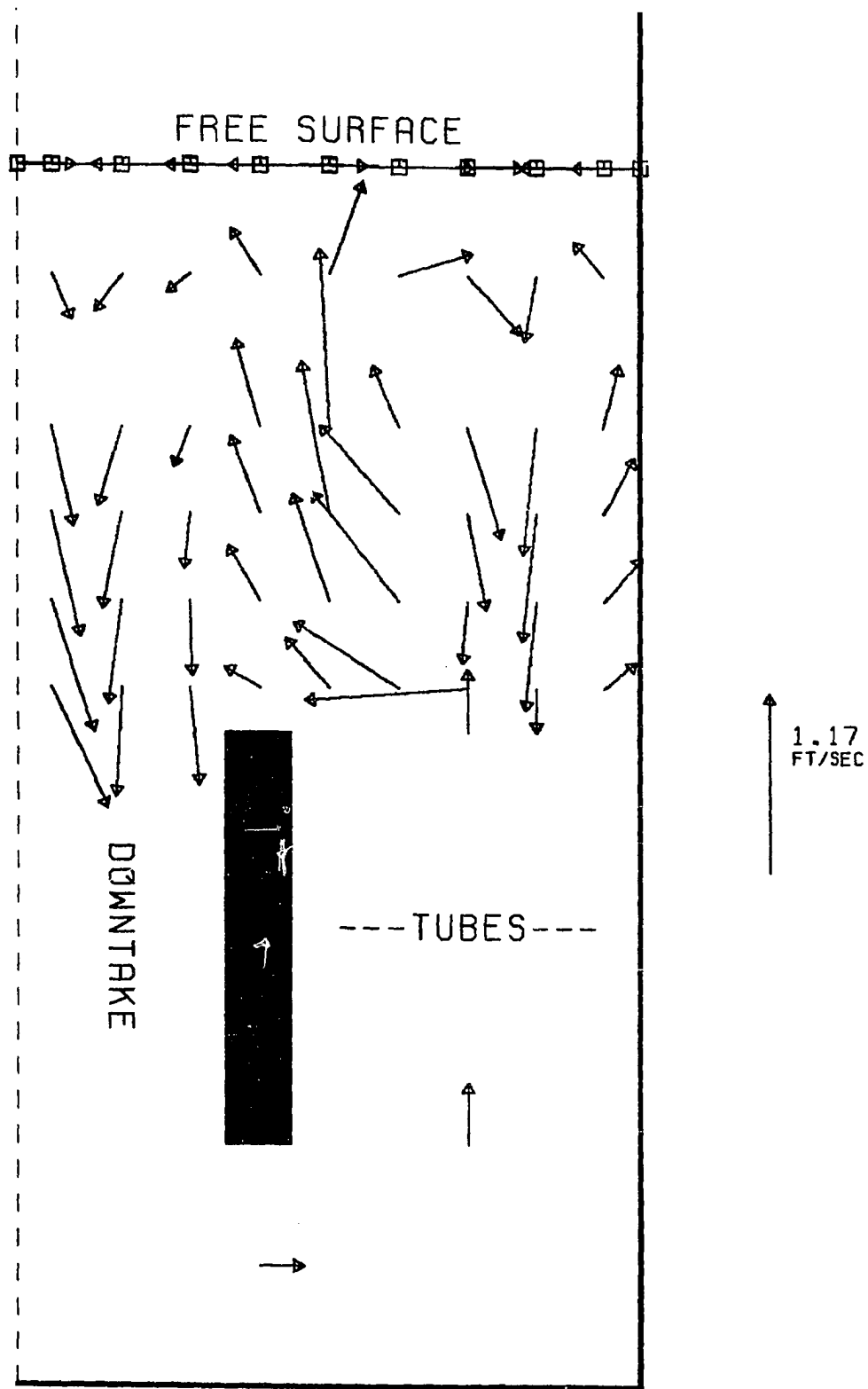
VELOCITY VECTORS

FIGURE II. 5 CASE 5



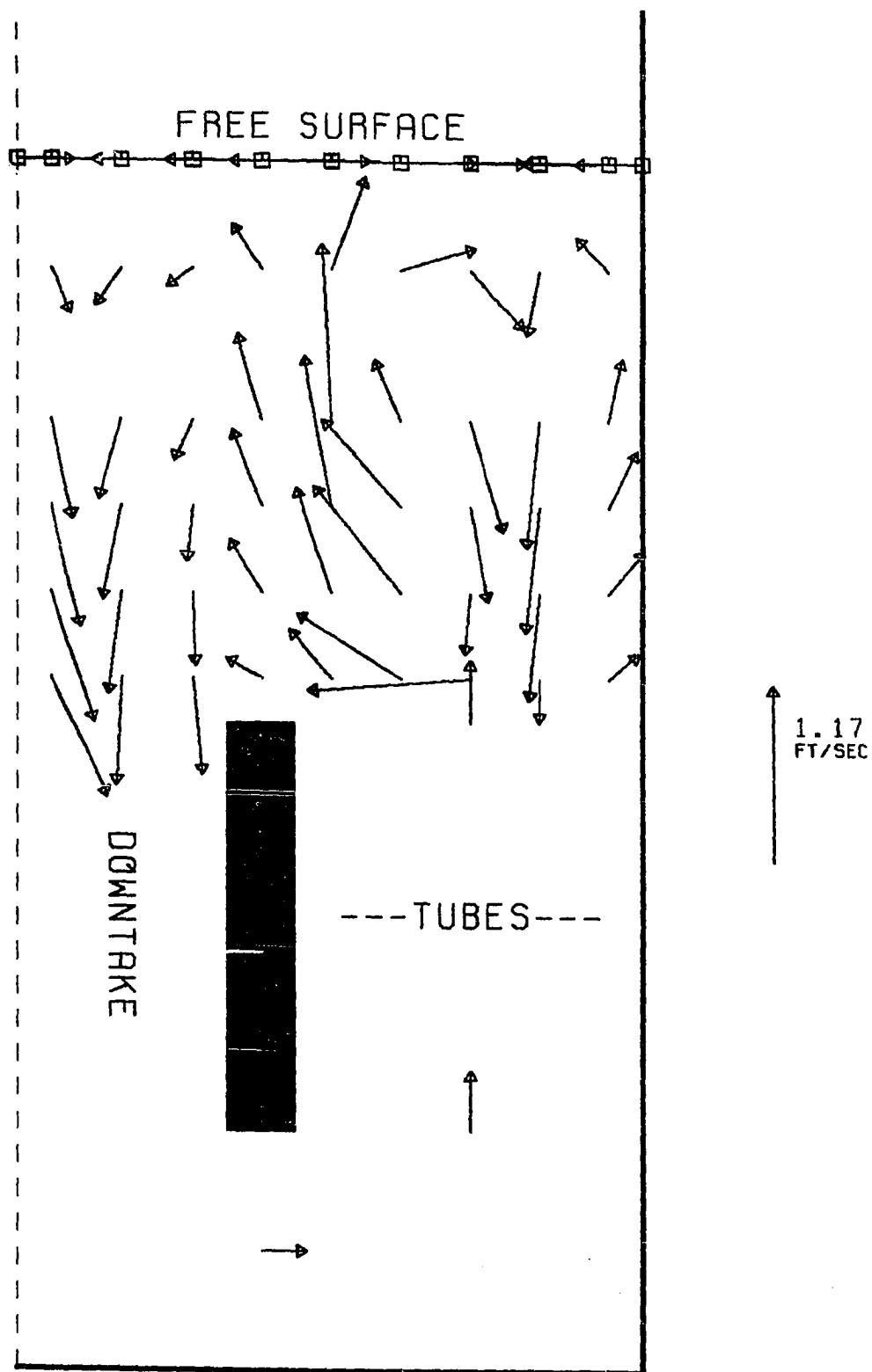
VELOCITY VECTORS

FIGURE II. 6 CASE 6



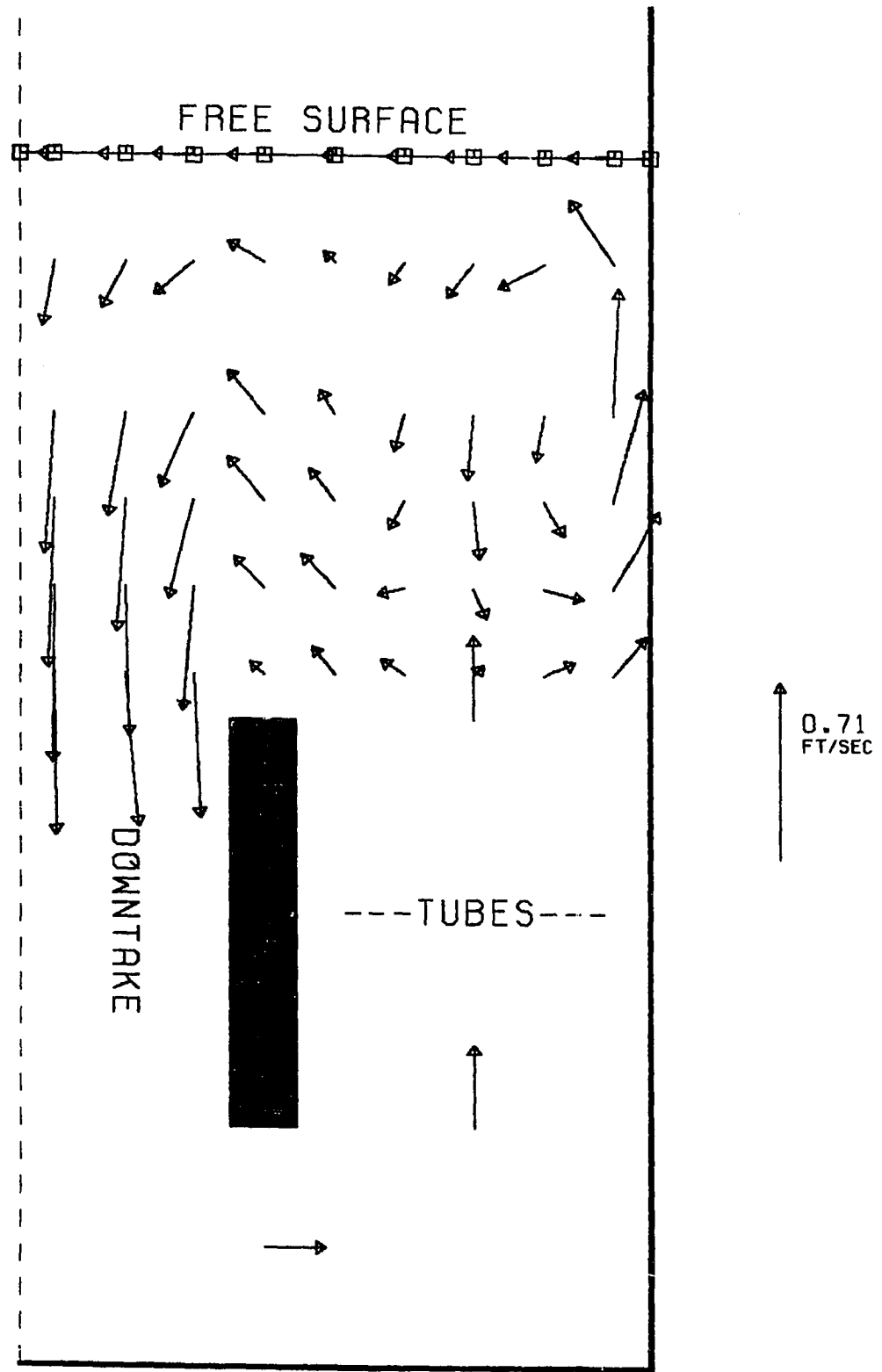
VELOCITY VECTORS

FIGURE II. 7 CASE 7



VELOCITY VECTORS

FIGURE II. 8 CASE 8



VELOCITY VECTORS

FIGURE II. 9 CASE 9

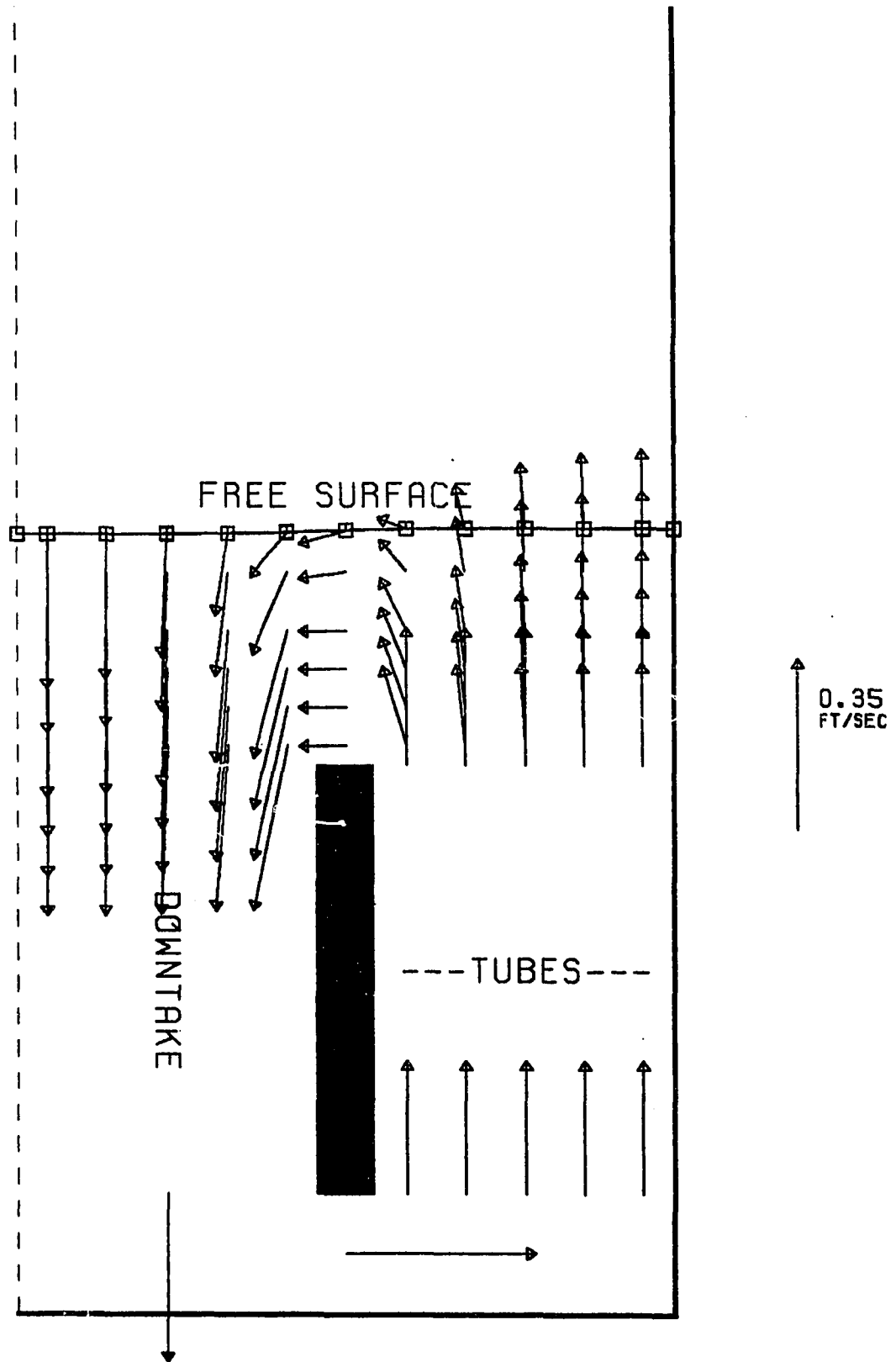
APPENDIX III

AN EXAMPLE OF DYNAMIC GRID

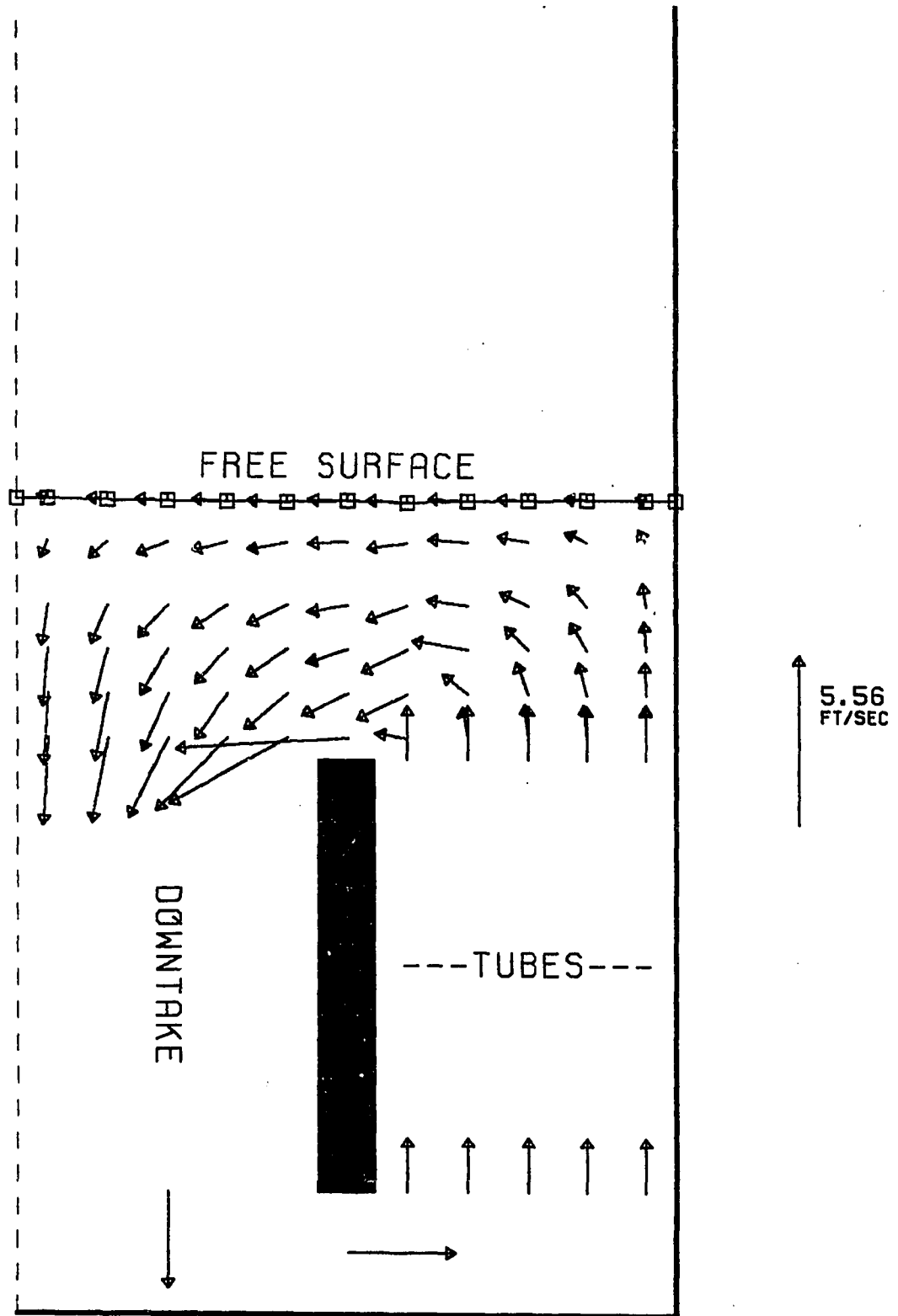
To demonstrate the dynamic grid, a test case was devised to simulate a typical moving interface under recirculating flow. The test simply consists of adding feed to a partially filled pan while recirculating the fluid in the Pan with a pump. The pump was simulated, as discussed in Chapter 4, by increasing the pressure drop from the Downtake to the Calandria by the amount of pressure head supplied by the pump. The recirculation is then caused by this pressure drop. The Figures III.1-III.3 are snapshots of the Pan at various times. Notice that the tank is filling and the grid formation is expanding in the vertical direction as designed. The total movement of the surface is about one foot. This simple case was devised only because it could be done in a small amount of computer time. A simulation of the Sugar Crystallizer with the same change in volume would take considerably more computer time to demonstrate how the dynamic grid works.

During a simulation of the Crystallizer the grid expands as the volume expands, and contracts when the accumulation of volume in the Pan is negative. This allows the simulation to continue from the beginning of a batch to the end, while the level is changing in

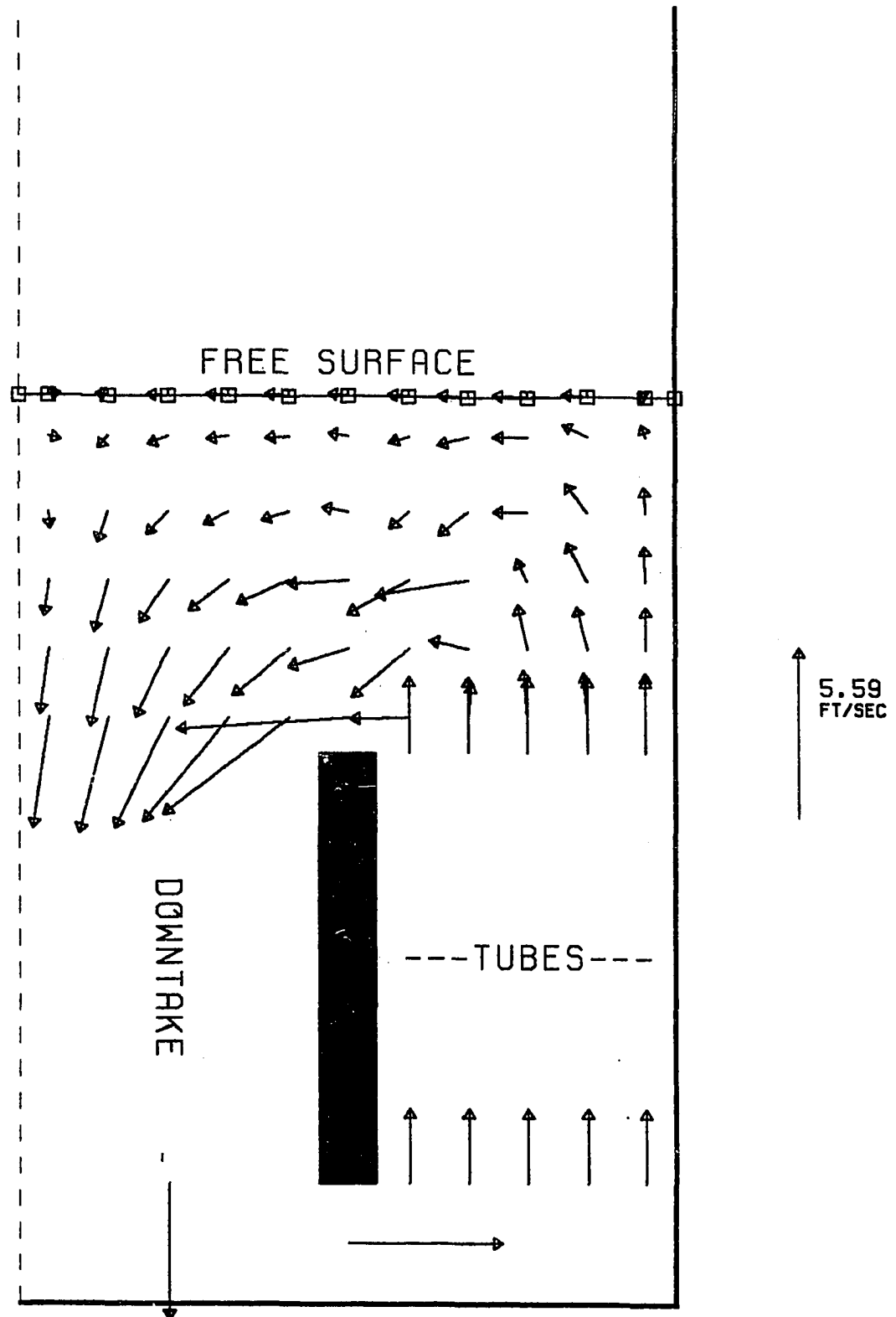
response to crystal growth, feed, and evaporation. Thus, the solution need not be stopped because the surface cell is too large or too small. Although the grid would normally be thought of as moving according to the dynamics of the surface, the movement of the grid can be arbitrary. Thus, with the proper programming, the grid can be made to move at the discretion of the programmer. The dynamic grid is an essential tool for free surface problems.



VELOCITY VECTORS FIGURE III. 1
 RUN I.D.: FREE SURFACE
 ELAPSED TIME: 0.000 HR.



VELOCITY VECTORS FIGURE III. 2
 RUN I.D.: FREE SURFACE
 ELAPSED TIME: 0.002 HR.



VELOCITY VECTORS FIGURE III. 3
 RUN I.D.: FREE SURFACE
 ELAPSED TIME: 0.008 HR.

VITA

Jack Jerome Bunton was born in Selma, Alabama on the twenty-ninth day of July, 1954. He is the son of Beulah G. Bunton of Mobile, Alabama and the late Oscar F. Bunton, retired United States Air Force T./Sgt. of twenty-three years.

He attended the University of South Alabama following graduation from high school and graduated with a B. S. in Chemical Engineering in 1976. In the Fall of 1976 he entered Graduate School at Louisiana State University and received a M. S. in Chemical Engineering in 1978.

He is married to the former Toni Lynn McLain of Mobile, Alabama. They have a lovely daughter, Brianna. They are presently living in Mobile, Alabama where he is employed by Ciba-Geigy Corp. as a Senior Process Engineer.

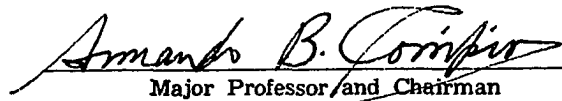
EXAMINATION AND THESIS REPORT

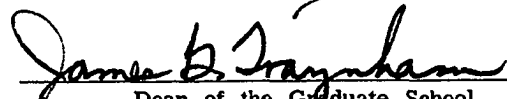
Candidate: Jack Jerome Bunton

Major Field: Chemical Engineering

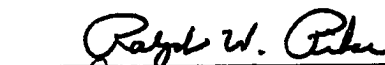
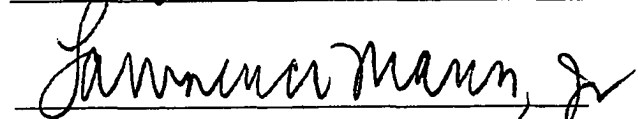
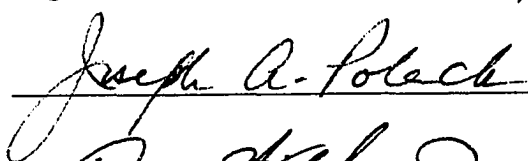

Title of Thesis: Natural Convection, Two-Phase Flow, and Crystallization
in a Vacuum Pan Sugar Crystallizer

Approved:


Major Professor and Chairman


Dean of the Graduate School

EXAMINING COMMITTEE:

Date of Examination:

November 25, 1980